

Final Report/Technical Completion Report
to
**California Department of Food and Agriculture
Fertilizer Research & Education Program,
University of California Water Resources Center,
California Tree Fruit Agreement**

**Long-term Nitrate Leaching
Below the Root Zone in
California Tree Fruit Orchards**

**Michelle Denton
Thomas Harter
Jan W. Hopmans
William R. Horwath**



February 2004



FINAL REPORT / TECHNICAL COMPLETION REPORT

to

**California Department of Food and Agriculture
Fertilizer Research and Education Program (FREP), Project 97-0365 M97-04**

University of California Water Resources Center, Project W-919

California Tree Fruit Agreement

Project Title: **Long-term Nitrate Leaching Below the Root Zone in California Tree Fruit Orchards / Transport and Fate of Nitrate-Nitrogen in Heterogeneous, Unsaturated Sediments below the Root Zone**

Project Location Kearney Agricultural Center, Parlier, California

Project Scientist Michelle Denton, Graduate Research Assistant, University of California, Davis

Project Leaders

Thomas Harter, Ph.D.
Assoc. CE Specialist, Subsurface Hydrology
thharter@ucdavis.edu

William R. Horwath, Ph.D.
Assoc. Prof., Soil Biogeochemistry
wrhorwath@ucdavis.edu

Jan Hopmans, Ph.D.
Professor, Water Management
jwhopmans@ucdavis.edu

Department of Land, Air, and Water Resources
University of California
Davis, CA 95616-8628

Cooperators

Scott Johnson, Ph.D.
Pomology Specialist
Kearney Agricultural Center
9240 S. Riverbend Ave.
Parlier, CA 93648

Dick Rice, Ph.D.
Entomologist, AES
Kearney Agricultural Center
9240 S. Riverbend Ave.
Parlier, CA 93648

Funding Support

Fertilizer Research and Education Program, *Project 97—0365 M97-04*, 1998 – 2001

\$ 86,905

Geoprobe Systems®, 3 months in-kind services: soil drilling and sampling device GH-40, 1997

\$ 18,000

California Tree Fruit Agreement, 1997-2000

\$ 26,189

California Water Resources Center, *Project W-919*, 1999-2001

\$ 54,500

TABLE OF CONTENTS

LIST OF TABLES	4
LIST OF FIGURES	5
OBJECTIVES	9
EXECUTIVE SUMMARY	9
ACKNOWLEDGEMENTS	11
1. INTRODUCTION	13
Problem Identification:	13
Current Approach:	13
Shortcomings of Current Approaches:	13
Past Research on Nitrate Flux in Deep Vadose Zones:	14
Research and Educational Needs:	14
2. SITE DESCRIPTION AND FIELD EXPERIMENTATION	15
2.1 Orchard Experiment Overview	15
2.2 Fertilizer Experiment and Nitrate Application	16
2.3 Irrigation	17
2.4 Weather Data	17
Precipitation	18
Reference Evapotranspiration	18
Air temperature	18
Solar radiation	19
Vapor pressure	19
Relative humidity	19
Dew point	20
Wind speed	20
Soil temperature	20
2.5 Plant yield and nutrient uptake	20
2.6 Bromide tracer experiment, October 2, 1996	22
2.7 Core sampling, 1997	22
3. LABORATORY METHODS	24
3.1 Hydraulic characterization: Multi-step outflow experiment	24
3.2 Hydraulic characterization- inverse modeling	25
3.3 Scaling	27
4. RESULTS	29
4.1 Geologic Framework	29
4.2 Laboratory Measurements	31
4.3 Multi-step Outflow Experiment and Parameter Estimation	33
4.4 Generating Pedotransfer Functions: NeuroMultistep	34

4.5 Scaling	35
5. DISCUSSION AND CONCLUSIONS	37
Link to FREP program goals:	39
Overcoming Site-Specificity:.....	39
New Products Generated by Project:	40
Extension Activities related to this project:	40
Technical/Scientific Conference Presentations:.....	41
6. REFERENCES	42

APPENDICES

- Appendix 1. *Reprint of:* Tuli, A., M.A. Denton, J.W. Hopmans, T. Harter, and J.L. Mac Intyre. 2001. Multi-step outflow experiment: From soil preparation to parameter estimation . Hydrology program, Dept of Land, Air, and Water Resources, University of California, Davis, CA, Paper number 100037.
- Appendix 2. *Preprint of:* Minasny, B., J. W. Hopmans, T. Harter, S. O. Eching, A. Tuli, and M. A. Denton, Neural networks prediction of soil hydraulic functions from multi-step outflow data, Soil Sci. Soc. of America Journal, 2004 (in print).

LIST OF TABLES

	<u>PAGE</u>
Table 2.2.1. Fertilizer amounts and application dates.	48
Table 2.3.1. Irrigation dates for the orchard. The date shown is the afternoon start date.	49
Table 2.4.1. Explanation of CIMIS report contents.	50
Table 2.4.2. Summary statistics for weather averages from 1983 to 1999. All values are monthly with exceptions noted.	50
Table 2.4.3. Department of Water Resources CIMIS Sensor Specifications	51
Table 2.5.1. Fruit yield, load and weight summary, including the 7 year average.	53
Table 2.5.2. Percent nitrogen in fruit on a dry mass basis (1983).	53
Table 2.5.3. Leaf nutrients.	54
Table 2.5.4. Soil nitrate concentration, in ppm, and pH in October, 1991.	55
Table 2.5.5. Soil nitrate concentration, in ppm, in January, 1995.	55
Table 3.3.1. Comparison of scaling subgroup assignments and data quality for each soil sample.	56
Table 4.2.1. Summary of DANR laboratory measurements.	59
Table 4.2.2. Summary statistics of DANR laboratory measurements	63
Table 4.3.1. Summary of the optimized van Genuchten parameters.	65
Table 4.3.2. Summary statistics of the van Genuchten parameters.	68
Table 4.5.1. Summary of percent reduction in sum of squares (SS) for subgroup "sandy loam" in groups 2, 3, and 4 using two scaling methods.	69

LIST OF FIGURES

	<u>PAGE</u>
Figure 2.1.1. Fantasia Nectarine Orchard Plot	71
Figure 2.2.1. Hand Application of Fertilizer	72
Figure 2.4.1. Average monthly precipitation from 1983 to 1999.	73
Figure 2.4.2. Average monthly ETo from 1983 to 1999.	73
Figure 2.4.3. Average monthly air temperature from 1983 to 1999.	73
Figure 2.4.4. Average monthly solar radiation from 1983 to 1999.	74
Figure 2.4.5. Average monthly vapor pressure from 1983 to 1999.	74
Figure 2.4.6. Average monthly relative humidity from 1983 to 1999.	74
Figure 2.4.7. Average monthly dew point from 1983 to 1999.	75
Figure 2.4.8. Average monthly wind speed from 1983 to 1999.	75
Figure 2.4.9. Average soil temperature from 1983 to 1999.	75
Figure 2.5.1a. Soil nitrate concentration measured in 1991 and 1995 for the 0 treatment subplot.	76
Figure 2.5.1b. Soil nitrate concentration for the 100 lbs N/acre subplot.	76
Figure 2.5.1c. Soil nitrate concentration for the 175 lbs N/acre subplot.	76
Figure 2.5.1d. Soil nitrate concentration for the 250 lbs N/acre subplot.	77
Figure 2.5.1e. Soil nitrate concentration for the 325 lbs N/acre subplot.	77
Figure 2.7.1. Fantasia Nectarine Soil Core Map	78
Figure 2.7.2. Deep Soil Profile Sampling Strategy	79
Figure 2.7.3. Soil Sample Numbering	80

	<u>PAGE</u>
Figure 3.1.1. Fantasia Nectarine Hydraulic Soil Core Map	81
Figure 4.1.1. Stratigraphic cross-section along a tree-row showing the major stratigraphic units.	82
Figure 4.2.1 a-i. Histograms for the nine laboratory measurements for 118 soil samples.	83-85
Figure 4.2.2a-b. Categorized box and whisker plots for bulk density.	86
Figure 4.2.3a-b. Categorized box and whisker plots for organic matter content.	87
Figure 4.2.4a-b. Categorized box and whisker plots for organic carbon content.	88
Figure 4.2.5a-b. Categorized box and whisker plots for porosity.	89
Figure 4.2.6a-b. Categorized box and whisker plots for saturated water content.	90
Figure 4.2.7a-b. Categorized box and whisker plots for the sand fraction.	91
Figure 4.2.8a-b. Categorized box and whisker plots for the silt fraction.	92
Figure 4.2.9a-b. Categorized box and whisker plots for the clay fraction.	93
Figure 4.2.10a-b. Categorized box and whisker plots for unsaturated hydraulic conductivity.	94
Figure 4.3.1a-b. Multi-step outflow experiment results and optimized curves for a sample with transient data.	95
Figure 4.3.2. Multi-step outflow results and optimized curve for a sample with steady state data.	96
Figure 4.3.3a-d. Histograms for the van Genuchten parameters for the samples.	97-98
Figure 4.3.4a-h. Categorized box and whisker plot for the van Genuchten parameters.	99-102
Figure 4.5.1a-e. Soil water retention (a) unscaled, (b) scaled using method 1, and (c) scaled using method 2. Original and de-scaled soil water pressure head using method 1 (d) and method 2 (e). All curves represent Group 1, Population 1.	103-104

	<u>PAGE</u>
Figure 4.5.1f-j. Unsaturated hydraulic conductivity (f) unscaled, (g) scaled using method 1, and (h) scaled using method 2. Original and de-scaled unsaturated hydraulic conductivity using method 1 (i) and method 2 (j). All curves represent Group 1, Population 1.	105-106
Figure 4.5.2a-e. Soil water retention (a) unscaled, (b) scaled using method 1, and (c) scaled using method 2. Original and de-scaled soil water pressure head using method 1 (d) and method 2 (e). All curves represent Group 2, Population 2.	107-108
Figure 4.5.2f-j. Unsaturated hydraulic conductivity (f) unscaled, (g) scaled using method 1, and (h) scaled using method 2. Original and de-scaled unsaturated hydraulic conductivity using method 1 (i) and method 2 (j). All curves represent Group 2, Population 2.	109-110
Figure 4.5.3a-e. Soil water pressure head (a)unscaled,(b) scaled using method 1, and (c) scaled using method 2. Original and descaled soil water pressure head using method 1(d) and method 2 (e). All curves represent Group 2, Population 1, subgroup sandy loam.	111-112
Figure 4.5.3f-j. Unsaturated hydraulic conductivity (f) unscaled, (g) scaled using method 1, and (h) scaled using method 2. Original and de-scaled unsaturated hydraulic conductivity using method 1 (i) and method 2 (j). All curves represent Group 2, Population 1, subgroup sandy loam.	113-114
Figure 4.5.4a-e. Soil water pressure head (a) unscaled (b) scaled using method 1,and (c) scaled using method 2. Original and descaled soil water pressure head curves using method 1 (d) and method 2 (e). All curves represent Group 3, Population 1, subgroup sandy loam.	115-116
Figure 4.5.4f-j. Unsaturated hydraulic conductivity (f) unscaled, (g) scaled using method 1,and (h) scaled using method 2. Original and descaled unsaturated hydraulic conductivity using method 1 (i) and method 2 (j). All curves represent Group 3, Population 1, subgroup sandy loam.	117-118
Figure 4.5.5a-e. Soil water pressure head (a) unscaled, (b) scaled using method 1, and (c) scaled using method 2. Original and descaled soil water pressure head curves using method 1 (d) and method 2 (e). All curves represent Group 4, Population 1, subgroup Sandy loam.	119-120

	<u>PAGE</u>
Figure 4.5.5f-j. Unsaturated hydraulic conductivity (f) unscaled, (g) scaled using method 1, and (h) scaled using method 2. Original and descaled unsaturated hydraulic conductivity (i-j) for Group 4, Population 1, subgroup sandy loam.	121-122
Photos 1 – 11. Flood irrigation of tree-row basins after bromide application.	123-125

OBJECTIVES

The objective of our work is to provide a better understanding of the processes governing the transport and fate of nitrate-nitrogen in deep alluvial unsaturated zones, which are typical for the eastern San Joaquin Valley. We develop and analyze an intensive field data set to determine the geologic, hydrologic, and geochemical framework that controls the long-term rate of nitrate leaching to groundwater under various fertilizer application rates. The field dataset provides the foundation for preparing a conceptual-numerical modeling analysis of the fate of nitrogen in deep unsaturated zones with high spatial variability and a significant potential for preferential flow. For this project, a site with a well-controlled fertilization trial was chosen. Our specific objectives are:

- to provide a detailed overview of the water and nitrogen conditions during a 12-year controlled fertilization experiment.
- to describe the heterogeneity of unsaturated alluvial sediments typical of the eastern San Joaquin Valley.
- to determine the physical and hydraulic properties of the deep unsaturated zone, and their relationship to sedimentary facies, texture.
- to develop a pedotransfer function tool that can be used to quickly determine soil hydraulic properties from inexpensively measured textural data.
- to provide an analysis of the spatial variability of hydraulic properties using the scaling concept, for later use in modeling studies.

The field and laboratory characterization is the foundation for the development and validation of various modeling tools that assess the fate of nitrogen in deep, heterogeneous vadose zones (ongoing work); and has provided an educational component for growers, farm advisors, and personnel from irrigation districts, water districts, and regulatory agencies on the leaching potential and attenuation rates of agricultural chemicals in similar areas.

EXECUTIVE SUMMARY

Nitrate-nitrogen in groundwater is the most widespread contaminant causing up to ten times as many well closures in the State of California as all other industrial contamination combined. While a large amount of research has focused on nitrogen cycling in the root zone (to depths of 6-10 feet), little is known about the fate of nitrogen between the root zone and the ground water table. Unlike in other agricultural regions of the United States, however, ground water levels in many areas of Central and Southern California are from 30 feet to over 100 feet deep. Therefore, the deep vadose zone is a critical link between agricultural sources and groundwater. Few studies have surveyed the hydrology and the fate of nitrogen at such depths or monitored leaching of nitrogen to a deep water table. Field-scale spatial variability of nitrate levels due to natural variability of soils and vadose zone sediments also remains unaccounted for in most work on groundwater quality impacts of agricultural nitrogen management.

Field, laboratory, and modeling research is carried out in conjunction with an eastern San Joaquin Valley site (near Reedley, Fresno County). The site was subject to a unique long-term nitrogen fertilizer study that investigated crop impacts of several alternative management practices, with fertilization rates ranging from 0 to 325 pounds of nitrogen per acre. Ground water levels at the orchard are approximately 50 feet below the surface, which is typical for many areas in the southern and eastern San Joaquin Valley. The unsaturated zone at the site has a heterogeneous profile that is characteristic for many alluvial soils and sediments found in the San Joaquin Valley and other alluvial basins in California.

Sixty continuous cores to 52 feet were obtained using the Geoprobe Systems Macrocore[®] direct push sampling technique. We identified ten major facies ranging in thickness from less than 30 cm to over 300 cm. Most of the identified facies are laterally continuous across the site. Sediment textures in these unsaturated zone facies range from clean medium sand (remnant of a former channel bed) to finely laminated clayey-silt loam (flood-plain deposits). The facies identification provides an overall framework of the unsaturated zone geology. Significant textural and structural variability was observed on the cores within each facies unit.

Over 1,000 samples were collected from the continuous cores for water content, pH, and nitrate analysis. Undisturbed cores were collected for analysis of unsaturated hydraulic properties using a multi-step outflow technique that we successfully modified to fit the relatively small diameter Macrocore[®] samples. For the approximately 100 undisturbed core samples, van Genuchten parameters for the hydraulic functions were obtained by inverse modeling of each individual multi-step experiment. All of the directly and indirectly measured sediment and hydraulic parameters are found to be highly variable within facies and across facies. For example, saturated hydraulic conductivity is log-normal distributed with a variance of over 5. The van Genuchten α and n parameters also have a skewed and highly variable distribution. Much of the variability is observed within facies, although between facies variability of hydraulic properties is also significant.

The hydraulic property database was used to develop pedotransfer functions from a neural network analysis of the relationship between textural sample composition and hydraulic properties of the samples. The pedotransfer functions are implemented within a simple-to-use computer program that can be used for other sites in the San Joaquin Valley to estimate hydraulic properties from the percent sand, silt, and clay content of individual soils or sediment facies. This tool provides the basis for site-specific unsaturated zone hydraulic analysis without the time-consuming step of measuring hydraulic functions.

We also determined scaling factors from the hydraulic property database. Scaling factors are a pseudo-geometric measure of the pore-space variability and have been used to capture, in a single parameter, the spatial variability of multiple hydraulic parameters (e.g., the van Genuchten parameters describing unsaturated hydraulic conductivity and soil water retention functions). We find that scaling indeed captures much of the observed variability. Including information about textural or facies membership into the scaling process significantly improves the predictive capability of the scaling factor.

Water content and nitrate distribution are also found to be highly variable. Nitrate concentrations vary over several orders of magnitude. This is consistent with the high variability of hydraulic properties. Apparently, the flow conditions in the deep unsaturated zone are such that narrow flow paths with a high flow rate (preferential flow paths) carry much of the nitrate leached from the root zone, while most of the unsaturated zone remains relatively stagnant and participates only to a limited amount in the transfer of water and nitrate to groundwater. Traditional approaches may therefore overestimate both the time nitrate remains in the unsaturated zone and the amount of attenuation or denitrification that occurs there. In a follow-up project, we are testing this hypothesis by implementing a detailed stochastic flow and transport model of the site that builds upon the extensive database of hydraulic properties, historic data, and scaling factors obtained for this site.

The research project provides a better understanding of the fate of nitrogen in deeper vadose zones under orchards and vineyards in the eastern San Joaquin Valley and similar alluvial basins in California. The resulting data and modeling tools are used to educate growers, farm advisors, irrigation and water districts, and regulatory agency personnel about nitrate leaching potential and attenuation rates and its time-frame in areas where the water table is substantially deeper than the root zone and where significant soil layering and spatial variability is observed.

ACKNOWLEDGMENTS

Under the supervision of the principal investigators, this project was implemented primarily by students and technical staff at UC Davis and the Kearney Agricultural Center. The project would not have been possible without their incredible enthusiasm, hard work, and dedication:

- Katrin Heeren was the field geologist in charge of the field operation in 1997 and completed a preliminary geologic report on the site geology in 1998.
- Anthony Cole, Chad Pyatt, and Rigo Rios, all undergraduate students from CSU Fresno, successfully implemented the drilling operations during the summer and fall of 1997 under the supervision of Katrin Heeren and Thomas Harter. Chad Pyatt later also completed all of the pH analyses
- Andrea DeLisle completed the nitrate analyses in 1997 on over 1,000 samples. Briefly, Cindy Bergens and Michael Ridolfi worked on chemical analyses. More recently, Tad Doane is in charge of the isotope and other chemical analyses (all under the supervision of Dr. William Horwath).
- Jim MacIntyre, hired for this project out of retirement, successfully adopted the multi-step outflow experiment in 1998 to work in conjunction with the Geoprobe Systems Macrocore[®] samples; and implemented all of the laboratory multi-step outflow experiments in 1998-1999.
- Michelle Denton is completing her M.S. thesis (1999-2003), which focuses on the inverse modeling of the multi-step outflow experiments, documentation of the updated experimental and modeling protocols, and interpretation of the soil

hydraulic data she obtained from the computer modeling of the lab experiments. She is the main author of this final report.

- Dr. Budi Minasny, Faculty of Agriculture, Food and Natural resources, The University of Sydney, Australia, in collaboration with Dr. Jan Hopmans used Michelle's dataset together with two similar datasets developed in Dr. Hopmans laboratory for the western San Joaquin Valley and the Sacramento Valley to generate a neural network based prediction tool for Central Valley soils.
- In a follow-up project (2002-2004), funded by FREP, Sevim Onsoy, Ph.D. student in our department, is taking the rich database generated for the Kearney site to complete the geostatistical analysis and to interpret the data within a stochastic framework to account for the tremendous heterogeneity encountered at the site.

1. INTRODUCTION

Problem Identification:

Pollution of groundwater from agricultural fertilization practices has become one of the largest ground-water quality issues in the intensively used agricultural areas of California. The number of well closures due to contamination with nitrate is almost ten times larger than the number of well closures due to industrial contamination (Metropolitan Water District of Southern California, 1987). Nitrate contamination of groundwater is particularly widespread in Southern California and along the east side of the San Joaquin Valley. High nitrate levels in ground water are caused by leaking septic systems, percolation of animal waste, and leaching of nitrogen fertilizer in agricultural fields. In a USDA document (Kellogg et al., 1992), it was estimated that 14 percent of California's rural lands have significant potential for nitrate leaching. The same report also concludes that more research is needed to understand the physical and biogeochemical processes dictating the fate of chemicals applied to crops and their transport in soil and water systems.

Current Approach:

Minimizing the impact on groundwater quality is an important aspect of fertilizer research and management. Commonly, nitrate leaching is evaluated by monitoring root zone nitrate levels with a small number of soil or lysimeter samples over one to several crop periods. Nutrients are rarely monitored below a depth of six feet. Tanji et al. (1977) and Tanji et al. (1979) presented a conceptual model for estimating nitrogen emissions from cropped lands, which was tested for a corn crop. Their model considers fluxes to and from the root zone and assumes that both water and nitrate fluxes are at steady-state. Similar but somewhat less sophisticated nitrogen balance models are typically used in many nitrogen field studies used to estimate fertilizer nitrogen impact on groundwater quality (e.g., Hartz and Costa, 1995; Lovatt, 1995; Miller and Friedman, 1995; Weinbaum and Goldhamer, 1995; Lovatt and Morse, 1995; Meyer, 1995). The common assumption is that nitrate losses to below approximately six feet represent the amount of nitrate leached into ground water. This assumption is justified for many areas in the United States, where ground water is found at depths of less than 10 to 20 feet.

Shortcomings of Current Approaches:

In many agricultural areas of California, in contrast, ground water levels are 30 to 100 feet deep and little is known about the fate of nutrients between the root zone and the ground water table. Few studies have surveyed nitrate levels at such depths or monitored leaching of nitrate to deep water table. Also, most of the intensively used agricultural areas in California are located in large to very large basins filled with alluvial deposits (Central Valley, Salinas Valley, Southern California and Mojave Desert basins) adding further complication to real time assessment of nitrate leaching to ground water. Vertical stratification of the alluvial soils and horizontal discontinuity of both coarse and fine grained soil material causes significant spatial variability in water percolation rates, nitrate concentrations, and denitrification rates (intrinsic variability). Spatial variability in both the horizontal and vertical direction limits the value of composite root zone soil

samples with respect to predicting nitrate leaching rates. Our current understanding of the spatial variability of hydraulic properties and their impact on nitrate fate and transport below the root zone is therefore limited and based on greatly simplified models.

Past Research on Nitrate Flux in Deep Vadose Zones:

Pioneering work on nitrate in deep soil profiles was presented by Pratt et al. (1972), who investigated nitrate profiles in a southern California citrus orchard to depths of 100 feet. The experimental site was subject to differential nitrogen treatment for 35 years from 1927 to 1962. Nitrogen treatments ranged from 50 to 350 lbs/ac. During the period from 1963 to the time of sampling in 1969, uniform treatment was applied at a rate of 150 lbs/ac. The soil under the orchard was classified as a Greenfield sandy loam. From their observations, the authors estimated that it would take between 10 and 50 years to leach nitrate to a depth of 100 feet. Average nitrate-nitrogen levels below the root zone varied from 15 to 35 ppm under the 50 lbs/ac treatment and from 35 to 55 ppm under the 350 lbs/ac treatment. Estimated differences between nitrate applied and nitrate uptake in the fruit plus nitrate remaining in the soil profile increased with application rates, suggesting that denitrification may account for up to 50% of nitrate losses in the soil profile when application rates are high. Not enough data was available to further confirm that denitrification was occurring. Lund et al. (1974) argued that differences in unaccounted nitrate losses (presumed to be due to denitrification) are strongly correlated with the textural properties of the soil. High losses were found in soils with pans or textural discontinuities, while losses were limited in relatively homogeneous, well draining soils. Later work by Gilliam et al. (1978), Klein and Bradford (1979), and Rees et al. (1995) in other areas of southern California supported these observations. No such studies are available for tree fruit orchards or vineyards. More importantly, none of these studies explicitly account for spatial variability in either the horizontal or vertical direction to quantify the risk for ground water pollution from fertilizer applications. Recently, Fogg et al. (1995) estimated the residence time of nitrate in groundwater of the Salinas valley, where vegetable crops are dominant. Their work, which accounted for spatial variability only in the saturated zone, demonstrated that it may take decades before changes in agricultural practices have a significant impact on ground water quality. They pointed out the need to better understand nitrogen transport processes in the deep vadose zone as a key to assessing the long-term impact of agricultural management practices on groundwater quality.

Research and Educational Needs:

Recently, geostatistical and stochastic methods have been developed to evaluate spatial variability of soil characteristics and to assess its effect upon solute transport. It has been shown, theoretically and in field experiments, that spatial variability can significantly impact the amount of solute leaching in soils and that concentrations of nitrate may vary significantly over short distances as a result of soil heterogeneity (e.g., Lund et al., 1974; Harter and Yeh, 1996). This may lead to large amounts of nitrate being leached quickly in some portions of the soil profile, while others retain nitrate for very long periods of time. The geostatistical-stochastic approach provides a well-suited framework to better understand the fate of nitrogen in California's deep, heterogeneous vadose zones. The Kearney Agricultural Center research orchard provides a unique, extensively sampled

and characterized field site with a well controlled, long-term field research experiment completed prior to our intensive deep vadose zone sampling campaign. Our goal in developing the site is to better understand the degree of spatial variability in hydraulic, transport, and chemical properties in the unsaturated zone and to provide the basis for adapting the stochastic approach specifically for nitrogen fate and transport. In a current follow-up project we demonstrate its utility for the assessment of nitrogen fluxes in deep vadose zones under irrigated agriculture. Ultimately, this project will provide significant information to better understand the risk of groundwater pollution and the associated costs and benefits of fertilizer treatments in tree orchards.

2. SITE DESCRIPTION AND FIELD EXPERIMENTATION

2.1 Orchard Experiment Overview

The research site, a former nectarine orchard, is located on the east side of the San Joaquin Valley, approximately 30 km southeast of Fresno, California, at the University of California Kearney Research Center. The orchard was planted by Marvin Gertz in 1975 and had four varieties of nectarines, each covering approximately 2 acres. A controlled fertilization management experiment was conducted in the orchard over a period of 12 years (Johnson et al., 1995) beginning in September 1982 and continuing through 1995. The experiment was conducted only on the Fantasia variety of nectarine. The ID number assigned to the experimental site was KAC #92-74 and was later renumbered to KAC #663. Trees were planted in a 15-tree by 15-tree matrix spaced 20 feet apart on berms approximately 4 ft wide and 1 ft high (Figure 2.1.1), creating 16 ft wide shallow furrows between tree rows.

As in many other surrounding areas, groundwater levels at the orchard are significantly deeper than the root zone. Since 1970, water levels have fluctuated between approximately 35 and 67 feet below the surface. In 1997, the unsaturated zone was approximately 50 feet thick. For the site, relatively accurate records about fertilization methods are available including exact dates and quantities. Dates and approximate amounts of applied irrigation water (flood irrigation) and climate conditions during the past 15 years are also available and are documented here. These data are important for the interpretation of any deep vadose zone hydrology and nitrogen data, because they define the water and nitrogen fluxes across the root zone of the orchard, which are driven by water applications, precipitation, and evapotranspiration.

The site is located on the Kings River alluvial fan, a highly heterogeneous sedimentary system consisting of coarse channel deposits, fine flood deposits, paleosols, and fine eolian deposits. Sedimentary layers exposed to the surface for sufficient amount of geologic time have developed soil profiles with distinguishable horizons. The type of sedimentary layering, the paleosols encountered, and the range of soil textural classes encountered at this site are rather typical for many areas in the San Joaquin Valley that have deep vadose zones (Weissmann and Fogg, 1996). Similar alluvial conditions are

also found in the Salinas Valley and in the desert basins of Southern and Southeastern California.

2.2 Fertilizer Experiment and Nitrate Application

The fertilizer experiment consisted of five application treatments in a random block design. The five nitrogen application treatments (0, 100, 175, 250, and 325 lbs N/acre/year, not including nitrogen applied via irrigation water) were applied in 3 replicates, with the exception of the 0 treatment having 2 replicates. This results in the orchard being divided into 14 subplots. Each subplot consists of a row of 5 trees. Two border trees and one border row on either side of a subplot separate treatments (Figure 2.2.1).

Except for the 0 lbs N/acre/year treatment plots, all trees received a broadcast application of 100 lbs N/acre nitrogen in September of each year. The fertilizer was applied from berm edge to berm edge using a tractor-mounted spreader. Application uniformity was not measured but anecdotal evidence indicates that greater amounts were applied near the edge of the furrows and less in the center of the furrows (Scott Johnson, personal communication). Generally, the fertilizer was not disked into the soil but was left at the soil surface.

In spring, additional fertilizer was applied by hand to the 175, 250, and 325 lbs N/acre plots in 75 lbs N/acre increments. It was applied 2-3 ft wide (normal to the berm) and about 12 ft in length, starting 6 ft on one side of a tree and ending 6 ft on the other side, leaving an 8-foot fertilizer-less gap between trees (Figure 2.2.2). Fertilizer application was repeated in this manner two or three times depending on the total treatment desired. These applications were separated by a few weeks.

Ammonium sulfate was used in the first application in September 1982. However, it was believed that the ammonium sulfate was acidifying the soil so ammonium nitrate and calcium nitrate were substituted for the remainder of the experiment. No fertilizer was applied in 1995. On September 25, 1996 a single application of 100 lbs N/acre was applied to the entire 20 year old orchard.

Fertilization records detailing the amount of fertilizer applied and the application dates are available from 1982 through 1994 and are shown in Table 2.2.1. Notice that the amount reported is on a per tree basis and is in reference to the amount of fertilizer and not the amount of nitrogen.

The orchard received further nitrogen from nitrate in precipitation (less than 5lbs N/acre) and from nitrate in irrigation water (30-50 lbs N/acre assuming 4-5 ppm of nitrate-N in 3-4 acft/acre of irrigation water).

2.3 Irrigation

As is common for many orchards and vineyards in the area, the orchard was flood irrigated every 2-3 weeks from April through September. The orchard was irrigated from 1983 to 1997. The irrigation water was supplied by a pipe located at the east side of the orchard. The water was turned on to a low flow rate (described as a “trickle”) in the late afternoon (between 3 and 4 o’clock) and was left on overnight. In the morning the flow rate was increased and was shut off after 2-3 inches water depth was achieved at the opposite end of the row (around 1pm). In 1997, the orchard received regular irrigations only through early July, when field sampling began. One additional irrigation was applied in late September 1997 (to facilitate coring through the hardpan at 10’ depth), after approximately two-thirds of all cores were taken.

A typical irrigation applied approximately 4-6 inches of water with an average application rate of 16gpm for roughly 21 hours (10-15 gpm for 15 hours (4pm – 7am) and 20-30 gpm for 6 hours (7 a.m. – 1 p.m.)). On average, 12 irrigations totaling 48 to 72 inches, or 4 to 6 feet, of water were applied to the orchard annually. This is slightly higher than the typical 45 in/year applied for a well managed nectarine orchard under furrow irrigation. Photos 1-11 show an irrigation event from start to finish.

Average consumptive use of the mature orchard is estimated to be 3 feet per year. Average net infiltration to below the root zone is therefore estimated to be on the order of 1 to 3 feet. The groundwater level at the site varies from 45-60 feet below ground surface. Assuming an average effective water content of 15%, travel time to the water table is on the order of 3-8 years.

Unfortunately, irrigation records are only available for 1983 and 1990-1997. Records for 1984-1989 have not been found. These records also include dates for fertilization, mowing, rotovating, pruning, thinning, harvesting, and application of chemicals other than fertilizer, such as herbicides. It is important to remember that irrigation data come with some uncertainty. For example, sometimes the irrigation event would last 1 day and sometimes it would span 3 days. Also, uniformity of water application is thought to be low and the trees at the end of a row are likely to receive less water than those trees near the supply pipe. Table 2.3.1 shows the dates of the irrigation events.

2.4 Weather Data

Climate records from June 1983 to December 1999 were obtained from the California Irrigation Management Information System (CIMIS) web site for the Parlier Station (#39) located near the site.

CIMIS is an integrated network of over 100 computerized weather stations located at key agricultural and municipal sites throughout California. By measuring values for various sensors, such as wind speed, air temperature, solar radiation, etc., we can calculate ETo and other useful factors. Providing information for improving water and energy

management through efficient irrigation practices is the primary use of the CIMIS system. The URL for CIMIS is <http://www.cimis.water.ca.gov>.

Several types of reports are available from CIMIS including hourly, 7-day daily, and monthly reports. For each of these the values are averaged over the time period of the report. For example, the hourly report consists of hourly averages. Table 2.4.1 summarizes the various report contents. The values within this report are monthly averages.

The following nine sub-sections briefly describe the CIMIS weather data for 1983 to 1999. Table 2.4.2 summarizes the basic statistics for the weather data. The sensor specifications are summarized in Table 2.4.3. The information in this table was copied directly from the CIMIS web site.

Precipitation

Assuming a water year is from October 1 to September 30, average annual precipitation is 13 inches with a standard deviation of 4.7 inches. The range is from 3.9 to 22.6 inches with the driest year being 1996 (October 1995 to September 1996) and the wettest year being 1995.

In most years essentially no precipitation is recorded between late May and early October. For monthly averaged precipitation, the range is from 0 to 8.7 inches with a mean of 1.07 inches and a standard deviation of 1.5 inches. This tells us what we already know: rainfall is quite variable. Figure 2.4.1 shows the average monthly precipitation in inches from 1983 to 1999.

Reference Evapotranspiration

Evapotranspiration is the combined process of water loss by evaporation and water transfer to the air through plant tissues. Reference evapotranspiration (ET_o) is a term used to describe the evapotranspiration rate from a known surface, such as grass or alfalfa. ET_o is expressed in either inches or millimeters. Crop Coefficients, K_c, are used with ET_o to estimate specific crop evapotranspiration rates. The reference crop used here is grass, which is closely clipped, actively growing, completely shading the soil, and well watered.

The average annual ET_o is 53.3 inches with a standard deviation of 2.7 inches. The range is from 46.8 to 56.4 inches.

The average monthly maximum ET_o occurs in July and the minimum occurs in December or January. The range is from 0.4 to 8.8 inches. The mean monthly ET_o is 4.5 inches with a standard deviation of 2.6 inches. Figure 2.4.2 shows the average monthly ET_o in inches from 1983 to 1999.

Air temperature

Maximum, minimum, and average air temperatures are reported on a monthly average basis (CIMIS web site). The maximum air temperature has 3 anomalous values that have

been flagged. These occur during July 1983, December 1985, and December 1988 at values of 105.4, 71, and 83.6 °C, respectively (possibly a temperature conversion error). There is no notation as to which day or days the errors occur on nor is there any explanation as to why the errors occurred. The error message is “one or more daily values flagged”. It could be due to a variety of instrumentation errors.

Without the anomalies, the range for the maximum monthly air temperature is 8.4 to 37.2°C. The mean is 24.6 °C with a standard deviation of 7.9 °C. The range for the minimum monthly air temperature is -2.6 to 18.9 °C. The mean is 9.1 °C with a standard deviation of 5.3 °C. The range for the average monthly air temperature is 3.3 to 27.5 °C. The mean is 16.5 °C with a standard deviation of 6.7 °C. Figure 2.4.3 shows the maximum, minimum, and average monthly air temperatures from 1983 to 1999 and includes the anomalies.

Solar radiation

Net radiation at the earth's surface is the major energy input for evaporation of water (Chow, et. al., 1988). Solar radiation makes up one component of net radiation.

The average monthly maximum solar radiation occurs during the summer, in June or July, and the minimum occurs during the winter, in December or January. The range is from 51 to 355 Watts/m². The mean is 206.02 Watts/m² and standard deviation is 91.5 Watts/m². Figure 2.4.4 shows the average monthly solar radiation from 1983 to 1999.

Vapor pressure

Besides the supply of heat energy, the second factor controlling evaporation is the ability to transport vapor away from the surface (Chow, et. al., 1988). Vapor pressure is calculated from the relative humidity and the air temperature.

The average monthly maximum occurs in July or August. The minimum occurs mostly from December to February. The range is from 0.4 to 2 kPa. The mean is 1.23 kPa and the standard deviation is 0.35 kPa. Figure 2.4.5 shows the average monthly vapor pressure from 1983 to 1999.

Relative humidity

For a given air temperature there is a maximum moisture content the air can hold. The corresponding vapor pressure is called the saturation vapor pressure. The relative humidity is the ratio of the actual vapor pressure to its saturation vapor pressure (Chow, et. al., 1988).

Maximum, minimum, and average relative humidity are reported on the CIMIS site on a monthly average basis. There is a period, March 1990 to January 1994, during which the relative humidity seems to not follow the same trend that is exhibited during the leading and following years. The precipitation shows larger peaks during this time period (Figure 2.4.1). Also, the vapor pressure (Figure 2.4.5) and dew point (Figure 2.4.7) exhibit a different than usual trend during this period. Vapor pressure, dew point, and relative humidity are interdependent variables.

The range for the maximum relative humidity is from 40 to 100% with a mean value of 88.9% with a standard deviation of 11.2%. The range for the minimum relative humidity is from 17 to 84% with a mean value of 41.9% and a standard deviation of 16.7%. The range for the average relative humidity is from 27 to 95% with a mean value of 64.8% and a standard deviation of 14.6%. The maximums occur in winter and the minimums occur in summer. Figure 2.4.6 shows the maximum, minimum, and average monthly relative humidity from 1983 to 1999.

Dew point

The temperature at which air would just become saturated at a given specific humidity is the dew-point temperature (Chow, et. al., 1988). The range is from -6.1 to 17.7 °C. The lows are mostly in December and January and the highs are in July and August. The mean is 9.2°C and the standard deviation is 4.5°C. Figure 2.4.7 shows the average monthly dew point temperature from 1983 to 1999.

Wind speed

It is windiest in April and May and the least windy in November. The range is from 1 to 2.5 m/s. Mean wind speed is 1.7 m/s with a standard deviation of 0.36 m/s. Figure 2.4.8 shows the average monthly wind speed from 1983 to 1999.

Soil temperature

Soil temperature values were not reported for April and May 1998. Soil temperature was at a minimum in December and January and at a maximum in July and August. The range is from 6.2 to 29.6 °C. The mean is 17.8°C with a standard deviation of 6.3°C. The point of measurement is 6 inches below the soil surface under irrigated grass. Figure 2.4.9 shows the average monthly soil temperature from 1983 to 1999.

2.5 Plant yield and nutrient uptake

As part of the fertilizer management project implemented at the site the following were measured:

- fruit yield
- nitrogen concentration in fruit (flesh, pit, and seed)
- leaf nutrients (%N, %P, and %K)
- soil nitrate and pH

Table 2.5.1 shows the fruit yield summary (in kg/tree) for 1983-1985 and 1991-1994 for all five treatment plots. Average individual fruit weight is obtained by dividing the total kilograms of fruit per tree by the number of fruit per tree. Yield in 1983 responded positively to the increasing fertilizer rate. The 7-year average yield, however, dropped in all subplots. A significant drop was seen in the control subplot. The 0 lbs N/acre subplot likely consumed the reserved N storage at the beginning of the experiment and thus, there was no significant difference in yield compared to other treatments in 1983. Once the reserve N was depleted the drop in yield became apparent. The yield from subplot 325 lbs

N/acre gave the second lowest yield after the control subplot, indicating a negative response to the high fertilizer application rate.

Percent nitrogen in fruit (flesh, pit, and seed) was measured in dry fruit mass in 1983 for each treatment group except the 0 treatment plots and is shown in Table 2.5.2. Dry weight is approximately 10% of wet fruit weight. Although fruit yields varied little between treatments total fruit N levels varied greatly from treatment to treatment. There is an increasing trend in nitrogen content in fruit flesh with nitrate application but there is no evident trend in nitrogen content in seeds or pits. For the 0, 100, and 325 lbs N/acre treatments, fruit harvest is estimated to remove 35, 70, and 110 lbs N/acre, respectively (Scott Johnson, personal communication).

Table 2.5.3 summarizes the measured leaf nutrients (%N, %P, and %K) for 1983-1985 and 1991-1994 for all five treatment plots. It is observed that nitrogen content in leaves increases with nitrate application. An opposite trend is seen in %P and %K. Leaf and cover crop N uptake are assumed to be returned to the soil via leaf fall, decomposition, and mechanical incorporation into the soil.

Average soil nitrate-N data are available for October 1991 and January 1995 to a depth of 10 feet at a measurement interval of 1 foot for each treatment subplot. Data for pH were measured to a depth of 1 foot with a measurement interval of 0.5 foot and are only available for October, 1991. The soil nitrate and soil pH data are shown in Table 2.5.4 and Table 2.5.5, respectively. The values reported for soil nitrate are arithmetic means of 6 to 9 soil samples. The time progression of soil nitrate through the soil profile from 1991 to 1995 for each subplot is illustrated in Figure 2.5.1a-e. Nitrogen concentration increases with time and depth as the nitrogen has an opportunity to transport through the soil. The peak concentration decreases due to N removal from the trees, possibly through denitrification, and perhaps lateral transport. The peak concentration depths for 100, 175, 250, and 325 lbs N/acre are 4, 6, 6, and 7 feet, respectively. Nitrogen concentration at the surface decreases from 1991 to 1995 because the 1991 measurement was taken shortly after a fertilizer application whereas the 1995 measurement was taken 5 months after any fertilizer application. The greater concentration at the surface for this subplot in 1991 may be explained by lateral flow from the surrounding treatment plots. That is, during times of fertilization there may have been some lateral flow. When fertilization ceased we see a decrease in the nitrate concentration at the surface of this plot. Additionally, the fertilizer application is not exact and some may have been inadvertently applied to the 0 lbs/ac plot. Also remember there is some nitrogen in the irrigation water and in precipitation. Soil pH increases with depth from an average of 6.75 in the upper 6 feet (Hanford fine sandy loam) to 7.19 at a depth of 40-50 feet. Differences in pH between fertilizer treatments are not significant.

From an agronomic perspective annual nitrogen losses (either to leaching below the root zone or to denitrification) can be estimated using a simple mass balance model for the root zone:

$$\text{net N losses} = \text{Fertilizer N} + \text{Irrigation water N} - \text{Harvest N}$$

This simple approach neglects N volatilization during plant material and root decay and ignores rainfall and evapotranspiration. Based on this equation, net N losses are estimated to be on the order of 0, 60 and 280 lbs N/acre for the 0, 100, and 325 lbs N/acre treatments. In the 0-treatment plot it is assumed that irrigation water supplied the bulk of the nitrogen, while large lateral roots into neighboring tree rows may have captured additional nitrogen. Approximately 90% of the root density is 10 ft in depth. In mature trees individual roots are expected to grow up to 20-30 feet horizontally. If all losses reach groundwater (assuming no denitrification), at an annual net water leaching rate of approximately 2 acre-ft/acre, the resulting concentration in the deep unsaturated zone leachate is approximately 0, 10, and 50 ppm for the three plots, respectively.

2.6 Bromide tracer experiment, October 2, 1996

Dr. Johnson's fertilization trial was completed in 1994. No fertilizer was applied in 1995. A single 75 lbs N/acre broadcast was applied to the entire orchard on September 12, 1996. On October 2, 1996 a simple tracer experiment was conducted to follow solute movement from the fertilization. The tracer experiment covered approximately one-fifth of the orchard including two of the three subplots that were later used for core drilling. Lab-grade potassium bromide solution was filled into a hand sprayer (backpack type) and sprayed in length wise passes across the entire area between tree-rows ("basin") from tree 14 to tree 10 until all solution was used. The only exception is the southernmost treatment basin, where the application is from tree 14 to tree 9. The treatment basins are between tree rows 8-9, 9-10, 10-11, and 11-12. Tree-rows are counted starting from the southernmost row, the tree number is counted starting from the westernmost tree in a tree-row. The bromide application rate averaged 13g/m². Prior to the bromide application, the orchard was mowed and rotovated to 6" depth. Following the application, the field was rotovated and irrigated.

2.7 Core sampling, 1997

During 1997, upon completion of the fertilizer experiment, three subplots (fertilized at the annual rate of 0, 100, 325 lb N/acre and referred to henceforth as subplots A, B, and C, respectively) were selected for detailed sampling and intensive data analysis (boxed areas in Figure 2.7.1). Approximately 3000 ft of geologic material were obtained from 62 continuous soil cores drilled to the water table (~ 52 feet). At each of the three subplots, 18-19 cores were collected. Spacing of the borehole locations varied from 4 to 10 feet in a transect that is approximately 300 ft long and 8 ft wide (Figure 2.7.1 and Figure 2.7.2). An additional north-south transect throughout the entire orchard, consisting of 6 cores spaced 40 feet apart, was sampled to obtain estimates of nitrate distribution at the scale of the entire orchard.

The drilling was implemented with the Geoprobe Systems® GH-40 direct push sampling device provided free of charge from the manufacturer. This method allows for more efficient field sampling and comparatively less disturbed sediment cores than auger drilling. The cores were obtained in hard plastic liners in segments of 1.2 m length with a

diameter of 4.0 cm. The sampler (Macrocore®) consists of a stainless steel cutting shoe attached to a 1.2 m long stainless steel cylinder with an equally long plastic tube that receives the core sample. The inner diameter of the plastic liner is 2 mm larger than the inner diameter of the cutting shoe to minimize compression inside the liner. Before lowering the sampler to the desired depth the cutting shoe was plugged with a removable tip to prevent slough accumulating at the bottom of the borehole from entering the sample. Upon reaching the top of the depth interval to be sampled, the tip was removed and the sample collected by pushing the sampler 1.2 m into undisturbed sediment. The sampler was then raised out of the borehole.

Following the extraction of the 1.2 m core, the 4 cm diameter core liner was laid out horizontally, cut lengthwise, and the upper half of the liner removed to expose the entire length of the core. Immediately, a complete sedimentologic description by color, texture and moisture was made on the continuous core. We determined major textural classes using USDA-SCS 1994 Field Estimation, sediment color based on the Munsell Color Chart, and grain-size for sands and gravels. Major textural units identified within the predominantly horizontally stratified transect span a wide range from finely cross-bedded clayey silts to paleosols, hardpans, and uniform medium sand. Major identifiable stratigraphic units vary in thickness from a few centimeters to several meters across the transect.

Based on the sedimentologic description, (disturbed) samples were collected approximately every 2 – 3 feet. A total of 1,200 samples were collected. Samples consisted of 22.5 cm length of core, collected from as many identifiable sedimentologic strata or sub-strata as possible.

Each 22.5 cm sample was subdivided into sections for various analysis:

- Nitrate analysis: a 5 cm sample section
- Water content: a 1.25 cm sample section
- pH analysis: a 1.25 cm sample section
- Isotope and other chemical analysis: a 15 cm section

In approximately one third of the boreholes, a slightly different sampling protocol was applied to also collect undisturbed core samples for the analysis of soil hydraulic properties. In those boreholes, the sampling protocol for all samples was as follows:

Prior to cutting the core, sampling locations were determined from visual inspection of the core through the clear plastic liner. At each sampling location in the core, a 10 cm lined section was cut and sealed with caps on each end (black cap at the bottom, red cap at the top). The remaining core was then sliced open lengthwise. Sub-samples were collected from the core sampling locations in the following sequence:

- pH analysis: a 1.25 cm sample section
- (soil hydraulic analysis: a 10 cm undisturbed core taken prior to taking disturbed samples)
- Water content: a 1.25 cm sample section
- Nitrate analysis: a 5 cm sample section

- Isotope and other chemical analysis: a 5 cm section

All disturbed soil samples were collected with a clean knife and spoon (rinsed with clean water in between different units) and stored in zip-blocs, envelopes and containers:

- Water content samples are put in tin boxes (21 grams) and immediately weighed. Samples were then oven-dried at 105 degrees Celsius for 2-3 days and weighed again for gravimetric determination of moisture content (Klute, 1986).
- pH samples: approximately 20 g are collected into a paper envelope and air-dried. Soil pH was later measured with KCl electrometric method using 10g of air-dry soil (see standard soil pH measurement, SSSA Book, Part 3, p. 487).
- Chemical analysis samples are collected into zip-lock bags and stored in ice-chests until the end of the field day

After every field day, soil samples for nitrate and hydraulic properties were moved to cold storage at -1°C . Soil samples for isotope and other chemical analysis were moved to a freezer (-10°C to -20°C).

Sample Numbering System: Soil cores are numbered in reference to the trees. The set of 6 cores to the east of a tree are associated with that tree. Soil cores are numbered with the tree column number first, then the row number, then the soil sample location (1-6). For example, the soil sample shown in Figure 2.7.3 is numbered 11-10-4. A fourth number, in reference to the 2.5 ft interval sub-sample is tagged on to the core number (increasing number with depth).

3. LABORATORY METHODS

3.1 Hydraulic characterization: Multi-step outflow experiment

In 19 of the 62 cores, samples were collected for hydraulic characterization (Figure 3.1.1). Hydraulic characterization was performed on 120 undisturbed core samples from those 19 core locations. Hydraulic characterization included determination of soil moisture content at the time of sampling (see above), determination of the saturated hydraulic conductivity, determination of grain size distribution, and measurement of the dependence between unsaturated hydraulic conductivity, moisture content, and soil water pressure. Additional measurements include bulk density and sand, silt, and clay fractions.

Saturated hydraulic conductivity was measured using the constant head method (Klute, 1986). The UC Agriculture and Natural Resources laboratory determined soil texture based on the percentages by weight of sand, silt, and clay (hydrometer method, ASTM, 1985). Bulk density was obtained gravimetrically from the undisturbed cores.

The soil-water retention and unsaturated hydraulic conductivity relations are basic elements necessary for the simulation and prediction of flow and transport in the vadose zone. We use the multi-step outflow (MSO) technique (Eching and Hopmans, 1993) to determine these relationships. The principle of the multistep outflow technique is to observe water outflow from and soil water suction changes in an initially saturated soil

core sample at increasing steps of dryness. The method has two components: implementation of a laboratory experiment, and computer analysis of the laboratory experiment to determine the hydraulic parameters of unsaturated hydraulic conductivity function and of the soil water retention curve.

For the laboratory experiment, a saturated sample is placed into a specially developed pressure/suction chamber (Tempe cell) at atmospheric pressure conditions. During the experiment, air pressure is increased in several discrete steps over the course of several days (typical for sands) to several weeks (typical for clays). Each step-wise increase in air-pressure forces water to flow out of the soil core sample until soil water suction in the pores matches the applied air pressure. Using high-precision instrumentation, we monitor how quickly the soil pressure inside the core changes in response to each pressure step and we monitor the outflow rate from the core over time. The core is instrumented with a tensiometer at the center of the core measuring the soil water suction. A burette connected to the core captures the outflow. Soil pressure and outflow are recorded automatically with these sensors and the data are sent to a computer. After completion of each experiment, the measurement data are cleaned up and converted into meaningful units using laboratory-derived calibration curves.

For this project, the original multistep outflow technique was modified to accept the 1.7" Geoprobe Macrocore[®] core samples such that they fit tightly inside the Tempe cell. The semi-permeable membrane on the outflow side of the Tempe cell was modified from a 1 bar ceramic plate to a 2 micron nylon filter. Various changes in the pressure and outflow tubing design have been made to allow for faster and safer connections, simplified trouble-shooting, and superior system testing. Special attention had to be paid to the development of air-bubbles in the outflow tubing to avoid erroneous measurements. A standard protocol has been developed and tested for the uniform handling of all core samples in each texture class (Tuli and Denton, 2001; Appendix 1).

To streamline the implementation of the multi-step laboratory experiments, the samples were arranged into 12 sets (or Runs) of 10 samples (or cells) per set resulting in 120 samples. The samples were identified using the naming convention described at the end of Section 2.7 and can also be identified by the run and cell number. The implementation of a single set of ten parallel laboratory multi-step experiments typically took 3-6 weeks including set-up and take-down, depending on the texture of the samples. Coarse textured samples are typically faster to run than fine textured samples due to their faster response to pressure changes. The multi-step outflow experiments were successfully completed for 118 undisturbed cores representing 9 major textural classes identified in the field cores: sand, loamy sand, sandy loam and silty loam to sandy loam, Hanford fine sandy loam (surface soil), loam, clay loam, clay, hardpan, deep paleosol. Due to a variety of experimental complications and errors, the multi-step outflow data were for 21 soil cores were unusable resulting in 97 viable samples for the inverse modeling process.

3.2 Hydraulic characterization- inverse modeling

To compute the hydraulic properties of the soil core, the multi-step outflow experiment is emulated in computer simulations. The hydraulic parameters of the computer model are adjusted until results from the computer simulation match the measurements from the outflow experiment. This process is referred to as “inverse modeling”, “parameter estimation” or “optimization”. The end product of the inverse modeling is a set of hydraulic parameters for the soil water retention and unsaturated hydraulic conductivity functions that can then be used to describe flow beneath the orchard. The computer model solves the one-dimensional Richards equation of unsaturated flow. In its one-dimensional form with the vertical coordinate, $z(L)$, taken positive upward Richard’s equation is written as:

$$C(h) \frac{\partial h}{\partial t} = \frac{\partial}{\partial z} \left[K(h) \left(\frac{\partial h}{\partial z} + 1 \right) \right]$$

where $C = d\theta/dh$ is the water capacity (L^{-1}), h is soil matric head (L), K is unsaturated hydraulic conductivity (LT^{-1}), and t denotes time (T).

An existing finite element code, SFOPT, has been adopted to simultaneously optimize the soil-water retention, $\theta(h)$, and unsaturated hydraulic conductivity, $K(\theta)$, parameters given our particular experimental setup. Several models have been developed that describe $\theta(h)$ and $K(\theta)$. We chose to use the soil water retention function proposed by van Genuchten (1980):

$$S_e = \left[1 + |\alpha h|^n \right]^{-m} \quad [1]$$

with

$$S_e = \frac{\theta(h) - \theta_r}{\theta_s - \theta_r}$$

and $m = 1 - 1/n$, where S_e is called effective water saturation ($0 \leq S_e \leq 1$), θ_s and θ_r are the saturated and residual water content (L^3 and L^{-3}), respectively, and α (L^{-1}) and n are empirical parameters. Substituting Eq. [1] in the capillary model of Mualem (1976), van Genuchten (1980) derived the following unsaturated hydraulic conductivity model:

$$K(h) = K_s S_e^l \left[1 - \left(1 - S_e^{1/m} \right)^m \right]^2$$

The parameters K_s and l denote saturated hydraulic conductivity (LT^{-1}) and tortuosity/connectivity coefficient, respectively. S_e and m are the same parameters as used in Eq. [1]. From the analysis of a variety of soils, Mualem (1976) proposed a value for $l = 0.5$, although l can be considered as another fitting parameter as well (Hopmans et al., 1994; Hopmans et al., 2002).

Other models describing these relationships that could be applied to interpret the experimental data are the lognormal model derived by Kosugi (1994) and the typical algebraic equations proposed by Brooks and Corey (1964), Gardner (1958), and Haverkamp and others (1977). The parameters necessary to mathematically describe the measured hydraulic conductivity and soil moisture retention curves are simultaneously determined in the computer model with an optimization algorithm using the Levenberg-Marquardt method. The inverse method is an iterative process that uses an initial guess for the parameters as a starting point. We repeat the optimization process with different initial guesses to ensure that the parameter estimates obtained from the computer model can be trusted (combined manual-automatic calibration).

Among the 97 samples, transient data were unavailable for all the samples in Runs 7 and 8 (20 samples). Due to transducer failure seven samples in Run 4 also had unusable transient data. The total number is now reduced to 71 samples. For the 27 samples with missing transient data there exists handwritten data for the equilibrium conditions between pressure steps during the outflow experiment. One sample in Run 10 (Cell 1 or 4-10-5 #13) did not converge using SF-OPT thus reducing the number of samples with transient data that will be considered in the remaining analyses (for example, scaling) to 70. Implementation of the inverse modeling for these 27 samples and the remaining 70 samples with transient data is described in detail in Chapter 6 in Tuli and Denton (2001) (Appendix 1).

The consequence of having a collection of samples with transient data and another with only equilibrium data is that the samples must be categorized into populations according to the information available for each sample. Those categorizations affect both the parameter estimation and the scaling as will be discussed below and in Section 4.3 and Section 4.5.

3.3 Scaling

Scaling is a technique used to simplify the analysis of hydraulic parameter datasets in heterogeneous unsaturated sediments. Scaling is based on the concept that the various hydraulic parameters, e.g., K_s , α , n , θ_s , θ_r , are all related to the pore size distribution and pore geometry. Heterogeneity of sediments or soils is reflected in the heterogeneity of pore geometry and pore size. Coarse soils have large pores, while heavy, fine-grained soils or soils with a high content of fines have very small pores. As the pore geometry varies with the type of sediment, the various hydraulic parameters vary accordingly. The scaling factor is a measure of that change in pore geometry and relates the actual hydraulic function derived for a sample to the scaled hydraulic function. The variability of the hydraulic parameters can, with some limitations, be directly related to the variability of the scaling factor and vice versa. The scaling method is based on the similar media theory introduced by Miller and Miller (1956) which assumes that the structure of pore spaces is geometrically similar among different locations. That is, similar media differ only in the scale of their geometry. An existing model, SCALE, was used to scale the hydraulic data (Clausnitzer, 1990). There are several options in the program including (A) to scale either water retention or (B) hydraulic conductivity data only; (C)

simultaneous scaling of soil water pressure head, h , and the natural logarithm of hydraulic conductivity K ; and (D) simultaneous scaling of the logarithm of both h and K .

The soil water retention and unsaturated hydraulic conductivity curves obtained for the 97 samples (70 with transient data and 27 with equilibrium data) were scaled simultaneously using methods C and D. The scaling yields a single set of scale factors, λ , thus simplifying the description of heterogeneity from a set of multi-variate probability functions (K_s , α , n , θ_s , θ_r) to a single-variable probability function for λ that relates to a reference soil. That is, scale factors, λ , are conversion factors relating the characteristics of a system to those of another system. In the case of soil hydraulic parameters the scale factors relate the multi-variate functions of soil water retention and unsaturated hydraulic conductivity to a reference soil via a single factor. Take, for instance, a group of 10 soils whose hydraulic functions are to be scaled. The result would be 10 scale factors relating the original functions to one reference soil. The reference soil's hydraulic parameters are determined via the SCALE program using Powell's optimization (Powell, 1964) method in combination with a Newton-Raphson iterative procedure.

In our case there are 97 samples representing many texture classes and stratigraphic units. The samples were grouped in four ways:

- Group 1.** Soils scaled all together. No a priori knowledge, such as texture, was used.
- Group 2.** Scaled within individual sub-groups, where sub-groups represent texture classes (USDA soil triangle) as determined in sieve analyses obtained by the DANR lab, without regard to the specific facies that the samples belonged to.
- Group 3.** Scaled within individual sub-groups, where sub-groups represent field determined texture classes (visual determination), but without regard to facies location.
- Group 4.** Scaled samples within individual sub-groups, where each sub-group is associated with a specific facies location (primarily texture-driven). See Figure 4.1.1.

Each group, except group 1, is a collection of subgroups. The subgroups for Group 2 are loamy sand, sand, sandy loam, silt loam, and silt. The subgroups for Group 3 are clay, hardpan, loam, loamy sand, paleosol, sand, sandy loam, silt loam, and Hanford sandy loam. The subgroups for Group 4 are sand, sandy loam (sL), silt/silt loam/loam/silty clay loam (CSiL), hardpan (HP1), paleosol (HP2), and two facies named "var1" and "var2" that contain various sedimentary structures within the unit but are distinguishable as a facies separate from the adjacent facies. Each soil sample was assigned to one of the subgroups of scaling groups 2-4 (group 1 has no subgroups). For example, sample 5-10-2 #20 is a sand in group 2, a loamy sand in group 3, and a sandy loam in group 4. Sometimes the subgroup designation is the same for all groups as is the case for sample 10-10-2 #8 (sand).

Additionally, each sample's data set was determined to be of good or poor quality. The samples were assigned to two populations according to the data quality for that sample.

Data quality is defined as follows: 1) if transient data exist the quality is considered to be good, 2) if only equilibrium data exist then the quality is considered to be poor. The first population consists of a mixture of good and poor quality data sets (97 soil samples) and will be referred to as Population 1. The second population contains only good quality data sets (70 soil samples) and will be referred to as Population 2. The subgroup designations and data quality for each sample are shown in Table 3.3.1 where a “1” indicates a transient data set and a “0” indicates an equilibrium data set only.

Each population is scaled with two methods. Method 1 simultaneously scales soil-water pressure, h , and the log of unsaturated hydraulic conductivity, $\ln K$. Method two simultaneously scales $\ln h$ and $\ln K$. The results are presented in Section 4.5. Soil water retention curves were scaled over 11 equally spaced pressure increments (0, 50, ..., 500 cm) with the exception of the sands which were scaled over 16 steps (0, 10, ..., 150 cm). Hydraulic conductivity curves were scaled at degree of saturation (S) values corresponding to these same pressure increments. The values for these curves were calculated using the van Genuchten functions and the associated van Genuchten parameters obtained for individual samples from the inverse modeling of the multi-step outflow experiment. The optimized saturated hydraulic conductivity was used for the 70 soil samples in the “good quality” group and the measured saturated hydraulic conductivity was used for the 27 soil samples in the “poor quality” group.

4. RESULTS

4.1 Geologic Framework

The site is located on the Kings River alluvial fan, approximately 2 miles west of the current river channel. The alluvial unconsolidated sediments are derived exclusively from the hard, crystalline Sierran bedrock. They appear as intercalated, thick and thin lenses of clay, silt, sand, and gravel. The deposits contain fairly well sorted subangular to subrounded sand and gravel, and intercalated lenses of silt, sand and gravel with some lenses of clay, showing a downstream decrease in grain-size (Page and LeBlanc, 1969).

The material obtained in the borehole cores is exclusively composed of unconsolidated sediments. The top section of the core material is a recent soil (Hanford fine sandy loam). The sediments can be classified into textural groups ranging in grain-size from clay to pebble and cover a wide spectrum of silty and sandy sediments in between. The colors of the sediments range from grayish brown to yellowish brown, more randomly to strong brown (no significant reduction zones). The thickness of the beds varies from less than 1 cm for clayey material to more than 2.5 m for sandy deposits. Both, sharp and gradual vertical transitions are present between texturally different units. Five textural units are found the cores: 1) sand, 2) sandy loam, 3) silt loam/loam, 4) silt/clay loam/clayey silt/clay, 5) paleosol. The relative occurrence of each category in percent of the vertical profile length (in 5 cm sections) are 17.2% sand, 47.8% sandy loam, 13.8% silt loam/loam, 8.3% clay loam/clay and 12.9% paleosol.

The sand is quartz-rich, contains feldspar, muscovite, biotite, hornblende and lithic fragments consistent with the granitic Sierran source. Cross-bedding at the scale of few cm could be observed occasionally within fine-grained sand, showing reddish-brown layers intercalated with gray-brown ones. The dominant color of the sand is a light gray to light brown, the brown hue increasing with increasing loam content. The thickness of the sand beds is as much as 2.5 m and is dependent on the location of the core relative to the course of an ancient secondary distributary channel in which the sediments deposited. The channel appears to have a northeast-southwest orientation, diagonally through the orchard site. The mean thickness is 1.7 m. Very coarse sand and particles up to pebble grain-size (up to 1 cm) could be observed occasionally at the bottom of sand units, but were not present in all the cores. These are probably channel lag deposits and were laid down in deeper parts of the channels.

Sandy loam is the most frequent category within the profile. The color is usually light olive to yellowish brown. Some of the sandy loam sediments are considered to be weakly developed paleosols because of their stronger brownish color, root traces and presence of aggregates. Mean bed thickness is 50 cm. Individual beds can be as much as 2 m thick. The sorting is moderate to good. Clay flasers and thin (0.5-1 cm) clay layers occasionally occur in sandy loam units. Sandy loam sediments are assumed to have developed at the edge of channels, as levee or as proximal floodplain deposits near the channels.

Silt loam, loam and silty clay loam are usually slight olive brown to brownish gray in color. The bed thickness is within a scale of a few cm to dm. Fine grained sediments often show sharp contacts between the units. Changes from one unit to the next exist on small distances. Cross-bedding can more frequently be observed within silty sediments than in fine sands. Root traces and rusty brown colored spots are quite common. The depositional environment was presumably the proximal to distal floodplain of the alluvial fan, an area dissected by distributary branched braided streams.

The finest sediments are grouped in the 4th category: Silt, clay and clay loam. These are believed to have been deposited in the distal floodplain and in ponds that developed in abandoned channels. The main color is brownish gray to olive brown. Fine, less than 1 mm thick root traces and rusty brown spots are quite frequent also in the clay sediments. Statistics for the thickness of clay layers in the unit between 8 and 13 m depth show a mean thickness of 12.8 cm, but the mode is about 3 cm. A thick clay bed even extends to 50 cm and is observed in most of the cores.

Paleosols could be recognized in different stages of maturity. They show a brown to strong brown, slightly reddish color, exhibit aggregates, ferric nodules and concretions, few calcareous nodules and hard, cemented layers. They also display a sharp upper and a gradual lower boundary as is typical for paleosols (Retallack, 1990). Clay content decreases downwards in the paleosols. Another feature is fine root traces. Paleosols formed in periods of stasis marked by non-erosion and non-deposition, during the interglacials. Thickness of the paleosol horizons ranges from 50 cm to about 2 m.

Several thicker units are recognized throughout the orchard and are used to construct a large scale geologic framework for the research site (Figure 4.1.1). The deepest parts of the cores from 15.8 to 15 m display a strong brownish colored, partly clayey paleosol hardpan. This paleosol marks the top of the Turlock Lake II formation (see below). From a depth of 15 to 12 m below surface, the main textural units are sandy loam to fine sandy loam, occasionally coarse sand and gravel, and occasionally fine-grained sediments right on top of the paleosol. In the cores with fine sediment at the bottom of this unit a coarsening-upward, in the other cores a fining-upward cycle can be observed. The sediments show a remarkable wetness due to proximity to aquifer water table. The sediments are vertically and laterally quite heterogeneous with relatively thin bedding (thickness cm to dm) between about 12 and 8 m depth, consisting mainly of clayey, silty and loamy material. Another strong brownish paleosol can be distinguished at a depth of 9-10 m. Between 9 and 6 m below surface a sand layer is found with laterally varying thickness averaging 1.7 m. A weak, mostly eroded paleosol is developed on top of the sand unit. Up to about 4-3 m below surface, sandy loam with intercalated sand, clayey and silty material is found. Different trends of upward-fining and -coarsening are found on top of each other and laterally next to each other within this unit. A 0.2 m to more than 1 m thick paleosol hardpan occurs at a depth of about 4-3 m. This paleosol marks the top of the Modesto formation. Sandy loam and subordinated loamy sand and loam are present from the top of the hardpan to the surface. 2.5 m below surface a laterally continuous clay horizon with a thickness of few cm is found in most of the cores.

Stratigraphically, the Quaternary deposits in this part of the valley can be divided into four units (Marchand & Allwardt, 1981). The Turlock Lake, Riverbank and Modesto Formations are of Pleistocene age (which began 2 million years ago). The Post-Modesto Formation belongs to the Holocene (which began 10,000 years ago). Most of the stratigraphic units found at the site are believed to represent separate alluvial episodes related to Sierran glaciations. The deposits are likely related to flood events that predominantly occurred during the end of a glaciation period. Paleosols, on the other hand, are indicative of substantial time intervals (several thousands to tens of thousands of years) between periods of aggradation (Marchand & Allwardt, 1981) and represent stratigraphic sequence boundaries. Paleosols are buried soil horizons that were formed on stable upper-fan, terrace or hillslope surfaces during interglacial periods (Lettis, 1982). At the site, they consist of strongly cemented sand to sandy loam with a characteristic reddish-brown color. Cementation is primarily by Fe-oxide and Mn-oxide, but also from calcification. They result from initial stratification or drainage boundaries in soil parent material (Harden & Marchand, 1977). Soils that formed on top of the upper Turlock Lake Formation are estimated to be 600 Ka (1Ka = 1000 years) old (Harden, 1987). The estimated age of the Riverbank formation is 130-450 Ka. The Modesto Formation corresponds to the most recent glaciation period (Huntington, 1980).

4.2 Laboratory Measurements

Table 4.2.1 summarizes the Division of Agriculture and Natural Resources analytical laboratory (DANR) results which include:

- sand, silt, and clay fractions,
- saturated hydraulic conductivity (K_s),
- bulk density,
- saturated water content (θ_s),
- porosity,
- percent organic matter,
- percent organic carbon.

The USDA texture classification for each soil sample is also included in Table 4.2.1. In contrast to the field texture identification, this classification is referred to as “DANR texture”. The results are organized by the run and cell number associated with the multi-step outflow sets. The core ID and sample number are also included. Hard copies of the results are in the green laboratory folders compiled by Jim MacIntyre and can be obtained from Thomas Harter. Additional measurements performed on the MSO and other samples (including, but not limited to, nitrate concentration, dry and wet soil weight, depth, field water content, and pH) are tabulated in a master database. The master database is too large to include in this report but may be obtained in electronic format from Thomas Harter.

Table 4.2.2 shows a summary of the basic statistics for the 118 MSO soil samples 1) as a whole and, 2) grouped according to the DANR texture. Notice that any missing data, as explained in Section 3.2, are reflected in the first column of the table (Valid N). For example, recall that 6 samples did not have measured K_s values. This can be seen in the “All” category in which there are 118 soil samples for each measurement except K_s which has 112.

Figure 4.2.1a-i shows the histograms for each of the 9 lab measurements for the soils grouped as a whole. The bulk density is fairly uniformly distributed with about 97% of the samples having a bulk density between 1.4 and 1.9 g/cm³ (Figure 4.2.1a). The organic matter and organic carbon are both nearly normally distributed with an average value of 0.094% and 0.054%, respectively (Figures 4.2.1b-c). About 91% of the samples have a saturated water content between 0.2 and 0.4 (Figure 4.2.1h). There is much more variability in the sand and silt content than in the clay content (Table 4.2.2). Overall, the soils have a surprisingly high sand content, much higher than silt or clay content. In fact, over 75% of the samples have a sand content greater than 60% (Figure 4.2.1d). Each of the grain size fractions has a skewed distribution (Figures 4.2.1d-f). About 84% of the samples have a measured saturated hydraulic conductivity less than 10 cm/hr. (Figure 4.2.1i). This is to be expected as K_s is generally log-normally distributed. The geometric mean of K_s is 0.712 cm/hr.

The box and whisker plots in Figures 4.2.1a-b to Figure 4.2.10a-b show the nine lab measurements categorized by DANR texture. Each measurement has two box and whisker plots, one showing the mean, standard deviation, and twice the standard deviation and the other showing the minimum, maximum, and lower and upper quartiles. The graphs for the silt texture show a single point and no box or whiskers because this

texture consists of only one sample. The arithmetic mean is used for all measurements except for K_s for which we use the geometric mean.

The loam has the least amount of variability in bulk density, while the loamy sand and silt loam have the most variability (Figure 4.2.2a-b). Organic matter content is very low in all samples. Sand has the least amount of organic matter and organic carbon at 0.06% and 0.03%, respectively. Loam, sandy loam, and silt loam have approximately the same amount of organic matter and organic carbon at about 0.11% and 0.063%, respectively. The loamy sand has slightly less organic matter and organic carbon at 0.09% and 0.05%, respectively (Figure 4.2.3a-b and Figure 4.2.4a-b). The silt loam, some of which could be loess deposits, has the greatest porosity and saturated water content while the loam has the least amount of spread in these two parameters (Figure 4.2.5a-b and Figure 4.2.6a-b). The amount of sand, silt, and clay in each texture is straight forward as the designation of each sample to a texture is directly based upon these fractions (Figures 4.2.7a-b, 4.2.8, and 4.2.9a-b). The sand has the most variability in the saturated hydraulic conductivity while the loam has the least (Figure 4.2.10a). Loamy sand, sandy loam, and silt loam have similar geometric mean K_s at 0.636, 0.325, and 0.289 cm/hr, respectively (Table 4.2.2).

4.3 Multi-step Outflow Experiment and Parameter Estimation

The experimental data obtained from the multi-step outflow experiment for one sample are shown in Figure 4.3.1a-b. The sample shown is one with transient data. Figure 4.3.1a displays the transient pressure head and Figure 4.3.1b displays the transient water outflow. The measured values are shown (as blue dots) along with the optimized curves resulting from the low, medium, and high initial guesses.

Figure 4.3.2 shows the results for a sample having only handwritten equilibrium points (pressure head vs. water content). Notice that there may be some data points at the same pressure with different water content values especially at the higher pressure heads. This is because the experimenter continued to make measurements until it was certain that the sample had reached equilibrium.

The van Genuchten parameters obtained either through optimization of the transient data with SFOPT or optimization of the steady-state data points with a spreadsheet function (MS Excel) are summarized in Table 4.3.1. The bold numbers are the chosen results that have been considered to be the best parameter fits and were chosen for further statistical analysis and scaling ("final parameter set"). The final parameter set was selected specifically by comparing the mass balance error (%mbe) of the computed flow simulation and the sum of the squared residual (ssq) of measured vs. simulated data. There are blanks for some of the samples for K_s because these samples do not have transient data and therefore do not have an optimized K_s value. These samples also do not have a value for %mbe because the Excel solver does not calculate that value. In some cases, a particular guess did not converge and these are denoted with an "n/a" entry.

The basic statistics for the chosen van Genuchten parameters for the 97 soil samples grouped 1) grouped as a whole and 2) grouped according to the texture, are in Table 4.3.2. Notice that there are 70 values for K_s , because optimized K_s values exist for only 70 samples. All the texture groups will have fewer K_s samples than α , n , and θ_r samples. Notice that the number of samples in the loam category has been reduced from 4 to 2. That is because Run 6 Cell 4 and Run 10 Cell 1 (both loams) were removed because of SF-OPT convergence problems.

Figure 4.3.3a-d shows the histograms for the van Genuchten (optimized) K_s , α , n , and θ_r for the 97 samples. K_s is log-normally distributed with 84% of the samples having an optimized K_s less than 20 cm/hr. The maximum and minimum optimized K_s are 99.5 cm/hr (associated with a sand sample) and 0.0077 cm/hr (associated with a silt loam), respectively. The remaining 3 parameters (α , n , and θ_r) all appear to be log-normally distributed.

Figure 4.3.4a-h shows categorized box and whisker plots for the van Genuchten parameters. Notice there is not a K_s box and whisker plot for the loam texture since there are no optimized K_s values for the loam. Also, the box and whisker plots for the loam texture showing the minimum and maximum, interquartiles, and median have no whiskers because there are only 2 loam samples. The sand has the highest mean and greatest amount of variation in K_s , α , and n but has the least amount of variation in θ_r .

4.4 Generating Pedotransfer Functions: NeuroMultistep

The extensive database generated from the nearly one-hundred multi-step outflow experiments constitutes a unique opportunity to fine-tune pedotransfer functions for the type of unsaturated sediment conditions typically encountered in the eastern San Joaquin Valley. "Pedotransfer function" refers to any kind of tool that allows a user to determine the unsaturated hydraulic conductivity and water retention functions and their parameters (which are time-consuming and expensive to measure) from inexpensive, quickly measurable soil properties. Common pedotransfer function tools estimate unsaturated (soil) hydraulic properties from information about the sand, silt, and clay content of a sample. In addition, saturated water content and bulk density, which can also be measured inexpensively, are sometimes used as input. A popular pedotransfer function tool is Rosetta (Schaap et al., 2001). Rosetta can be obtained for free from the internet (<http://www.usssl.ars.usda.gov/models>). The user provides the textural analysis (% sand, % silt, % clay) and, optionally, bulk density and saturated water content. With this input (entered through a Microsoft Windows interface), the software tool estimates the unsaturated hydraulic functions. These estimates are not accurate measurements and are provided with a confidence interval.

Pedotransfer function tools are based on a sophisticated regression-like analysis of extensive soil hydraulic property databases, that contain information from hundreds of soil samples from often dozens of sites where both, textural data and hydraulic properties have been determined. The drawback of these databases is that they combine data from

many different sites, measured by many different methods. Few have considered unsaturated hydraulic properties below the root zone.

Our multi-step outflow experiments completed a series of three multi-year projects in Dr. Hopmans unsaturated zone hydraulics laboratory, each of which examined extensive collections of soil samples from three different locations in the Central Valley: In addition to our Eastern San Joaquin Valley site, these projects investigated soils (limited to within the root zone) in Yolo County (fine-grained, relatively heavy soils), and in the western San Joaquin Valley (wide range of textures, well drained uniform soil profiles).

We used a regression-like technique, known as neural network analysis, to generate pedotransfer functions from these three datasets that are specifically useful for unsaturated sediments and soils in the Central Valley or locations with similar alluvial sediments and soils. Using the dataset described in the previous section, we developed a pedotransfer function tool that is based on our Central Valley specific dataset (“training dataset”) obtained under identical measurement protocols. We find that the resulting tool predicts unsaturated hydraulic properties for Central Valley soils with significantly higher accuracy than Rosetta due to the consistency of the measurement method with which the training dataset was obtained. Prediction errors for water content, for example, are approximately 3% to 4%. The pedotransfer function software, called *NeuroMultistep*, is available for free from Dr. Jan Hopmans (jwhopmans@ucdavis.edu) or at <http://www.agric.usyd.edu.au/acpa>. See Appendix 2 for detailed information on the neural network analysis and pedotransfer functions.

4.5 Scaling

Recall from Section 3.3 that the samples were assembled into 4 groups:

- Group 1.** Soils scaled all together. No a priori knowledge, such as texture, was used.
- Group 2.** Scaled within individual sub-groups, where sub-groups represent texture classes (USDA soil triangle) as determined in sieve analyses obtained by the DANR lab, without regard to the specific facies that the samples belonged to.
- Group 3.** Scaled within individual sub-groups, where sub-groups represent field determined texture classes (visual determination), but without regard to facies location.
- Group 4.** Scaled samples within individual sub-groups, where each sub-group is associated with a specific facies location (primarily texture-driven). See Figure 4.1.1.

Also recall from Section 3.3 that for each scaling group there are two populations. The first population consists of a mixture of good and poor quality data sets (97 soil samples) and will be referred to as Population 1. The second population contains only good quality data sets (70 soil samples) and will be referred to as Population 2. Each population is scaled with two methods. Method 1 simultaneously scales soil-water pressure, h , and the natural logarithm of hydraulic conductivity, $\ln K$. Method two simultaneously scales $\ln h$

and $\ln K$. Each group, except group 1, has a series of subgroups. For each subgroup there are 5 graphs for pressure head and 5 graphs for unsaturated hydraulic conductivity:

- the original data are graphed with the Powell curve (initial guess curve),
- the scaled values and scaled mean curve using pressure head and the log of the conductivity (method 1),
- the scaled values and scaled mean curve using the log of pressure head and the log of the conductivity (method 2),
- a comparison of the original data and de-scaled data for method 1
- a comparison of the original data and de-scaled data for method 2

In the following figures the two solid curves represent the best fit through the unscaled data and the optimized scaled mean curves. The open triangles represent the unscaled data, the open diamonds represent the scaled data using Method 1, and the open squares represent the scaled data using Method 2. The closed diamonds and the closed squares on the 1:1 graphs represent Method 1 and Method 2, respectively. The correlation between the original data and the estimated or de-scaled values (1:1 graph) is an indicator of the degree of success of the scaling procedure. The estimates are calculated by multiplying the mean curve by the appropriate scale factor. The percent reduction in the sum of the squares (SS) is another indicator for the degree of success of the scaling procedure.

Figure 4.5.1a-j shows scaled and unscaled soil-water pressure and unsaturated hydraulic conductivity curves and the 1:1 curves for Group 1 Population 1 using both scaling methods. Both the retention and conductivity curves span a large range of values making it clear that this group contains soil samples that do not have similar flow properties. As seen in the scaled and 1:1 curves for h , method 2 yields better results in scaling h while the scaled curve and 1:1 curves for $\ln k$ show that method 1 yields better results for $\ln K$. In the 1:1 curves for h some values stray significantly from the 1:1 line. These values are primarily associated with sands. The percent reductions in SS (the individual sum of squares reduction for h and $\ln K$ are not considered) for method 1 and method 2 are 93% and 66.4%, respectively, indicating that method 1 yields superior results than method 2.

Figure 4.5.2a-j shows scaled and unscaled soil-water pressure and unsaturated hydraulic conductivity curves and the 1:1 curves for Group 1 Population 2 using both scaling methods. As before, it appears that method 2 yields better results for h and method 1 yields better results for $\ln K$. The SS reduction for method 1 is 90.2% and for method 2 it is 62.4%. Again, overall method 1 yields better results than method 2.

To evaluate groups 2-4 the percent reduction in SS for the sandy loam subgroup, appearing in all three groups, was compared. In Group 2 the sandy loam subgroup has 39 samples, in Group 3 the sandy loam subgroup has 20 samples, and in Group 4 the sandy loam subgroup has only 4 samples. Refer to Table 3.3.1 to recall the subgroup designations.

Figure 4.5.3a-j shows scaled and unscaled soil-water pressure and unsaturated hydraulic conductivity curves and the 1:1 curves for Group 2 Population 1. Figure 4.5.4a-j shows

scaled and unscaled soil-water pressure and unsaturated hydraulic conductivity curves and the 1:1 curves for Group 3 Population 1. Figure 4.5.5a-j shows scaled and unscaled soil-water pressure and unsaturated hydraulic conductivity curves and the 1:1 curves for Group 4 Population 1. Table 4.5.1 summarizes the SS percent reduction using both scaling methods for the sandy loam subgroup. Method 1 appears to be the superior method for scaling these data sets. The greatest reduction in SS is in group 4 which is the group that uses facies information along with location information. This leads one to ask whether *a priori* knowledge of facies will aid us in scaling the other subgroups. To answer this question a complete statistical analysis will be performed and presented in Michelle Denton's thesis (*in progress*).

5. DISCUSSION AND CONCLUSIONS

The geologic analysis reveals a significant amount of textural and structural variability throughout the thick unsaturated zone at the site. In the cores, sub-facies structures have been identified at the millimeter, centimeter, and decimeter scale, particularly in the finer-grained sedimentary facies units. More uniformity is observed in the thicker coarse grained sand facies. Several major geologic units (facies) have been identified at the site, some with significant textural contrasts to their neighboring facies, some with gradual transition into the adjacent facies. Within all of the major facies, the smaller scale variability has been thought to contribute significantly to the overall geologic and hydrologic variability within the unsaturated zone.

Hence, when analyzing the observed hydraulic characteristics of the sediments at the site, we must distinguish between two major scales of variability: the variability between the major sedimentologic facies, and the much smaller-scale variability within individual sedimentologic facies identified at the site.

We note that the major sedimentologic facies are horizontally continuous layers throughout the field site, albeit of somewhat variable thickness. As Weissmann et al. points out, these facies themselves are variable, but at a scale that is much larger than our site. For example, if we repeated the same investigation several thousand feet away from the site, we would encounter a similar range of facies types, but their vertical assemblage or sequence, and their thickness would be significantly different.

On the other hand, we find little lateral continuity in the sub-facies structures observed in the continuous cores. These small scale geologic patterns vary not only over short vertical distances, but appear to also vary rapidly in the lateral direction. The lateral spacing of our cores (4 feet minimum distance) is mostly too large to map identifiable sub-facies units across two or more boreholes. Their lateral continuity is therefore limited to generally much less than 1m.

Are the two scales evident in the spatial variability of the hydraulic properties? The significance of this question relates to our ability to appropriately model the spatial heterogeneity of the unsaturated flow and transport processes. Indeed, the extensive

database of soil hydraulic properties, with more than ten samples from each major textural unit, strongly indicates that much hydraulic variability exists at the smaller, sub-facies scale. In fact, much of the overall variability of most soil properties (Table 4.2.2) and estimated hydraulic parameters (Table 4.3.2) and even of the scaling factor occurs at the sub-facies scale. The variance of the sub-facies grouped samples are not much smaller than the overall variance of soil properties found at the site (Table 4.2.2, 4.3.2). However, the difference in within-facies variability and total variability is significant, supporting the hypothesis that an identification of the major sedimentologic facies at a site may help identify a significant part of the hydraulic variability acting at the site. In particular, the grain size distribution, as expected, is significantly less variable within facies than in the total sample population.

We expect that similar properties and similar variability exists in facies with comparable textural classification. The statistical data shown in Table 4.2.2 and 4.3.2 are therefore transferable to other sites in the eastern San Joaquin Valley with similar facies textures, even if the facies assemblage or sequence is different.

The amount of spatial variability of the hydraulic properties (within facies and between facies) is tremendous: the variance of $\ln K_s$ exceeds 5, the coefficient of variation of α is greater than 1, that of n is approximately 50% (Table 4.2.2, 4.3.2). Theoretical work on the effects of such strong spatial variability for water and solute transport (Harter et al., 1996, 1998, 1999) suggests, that highly heterogeneous flow conditions are prevalent at the site with strong fingering or preferential flow paths channeling much of the water flow and solute transport through a relatively small portion of the unsaturated domain. This theoretical work suggests that infiltration and downward displacement velocities are log-normally distributed with high variance, which leads to highly variable distribution of nitrate. This is indeed consistent with the site conditions, where nitrate is found to vary over several orders of magnitude. On the other hand, we have found relatively uniform distribution of chloride and bromide (when compared to the variability of nitrate) in a few selected samples from the upper 15 feet (not reported above). The variability of chloride and bromide is comparable to that of the organic matter content, which varies within less than two orders of magnitude. The discrepancy in variability between nitrate and chloride (or bromide) should be explored further in future work.

Highly heterogeneous flow-paths, suggested by the variability of hydraulic properties and nitrate, are further enhanced by the strong fingering created by the infiltration and redistribution of water in the sandy loamy root zone at the site, as described in Wang et al., 2003. On the other hand, low permeability layers such as the hardpans and the fine grained facies below the channel deposits may counteract some of the flux variability; however those effects can only be quantified using explicit computer modeling based on the parameter distributions defined above (we are currently investigating these effects in a follow-up project).

The highly heterogeneous, log-normally distributed flow conditions that apparently dominate unsaturated flow at the site are considered to be representative for the flow patterns in most unsaturated zones in the Eastern San Joaquin Valley. Extrapolating the

field data based on our theoretical understanding of flow in such systems, we expect water flux to be as variable as or more variable than hydraulic conductivity. With that degree of heterogeneity in the flow pattern, flow in the unsaturated zone is essentially divided into two phases: much of the unsaturated zone is moist with almost stagnant water; a small fraction of the unsaturated zone – possibly less than one-fifth of its volume, is part of narrow, tortuous flow paths that are relatively wet and transmit the bulk of the recharge water and consequently, the bulk of nitrate.

From the analysis of the long-term annual water balance, we determined that the uniform mean vertical water displacement in and below the root zone in the orchard is approximately 10 feet per year. Under uniform flow conditions, it would therefore take nearly five years for nitrate and water to travel from the land surface to the water table (depth to water at our site is 52 feet). However, given the large variance in geologic, textural, and hydraulic properties, it can be shown that much of the nitrate mass that near the vadose zone surface is washed into preferential flow paths from where it is transported quickly out of the unsaturated zone, possibly within one to two years or even less. This would explain, at least partially, the relatively low amounts of total nitrogen found in the deep unsaturated zone.

These findings, if confirmed with our ongoing stochastic modeling project, have major implications for the interpretation of nitrate or other chemical distributions in the unsaturated zone: In estimating the net annual losses from core samples, one of the standard practices is to collect composite soil samples from the bottom of the root zone (usually 120 cm – 180 cm). Composite samples provide an arithmetic average nitrate concentration. They are interpreted using uniform flow conditions as the underlying conceptual model for estimating nitrogen losses. Based on the findings reported here, which suggest that preferential flow conditions may prevail in the root zone, but also throughout a thick unsaturated zone, we hypothesize that such a uniform flow based interpretation may significantly underestimate the nitrogen leaching rate.

Link to FREP program goals:

The project partially addresses three of FREP's priority areas, 'education and public information', 'fertilization practices', and 'site specific fertilizer technology'. All three program goals identify the relationship between fertilizer, fertilization practices/technology, and the environment as a research priority area. For a set of three fertilization practices in a tree fruit orchard, this project focused on providing the foundation for qualitatively and quantitatively defining the relationship between identifiable geology, hydraulic properties of the subsurface above the water table, fertilizer, fertilization practices/technology and nitrate loading to groundwater.

Overcoming Site-Specificity:

How can results from this particular research orchard be extrapolated to other sites? The particular conditions at the Kearney site are typical for the tree fruit orchard areas in much of Fresno and Tulare County east of Highway 41. The field research component helps built a much improved understanding of the general relationship between characteristics of geologic and soil heterogeneity in alluvial unsaturated sediments

(horizontal and vertical variability, range of layer thickness, contrast of soil textures encountered, degree of interbedding with clays, silty clays, and hardpan) and the overall characteristics of the fate and transport of nitrate in such sediments. With these data, we are able to develop and validate a new approach to model nitrate leaching in deep vadose zones, which is the second (and ongoing) research component of this project. It is the detailed site geologic and hydrologic characterization, combined with the improved understanding and nitrate transport modeling capability that will most benefit the assessment of nitrate leaching at other sites with thick vadose zones of alluvial sediments. To overcome site-specificity, we developed pedotransfer functions that allow users to compute unsaturated hydraulic properties from soil texture data. We also characterized the spatial variability found in typical alluvial fan deposits of the eastern San Joaquin Valley. The statistical properties of unsaturated hydraulic properties and their scale factors are tabulated as a function of typical facies groups. We believe that these are representative for such facies at other locations in the eastern San Joaquin Valley as well. Together, the pedotransfer functions and the scaling factor analysis provide a unique, site-independent database for soil physicists and others needing to characterize the hydraulic properties of the unsaturated zone from texture data or facies description of soil or sediment cores.

New Products Generated by Project:

- Large database of texture and facies specific geologic, texture, and hydrologic data;
- *NeuroMultistep*, a simple hands-on computer tool to predict hydraulic properties of soils from simple texture data;

Extension Activities related to this project:

- Harter, T., "Drilling in a tree orchard to assess nitrate leaching", 2 field tours to researchers, water district personnel, farmers, tree fruit industry, fertilizer industry representatives, 7/22/97; 7/25/97; 8/6/97; 9/17/97; 9/19/97; 9/30/98.
- Harter, T., "Understanding nitrate and pesticide contamination when locating water supply wells: spatial variability and long-term trends", California/Nevada American Water Works Association, Fall Conference, Los Angeles, 10/22/97.
- Harter, T., "Nitrate management and groundwater contamination: Walking on the razor's edge?", California Fertilizer Association Nutrient Seminar, Fresno, 10/8/98.
- Harter, T., "Groundwater resources management in the vineyard", UC Coop. Ext. San Luis Obispo County, Vineyard Water Management Shortcourse, Paso Robles, 5/11-13/99.
- Harter, T., "Drinking water source protection through nutrient management", FREP/SAREP Joint Annual Conference, Modesto, 11/30/99.
- Harter, T., "Nitrate distribution in a deep, alluvial unsaturated zone: Geologic control vs. fertilizer management", California chapter of the American Society of Agronomy (CASA) Annual Meeting, Fresno, 2/6/02.

- Harter, T., “Nitrate in the deep alluvial unsaturated zone: Linking agriculture with groundwater quality?”, Monterey County Water Resources Management Agency, Nitrate Technical Advisory Committee Meeting, 6/27/02.
- Harter, T., *Member*, Monterey County Nitrate Technical Advisory Committee, 1997-current.
- Harter, T., *Member*, Subcommittee on denitrification, USDA-NRCS Technical Committee for developing the Comprehensive Nutrient Management Plans for confined animal farming operations, 2002-current.
- Harter, T., *Member*, CALFED Panel on Appropriate Water Measurement in Agriculture, 2001-current.

Technical/Scientific Conference Presentations:

- Harter, T., “Flow and transport processes in the non-shallow vadose zone: Heterogeneity and uncertainty”, Dept. of Geological and Environmental Sciences, Stanford University, 2/25/98.
- Harter, T., “Field-scale transport of reactive contaminants in the vadose zone”, American Geophysical Union Fall Meeting, San Francisco, 12/7/98.
- Denton, M., T. Harter, J. W. Hopmans, W. R. Horwath, “Spatial variability of hydraulic properties in unsaturated alluvial sediments”, American Geophysical Union Fall Meeting, San Francisco, 12/19/00.
- Harter, T., Nonpoint source pollution from animal farming in Semi-arid regions: Spatio-temporal variability and groundwater monitoring strategies”, UNESCO Conference on Future Groundwater Resources at Risk, Lisbon, Portugal, 6/25/01
- Harter, T., “Stratigraphic control of nonpoint source pollution in alluvial aquifer systems”, Dept. of Civil Engineering, Universidad Polytechnica Barcelona, Spain, 7/3/01.
- Harter, T., “Stratigraphic control of nonpoint source pollution in alluvial aquifer systems”, Dept. of Environmental & Applied Geology, Tuebingen University, Germany, 7/10/01.
- Denton, M., T. Harter, J. W. Hopmans, W. R. Horwath, “Nitrogen transport in thick, unsaturated, spatially variable alluvial sediments”, American Geophysical Union, Fall Meeting, San Francisco, 12/15/01.

6. REFERENCES

- ASTM, Standard test method for particle-size analysis of soils, D 422-63, *1985 Annual Book of ASTM Standards, 04.08*, 117-127, American Society for Testing and Materials, Philadelphia, 1985.
- Brooks, R.H., and A.T. Corey, 1964. Hydraulic properties of porous media. Fort Collins, Colorado State University Hydrology Paper no. 3, 27 p.
- Chow, Ven Te, D.R. Maidment, and L.W. Mays, 1988. *Applied Hydrology*, McGraw-Hill, New York.
- Clausnitzer, V., J.W. Hopmans and D.R. Nielsen, 1992. Simultaneous scaling of soil water retention and hydraulic conductivity curves, *Water Resources Research*, 28: 19-31.
- Clausnitzer, V., J.W. Hopmans and D.R. Nielsen, 1990. A comprehensive algorithm for simultaneous scaling of soil water retention and hydraulic conductivity data. Dept of Land, Air, and Water Resources, University of California, Davis, CA, Paper number 100018.
- Eching, S. O., and J. W. Hopmans, 1993. Optimization of hydraulic functions from transient outflow and soil water pressure head data *Soil Sci. Soc. Amer. J.*, 57: 1167-1175.
- Eching, S. O., J. W. Hopmans, and O. Wendroth, 1994. Unsaturated hydraulic conductivity from transient multi-step outflow and soil water pressure data, *Soil Sci. Soc. Amer. J.*, 58: 687-695.
- Fogg, G.E., D.E. Rolston, E.M. LaBolle, K.R. Burow, L.A. Maserjian, D. Decker, and S.F. Carle, 1995. Matrix diffusion and contaminant transport in granular geologic materials, with case study of nitrate contamination in Salinas Valley, California: Final Technical Report submitted to Monterey County Water Resources Agency and U.S. Geological Survey in fulfillment of Water Resources Research Award No. 14-08-0001-G1909, 65 p.
- Gardner, W.R., 1958. Some steady-state solutions of the unsaturated moisture flow equation with application to evaporation from a water table. *Soil Science*, vol. 85, no. 1, p. 228-232.
- Gilliam, J. W., S. Dasberg, L. J. Lund, and D. D. Focht, 1978. Denitrification in four California soils: Effect of soil profile characteristics, *J. Soil Sci. Soc. of Amer.*, 42, 61-66.

- Harden, J.W., 1987. Soils developed in granitic alluvium near Merced, California. U.S Geological Survey Bulletin 1590-A, 65p.
- Harden, J.W., and Marchand, D.E., 1977. The soil chronosequence of the Merced River area. In: Singer, M.J. (ed.). Soil development, geomorphology, and Cenozoic history of the northeastern San Joaquin Valley and adjacent areas, California. Soil Science Society of America-Geological Society of America joint field session, 1977, guidebook, p. 22-38.
- Harter, T., and T.-C. J. Yeh, 1996. Stochastic analysis of solute transport in heterogeneous, variably saturated soils. *Water Resour. Res.*, 32(6): 1585-1595.
- Harter, T., and T. C. J. Yeh. 1998, Flow in unsaturated random porous media nonlinear numerical analysis and comparison to analytical stochastic models. *Advances in Water Resources*. 22 (2): 257-272.
- Harter, T., and D. Zhang. 1999. Water flow and solute spreading in heterogeneous soils with spatially variable water content. *Water Resour. Res.* 35(2), 415-426.
- Hartz, T. K., and F. Costa, 1995. Nitrogen movement through intensive on-farm monitoring, in: Walsh Cady, C. and R. Coppock (eds.), *Proceedings of the Third Annual Fertilizer Research and Education Program Conference*, California D.F.A., 1220 N Str. Sacramento, CA 95814, p. 20-22.
- Haverkamp, R. et al, 1977. A comparison of numerical simulation models for one-dimensional infiltration. Soil Science Society of America Proceedings, vol. 41, p. 285-294.
- Hopmans, J.W., J.C. van Dam, S.O. Eching, and J.N.M. Stricker. 1994. Parameter estimation of soil hydraulic functions using inverse modeling of transient outflow experiments. *Trends in Hydrology*, 1:217-242.
- Hopmans, J.W., J. Simunek, N. Romano and W. Durner. 2002. Simultaneous determination of water transmission and retention properties-inverse methods. In J. Dane, D.E. Elrick, D. Reynolds and B Clothier (eds). *Methods of Soil Analysis. Part I. Third Edition* American Society of Agronomy, Monograph No. 9, Madison, WI.
- Horwath, W. R. and E. A. Paul. 1994. Microbial Biomass. *In* *Methods of Soil Analysis-Part2-Microbiological and Biochemical Properties*. Weaver, R. W., J. S. Angle, and P. S. Bottomley, eds., Soil Science Society of America, Madison, WI, pp. 753-773.
- Huntington, G.L., 1980. Soil-land form relationships of portions of the San Joaquin River and Kings River alluvial depositional systems in the Great Valley of California. Ph.D. dissertation, University of California, Davis, 147p.

- Johnson, R.S., F.G. Mitchell, and C.H. Crisosto, 1995. Nitrogen fertilization of Fantasia nectarine – A 12 year study. UC Kearney Tree Fruit Review Vol 1, 14-19.
- Kellogg, R.L., M.S. Maizel, and D.W. Goss, 1992. *Agricultural chemical use and ground water quality: Where are the potential problem areas?* USDA-SCS National Center for Resource Innovations, Washington, D.C.
- Klein, J.M., and W.L. Bradford, 1979. Distribution of nitrate and related nitrogen species in the unsaturated zone, Redlands and vicinity, San Bernardino County, California, *United States Geological Survey Water Resources Investigations Report 79-60*, 81 p.
- Klute, A (ed.), 1986. *Methods of Soil Analysis, Part 1: Physical and Mineralogical Methods*, 2nd Edition, American Society of Agronomy, Soil Science Society of America, Madison, WI, 1188p.
- Kosugi, K., 1994. Three parameter lognormal distribution model for soil water retention. *Water Resources Research*, 30: 891-901.
- Lettis, W.R., 1982. Late Cenozoic stratigraphy and structure of the western margin of the central San Joaquin Valley, California. U.S. Geological Survey Open-File Report, 82-526, 203 p.
- Lovatt C. J., 1995. Avocado growers can reduce nitrate groundwater pollution and increase yield and profit, in: Walsh Cady, C. and R. Coppock (eds.), *Proceedings of the Third Annual Fertilizer Research and Education Program Conference*, California D.F.A., 1220 N Str. Sacramento, CA 95814, p. 32-33.
- Lovatt, C.J., and J.G. Morse, 1995. Citrus growers can reduce nitrate groundwater pollution and increase profits by using foliar urea fertilization, in: Walsh Cady, C. and R. Coppock (eds.), *Proceedings of the Third Annual Fertilizer Research and Education Program Conference*, California D.F.A., 1220 N Str. Sacramento, CA 95814, p. 45-47.
- Lund, L. J., D. C. Adriano, and P. F. Pratt, 1974. Nitrate concentrations in deep soil cores as related to soil profile characteristics, *J. Environ. Qual.*, 3, 78-82.
- Marchand, D.E. and Allwardt, A., 1981. Late Cenozoic Stratigraphic Units, Northeastern San Joaquin Valley, California: US Geological Survey Bulletin 1470.
- Metropolitan Water District of Southern California, 1987. Groundwater quality and its impact on water supply in the Metropolitan Water District service area, *Report No. 969, Los Angeles, Metropolitan Water District of Southern California*, 45 p.

- Meyer, R. D., 1995. Potential nitrate movement below the root zone in drip irrigated almonds, in: Walsh Cady, C. and R. Coppock (eds.), *Proceedings of the Third Annual Fertilizer Research and Education Program Conference*, California D.F.A., 1220 N Str. Sacramento, CA 95814, p. 50-51.
- Miller, R. O., and R. Friedman, 1995. Use of ion exchange resin bags to monitor soil nitrate in tomato cropping systems of Yolo County, in: Walsh Cady, C. and R. Coppock (eds.), *Proceedings of the Third Annual Fertilizer Research and Education Program Conference*, California D.F.A., 1220 N Str. Sacramento, CA 95814, p. 35.
- Miller, E.E. and R.D. Miller, 1956. Physical theory for capillary flow phenomena, *J. Applied Physics*, 27(4), 324-332.
- Mualem, Y. 1976. A new model for predicting the hydraulic conductivity of unsaturated porous media. *Water Resour. Res.* 12:513-522.
- Page, R.W. and LeBlanc, R.A., 1969. Geology, hydrology and water quality in the Fresno area, California. USGS Open-File Report, 70p.
- Powell, M.J.D., 1964. An efficient method for finding the minimum of a function of several variables without calculating derivatives. *The Computer Journal* 7:155-162.
- Pratt, P. F., W. W. Jones, and V. E. Hunsaker, 1972. Nitrate in deep soil profiles in relation to fertilizer rates and leaching volume, *J. Environ. Qual.*, 1, 97-102.
- Rees, T. F., D. J. Bright, R. G. Fay, A. H. Christensen, R. Anders, B. S. Baharie, and M. T. Land, 1995. Geohydrology, water quality, and nitrogen geochemistry in the saturated and unsaturated zones beneath various land uses, Riverside and San Bernardino Counties, California, 1991-93, *United States Geological Survey Water Resources Investigations Report 94-4127*, 267p.
- Retallack, G.J., 1990. Soils of the Past – An introduction to paleopedology. Unwin Hyman (Ed.), Winchester/Mass., 520p.
- Schaap, M.G., F.L. Leij, and M.Th. van Genuchten, 2001. Rosetta: a computer program for estimating soil hydraulic parameters with hierarchical pedotransfer functions. *J. Hydrol.* 251:163-176
- Tanji, K. K., M. Fried, and R. M. Van De Pol, 1977. A steady-state conceptual nitrogen model for estimating nitrogen emissions from cropped lands, *J. Environ. Qual.*, 6, 155-159.

- Tanji, K. K., F. E. Broadbent, M. Mehran, and M. Fried, 1979. An extended version of a conceptual model for evaluating annual nitrogen leaching losses from croplands, *J. Environ. Qual.*, 8, 114-120.
- Tuli, A., M.A. Denton, J.W. Hopmans, T. Harter, and J.L. Mac Intyre. 2001. Multi-step outflow experiment: From soil preparation to parameter estimation . Hydrology program, Dept of Land, Air, and Water Resources, University of California, Davis, CA, Paper number 100037.
- van Genuchten, M.TH., 1980. A closed form equation for predicting the hydraulic conductivity of unsaturated soils. *Soil Sci. Soc. Am. J.* 44:892-898.
- Wang Z., A. Tuli, and W.A. Jury. 2003. Unstable flow during a redistribution period in homogeneous soil. *Vadose Zone Journal*, 2:52-60.
- Weinbaum, S. A., and D. A. Goldhamer, 1995. Nitrogen fertilizer management to reduce groundwater degradation, in: Walsh Cady, C. and R. Coppock (eds.), *Proceedings of the Third Annual Fertilizer Research and Education Program Conference*, California D.F.A., 1220 N Str. Sacramento, CA 95814, p. 38-40.
- Weissmann, G.S., S.F. Carle, and G.E. Fogg, 1999. Three-dimensional hydrofacies modeling based on soil surveys and transition probability geostatistics. *Water Resources Research*, 35: 1761-1170.
- Wraith, J.M. and D. Or. 1998. Nonlinear parameter estimation using spreadsheet software. *J. Nat. Resour. Life Sci. Edu.* 27: 13-19.

TABLES

Key

AS = Ammonium Sulfate (21% N)

CN = Calcium Nitrate (15.5% N)

AN = Ammonium Nitrate (34% N)

Table 2.2.1. Fertilizer amounts and application dates.

	TREATMENT PLOTS			
	100 lbs/acre N	175 lbs/acre N	250 lbs/acre N	325 lbs/acre N
DATE				
9/14/1982	5 lbs Ammonium Sulfate per tree to all trees			
2/24/1983			5# AS	5# AS
4/22/1983			2.5# AS	2.5# AS
5/26/1983		4.9# CN		4.9# CN
9/15/1983	2.6 lbs Ammonium Nitrate per tree to all trees			
3/13/1984			3# AN	3# AN
4/26/1984			1.5# AN	1.5# AN
5/23/1984		4.9# CN		4.9# CN
9/11/1984	2.1 lbs Ammonium Nitrate per tree to all trees			
3/20/1985			3# AN	3# AN
5/1/1985			1.5# AN	1.5# AN
5/29/1985		4.9# CN		4.9# CN
9/4/1985	3.2 lbs Ammonium Nitrate per tree to all trees			
3/7/1986			3# AN	3# AN
4/17/1986			1.5# AN	1.5# AN
5/29/1986		5# CN		5# CN
9/9/1986	3.3 lbs Ammonium Nitrate per tree to all trees			
Mid-March 1987			3# AN	3# AN
Mid-April 1987			1.5# AN	1.5# AN
6/1/1987		5# CN		5# CN
9/18/1987	~3 lbs Ammonium Nitrate per tree to all trees			
4/5/1988			3# AN	3# AN
5/5/1988			1.5# AN	1.5# AN
6/6/1988		5# CN		5# CN
9/7/1988	3.0 lbs Ammonium Nitrate per tree to all trees			
3/29/1989			3# AN	3# AN
5/1/1989			1.5# AN	1.5# AN
June 1989		5# CN		5# CN
9/27/1989	2.6 lbs Ammonium Nitrate per tree to all trees			
3/28/1990			3# AN	3# AN
5/7/1990			1.5# AN	1.5# AN
6/4/1990		5# CN		5# CN
9/17/1990	3.6 lbs Ammonium Nitrate per tree to all trees			
3/22/1991			3# AN	3# AN
5/2/1991			1.5# AN	1.5# AN
6/3/1991		5# CN		5# CN
9/5/1991	3.6 lbs Ammonium Nitrate per tree to all trees			
3/20/1992			3# AN	3# AN
4/29/1992			1.5# AN	1.5# AN
5/28/1992		5# CN		5# CN
9/9/1992	3.1 lbs Ammonium Nitrate per tree to all trees			
3/17/1993			3# AN	3# AN
5/3/1993			1.5# AN	1.5# AN
6/1/1993		5# CN		5# CN
9/13/1993	3.1 lbs Ammonium Nitrate per tree to all trees			
3/21/1994			3# AN	3# AN
5/10/1994			1.5# AN	1.5# AN
6/1/1994		5# CN		5# CN
9/16/1994	3.3 lbs Ammonium Nitrate per tree to all trees			

Table 2.3.1. Irrigation dates for the orchard. The date shown is the afternoon start date.

1983	1990	1991	1992	1993	1994	1995	1996	1997
28-Apr	29-Mar	7-Feb	22-Apr	19-Mar	21-Mar	1-May	1-May	25-Mar
19-May	17-Apr	3-May	29-Apr	16-Apr	14-Apr	10-May	9-May	10-Apr
31-May	8-May	22-May	7-May	3-May	10-May	22-May	21-May	21-Apr
14-Jun	4-Jun	3-Jun	18-May	18-May	23-May	31-May	3-Jun	5-May
24-Jun	14-Jun	20-Jun	28-May	1-Jun	1-Jun	8-Jun	25-Jun	15-May
30-Jun	21-Jun	1-Jul	3-Jun	9-Jun	9-Jun	20-Jun	2-Jul	27-May
11-Jul	27-Jun	15-Jul	9-Jun	18-Jun	16-Jun	3-Jul	30-Jul	9-Jun
21-Jul	3-Jul	30-Jul	18-Jun	24-Jun	23-Jun	10-Jul	11-Sep	19-Jun
1-Aug	10-Jul	8-Aug	25-Jun	1-Jul	30-Jun	25-Jul	3-Oct	30-Jun
9-Aug	24-Jul	6-Sep	1-Jul	9-Jul	16-Jul	7-Aug		10-Jul
22-Aug	9-Aug		8-Jul	16-Jul	28-Jul	23-Aug		21-Jul
29-Aug	5-Sep		23-Jul	30-Jul	8-Aug	6-Sep		1-Aug
19-Sep	18-Sep		6-Aug	9-Aug	16-Sep	4-Oct		13-Aug
			20-Aug	24-Aug				21-Aug
			31-Aug	2-Sep				2-Sep
			10-Sep	14-Sep				16-Sep
			28-Sep					

Table 2.4.1. Explanation of CIMIS report contents.

CIMIS Report Types	
Standard Daily report	<p>This report will provide average daily data for the stations and date range provided.</p> <p>Consists of 14 pre-determined sensors: ETo; precipitation; solar radiation; average vapor pressure; maximum, minimum, and average air temperature; maximum, minimum, and average relative humidity; dew point; wind speed; wind run; and average soil temperature.</p>
Standard Hourly report	<p>This report will provide average hourly data for the stations and date range provided.</p> <p>Consists of 10 pre-determined sensors: ETo; precipitation; solar radiation; vapor pressure; air temperature; relative humidity; dew point; wind speed; wind direction; and soil temperature.</p>
Standard Monthly report	Allows you to select weather stations for which you will receive monthly summaries for a variety of sensors.

Table 2.4.2. Summary statistics for weather averages from 1983 to 1999. All values are monthly with exceptions noted.

	Min	Max	Mean	Standard deviation
Total Precipitation (in.) annual	3.9	22.6	13.0	4.7
Total Precipitation (in.) monthly	0	8.7	1.1	1.5
Evapotranspiration (in.) annual	46.8	56.4	53.3	2.7
Evapotranspiration (in.) monthly	0.4	8.8	4.5	2.6
Average Solar Radiation (W/m ²)	51	355	206.02	91.5
Vapor Pressure (kPa)	0.4	2	1.23	0.35
Maximum Air Temperature (°C)	8.4	37.2	24.6	7.9
Minimum Air Temperature (°C)	-2.6	18.9	9.1	5.3
Average Air Temperature (°C)	3.3	27.5	16.5	6.7
Maximum Relative Humidity (%)	40	100	88.9	11.2
Minimum Relative Humidity (%)	17	84	41.9	16.7
Average Relative Humidity (%)	27	95	64.8	14.6
Average Dew Point (°C)	-6.1	17.7	9.2	4.5
Average Wind Speed (m/s)	1	2.5	1.7	0.36
Average Soil Temperature (°C)	6.2	29.6	17.8	6.3

Table 2.4.3. Department of Water Resources CIMIS Sensor Specifications

The following sensor specifications, except sensor heights, are provided by the particular manufacturer.

Precipitation

Sensor:	Tipping-bucket rain gauge with magnetic reed switch
Model:	TE525MM
Maker:	Texas Electronics
Height:	1.0 meters
Specifications Orifice:	24.5 cm (9.644 in)
Resolution:	0.1 mm
Accuracy:	± 1% at 5 cm/hour or less

Air temperature/ Relative humidity

Sensor:	Fenwal Thermistor/ HUMICAP H-sensor
Model:	HMP35C
Maker:	Vaisala/ modified by Campbell Scientific, Inc.
Height:	1.5 meters
Specifications Range:	0 to 100% RH, -35 to 50 °C
Accuracy:	± 2% RH (0-90% RH), ±5% RH (90-100% RH), ±0.1 °C over -24 to 48 °C range.
Note:	Both sensors are enclosed in a 12-plate naturally aspirated radiation shield made by R.M. Young.

Total solar radiation

Sensor:	Pyranometer—high stability silicon photovoltaic detector (blue enhanced)
Model:	LI200S
Maker:	Li-Cor
Height:	2.0 meters
Specifications	
Sensitivity:	±5% error under natural sunlight conditions. Typically 80 micro Ampere per 1000 watts per square meter.
Linearity:	Maximum deviation of 1% up to 3000 watts per square meter.
Response time:	10 micro seconds
Correction:	Cosine corrected up to 80 degrees angle of incidence
Azimuth:	±1% error over 360 degrees at 45 degrees elevation

Table 2.4.3 cont. Department of Water Resources CIMIS Sensor Specifications

Wind speed

Sensor:	Three-cup anemometer utilizing a magnet activated reed switch whose frequency is proportional to wind speed
Model:	014A
Maker:	Met-One
Height:	2.0 meters
Specifications Range:	0-45 m/s (0-100 mph)
Threshold:	0.45 m/s (1 mph)
Gust Survival:	0-53 m/s (0-120 mph)
Accuracy:	1.5% or 0.11 m/s (0.25 mph)

Soil temperature

Sensor:	Soil Thermistor—Fenwal Electronic UUT51J1 thermistor in water resistant coating.
Model:	107B
Maker:	Fenwal/modified by Campbell Scientific, Inc.
Height:	15 cm (6 in) below soil surface under irrigated grass
Specifications Accuracy:	Worst case ± 0.4 °C over -33 to 48 °C, ± 0.5 °C at -40 °C

Table 2.5.1. Fruit yield, load and weight summary, including the 7 year average.

Yield (kg fruit/tree)		YEAR							
		<u>1983</u>	<u>1984</u>	<u>1985</u>	<u>1991</u>	<u>1992</u>	<u>1993</u>	<u>1994</u>	<u>7 yr.</u> <u>Ave.</u>
Treatment (lbs N/acre)									
0		191.0	155.9	126.1	132.2	126.3	100.2	103.3	133.6
100		202.4	194.9	202.8	207.2	203.1	160.4	155.9	189.5
175		198.9	187.2	171.1	193.6	214.5	143.4	165.5	182.0
250		201.4	205.5	186.9	222.1	209.8	160.2	177.9	194.8
325		203.5	190.4	170.7	197.9	187.7	134.0	159.4	177.7

Fruit Load (# fruit/tree)		YEAR						
		<u>1983</u>	<u>1984</u>	<u>1985</u>	<u>1991</u>	<u>1992</u>	<u>1993</u>	<u>1994</u>
Treatment (lbs N/acre)								
0		1130	945	856	906	868	641	657
100		1199	1130	1352	1313	1267	917	827
175		1118	1074	1100	1134	1418	754	933
250		1128	1191	1217	1393	1342	912	949
325		1150	1087	1135	1200	1214	745	911

Fruit Weight (grams/ fruit)		YEAR						
		<u>1983</u>	<u>1984</u>	<u>1985</u>	<u>1991</u>	<u>1992</u>	<u>1993</u>	<u>1994</u>
Treatment (lbs N/acre)								
0		168.6	152.3	139.1	130.5	137.8	149.9	145.5
100		172.8	173.8	154.4	165.8	160.3	179.2	184.7
175		176.4	172.0	153.2	167.9	153.8	187.3	181.3
250		179.3	177.9	154.0	169.4	157.1	179.9	189.8
325		177.1	172.9	150.8	166.8	152.5	176.8	175.5

Table 2.5.2. Percent nitrogen in fruit on a dry mass basis (1983).

Treatment (lbs N/acre)	Flesh	Pit	Seed	Total
100	1.57	0.60	5.71	7.88
175	1.66	0.47	5.63	7.76
250	1.78	0.78	5.92	8.48
325	2.05	0.50	5.76	8.31

Table 2.5.3. Leaf nutrients.

<u>%N</u>		<u>Year</u>						
Treatment (lbs N/acre)		<u>1983</u>	<u>1984</u>	<u>1985</u>	<u>1991</u>	<u>1992</u>	<u>1993</u>	<u>1994</u>
0		2.82	2.51	2.44	2.69	2.59	2.52	2.66
100		2.69	2.7	2.77	2.95	2.78	2.76	3.16
175		3.03	3.12	3.07	3.13	2.95	2.82	3.21
250		3.28	3.28	3.36	3.49	3.09	3.28	3.53
325		3.19	3.4	3.37	3.48	3.16	3.17	3.54

<u>%P</u>		<u>Year</u>						
Treatment (lbs N/acre)		<u>1983</u>	<u>1984</u>	<u>1985</u>	<u>1991</u>	<u>1992</u>	<u>1993</u>	<u>1994</u>
0		-	0.23	0.27	0.29	0.34	-	0.28
100		-	0.22	0.18	0.19	0.21	-	0.19
175		-	0.21	0.18	0.18	0.21	-	0.19
250		-	0.22	0.18	0.18	0.19	-	0.19
325		-	0.18	0.18	0.18	0.20	-	0.19

<u>%K</u>		<u>Year</u>						
Treatment (lbs N/acre)		<u>1983</u>	<u>1984</u>	<u>1985</u>	<u>1991</u>	<u>1992</u>	<u>1993</u>	<u>1994</u>
0		2.58	2.11	2.81	2.00	2.25	3.34	3.13
100		2.58	1.92	2.31	1.72	1.64	2.46	2.55
175		2.52	1.76	2.18	1.47	1.36	2.39	2.57
250		2.52	1.84	2.12	1.41	1.23	1.95	2.09
325		2.38	1.73	2.13	1.31	1.33	2.14	2.09

Table 2.5.4. Soil nitrate concentration, in ppm, and pH in October, 1991.

Depth (ft)	Treatments (lbs N/acre/year)				
	0	100	175	250	325
	<u>Nitrate (ppm)</u>				
0 – 0.5	6.4	23.1	46.0	23.6	14.4
0.5 – 1	3.4	13.4	20.6	12.5	7.4
1 – 2	1.9	8.2	10.0	9.4	5.3
2 – 3	1.5	6.3	10.9	10.3	8.3
3 – 4	1.9	5.2	12.8	9.3	3.4
4 – 5	2.1	4.2	18.0	6.5	6.8
5 – 6	2.4	4.6	8.3	8.6	4.7
6 – 7	3.2	4.3	4.4	6.4	4.7
7 – 8	1.7	3.9	5.9	9.0	6.5
8 – 9	1.8	4.1	11.5	11.9	9.0
9 – 10	1.6	4.2	7.3	9.1	10.8
	<u>pH</u>				
0 – 0.5	7.8	6.7	6.2	6.3	7.0
0.5 – 1	7.9	7.2	6.6	6.9	7.2

Table 2.5.5. Soil nitrate concentration, in ppm, in January, 1995.

Depth (ft)	Treatments (lbs N/acre/year)				
	0	100	175	250	325
	<u>Nitrate (ppm)</u>				
0 – 0.5	4.4	6.6	6.2	6.0	6.6
0.5 – 1	3.7	5.1	5.2	4.6	5.2
1 – 2	2.8	4.4	3.7	6.3	7.6
2 – 3	2.9	13.3	10.7	10.6	15.1
3 – 4	2.9	17.8	17.0	16.5	17.6
4 – 5	3.3	9.8	14.1	9.1	15.3
5 – 6	3.1	6.3	20.4	12.7	17.5
6 – 7	3.6	4.0	7.4	5.1	22.4
7 – 8	2.7	3.8	3.9	4.4	16.6
8 – 9	3.4	4.1	4.4	4.3	11.5
9 – 10	3.0	3.4	4.6	4.2	7.2

Table 3.3.1. Comparison of scaling subgroup assignments and data quality for each soil sample.

MSO run #	MSO cell #	Core #	Sample #	Group 2	Group 3	Group 4	Data quality
3	1	3-10-1	6	sand	sand	var1	1
3	2	3-10-2	3	sand	sand	var1	1
3	3	5-10-2	9	sand	sand	sand	1
3	4	5-10-2	10	sand	sand	sand	1
3	5	10-8-2	6	sand	sand	sand	1
3	6	10-8-2	8	sand	sand	CSiL	1
3	7	10-8-5	3	sand	sand	var1	1
3	8	10-8-5	7	sand	sand	sand	1
3	9	10-10-2	8	sand	sand	sand	1
3	10	10-10-2	9	loamy sand	sand	sand	1
4	1	5-10-2	20	sand	loamy sand	sandy loam	1
4	2	10-8-5	17	sand	loamy sand	sandy loam	1
4	3	10-10-5	3	sand	sand	var1	0
4	4	11-8-2	8	sand	sandy loam	sand	0
4	5	11-8-2	16	loamy sand	loamy sand	sandy loam	1
4	6	11-10-5	3	sand	sand	var1	0
4	7	12-10-2	3	sand	sand	var1	0
4	9	13-10-2	3	sand	loamy sand	var1	0
4	10	13-10-5	2	sand	loamy sand	var1	0
4	8	13-8-2	4	sand	sand	var1	0
5	1	4-10-5	10	sandy loam	sandy loam	CSiL	1
5	2	4-10-5	16	loamy sand	sandy loam	sandy loam	1
5	3	10-8-2	5	sandy loam	sandy loam	var2	1
5	4	10-8-2	13	loamy sand	sandy loam	sL	1
5	5	10-8-5	12	silt loam	sandy loam	CSiL	1
5	6	10-8-5	16	loamy sand	sandy loam	sL	1
5	7	11-8-2	7	sandy loam	sandy loam	var2	1
5	8	11-8-2	14	sandy loam	sandy loam	sL	1
5	9	13-8-5	7	silt loam	sandy loam	var2	1
5	10	13-8-5	11	sandy loam	sandy loam	CSiL	1
6	1	3-10-5	14	sandy loam	sandy loam	CSiL	1
6	2	3-10-5	17	loamy sand	sandy loam	CSiL	1
6	3	5-10-2	17	loamy sand	sandy loam	CSiL	1
6	5	10-10-2	6	loamy sand	sandy loam	var2	1
6	6	10-10-2	14	sandy loam	sandy loam	CSiL	1
6	8	12-10-2	13	loamy sand	sandy loam	sL	1
6	9	13-10-2	12	sandy loam	sandy loam	CSiL	1
6	10	13-10-5	11	loamy sand	sandy loam	CSiL	1
7	1	3-10-1	2	loamy sand	sL-Han	sL	0
7	2	3-10-1	5	loamy sand	sL-Han	sL	0
7	3	3-10-4	3	sandy loam	sL-Han	sL	0
7	4	3-10-4	4	loamy sand	sL-Han	sL	0
7	5	4-10-5	2	sandy loam	sL-Han	var1	0
7	6	10-8-5	2	loamy sand	sL-Han	clay	0
7	7	10-10-2	2	loamy sand	sL-Han	sL-Han	0
7	8	11-10-5	2	loamy sand	sL-Han	sL-Han	0
7	9	12-10-2	2	loamy sand	sL-Han	sL-Han	0
7	10	13-10-5	1	loamy sand	sL-Han	sL-Han	0

Table 3.3.1. continued

MSO run #	MSO cell #	Core #	Sample #	Group 2	Group 3	Group 4	Data quality
3	1	3-10-1	6	sand	sand	var1	1
3	2	3-10-2	3	sand	sand	var1	1
3	3	5-10-2	9	sand	sand	sand	1
3	4	5-10-2	10	sand	sand	sand	1
3	5	10-8-2	6	sand	sand	sand	1
3	6	10-8-2	8	sand	sand	CSiL	1
3	7	10-8-5	3	sand	sand	var1	1
3	8	10-8-5	7	sand	sand	sand	1
3	9	10-10-2	8	sand	sand	sand	1
3	10	10-10-2	9	loamy sand	sand	sand	1
4	1	5-10-2	20	sand	loamy sand	sandy loam	1
4	2	10-8-5	17	sand	loamy sand	sandy loam	1
4	3	10-10-5	3	sand	sand	var1	0
4	4	11-8-2	8	sand	sandy loam	sand	0
4	5	11-8-2	16	loamy sand	loamy sand	sandy loam	1
4	6	11-10-5	3	sand	sand	var1	0
4	7	12-10-2	3	sand	sand	var1	0
4	9	13-10-2	3	sand	loamy sand	var1	0
4	10	13-10-5	2	sand	loamy sand	var1	0
4	8	13-8-2	4	sand	sand	var1	0
5	1	4-10-5	10	sandy loam	sandy loam	CSiL	1
5	2	4-10-5	16	loamy sand	sandy loam	sandy loam	1
5	3	10-8-2	5	sandy loam	sandy loam	var2	1
5	4	10-8-2	13	loamy sand	sandy loam	sL	1
5	5	10-8-5	12	silt loam	sandy loam	CSiL	1
5	6	10-8-5	16	loamy sand	sandy loam	sL	1
5	7	11-8-2	7	sandy loam	sandy loam	var2	1
5	8	11-8-2	14	sandy loam	sandy loam	sL	1
5	9	13-8-5	7	silt loam	sandy loam	var2	1
5	10	13-8-5	11	sandy loam	sandy loam	CSiL	1
6	1	3-10-5	14	sandy loam	sandy loam	CSiL	1
6	2	3-10-5	17	loamy sand	sandy loam	CSiL	1
6	3	5-10-2	17	loamy sand	sandy loam	CSiL	1
6	5	10-10-2	6	loamy sand	sandy loam	var2	1
6	6	10-10-2	14	sandy loam	sandy loam	CSiL	1
6	8	12-10-2	13	loamy sand	sandy loam	sL	1
6	9	13-10-2	12	sandy loam	sandy loam	CSiL	1
6	10	13-10-5	11	loamy sand	sandy loam	CSiL	1
7	1	3-10-1	2	loamy sand	sL-Han	sL	0
7	2	3-10-1	5	loamy sand	sL-Han	sL	0
7	3	3-10-4	3	sandy loam	sL-Han	sL	0
7	4	3-10-4	4	loamy sand	sL-Han	sL	0
7	5	4-10-5	2	sandy loam	sL-Han	var1	0
7	6	10-8-5	2	loamy sand	sL-Han	clay	0
7	7	10-10-2	2	loamy sand	sL-Han	sL-Han	0
7	8	11-10-5	2	loamy sand	sL-Han	sL-Han	0
7	9	12-10-2	2	loamy sand	sL-Han	sL-Han	0
7	10	13-10-5	1	loamy sand	sL-Han	sL-Han	0
8	1	10-10-5	11	loam	loam	CSiL	0

Table 4.2.1. Summary of DANR laboratory measurements.

MSO run #	MSO cell #	Core #	Sample #	BD (g/cm ³)	OM (%)	C-org (%)	Sand (%)	Silt (%)	Clay (%)	Ksatm (cm/hr)	Porosity	Θ_s^m (cm ³ /cm ³)	texture
1	1	6-10-5	12	1.41	0.09	0.05	17	76	7	0.074	0.466	0.423	silt loam
1	2	6-10-5	13	1.48	0.09	0.05	15	81	4	0.071	0.441	0.389	silt
1	3	6-10-5	14	1.8	0.06	0.03	84	15	1	0.874	0.322	0.223	loamy sand
1	4	6-10-5	15	1.74	0.03	0.02	70	27	3	0.409	0.345	0.335	sandy loam
1	5	6-10-5	16	1.74	0.1	0.06	62	28	10	0.087	0.342	0.253	sandy loam
1	6	6-10-2	7	1.52	0.03	0.02	74	25	1	1.53	0.425	0.293	loamy sand
1	7	6-10-2	6	1.48	0.04	0.02	82	17	1	2.61	0.44	0.302	loamy sand
1	9	6-10-2	8	1.48	0.02	0.01	99	1	<1	67.32	0.443	0.327	sand
1	10	6-10-2	9	1.46	0.01	<.01	97	2	1	50.27	0.445	0.298	sand
2	1	6-10-2	2	1.72	0.17	0.1	67	28	5	<i>no data</i>	0.353	0.243	sandy loam
2	2	6-10-2	3	1.76	0.13	0.08	58	30	15	<i>no data</i>	0.336	0.31	sandy loam
2	3	6-10-2	4	1.73	0.09	0.05	71	22	7	<i>no data</i>	0.346	0.313	sandy loam
2	5	6-10-2	11	1.78	0.1	0.06	68	25	7	<i>no data</i>	0.327	0.254	sandy loam
2	6	6-10-2	15	1.58	0.09	0.05	53	41	6	<i>no data</i>	0.405	0.359	sandy loam
2	7	6-10-2	17	1.75	0.09	0.05	82	12	6	<i>no data</i>	0.341	0.289	loamy sand
2	8	6-10-5	8	1.51	0.12	0.07	95	2	3	65.22	0.429	0.372	sand
2	9	6-10-5	9	1.48	0.08	0.05	94	3	3	24.39	0.443	0.34	sand
2	10	6-10-5	10	1.47	0.07	0.04	94	2	4	20.63	0.445	0.306	sand
3	1	3-10-1	6	1.54	0.06	0.04	98	<1	2	1.702	0.421	0.322	sand
3	2	3-10-2	3	1.58	0.08	0.05	97	<1	3	2.018	0.405	0.307	sand
3	3	5-10-2	9	1.49	0.06	0.03	98	<1	3	0.407	0.439	0.339	sand
3	4	5-10-2	10	1.5	0.06	0.03	99	<1	1	51.148	0.434	0.331	sand
3	5	10-8-2	6	1.5	0.06	0.04	97	<1	3	54.902	0.436	0.369	sand
3	6	10-8-2	8	1.47	0.06	0.03	98	<1	2	72.471	0.447	0.354	sand
3	7	10-8-5	3	1.57	0.06	0.04	97	<1	3	0.718	0.407	0.3	sand
3	8	10-8-5	7	1.46	0.06	0.03	98	<1	2	61.271	0.45	0.367	sand
3	9	10-10-2	8	1.46	0.07	0.04	94	<1	7	1.976	0.45	0.399	sand
3	10	10-10-2	9	1.54	0.08	0.05	89	<1	12	4.195	0.418	0.341	loamy sand
4	1	5-10-2	20	1.81	0.09	0.05	87	11	2	0.699	0.317	0.222	sand
4	2	10-8-5	17	1.85	0.06	0.03	91	7	2	12.1	0.302	0.229	sand
4	3	10-10-5	3	1.53	0.04	0.03	98	1	1	7.67	0.422	0.267	sand
4	4	11-8-2	8	1.51	0.04	0.02	97	2	1	12.4	0.431	0.284	sand

Table 4.2.1. continued

MSO run #	MSO cell #	Core #	Sample #	BD (g/cm ³)	OM (%)	C-org (%)	Sand (%)	Silt (%)	Clay (%)	Ksatm (cm/hr)	Porosity	Θ_s^m (cm ³ /cm ³)	texture
4	5	11-8-2	16	1.87	0.04	0.03	84	15	1	0.644	0.293	0.237	loamy sand
4	6	11-10-5	3	1.6	0.07	0.04	96	3	1	18.5	0.398	0.237	sand
4	7	12-10-2	3	1.55	0.03	0.02	98	1	1	4.29	0.415	0.319	sand
4	8	13-8-2	4	1.56	0.04	0.02	99	<1	1	16.5	0.411	0.272	sand
4	9	13-10-2	3	1.55	0.03	0.02	99	<1	1	33.9	0.414	0.281	sand
4	10	13-10-5	2	1.54	0.04	0.02	97	2	1	10.6	0.419	0.283	sand
5	1	4-10-5	10	1.72	0.09	0.05	61	35	4	0.098	0.349	0.309	sandy loam
5	2	4-10-5	16	1.85	0.07	0.04	78	18	4	1.791	0.302	0.275	loamy sand
5	3	10-8-2	5	1.55	0.09	0.05	67	29	4	0.437	0.415	0.302	sandy loam
5	4	10-8-2	13	1.83	0.07	0.04	74	21	5	0.341	0.309	0.252	loamy sand
5	5	10-8-5	12	1.5	0.09	0.05	37	59	4	2.264	0.434	0.395	silt loam
5	6	10-8-5	16	1.81	0.06	0.03	78	17	5	0.772	0.317	0.269	loamy sand
5	7	11-8-2	7	1.51	0.06	0.03	63	32	5	1.552	0.43	0.329	sandy loam
5	8	11-8-2	14	1.75	0.08	0.05	87	8	5	1.922	0.34	0.263	sandy loam
5	9	13-8-5	7	1.62	0.08	0.05	42	54	4	0.308	0.389	0.329	silt loam
5	10	13-8-5	11	1.53	0.07	0.04	71	25	4	2.649	0.423	0.346	sandy loam
6	1	3-10-5	14	1.75	0.12	0.07	69	23	8	0.089	0.338	0.248	sandy loam
6	2	3-10-5	17	1.81	0.09	0.05	81	15	4	0.027	0.318	0.256	loamy sand
6	3	5-10-2	17	1.48	0.08	0.05	83	13	4	0.887	0.442	0.309	loamy sand
6	4	5-10-2	19	1.57	0.09	0.05	49	43	8	0.024	0.409	0.301	loam
6	5	10-10-2	6	1.71	0.07	0.04	82	13	5	0.208	0.354	0.248	loamy sand
6	6	10-10-2	14	1.51	0.07	0.04	71	24	5	0.812	0.43	0.345	sandy loam
6	7	12-10-2	10	1.6	0.09	0.05	77	16	7	0.316	0.396	0.133	loamy sand
6	8	12-10-2	13	1.7	0.07	0.04	86	10	4	0.555	0.36	0.278	loamy sand
6	9	13-10-2	12	1.71	0.07	0.04	66	30	4	0.276	0.355	0.285	sandy loam
6	10	13-10-5	11	1.66	0.06	0.03	75	21	4	0.43	0.375	0.267	loamy sand
7	1	3-10-1	2	1.65	0.17	0.1	74	23	3	0.0454	0.378	0.257	loamy sand
7	2	3-10-1	5	1.69	0.15	0.09	76	23	1	0.222	0.361	0.262	loamy sand
7	3	3-10-4	3	1.66	0.17	0.1	72	25	3	0.0192	0.373	0.245	sandy loam
7	4	3-10-4	4	1.69	0.14	0.08	74	23	3	0.247	0.361	0.265	loamy sand
7	5	4-10-5	2	1.56	0.16	0.09	72	26	2	0.946	0.41	0.287	sandy loam
7	6	10-8-5	2	1.59	0.16	0.09	82	17	1	0.593	0.399	0.254	loamy sand

Table 4.2.1. continued

MSO run #	MSO cell #	Core #	Sample #	BD (g/cm ³)	OM (%)	C-org (%)	Sand (%)	Silt (%)	Clay (%)	Ksatm (cm/hr)	Porosity	Θ_s^m (cm ³ /cm ³)	texture
7	7	10-10-2	2	1.63	0.13	0.07	76	21	3	0.386	0.386	0.27	loamy sand
7	8	11-10-5	2	1.63	0.12	0.07	83	16	1	0.842	0.384	0.229	loamy sand
7	9	12-10-2	2	1.65	0.1	0.06	83	15	2	4.27	0.376	0.288	loamy sand
7	10	13-10-5	1	1.64	0.12	0.07	82	16	2	1.07	0.383	0.245	loamy sand
8	1	10-10-5	11	1.57	0.13	0.07	43	50	7	0.0989	0.408	0.333	loam
8	2	10-10-5	12	1.8	0.13	0.08	69	22	9	0.121	0.321	0.245	sandy loam
8	3	11-10-5	5	1.77	0.13	0.08	74	18	8	0.0496	0.332	0.238	sandy loam
8	4	11-10-5	6	1.77	0.2	0.12	71	20	9	5.61	0.332	0.229	sandy loam
8	5	11-10-5	7	1.71	0.1	0.06	68	20	12	2.83	0.355	0.278	sandy loam
8	6	11-10-5	11	1.61	0.13	0.07	27	63	10	2.88	0.392	0.366	silt loam
8	7	11-10-5	13	1.64	0.18	0.1	57	36	7	3.56	0.381	0.328	sandy loam
8	8	12-10-2	12	1.71	0.1	0.06	68	22	10	24.6	0.355	0.325	sandy loam
8	9	13-8-2	11	1.26	0.17	0.1	40	53	7	15.4	0.525	0.471	silt loam
8	10	13-8-2	12	1.57	0.14	0.08	49	44	7	0.0169	0.408	0.307	loam
9	1	3-10-4	14	1.55	0.08	0.05	57	37	6	0.664	0.414	0.362	sandy loam
9	2	3-10-4	19	1.48	0.13	0.07	44	50	6	1.217	0.442	0.408	silt loam
9	3	3-10-5	13	1.49	0.06	0.03	34	63	3	0.327	0.437	0.385	silt loam
9	4	4-10-5	5	1.53	0.13	0.07	72	24	4	1.444	0.423	0.296	sandy loam
9	5	4-10-5	8	1.58	0.07	0.04	38	58	4	0.382	0.402	0.354	silt loam
9	6	10-8-5	14	1.55	0.13	0.08	25	71	4	0.799	0.415	0.426	silt loam
9	7	11-10-5	10	1.43	0.08	0.05	74	22	4	6.166	0.46	0.389	loamy sand
9	8	12-10-2	6	1.54	0.07	0.04	74	22	4	1.48	0.419	0.333	loamy sand
9	9	13-8-5	15	1.63	0.06	0.03	34	62	4	0.268	0.385	0.348	silt loam
9	10	13-10-2	13	1.59	0.1	0.06	40	54	6	0.092	0.402	0.386	silt loam
10	1	4-10-5	13	1.59	0.1	0.06	44	49	7	0.206	0.4	0.339	loam
10	2	4-10-5	14	1.52	0.1	0.06	51	43	6	0.188	0.427	0.397	sandy loam
10	3	5-10-2	18	1.31	0.18	0.1	13	70	17	0.00262	0.507	0.433	silt loam
10	4	10-8-2	10	1.37	0.12	0.07	29	67	4	0.199	0.484	0.458	silt loam
10	5	10-8-2	12	1.68	0.07	0.04	74	21	5	0.578	0.364	0.276	sandy loam
10	6	10-8-5	9	1.69	0.11	0.06	60	33	7	0.334	0.361	0.3	sandy loam
10	7	10-8-5	15	1.46	0.13	0.08	40	54	6	0.143	0.412	0.348	silt loam
10	8	10-10-5	13	1.32	0.14	0.08	15	76	9	0.0713	0.501	0.443	silt loam

Table 4.2.1. continued

MSO run #	MSO cell #	Core #	Sample #	BD (g/cm3)	OM (%)	C-org (%)	Sand (%)	Silt (%)	Clay (%)	Ksatm (cm/hr)	Porosity	Θ_s^m (cm³/cm³)	texture
10	9	11-8-2	10	1.41	0.12	0.07	27	70	3	0.18	0.469	0.408	silt loam
10	10	13-10-5	10	1.48	0.1	0.06	20	76	4	0.106	0.443	0.426	silt loam
11	1	3-10-1	8	1.85	0.07	0.04	76	17	7	0.0447	0.302	0.251	sandy loam
11	2	3-10-5	5	1.87	0.16	0.09	67	24	9	0.00447	0.294	0.23	sandy loam
11	3	5-10-2	3	1.64	0.2	0.12	57	34	9	0.0175	0.381	0.344	sandy loam
11	4	5-10-2	4	1.61	0.07	0.04	79	14	7	0.591	0.392	0.328	loamy sand
11	5	10-10-2	3	1.74	0.13	0.07	62	25	13	0.0132	0.343	0.303	sandy loam
11	6	10-10-2	4	1.87	0.07	0.04	69	20	11	0.00201	0.294	0.244	sandy loam
11	7	11-8-2	4	1.75	0.11	0.06	63	22	15	0.0831	0.34	0.297	sandy loam
11	8	11-10-5	4	1.79	0.15	0.09	64	24	12	0.0893	0.325	0.279	sandy loam
11	9	13-8-2	6	1.66	0.11	0.06	65	28	7	0.141	0.374	0.27	sandy loam
11	10	13-8-5	3	1.79	0.06	0.03	70	21	9	0.0505	0.325	0.283	sandy loam
12	1	10-8-2	14	1.67	0.07	0.04	74	18	8	1.149	0.37	0.279	sandy loam
12	2	10-8-2	15	1.8	0.12	0.07	69	21	10	0.137	0.321	0.281	sandy loam
12	3	10-8-5	18	1.8	0.11	0.06	68	23	9	1.523	0.321	0.239	sandy loam
12	4	10-10-5	19	1.69	0.09	0.05	72	21	7	0.188	0.362	0.255	sandy loam
12	5	11-8-2	17	1.78	0.14	0.08	70	20	10	5.247	0.328	0.237	sandy loam
12	6	11-10-5	17	1.6	0.09	0.05	77	16	7	2.667	0.396	0.315	sandy loam
12	7	12-10-2	15	1.59	0.09	0.05	76	16	8	0.505	0.4	0.275	sandy loam
12	8	13-8-2	16	1.69	0.14	0.08	74	18	8	14.841	0.362	0.293	sandy loam
12	9	13-8-5	17	1.77	0.07	0.04	78	15	7	0.39	0.332	0.238	loamy sand
12	10	13-10-2	15	1.74	0.04	0.02	66	28	6	0.333	0.343	0.263	sandy loam

Table 4.2.2. Summary statistics of DANR laboratory measurements

	Valid N	Mean	Median	Mode	Mode Frequency	Minimum	Maximum	Lower Quartile	Upper Quartile	Std. Deviation
<u>ALL</u>										
Bulk Density (g/cm ³)	118	1.621	1.605	1.48	7	1.26	1.87	1.52	1.74	0.134
Organic Matter (%)	118	0.094	0.09	0.07	18	0.01	0.20	0.07	0.12	0.040
Organic Carbon(%)	118	0.054	0.05	0.05	23	0.01	0.12	0.04	0.07	0.024
Sand (%)	118	69.415	72	74	10	13	99	61	83	21.59
Silt (%)	118	25.398	22	1	15	1	81	14	32	20.24
Clay(%)	118	5.347	5	4	21	1	17	3	7	3.41
K _s (cm/hr)	112	0.712*	0.619	0.19	2	0.002	72.471	0.162	2.749	15.257
Porosity	118	0.388	0.394	Multiple		0.293	0.525	0.345	0.425	0.050
Saturated Water Content	118	0.307	0.299	Multiple		0.133	0.471	0.263	0.341	0.059
<u>DANR - loam</u>										
Bulk Density (g/cm ³)	4	1.575	1.57	1.57	3	1.570	1.590	1.570	1.580	0.010
Organic Matter (%)	4	0.115	0.115	Multiple		0.090	0.140	0.095	0.135	0.024
Organic Carbon(%)	4	0.065	0.065	Multiple		0.050	0.080	0.055	0.075	0.013
Sand (%)	4	46.250	46.5	49	2	43	49	43.5	49.0	3.202
Silt (%)	4	46.500	46.5	Multiple		43	50	43.5	49.5	3.512
Clay(%)	4	7.250	7.0	7	3	7	8	7	7.5	0.5
K _s (cm/hr)	4	0.054*	0.062	Multiple		0.017	0.206	0.020	0.152	0.088
Porosity	4	0.406	0.408	0.408	2	0.400	0.409	0.404	0.409	0.004
Saturated Water Content	4	0.320	0.32	Multiple		0.301	0.339	0.304	0.336	0.019
<u>DANR - loamy sand</u>										
Bulk Density (g/cm ³)	27	1.664	1.65	Multiple		1.430	1.870	1.590	1.770	0.121
Organic Matter (%)	27	0.088	0.08	0.07	7	0.030	0.170	0.070	0.120	0.037
Organic Carbon(%)	27	0.051	0.05	0.04	7	0.020	0.100	0.040	0.070	0.021
Sand (%)	27	79.407	79	74	6	74	89	75	83	4.308
Silt (%)	27	16.889	16	15	5	1	25	15	21	5.056
Clay(%)	27	3.778	4	Multiple		1	12	1	5	2.562
K _s (cm/hr)	26	0.636*	0.619	Multiple		0.027	6.166	0.341	1.480	1.504
Porosity	27	0.372	0.376	0.361	2	0.293	0.460	0.332	0.399	0.045
Saturated Water Content	27	0.271	0.267	Multiple		0.133	0.389	0.248	0.293	0.047
<u>DANR – sand</u>										
Bulk Density (g/cm ³)	23	1.542	1.510	1	3	1.460	1.850	1.480	1.560	0.100
Organic Matter (%)	23	0.057	0.060	0	8	0.010	0.120	0.040	0.070	0.024
Organic Carbon(%)	23	0.033	0.030	Multiple		0.010	0.070	0.020	0.040	0.014
Sand (%)	23	96.391	97	Multiple		87	99	95	98	2.872
Silt (%)	23	2.087	1	1	14	1	11	1	2	2.353
Clay(%)	23	2.130	2	1	10	1	7	1	3	1.424
K _s (cm/hr)	23	11.072*	16.500	Multiple		0.407	72.471	2.018	51.148	25.266
Porosity	23	0.418	0.429	Multiple		0.302	0.450	0.411	0.443	0.038
Saturated Water Content	23	0.310	0.307	Multiple		0.222	0.399	0.281	0.340	0.047
<u>DANR - sandy loam</u>										
Bulk Density (g/cm ³)	46	1.695	1.715	1.74	4	1.510	1.870	1.640	1.770	0.099
Organic Matter (%)	46	0.108	0.100	Multiple		0.030	0.200	0.080	0.130	0.040
Organic Carbon(%)	46	0.062	0.060	Multiple		0.020	0.120	0.050	0.080	0.024
Sand (%)	46	67.565	68.500	Multiple		51	87	63	72	6.781
Silt (%)	46	25.000	24	Multiple		8	43	21	28	6.864
Clay(%)	46	7.500	7	7.0	8	2	15	5	9	3.017
K _s (cm/hr)	41	0.325*	0.334	0.188	2	0.002	24.600	0.089	1.523	4.451
Porosity	46	0.360	0.354	Multiple		0.294	0.430	0.332	0.381	0.037
Saturated Water Content	46	0.288	0.282	Multiple		0.229	0.397	0.253	0.313	0.040

Table 4.2.2. continued

	Valid N	Mean	Median	Mode	Mode Frequency	Minimum	Maximum	Lower Quartile	Upper Quartile	Std. Deviation
<u>DANR - silt loam</u>										
Bulk Density (g/cm ³)	17	1.475	1.48	Multiple		1.26	1.63	1.41	1.58	0.1149
Organic Matter (%)	17	0.112	0.12	0.13	4	0.06	0.18	0.09	0.13	0.03504
Organic Carbon(%)	17	0.064	0.07	0.07	4	0.03	0.1	0.05	0.08	0.02093
Sand (%)	17	30.706	34	40	3	13	44	25	40	10.01102
Silt (%)	17	63.294	63	Multiple		50	76	54	70	8.79463
Clay(%)	17	6.000	4	4	7	3	17	4	7	3.4821
K _s (cm/hr)	17	0.289*	0.268	Multiple		0.00262	15.4	0.106	0.799	3.68542
Porosity	17	0.441	0.437	0.402	2	0.385	0.525	0.402	0.469	0.04411
Saturated Water Content	17	0.400	0.408	Multiple		0.329	0.471	0.366	0.426	0.04147

* geometric mean used for K_s

Table 4.3.1. Summary of the optimized van Genuchten parameters.

LOW GUESS										MEDIUM GUESS						HIGH GUESS						
MSO run #	MSO cell #	core #	sample #	α (cm ⁻¹)	n	Θ_r (cm ³ /cm ³)	K _s (cm/hr)	% mbe	ssq	α (cm ⁻¹)	n	Θ_r (cm ³ /cm ³)	K _s (cm/hr)	% mbe	ssq	α (cm ⁻¹)	n	Θ_r (cm ³ /cm ³)	K _s (cm/hr)	% mbe	ssq	
3	1	3-10-1	6	0.035	5.367	0.000	0.045	0.125	4.351	0.031	7.469	0.069	3.057	0.746	0.492	n/a						
3	2	3-10-2	3	0.046	5.002	0.079	14.57	0.042	0.682	0.046	5.013	0.080	14.862	0.141	0.689	n/a						
3	3	5-10-2	9	n/a						0.046	4.611	0.055	37.793	0.392	2.568	n/a						
3	4	5-10-2	10	0.031	3.520	0.000	0.092	0.734	7.949	0.043	4.898	0.054	22.611	0.346	1.999	n/a						
3	5	10-8-2	6	0.027	4.133	0.000	0.078	0.254	1.672	0.037	5.018	0.093	99.534	0.279	1.819	0.022	2.576	0.0001	0.0302	0.7425	10.730	
3	6	10-8-2	8	0.044	5.046	0.060	60.49	0.420	3.653	0.044	5.130	0.062	69.624	0.122	3.656	0.034	4.421	0.0001	0.0611	0.8987	10.01	
3	7	10-8-5	3	0.037	3.605	0.000	0.133	0.559	5.171	0.052	5.246	0.122	24.237	0.848	1.575	0.053	5.243	0.1218	24.502	0.8630	1.575	
3	8	10-8-5	7	0.036	4.674	0.045	23.97	0.069	1.451	0.036	4.679	0.045	24.134	0.081	1.451	0.042	6.027	0.0001	0.0243	2.5369	13.65	
3	9	10-10-2	8	0.026	4.998	0.155	22.73	0.235	1.219	0.026	5.003	0.155	22.972	1.217	1.220	0.019	4.789	0.0001	0.0351	0.1066	6.043	
3	10	10-10-2	9	0.027	3.558	0.166	1.44	0.105	0.517	0.027	3.563	0.166	1.451	0.165	0.516							
4	1	5-10-2	20	0.005	2.734	0.000	0.12	1.208	0.309	0.005	3.081	0.032	0.152	4.112	0.302	n/a						
4	2	10-8-5	17	0.009	1.711	0.000	0.036	0.892	0.655	0.019	2.424	0.097	26.632	0.002	0.296	0.192	8.861	0.1570	0.0001	NaN	2.015	
4	3	10-10-5	3	0.055	4.970	0.050			0.004	0.055	4.970	0.050			0.004	0.055	4.970	0.0500			0.0040	
4	4	11-8-2	8	0.034	3.833	0.074			0.000	0.034	3.833	0.074			0.000	0.034	3.833	0.0738			0.0002	
4	5	11-8-2	16	0.003	3.063	0.000	0.178	0.104	0.138	0.003	3.433	0.046	0.232	0.378	0.141	n/a						
4	6	11-10-5	3	0.048	3.933	0.079			0.000	0.048	3.933	0.079			0.000	0.048	3.933	0.0786			0.0002	
4	7	12-10-2	3	0.077	3.597	0.063			0.000	0.077	3.597	0.063			0.000	0.077	3.597	0.0629			0.0004	
4	8	13-8-2	4	0.078	3.551	0.050			0.000	0.078	3.551	0.050			0.000	0.078	3.549	0.0500			0.0005	
4	9	13-10-2	3	0.061	3.910	0.060			0.001	0.061	3.910	0.060			0.001	0.061	3.910	0.0603			0.0012	
4	10	13-10-5	2	0.060	3.911	0.066			0.000	0.060	3.911	0.066			0.000	0.060	3.911	0.0664			0.0005	
5	1	4-10-5	10	0.007	2.700	0.258	0.029	0.212	0.201	0.007	2.760	0.258	0.028	0.199	0.201	n/a						
5	2	4-10-5	16	0.004	1.404	0.003	0.085	0.234	0.476	0.004	2.225	0.150	0.214	0.174	0.254	n/a						
5	3	10-8-2	5	0.009	3.290	0.143	0.811	0.023	1.264	0.008	3.933	0.148	1.203	0.307	1.090							
5	4	10-8-2	13	0.005	1.658	0.000	0.056	0.360	0.626	0.005	1.663	0.001	0.055	0.354	0.626	n/a						
5	5	10-8-5	12	0.004	1.237	0.008	0.602	0.181	0.497	0.004	1.547	0.210	0.356	0.248	0.465	0.002	1.6939	0.0001	0.0047	0.1669	1.311	
5	6	10-8-5	16	0.009	1.893	0.000	0.228	0.471	0.768	0.008	2.346	0.042	0.416	0.169	0.692							
5	7	11-8-2	7	0.006	2.003	0.000	0.072	0.391	0.883	0.006	1.983	0.000	0.074	0.398	0.883	n/a						
5	8	11-8-2	14	0.015	2.686	0.030	1.267	0.285	0.735	0.015	2.720	0.032	1.375	0.269	0.735	n/a						
5	9	13-8-5	7	0.003	1.271	0.075	0.017	0.249	0.412	0.002	1.400	0.064	0.018	0.219	0.348	n/a						
5	10	13-8-5	11	0.005	1.759	0.000	0.011	0.475	2.662	0.013	1.479	0.001	0.241	0.409	1.363	0.013	1.4771 6	0.0001	0.2420	0.4087 0	1.363	
6	1	3-10-5	14	0.008	4.557	0.211	0.630	0.221	0.296	0.008	4.586	0.211	0.652	0.162	0.295	0.090	1.0826	0.0001	30.0	0.1465	0.573	
6	2	3-10-5	17	0.005	1.384	0.000	0.310	0.225	0.334	0.006	1.932	0.131	0.260	0.231	0.319	0.005	1.3873	0.0002	0.3068	0.2098	0.3334	
6	3	5-10-2	17	0.007	1.046	0.033	0.739	0.216	0.770	0.015	2.667	0.279	2.230	0.600	0.305	n/a						
6	4	5-10-2	19							NO MSO DATA AVAILABLE FOR THIS SAMPLE												
6	5	10-10-2	6	0.011	2.721	0.154	0.223	0.610	0.385	0.011	2.717	0.155	0.254	0.211	0.363	0.005	1.7478	0.0001	0.0068	0.2299	1.545	
6	6	10-10-2	14	0.012	1.337	0.001	2.345	0.196	0.566	0.011	1.724	0.138	1.439	0.209	0.515	n/a						
6	7	12-10-2	10							NO MSO DATA AVAILABLE FOR THIS SAMPLE												
6	8	12-10-2	13	0.006	2.459	0.028	0.197	0.552	0.469	0.006	2.680	0.050	0.253	0.158	0.409	0.006	2.2187	0.0001	0.1887	0.1622	0.49	
6	9	13-10-2	12	0.002	2.066	0.000	0.057	0.251	0.231	0.003	2.599	0.130	0.126	0.138	0.222	0.002	2.0004	0.0002	0.0769	0.1039	0.226	

Table 4.3.1. continued

				LOW GUESS						MEDIUM GUESS						HIGH GUESS					
MSO run #	MSO cell #	core #	sample #	α (cm ⁻¹)	n	Θ_r (cm ³ /cm ³)	K_s (cm/hr)	% mbe	ssq	α (cm ⁻¹)	n	Θ_r (cm ³ /cm ³)	K_s (cm/hr)	% mbe	ssq	α (cm ⁻¹)	n	Θ_r (cm ³ /cm ³)	K_s (cm/hr)	% mbe	ssq
6	10	13-10-5	11	0.042	1.319	0.000	5.11	0.058	1.663	0.007	4.569	0.151	0.370	0.046	0.580	0.007	4.5638	0.1514	0.3685	0.0265	0.58
7	1	3-10-1	2	0.028	1.217	0.000			0.000	0.028	1.217	0.000			0.000	0.028	1.2315	0.0124			0.001
7	2	3-10-1	5	0.005	1.673	0.000			0.000	0.005	1.673	0.000			0.000	n/a					
7	3	3-10-4	3	0.017	1.435	0.090			0.000	0.017	1.435	0.090			0.000	n/a					
7	4	3-10-4	4	0.015	1.536	0.090			0.000	0.015	1.536	0.090			0.000	0.015	1.5364	0.0900			0.0003
7	5	4-10-5	2	0.007	1.657	0.019			0.000	0.007	1.691	0.031			0.000	0.007	1.7115	0.0368			0.0001
7	6	10-8-5	2	0.010	2.036	0.090			0.000	0.010	2.036	0.090			0.000	0.010	2.0360	0.0900			0.0001
7	7	10-10-2	2	0.027	1.300	0.000			0.000	0.027	1.300	0.000			0.000	0.027	1.2996	0.0001			0.0001
7	8	11-10-5	2	0.011	2.407	0.084			0.000	0.011	2.407	0.084			0.000	0.011	2.4069	0.0841			0.0001
7	9	12-10-2	2	0.022	2.197	0.090			0.001	0.022	2.197	0.090			0.001	0.022	2.1973	0.0900			0.0011
7	10	13-10-5	1	0.018	2.078	0.090			0.000	0.018	2.078	0.090			0.000	0.018	2.0781	0.0900			0.0004
8	1	10-10-5	11	0.007	1.183	0.000			0.000	0.008	1.237	0.084			0.000	0.008	1.2362	0.0809			0.0002
8	2	10-10-5	12	0.006	1.784	0.090			0.000	0.006	1.784	0.090			0.000	n/a					
8	3	11-10-5	5	0.017	1.474	0.090			0.000	0.017	1.474	0.090			0.000	n/a					
8	4	11-10-5	6	0.012	1.450	0.090			0.000	0.012	1.450	0.090			0.000	n/a					
8	5	11-10-5	7	0.016	1.342	0.090			0.000	0.016	1.342	0.090			0.000	0.016	1.3421	0.0900			0.0003
8	6	11-10-5	11	0.022	1.137	0.090			0.000	0.022	1.137	0.090			0.000	0.022	1.1368	0.0900			0.0003
8	7	11-10-5	13	0.019	1.114	0.000			0.000	0.021	1.136	0.061			0.000	0.020	1.1646	0.0896			0.0002
8	8	12-10-2	12	0.023	1.193	0.090			0.000	0.023	1.193	0.090			0.000	0.023	1.1927	0.0900			0.0004
8	9	13-8-2	11	0.016	1.128	0.058			0.000	0.016	1.141	0.090			0.000	0.016	1.1414	0.0900			0.0004
8	10	13-8-2	12	0.003	1.367	0.090			0.000	0.003	1.367	0.090			0.000	0.003	1.3669	0.0900			0.0001
9	1	3-10-4	14	n/a						0.005	2.407	0.172	0.212	0.109	0.832	0.004	1.6226	0.0187	0.1360	0.1202	0.8477
9	2	3-10-4	19	0.005	1.259	0.000	1.275	0.237	0.541	0.007	1.870	0.268	1.616	0.063	0.521	0.007	1.9569	0.2890	2.5175	1.2160	4.5040
9	3	3-10-5	13	n/a						0.003	2.511	0.075	0.391	0.575	0.526	0.003	2.1784	0.0001	0.3320	0.1854	0.5339
9	4	4-10-5	5	0.007	3.136	0.122	0.793	0.203	0.476	0.007	3.139	0.122	0.794	0.283	0.476	n/a					
9	5	4-10-5	8	n/a						0.007	1.161	0.155	2.286	0.166	2.347	0.002	5.0424	0.0002	0.0139	0.7388	0.2154
9	6	10-8-5	14	0.011	1.451	0.241	13.443	0.074	0.110	0.012	2.054	0.318	30.000	0.631	0.098	0.013	1.1522	0.0017	30.0	0.0459	0.1266
9	7	11-10-5	10	0.011	2.854	0.169	1.941	0.338	0.850	0.010	2.901	0.170	1.914	0.235	0.852	0.010	2.8949	0.1696	1.9394	0.1609	0.8512
9	8	12-10-2	6	0.009	5.298	0.164	9.554	1.424	0.223	0.009	5.355	0.164	10.285	2.302	0.225	n/a					
9	9	13-8-5	15	0.001	2.153	0.000	0.204	0.301	0.024	0.001	2.146	0.000	0.204	0.188	0.024	n/a					
9	10	13-10-2	13	0.004	1.247	0.000	1.184	0.191	0.211	0.009	2.638	0.311	12.246	1.118	0.112	0.002	1.8108	0.0001	0.0782	0.1539	0.2083
10	1	4-10-5	13	n/a						n/a						n/a					
10	2	4-10-5	14	0.004	1.616	0.003	0.357	0.236	1.004	0.004	1.695	0.054	0.393	0.222	1.013	0.003	2.6438	0.0001	0.0081	0.1442	2.9090
10	3	5-10-2	18	0.011	1.866	0.364	0.201	0.237	0.234	0.011	1.868	0.364	0.201	0.205	0.234	0.011	1.7259	0.3571	0.2027	0.2090	0.2364
10	4	10-8-2	10	0.002	1.735	0.000	0.296	0.394	0.992	0.008	1.487	0.255	12.783	0.583	0.545	0.007	1.1823	0.0002	30.0	0.5387	0.5534
10	5	10-8-2	12	0.005	1.986	0.000	0.126	0.373	1.268	0.005	2.067	0.017	0.150	0.201	1.256	n/a					
10	6	10-8-5	9	0.002	1.665	0.000	0.023	0.195	0.782	0.011	1.422	0.166	1.069	0.178	0.456	n/a					
10	7	10-8-5	15	0.004	3.143	0.245	2.115	0.838	0.003	0.004	3.132	0.245	2.055	1.821	0.003	0.002	2.8172	0.0001	0.0142	0.4233	0.3447
10	8	10-10-5	13	0.011	2.534	0.363	4.960	0.987	0.592	0.011	2.908	0.369	30.000	5.500	0.545	0.005	1.6936	0.2258	0.0510	0.3631	1.1270

Table 4.3.1. continued

				LOW GUESS						MEDIUM GUESS						HIGH GUESS					
MSO run #	MSO cell #	core #	sample #	α (cm ⁻¹)	n	Θ_r (cm ³ /cm ³)	K_s (cm/hr)	% mbe	ssq	α (cm ⁻¹)	n	Θ_r (cm ³ /cm ³)	K_s (cm/hr)	% mbe	ssq	α (cm ⁻¹)	n	Θ_r (cm ³ /cm ³)	K_s (cm/hr)	% mbe	ssq
10	9	11-8-2	10	0.001	1.233	0.022	0.937	0.522	0.034	0.003	2.533	0.339	0.565	0.888	0.026	0.001	1.6657	0.0001	19.6319	28.788	0.0587
10	10	13-10-5	10	n/a						0.013	1.624	0.396	0.202	0.347	0.252	0.007	1.7093	0.3960	0.0077	0.3941	0.2282
11	1	3-10-1	8	0.005	1.433	0.000	0.254	0.201	0.150	0.012	1.976	0.158	2.732	0.287	0.113	0.008	1.3055	0.0001	0.6544	0.1842	0.1574
11	2	3-10-5	5	0.005	2.810	0.165	0.251	0.152	0.170	0.005	2.995	0.169	0.318	0.482	0.170	0.377	10.0	0.2000	0.0001	NaN	1.9860
11	3	5-10-2	3	n/a						0.003	1.206	0.008	0.338	0.164	0.416	n/a					
11	4	5-10-2	4	0.007	1.501	0.138	0.179	0.265	0.243	0.007	1.502	0.138	0.179	0.266	0.243	n/a					
11	5	10-10-2	3	n/a						0.010	1.872	0.110	2.829	0.335	1.232	0.011	2.7195	0.1677	24.1866	0.8611	1.0820
11	6	10-10-2	4	n/a						0.002	1.290	0.000	0.027	0.162	0.348	0.006	1.1215	0.0001	0.4808	0.1702	0.3451
11	7	11-8-2	4	n/a						0.012	2.474	0.143	2.557	0.310	1.367	0.012	2.4707	0.1426	2.5282	0.3611	1.3670
11	8	11-10-5	4	n/a						0.011	2.859	0.234	0.319	0.437	0.337	n/a					
11	9	13-8-2	6	n/a						0.004	1.359	0.005	0.358	0.183	0.428	0.004	1.3551	0.0021	0.3578	0.1753	0.4281
11	10	13-8-5	3	0.006	2.138	0.139	0.141	0.209	0.359	0.006	2.125	0.138	0.141	0.166	0.361	0.004	1.787	0.0001	0.0177	0.1685	0.9009
12	1	10-8-2	14	0.011	2.460	0.144	1.283	0.350	0.551	0.011	2.463	0.144	1.289	0.367	0.551	n/a					
12	2	10-8-2	15	n/a						0.003	1.415	0.139	0.020	0.155	0.121	0.002	1.2562	0.0169	0.0246	0.1583	0.1196
12	3	10-8-5	18	0.008	1.840	0.151	0.221	0.249	0.196	0.008	1.837	0.152	0.227	0.204	0.196	n/a					
12	4	10-10-5	19	0.006	1.662	0.000	0.276	0.529	0.345	0.007	2.027	0.072	0.370	0.766	0.291	0.007	2.0264	0.0723	0.3696	0.7720	0.2905
12	5	11-8-2	17	0.007	1.564	0.115	0.129	0.299	0.246	0.008	1.954	0.153	0.157	0.284	0.236	n/a					
12	6	11-10-5	17	0.017	1.715	0.117	3.111	0.305	0.628	0.016	1.718	0.117	3.095	0.349	0.628	0.016	1.7187	0.1172	3.0966	0.0034	0.6276
12	7	12-10-2	15	0.033	1.274	0.000	3.627	0.108	0.979	0.008	2.466	0.133	0.163	0.163	0.400	0.008	2.4598	0.1325	0.1623	0.0016	0.3997
12	8	13-8-2	16	0.009	2.359	0.120	0.751	0.176	0.921	0.009	2.360	0.120	0.751	0.173	0.921	n/a					
12	9	13-8-5	17	0.007	2.575	0.074	1.040	1.608	0.808	0.007	2.579	0.075	1.040	1.601	0.808	0.007	2.573	0.0743	1.0341	1.5724	0.8078
12	10	13-10-2	15	0.007	3.316	0.172	0.690	0.204	0.686	0.007	3.321	0.172	0.687	0.171	0.686	n/a					

Table 4.3.2. Summary statistics of the van Genuchten parameters.

	Valid N	Mean	Median	Mode	Mode Frequency	Minimum	Maximum	Lower Quartile	Upper Quartile	Std. Deviation
<u>ALL</u>										
α	97	0.016	0.010	.0074700	2	0.001	0.078	0.006	0.018	0.017
n	97	2.619	2.359	Multiple		1.122	7.469	1.658	3.136	1.280
θ_r	97	0.114	0.090	0.090	12	0.000	0.396	0.054	0.155	0.092
K_s	70	0.863*	0.523	30.000	2	0.008	99.534	0.212	2.732	15.940
<u>DANR - loam</u>										
α	2	0.005	0.005	Multiple		0.003	0.007	0.003	0.007	0.003
n	2	1.275	1.275	Multiple		1.183	1.367	1.183	1.367	0.130
θ_r	2	0.045	0.045	Multiple		0.000	0.090	0.000	0.090	0.064
K_s	0	n/a		Multiple						
<u>DANR - loamy sand</u>										
α	22	0.012	0.010	Multiple		0.003	0.028	0.006	0.015	0.008
n	22	2.459	2.286	Multiple		1.217	5.298	1.673	2.717	1.002
θ_p	22	0.096	0.090	0.090	4	0.000	0.279	0.042	0.151	0.073
K_s	14	0.5*	0.315	Multiple		0.056	9.554	0.214	1.451	2.475
<u>DANR - sand</u>										
α	18	0.044	0.045	Multiple		0.005	0.078	0.034	0.055	0.019
n	18	4.454	4.642	Multiple		2.424	7.469	3.833	5.002	1.093
θ_r	18	0.072	0.065	.0500000	2	0.032	0.155	0.054	0.079	0.029
K_s	11	15.496*	23.974	Multiple		0.152	99.534	14.566	37.793	28.041
<u>DANR - sandy loam</u>										
α	39	0.009	0.008	Multiple		0.002	0.023	0.006	0.012	0.005
n	39	2.104	1.976	Multiple		1.122	4.586	1.450	2.599	0.787
θ_r	39	0.106	0.120	.0900000	6	0.000	0.258	0.032	0.153	0.069
K_s	31	0.447*	0.358	Multiple		0.025	24.187	0.163	1.203	4.290

Table 4.3.2. continued

	Valid N	Mean	Median	Mode	Mode Frequency	Minimum	Maximum	Lower Quartile	Upper Quartile	Std. Deviation
DANR - silt loam										
α	16	0.008	0.007	Multiple		0.001	0.022	0.003	0.011	0.006
n	16	2.195	1.962	Multiple		1.128	5.042	1.517	2.586	0.973
θ_r	16	0.210	0.250	Multiple		0.000	0.396	0.069	0.329	0.140
K_s	14	0.66*	0.478	30.000	2	0.008	30.000	0.201	12.246	10.869

* geometric mean used for K_s

Table 4.5.1. Summary of percent reduction in sum of squares (SS) for subgroup "sandy loam" in groups 2, 3, and 4 using two scaling methods.

Group	Reduction in SS (%)	
	Method 1	Method 2
Group 2	83.6	57.9
Group 3	85.3	60.0
Group 4	86.7	54.0

FIGURES

Figure 2.1.1. Fantasia Nectarine Orchard Plot

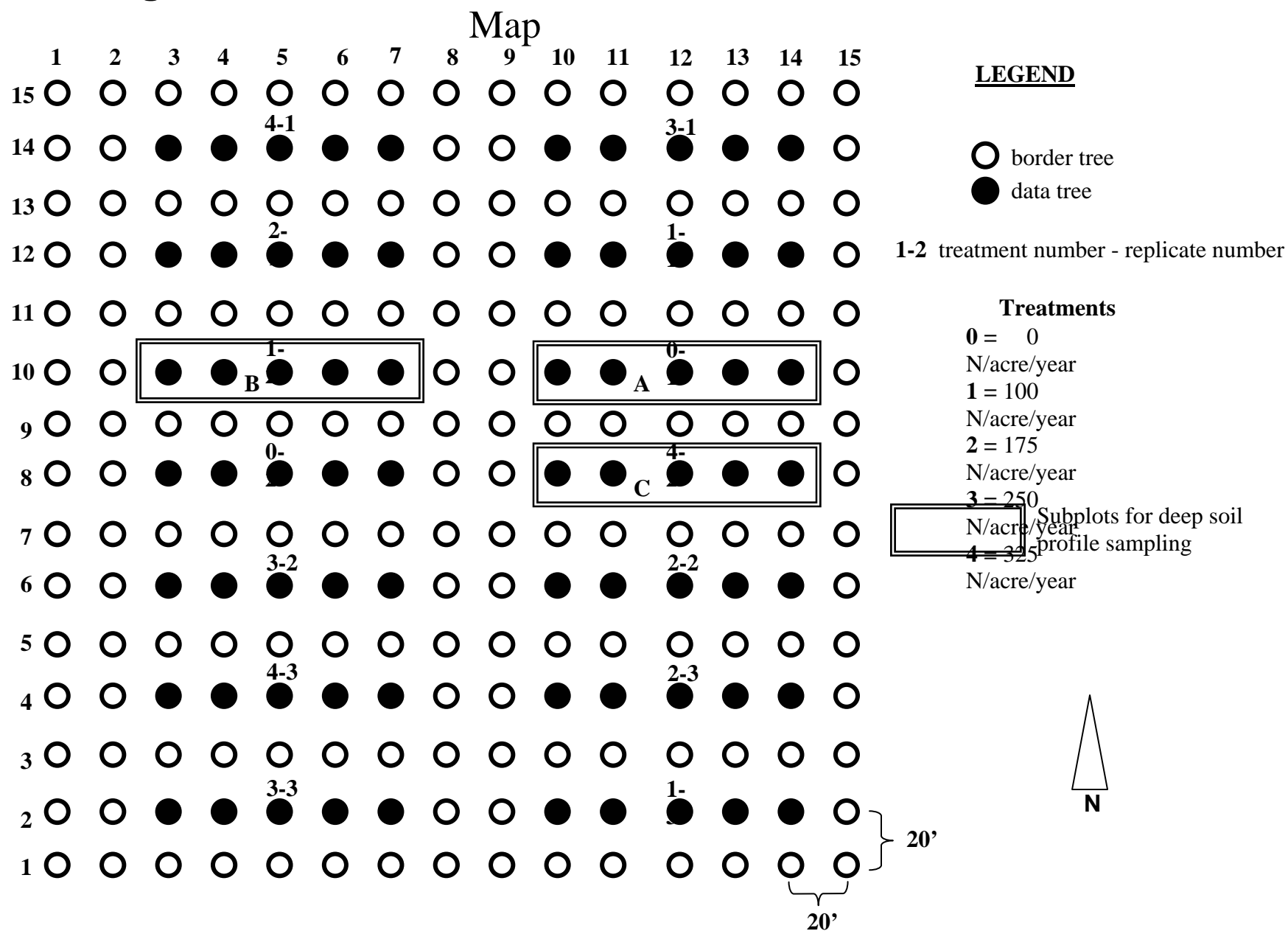
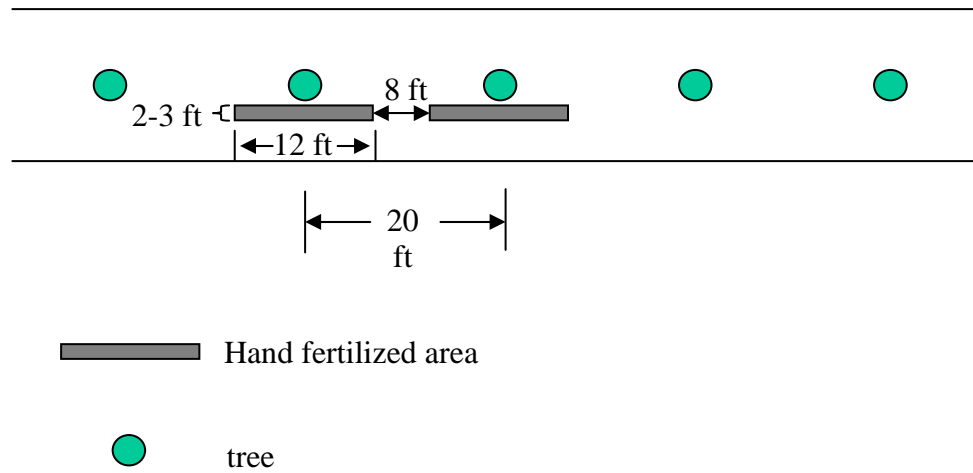


Figure 2.2.1. Hand Application of Fertilizer



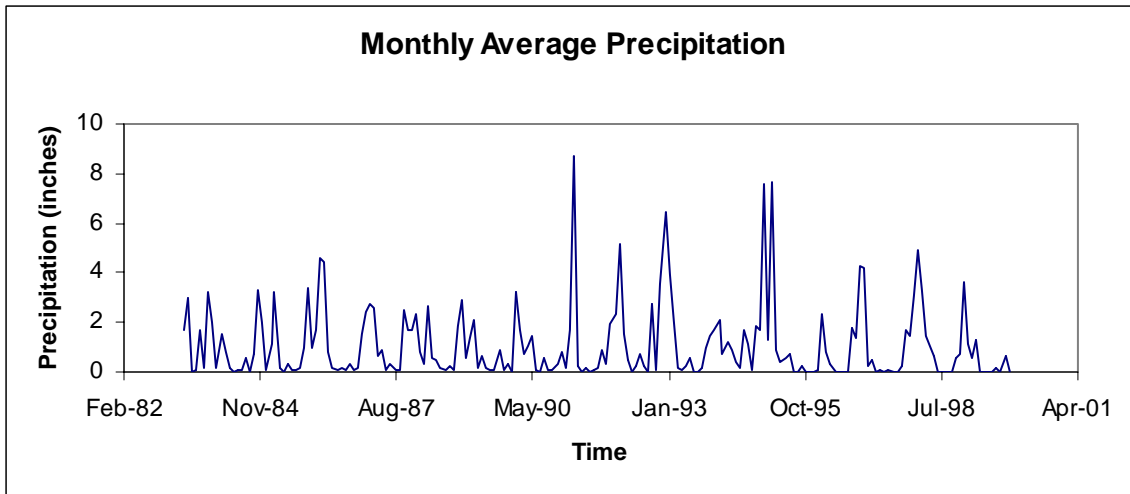


Figure 2.4.1. Average monthly precipitation from 1983 to 1999.

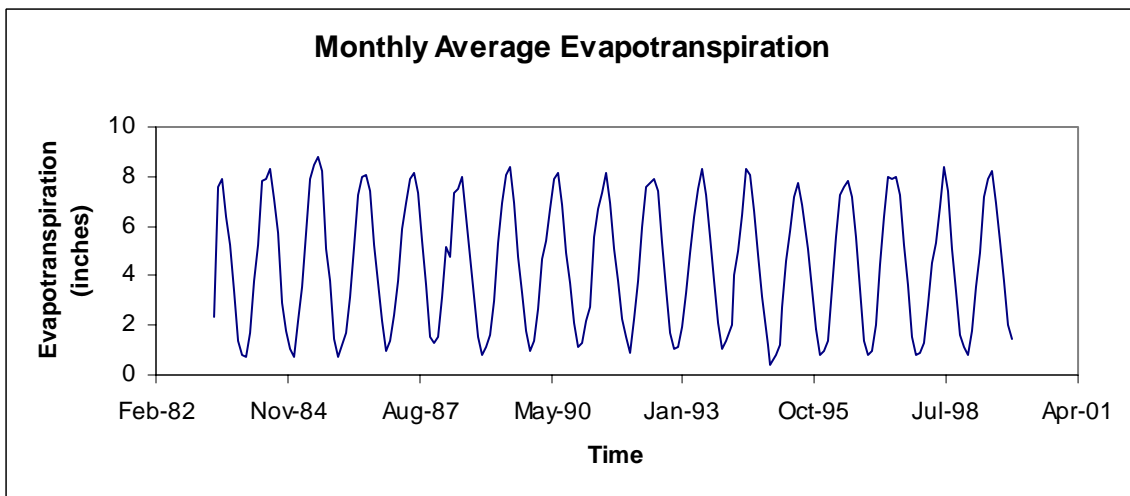


Figure 2.4.2. Average monthly ETo from 1983 to 1999.

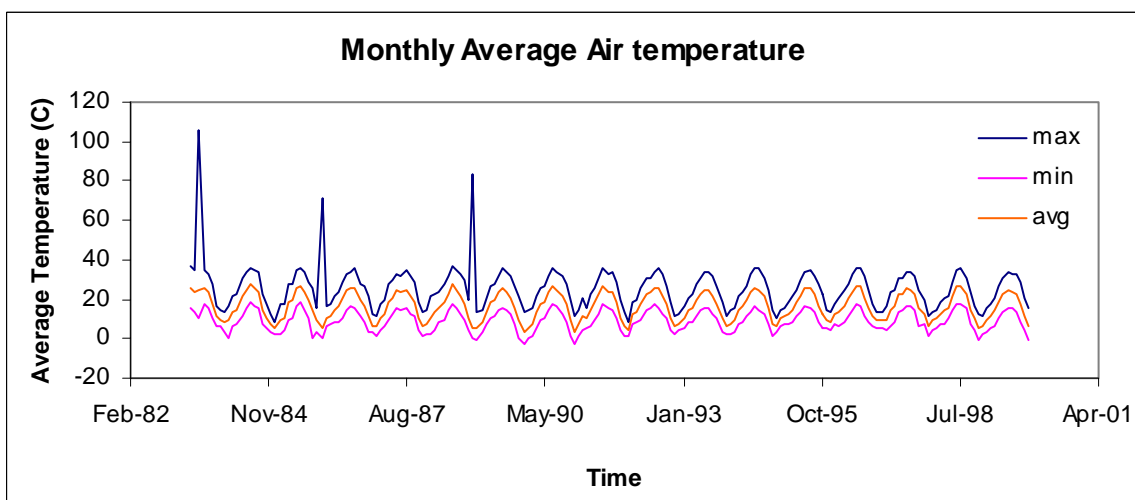


Figure 2.4.3. Average monthly air temperature from 1983 to 1999.

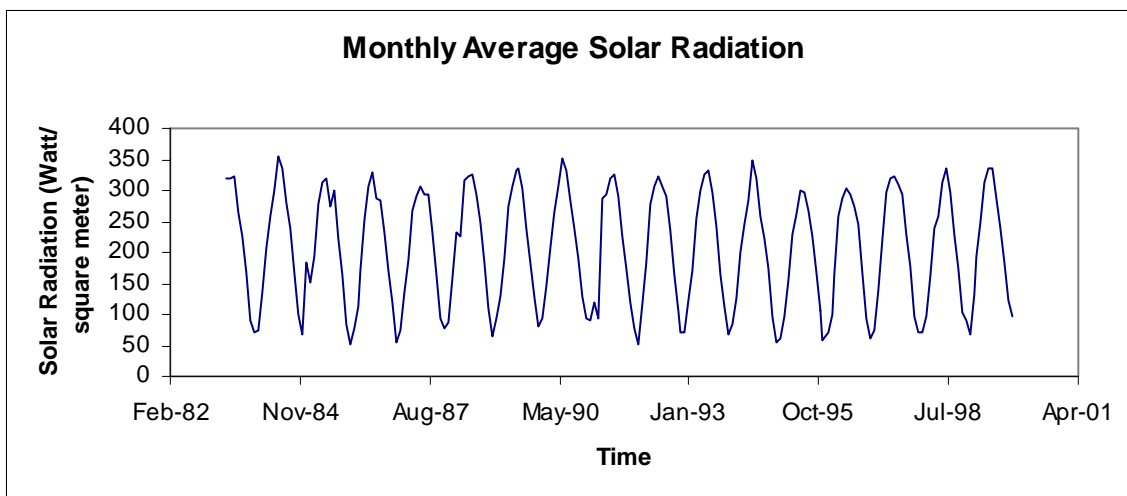


Figure 2.4.4. Average monthly solar radiation from 1983 to 1999.

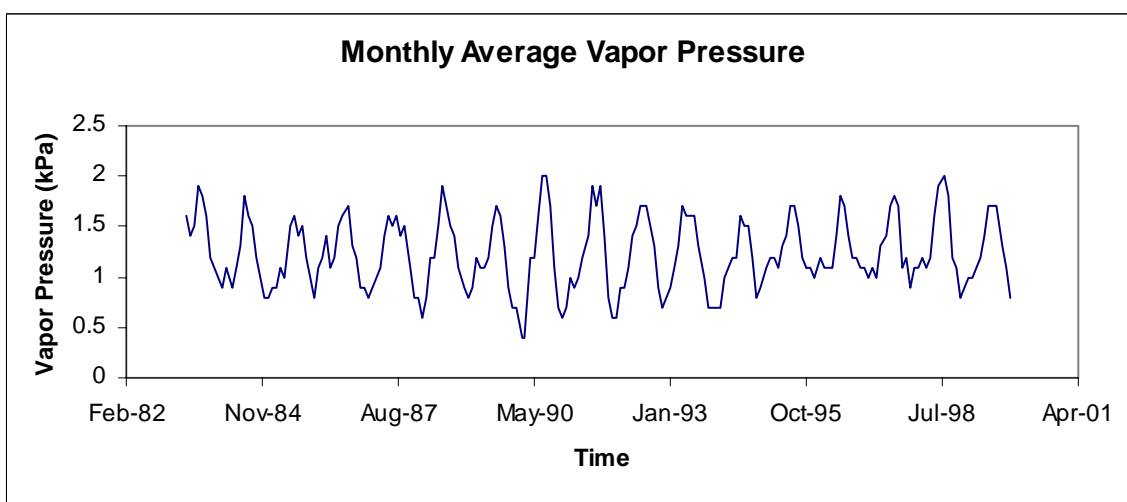


Figure 2.4.5. Average monthly vapor pressure from 1983 to 1999.

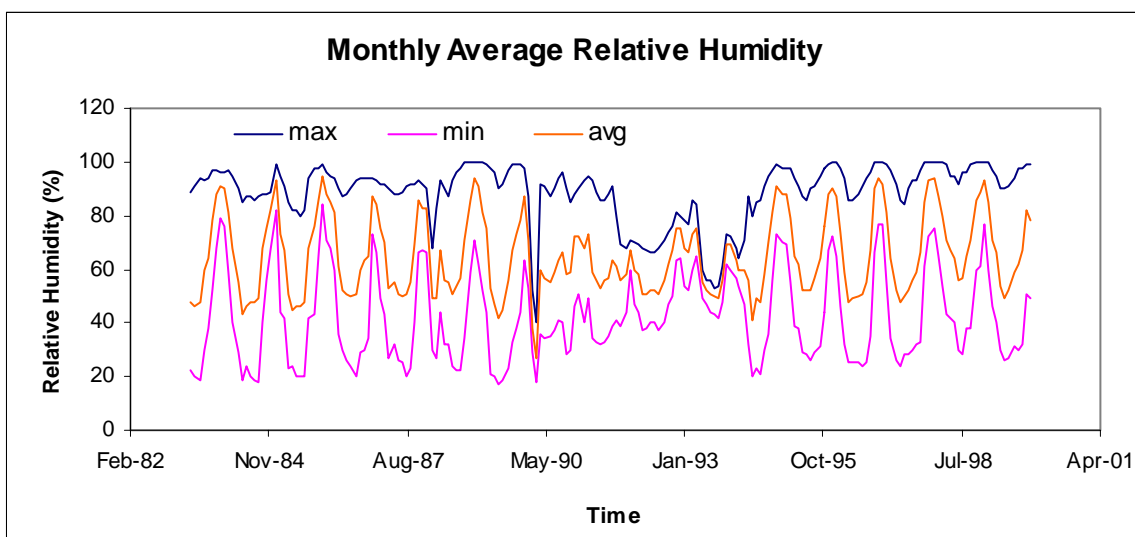


Figure 2.4.6. Average monthly relative humidity from 1983 to 1999.

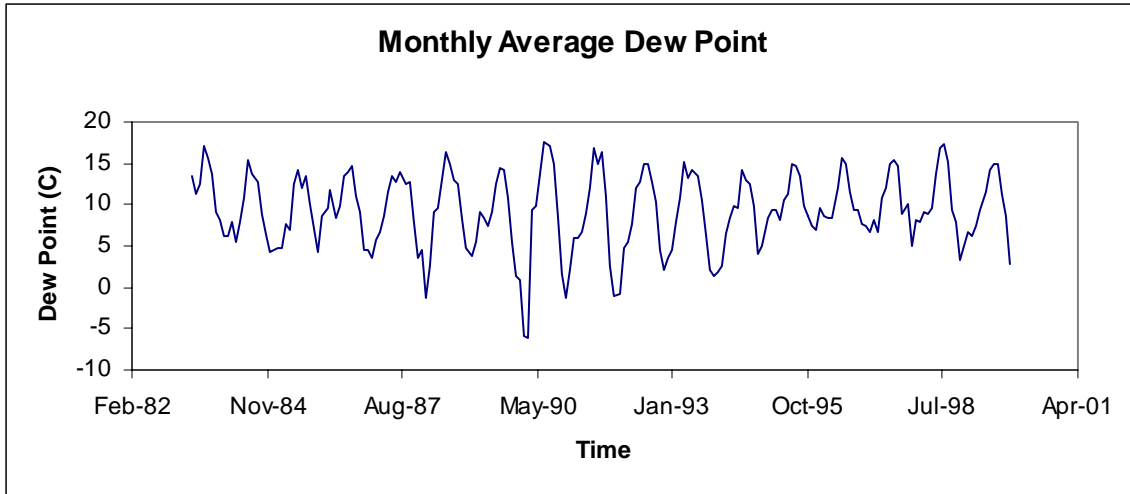


Figure 2.4.7. Average monthly dew point from 1983 to 1999.

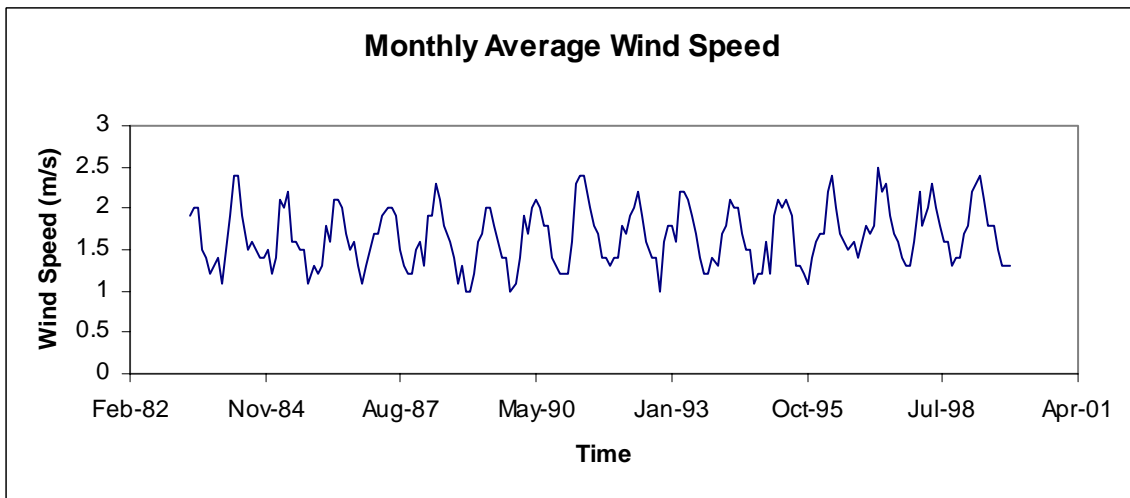


Figure 2.4.8. Average monthly wind speed from 1983 to 1999.

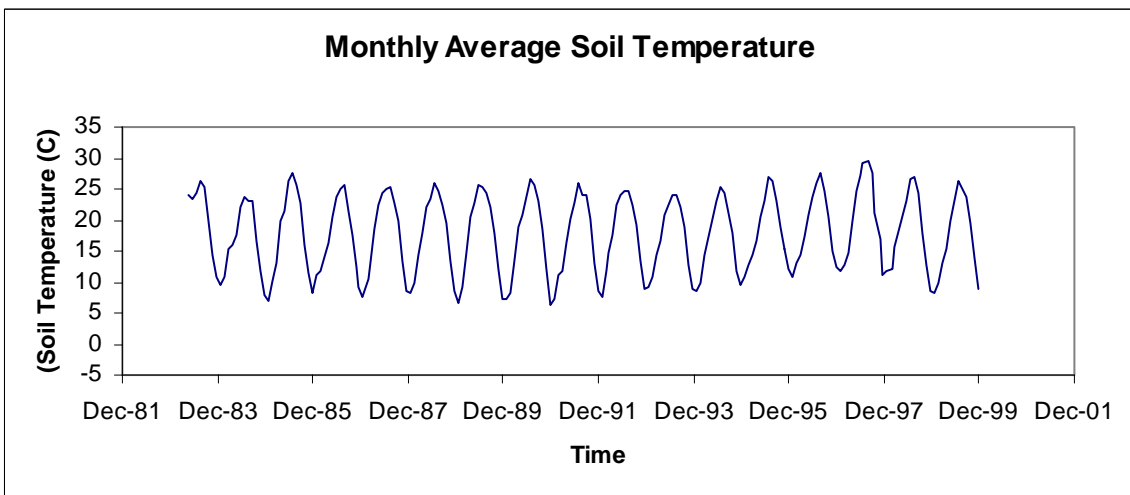


Figure 2.4.9. Average soil temperature from 1983 to 1999.

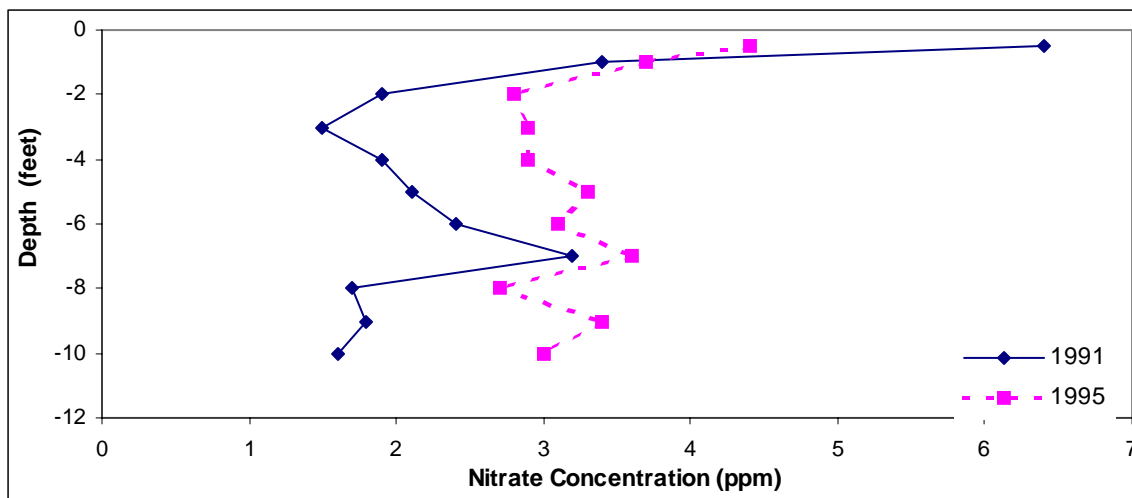


Figure 2.5.1a. Soil nitrate concentration measured in 1991 and 1995 for the 0 treatment subplot.

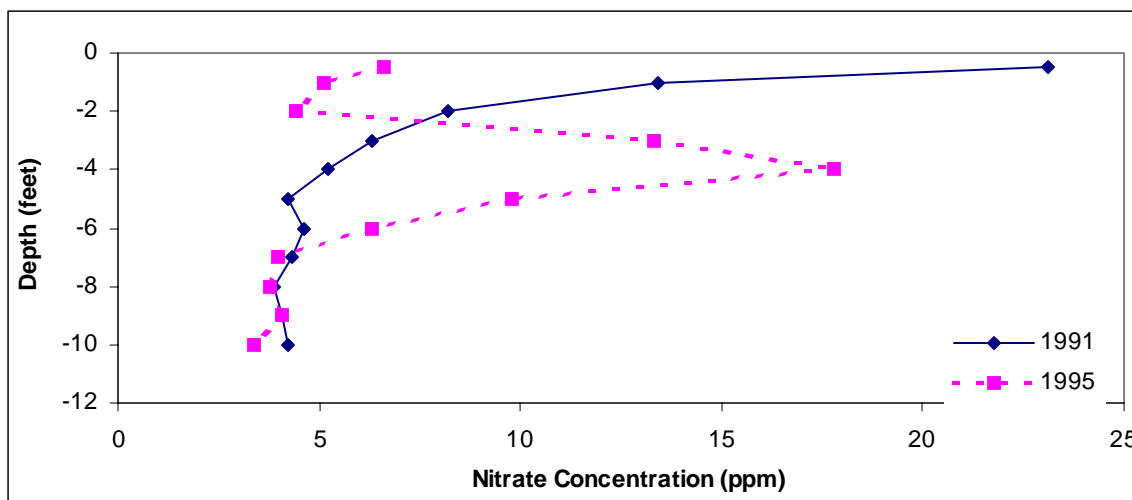


Figure 2.5.1b. Soil nitrate concentration for the 100 lbs N/acre subplot.

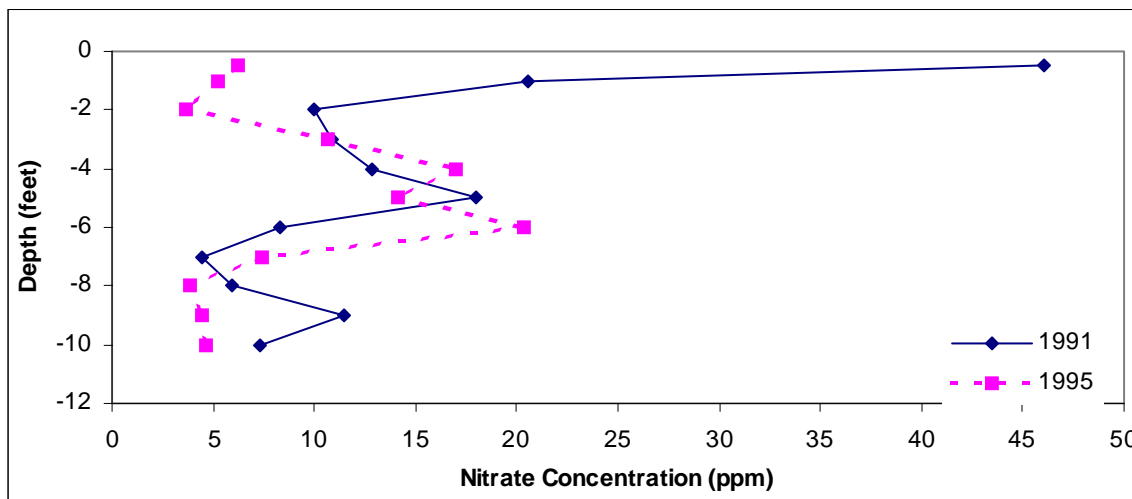


Figure 2.5.1c. Soil nitrate concentration for the 175 lbs N/acre subplot.

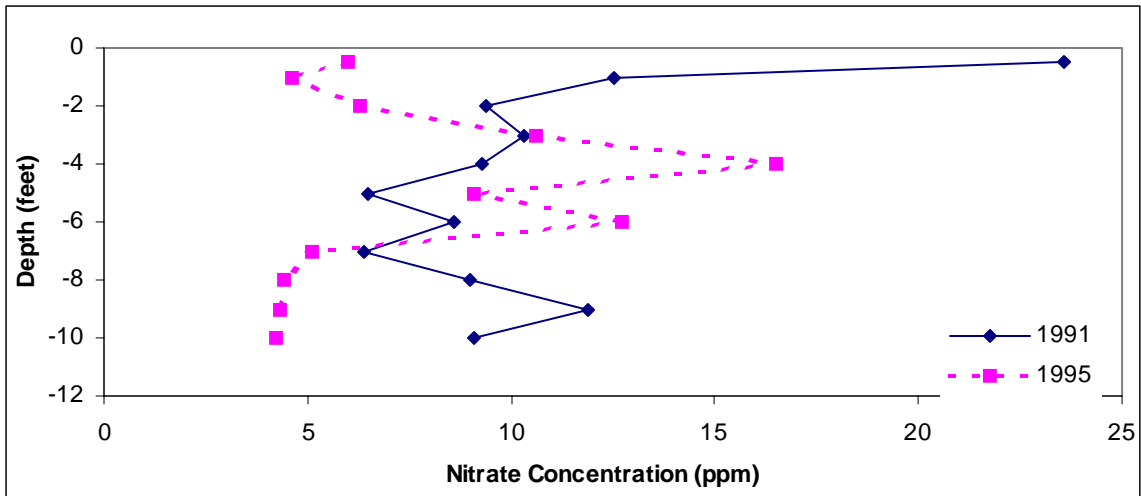


Figure 2.5.1d. Soil nitrate concentration for the 250 lbs N/acre subplot.

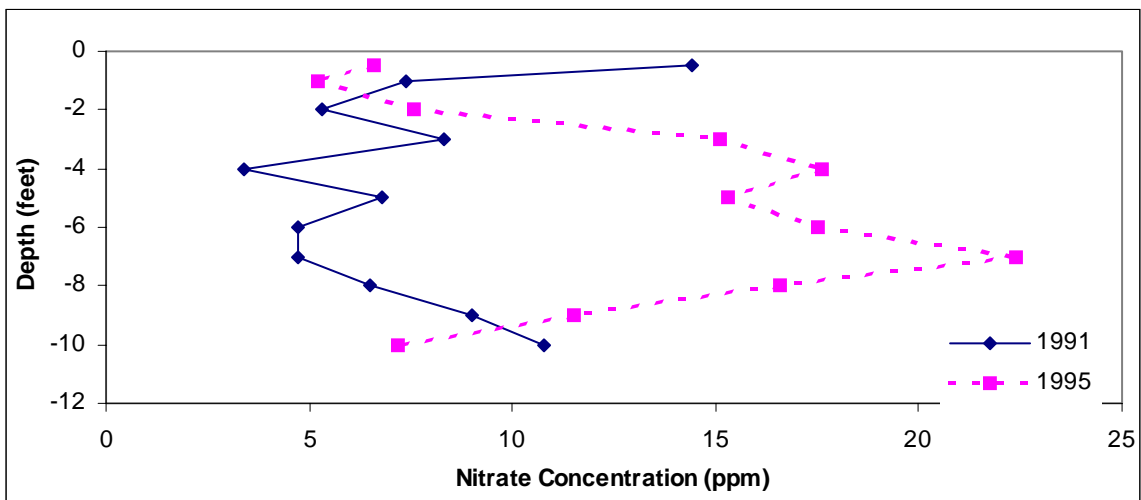


Figure 2.5.1e. Soil nitrate concentration for the 325 lbs N/acre subplot.

Figure 2.7.1. Fantasia Nectarine Soil Core Map

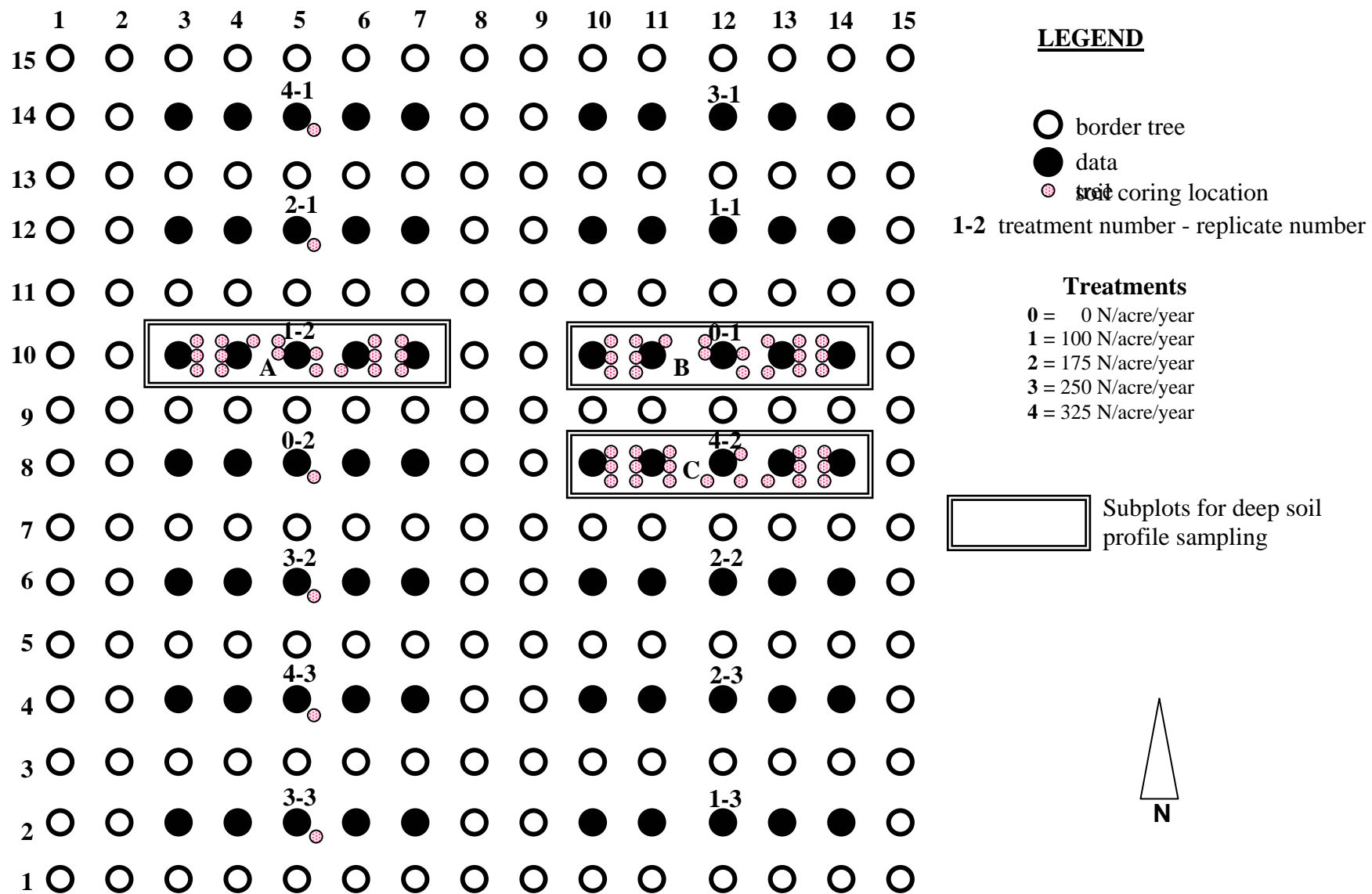


Figure 2.7.2. Deep Soil Profile Sampling Strategy

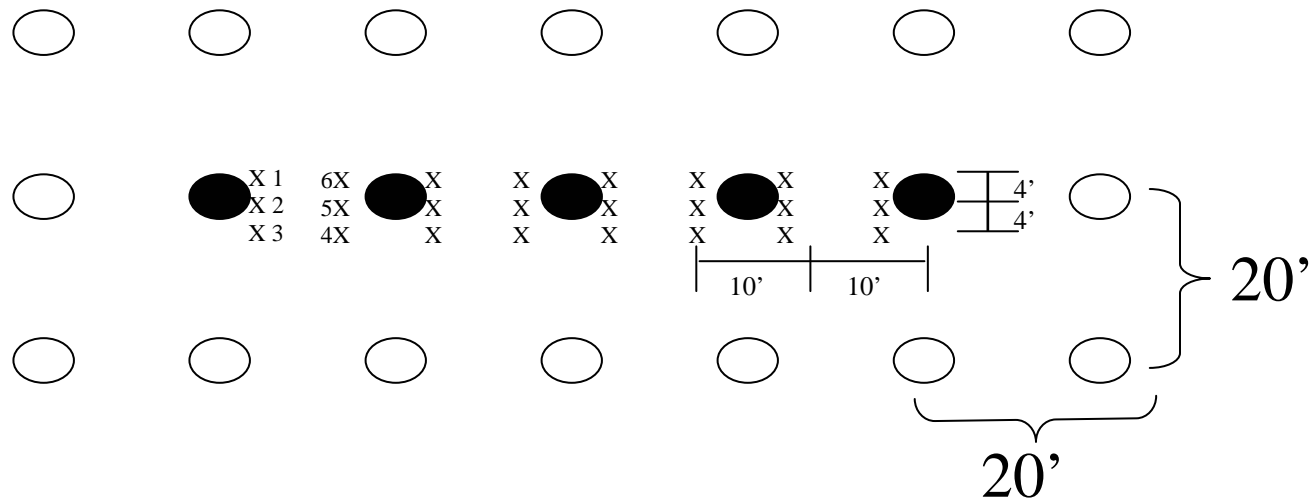
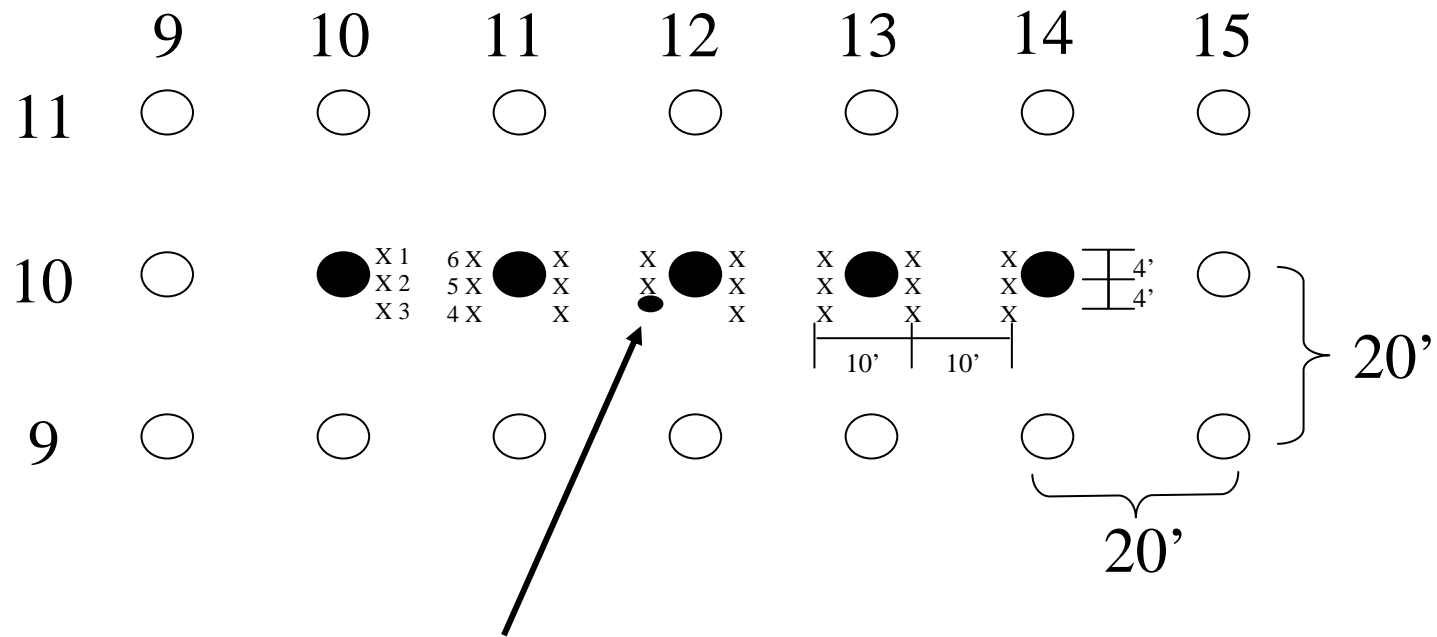
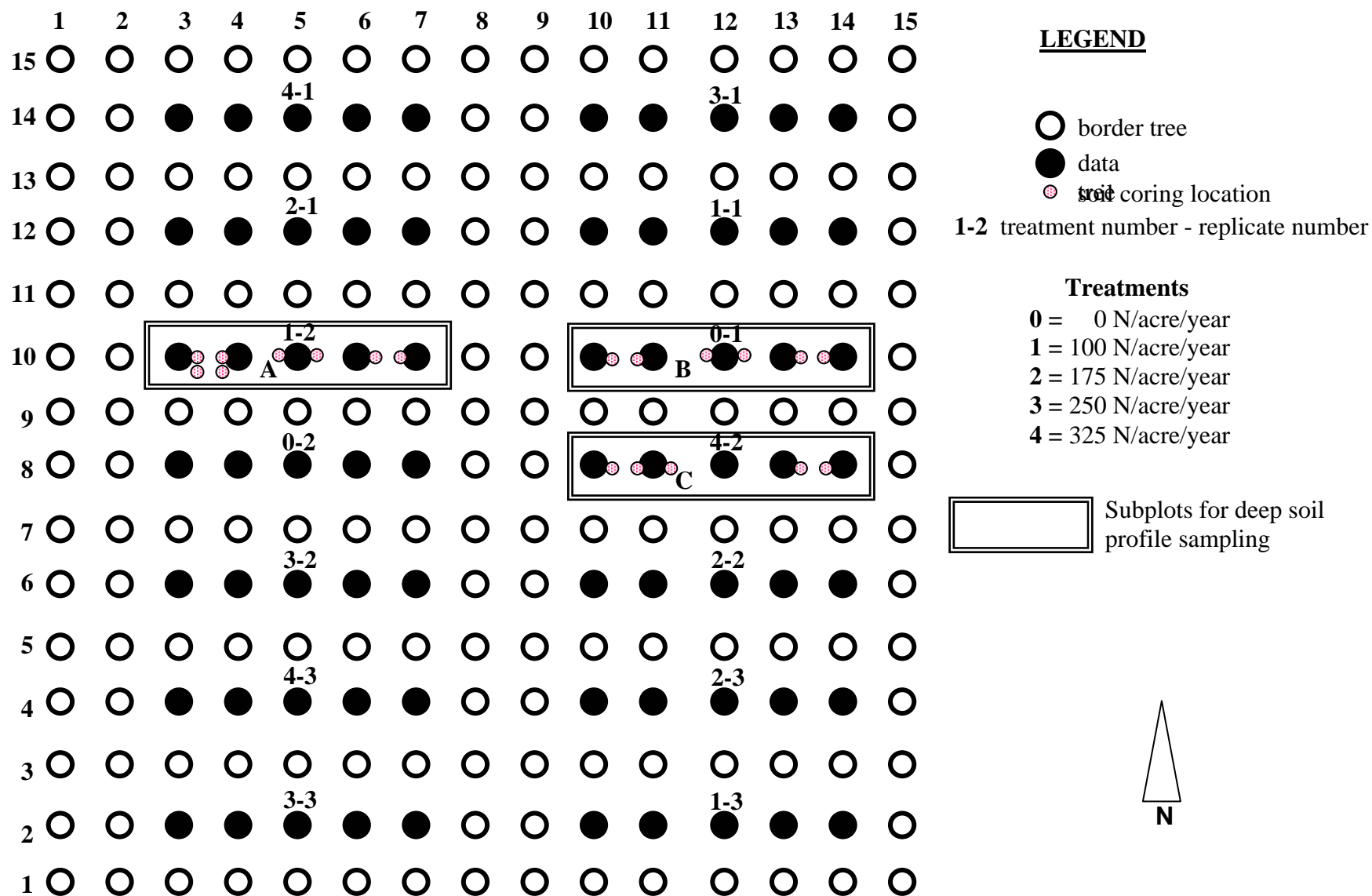


Figure 2.7.3. Soil Sample Numbering



Core number 11-10- 4

Figure 3.1.1. Fantasia Nectarine Hydraulic Soil Core Map



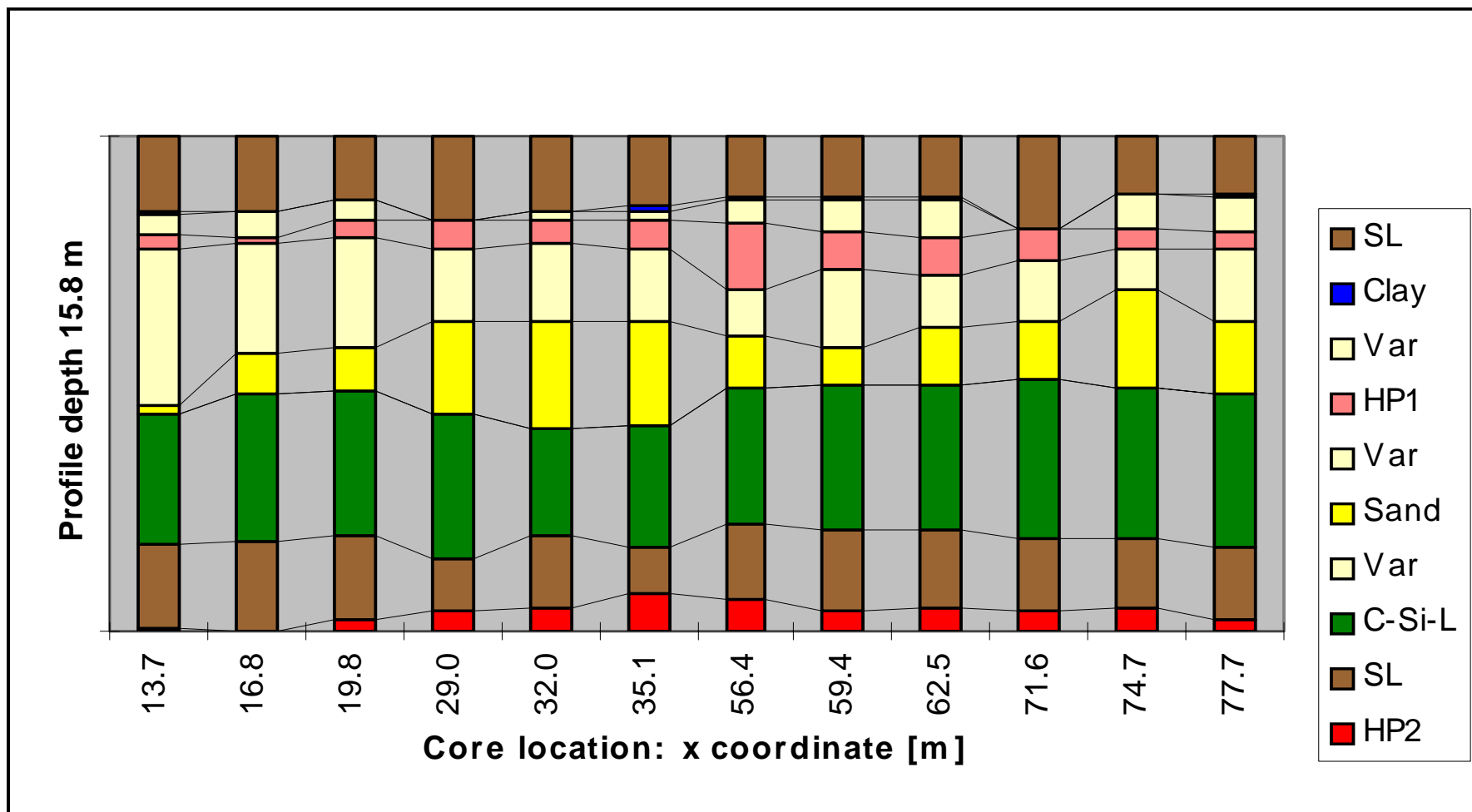
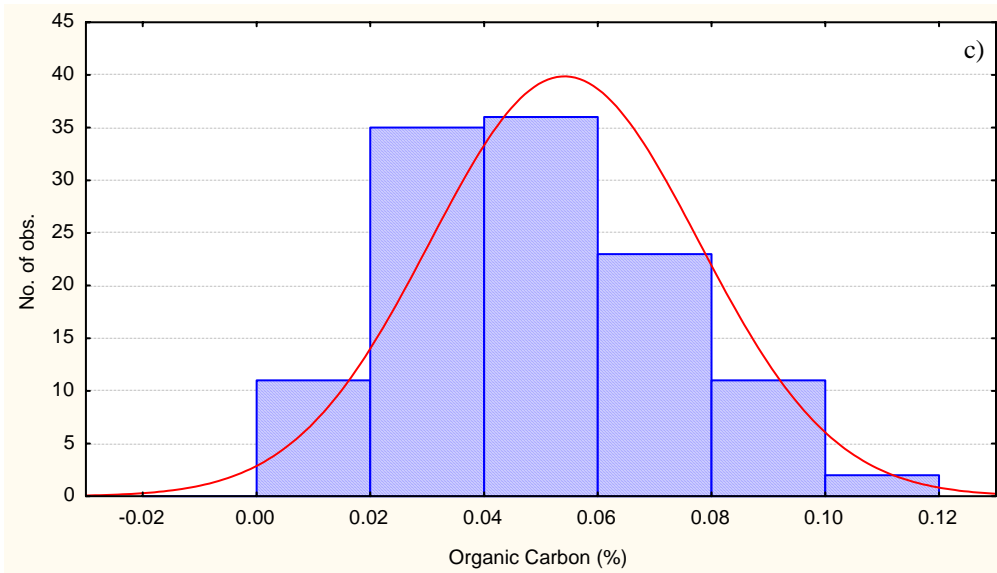
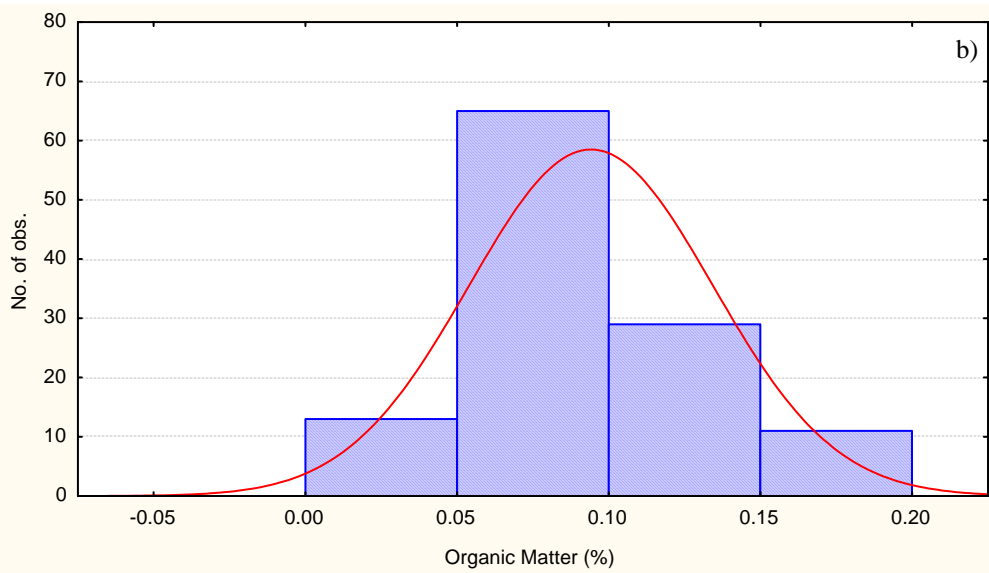
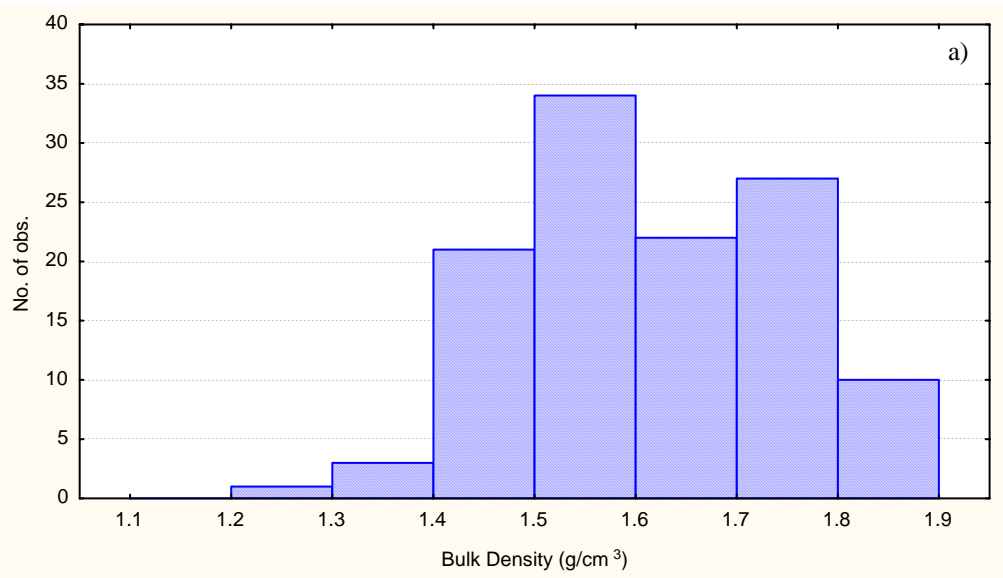
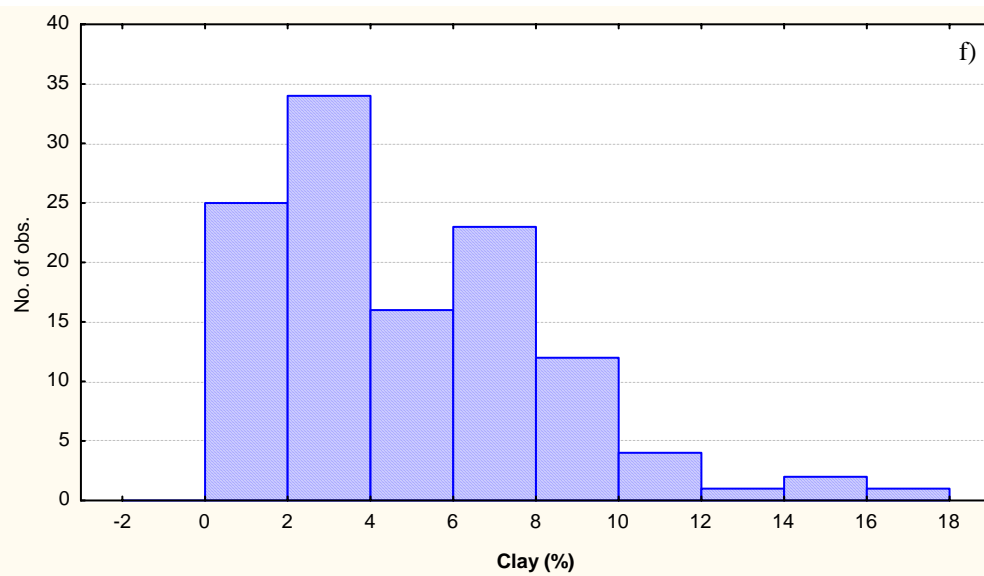
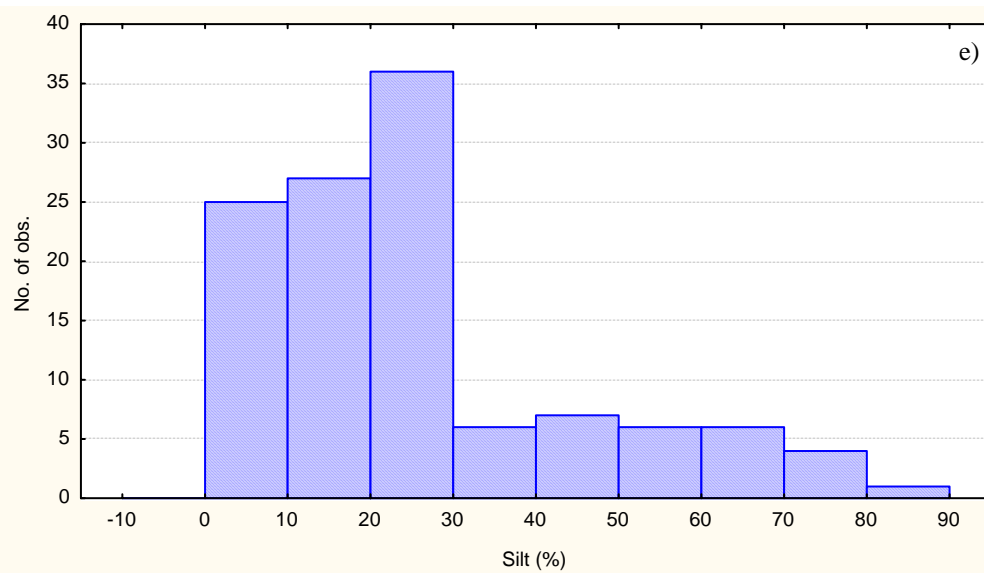
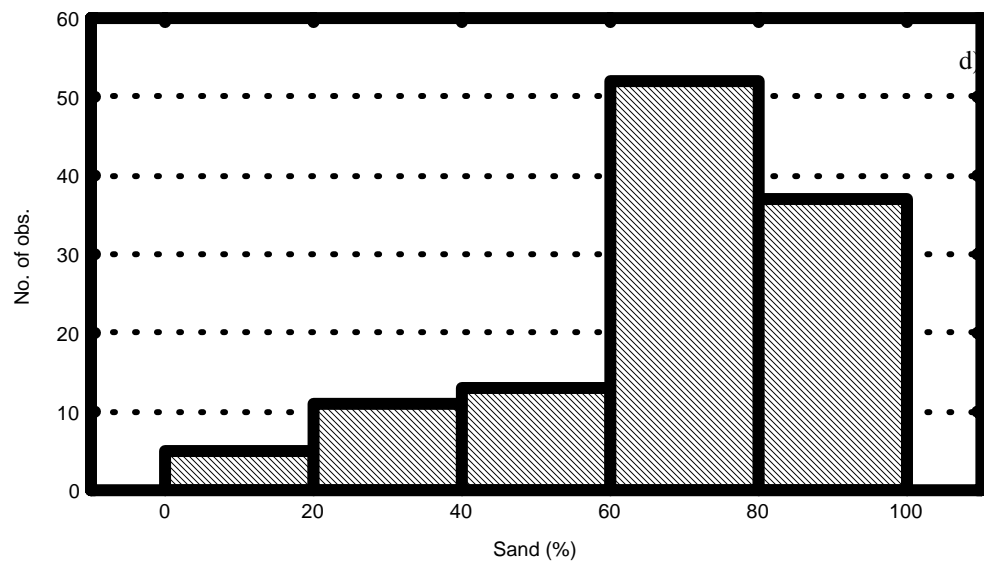


Figure 4.1.1. Stratigraphic cross-section along a tree-row showing the major stratigraphic units.





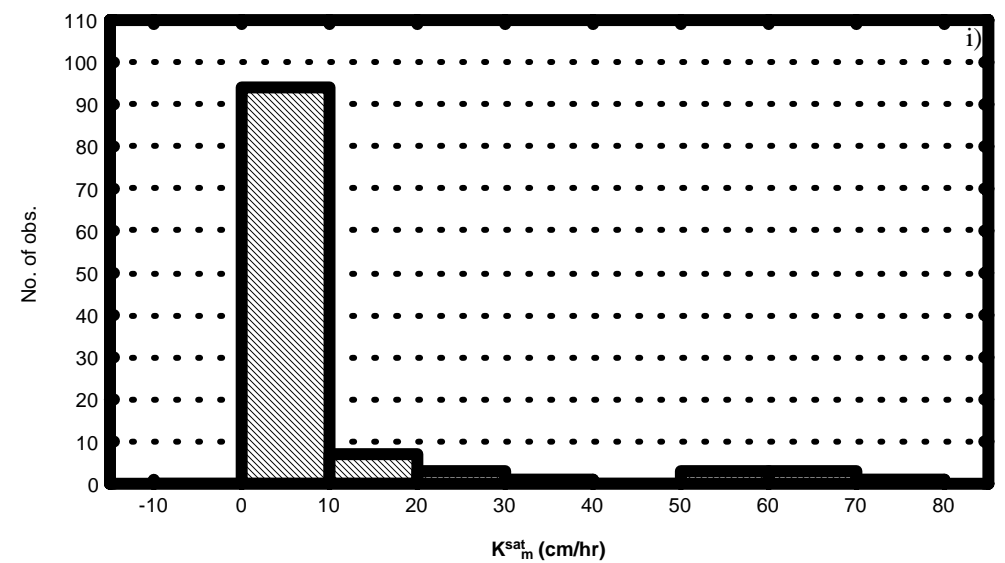
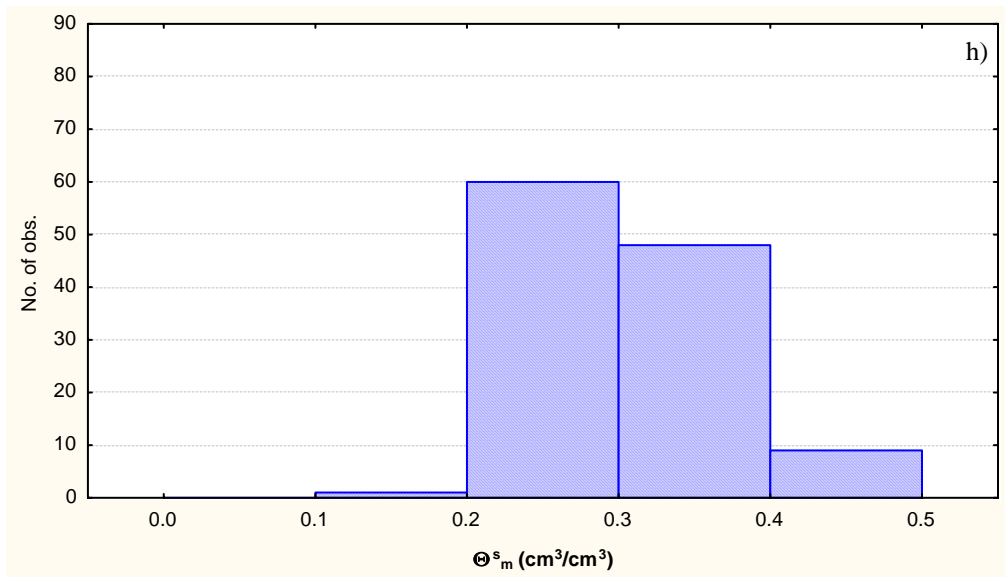
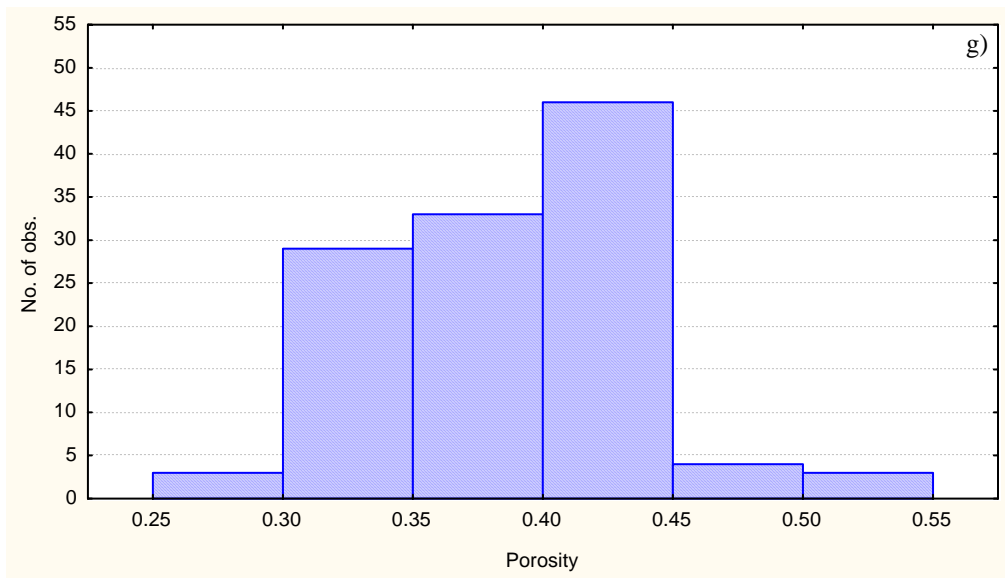


Figure 4.2.1 a-i. Histograms for the nine laboratory measurements for 118 soil samples.

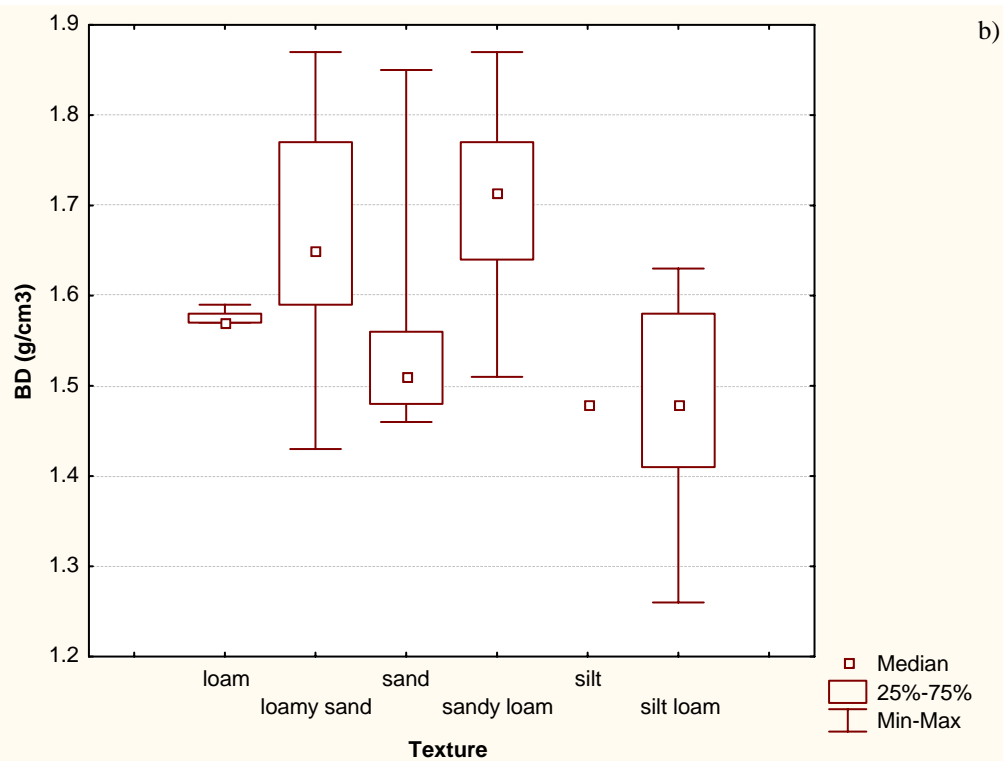
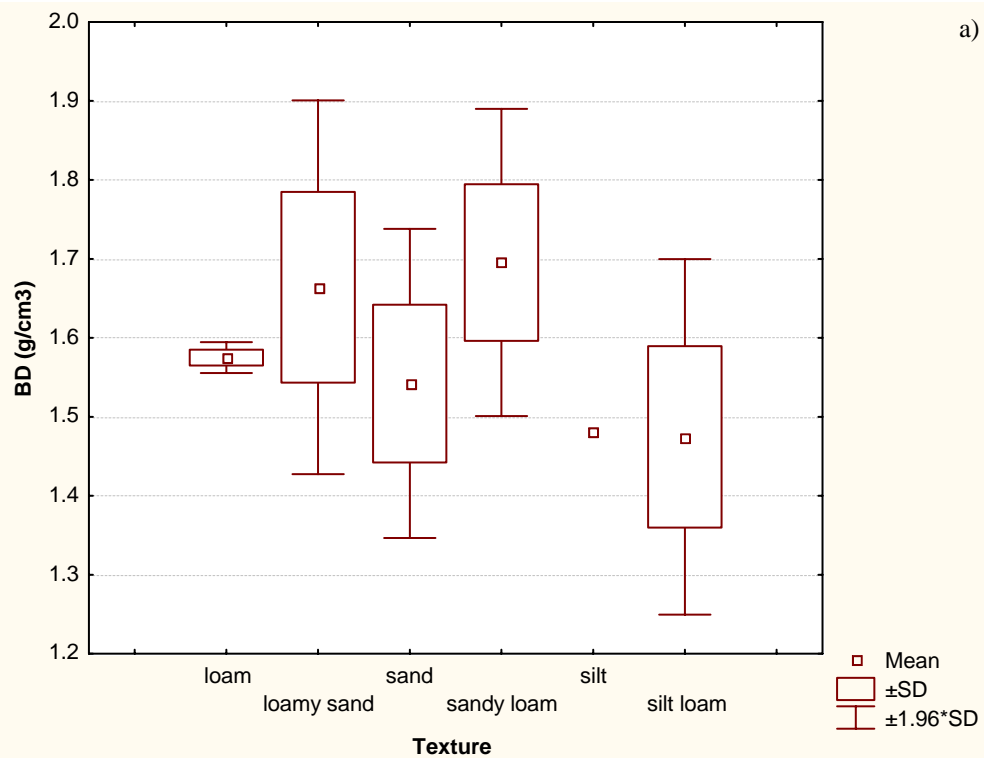


Figure 4.2.2a-b. Categorized box and whisker plots for bulk density.

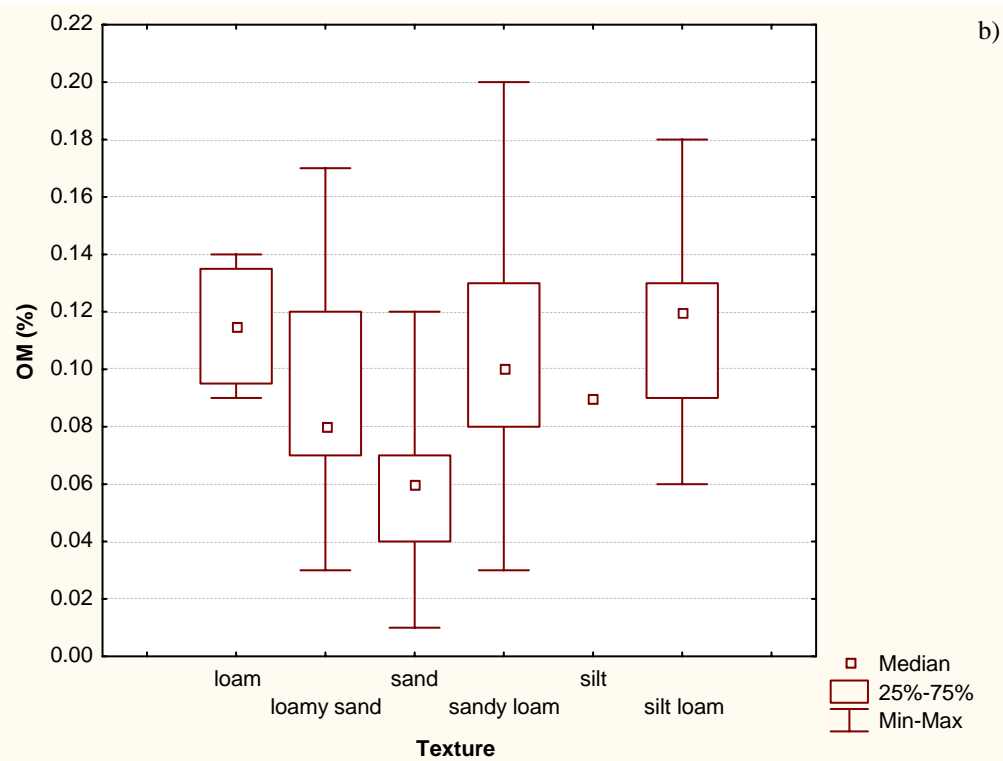
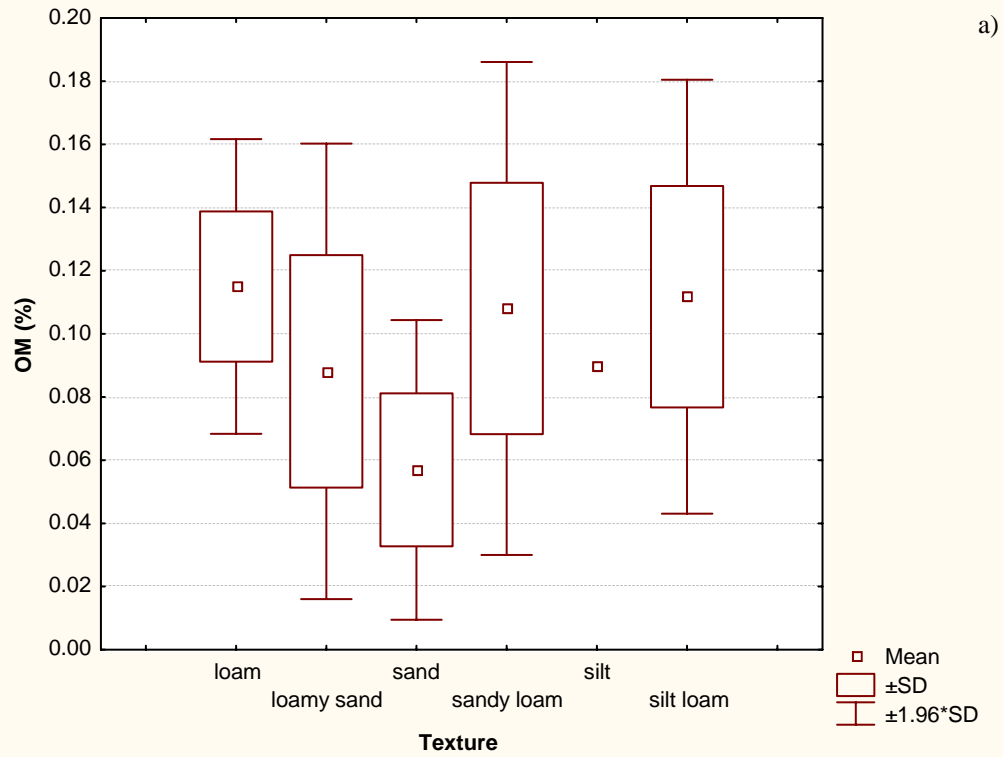


Figure 4.2.3a-b. Categorized box and whisker plots for organic matter content.

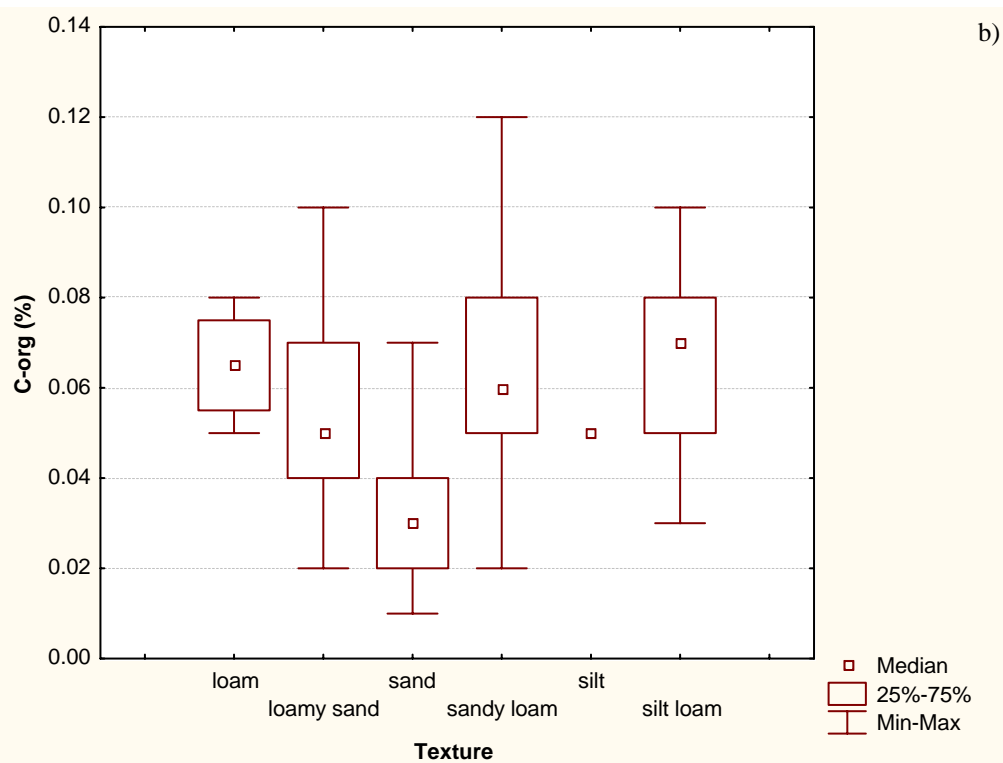
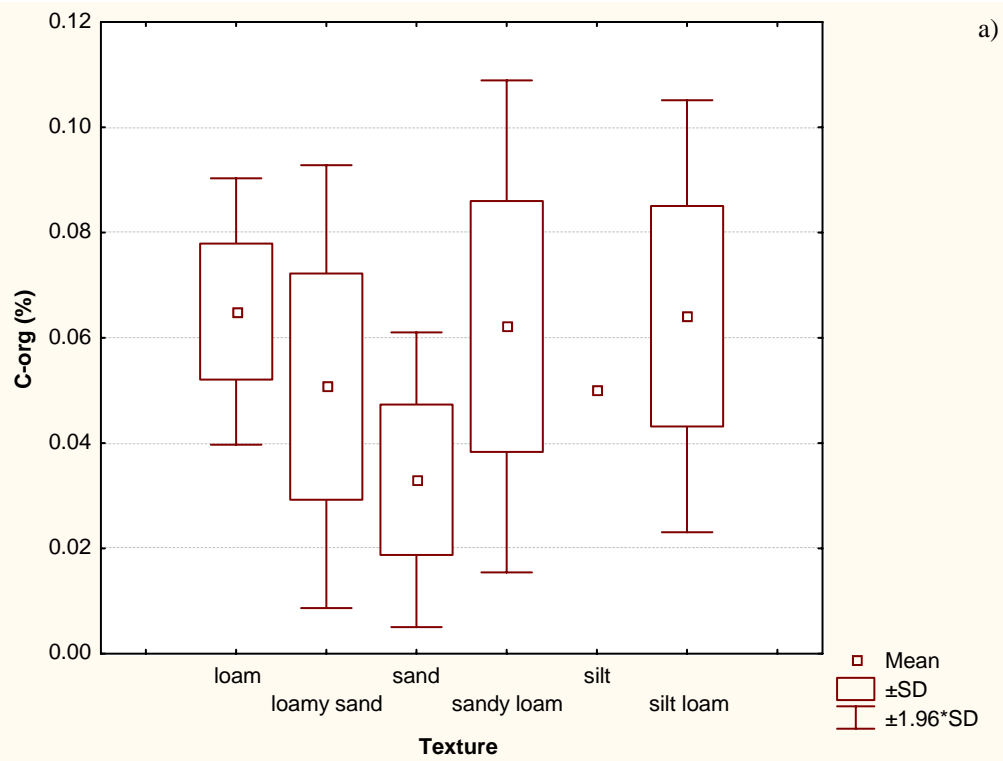


Figure 4.2.4a-b. Categorized box and whisker plots for organic carbon content.

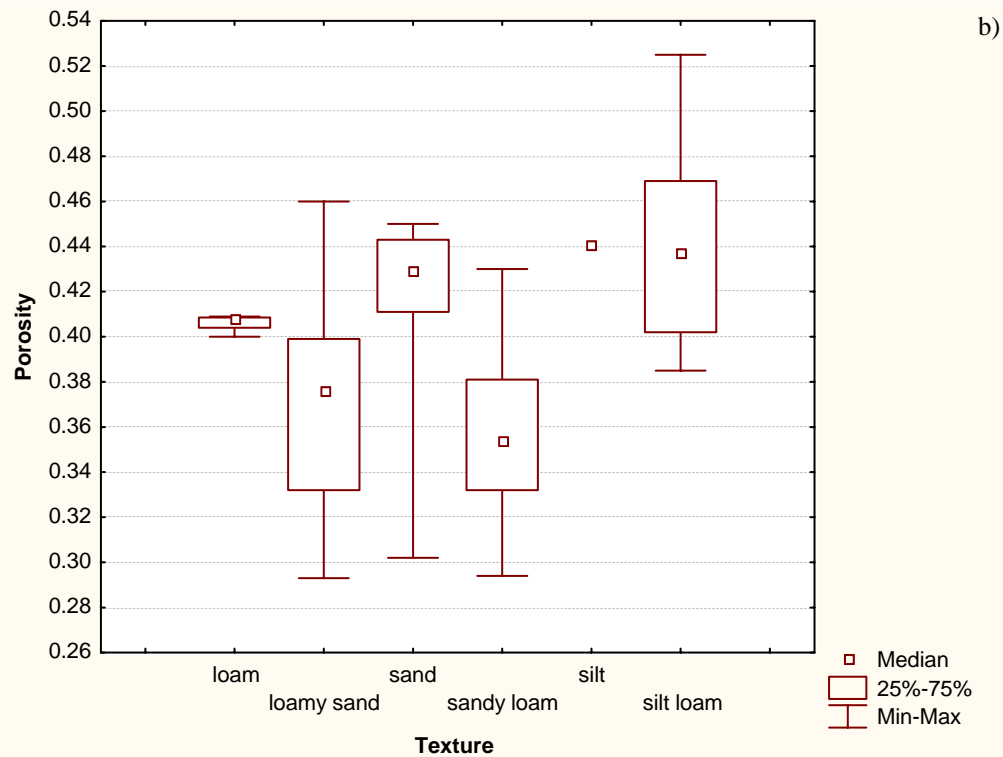
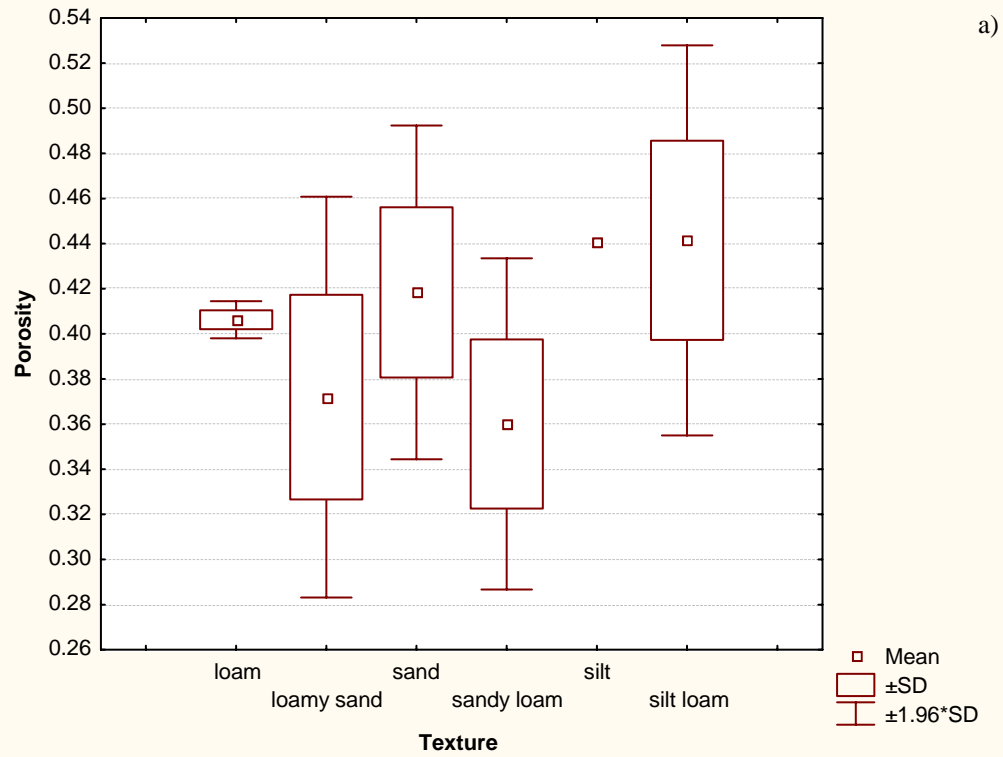


Figure 4.2.5a-b. Categorized box and whisker plots for porosity.

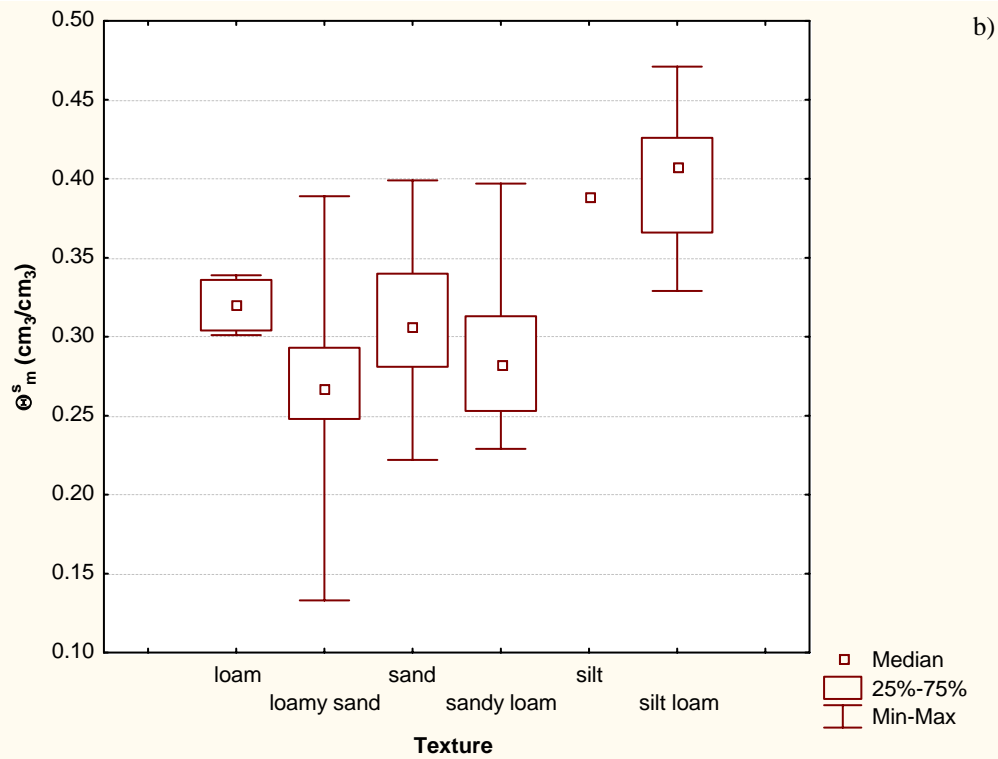
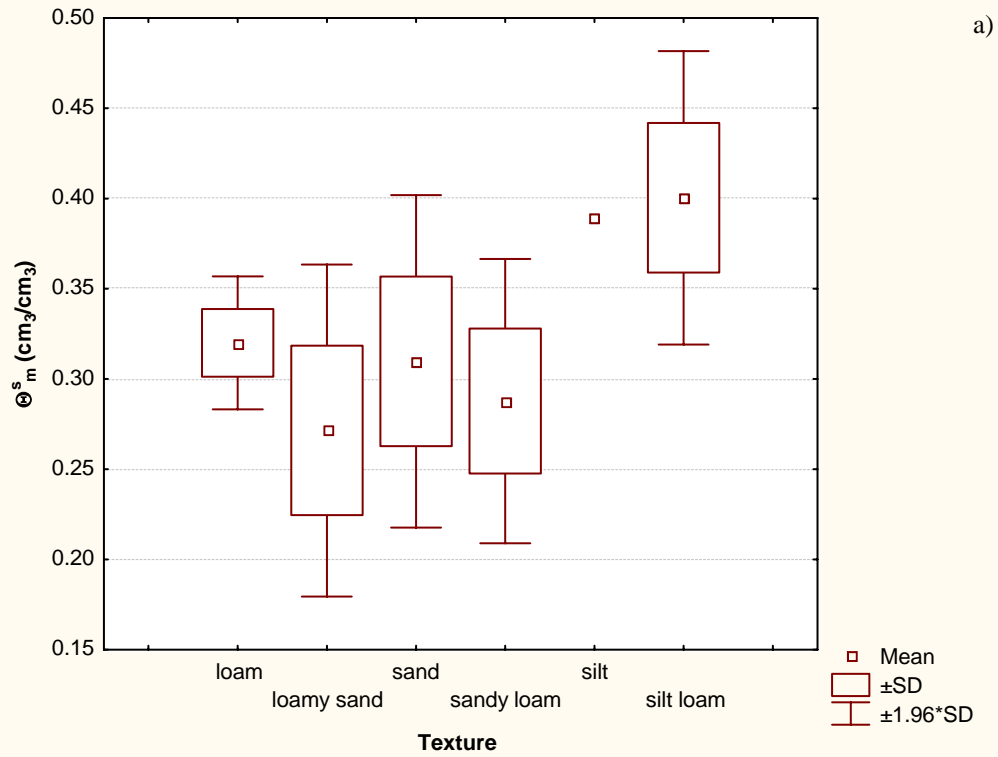


Figure 4.2.6a-b. Categorized box and whisker plots for saturated water content.

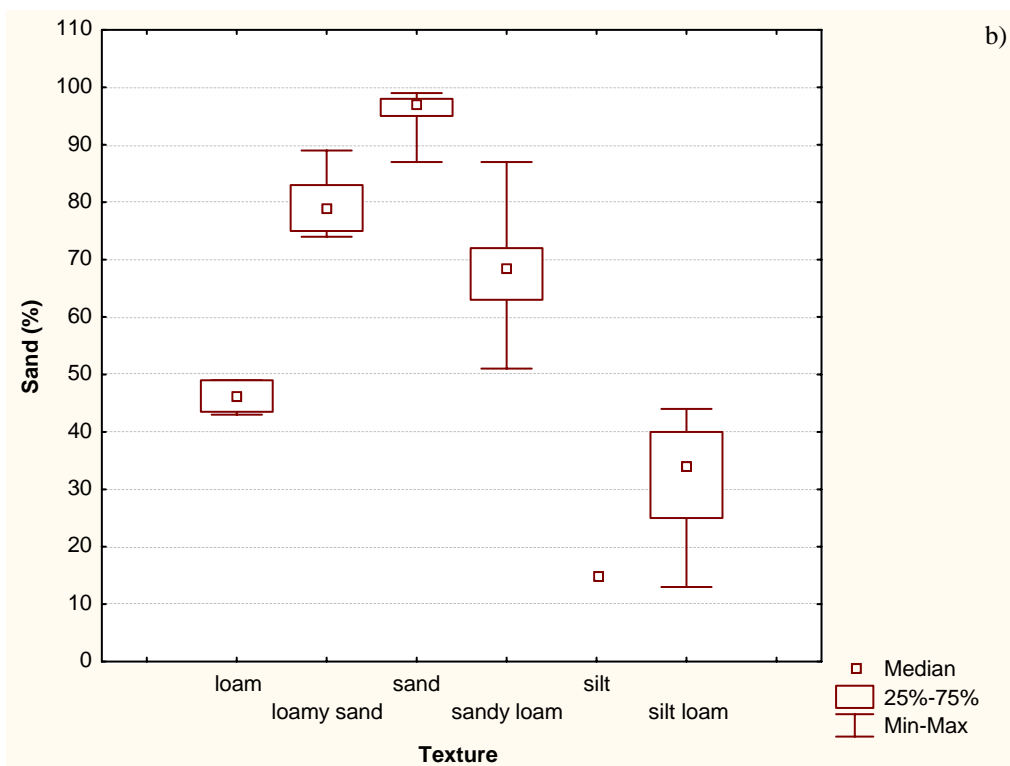
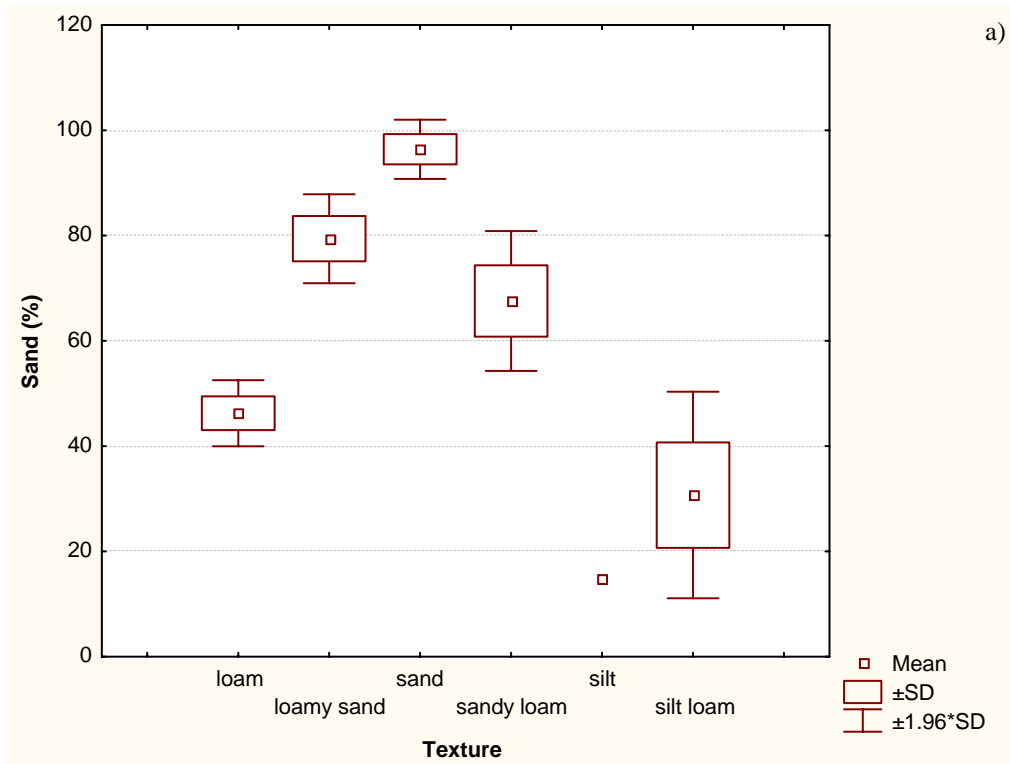


Figure 4.2.7a-b. Categorized box and whisker plots for the sand fraction.

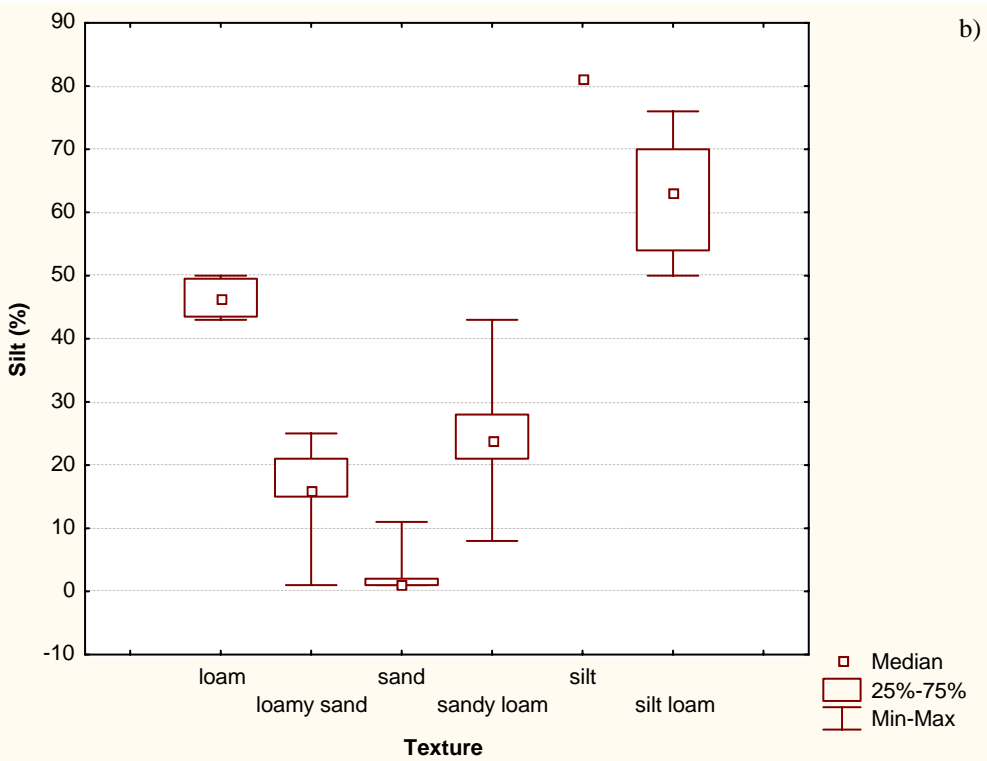
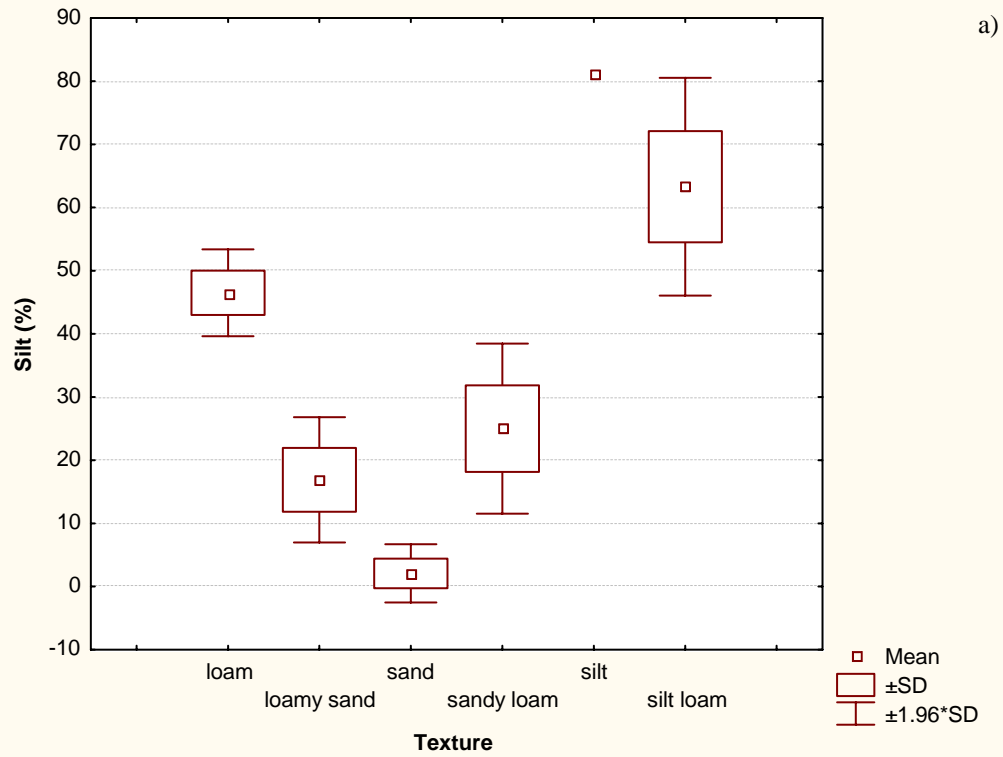


Figure 4.2.8a-b. Categorized box and whisker plots for the silt fraction.

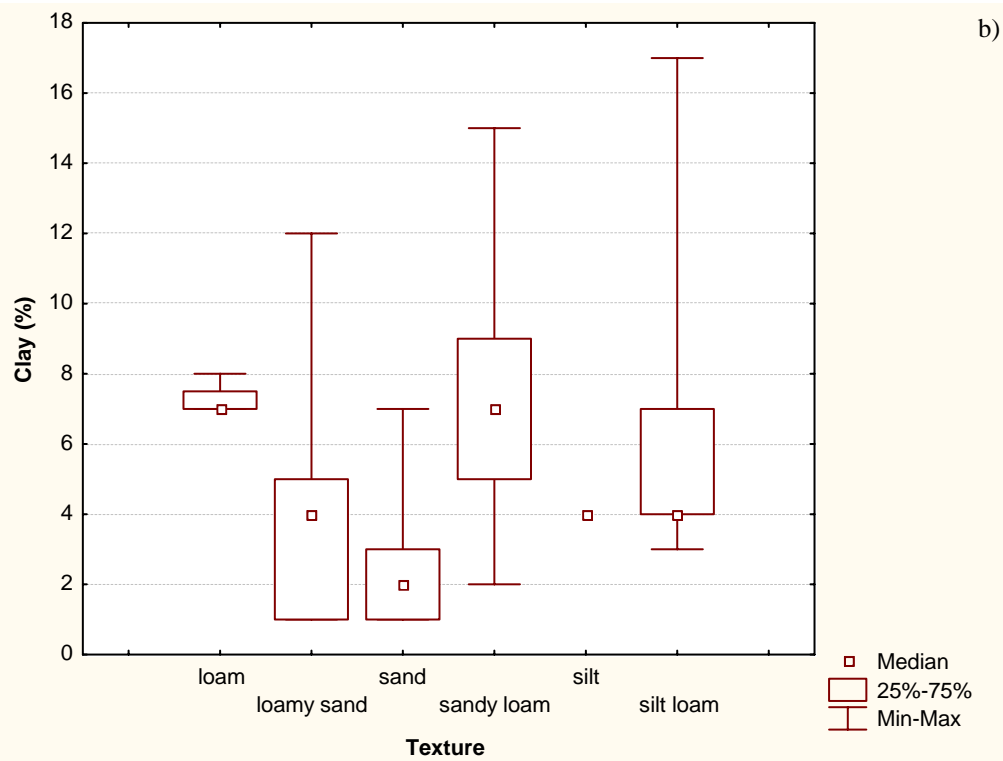
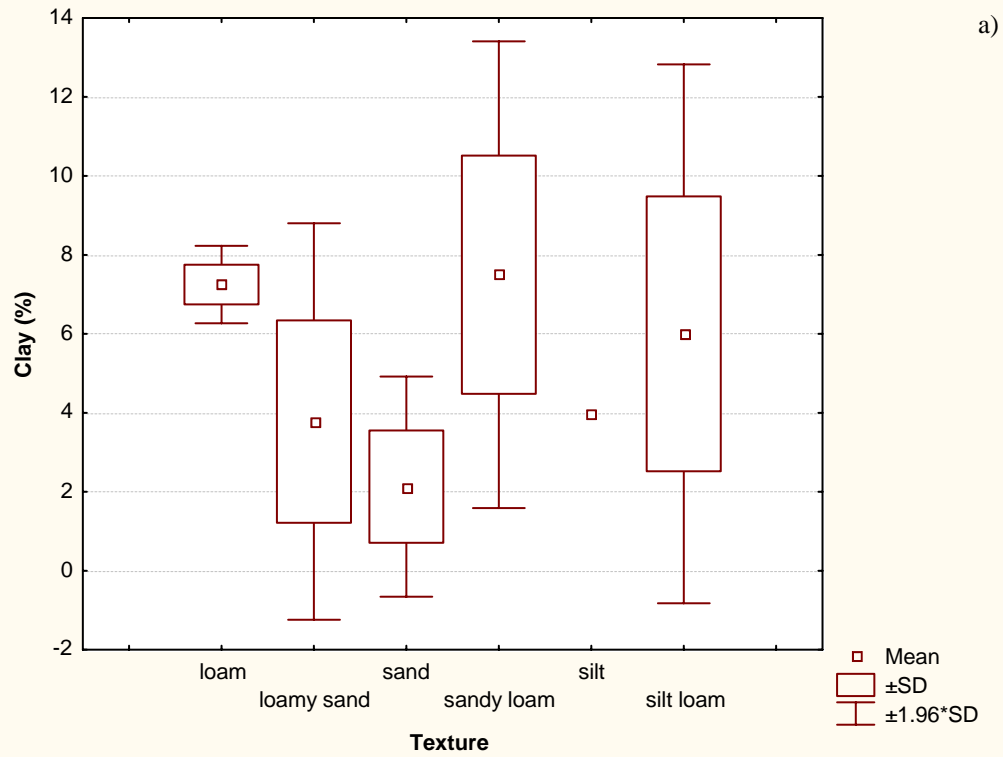


Figure 4.2.9a-b. Categorized box and whisker plots for the clay fraction.

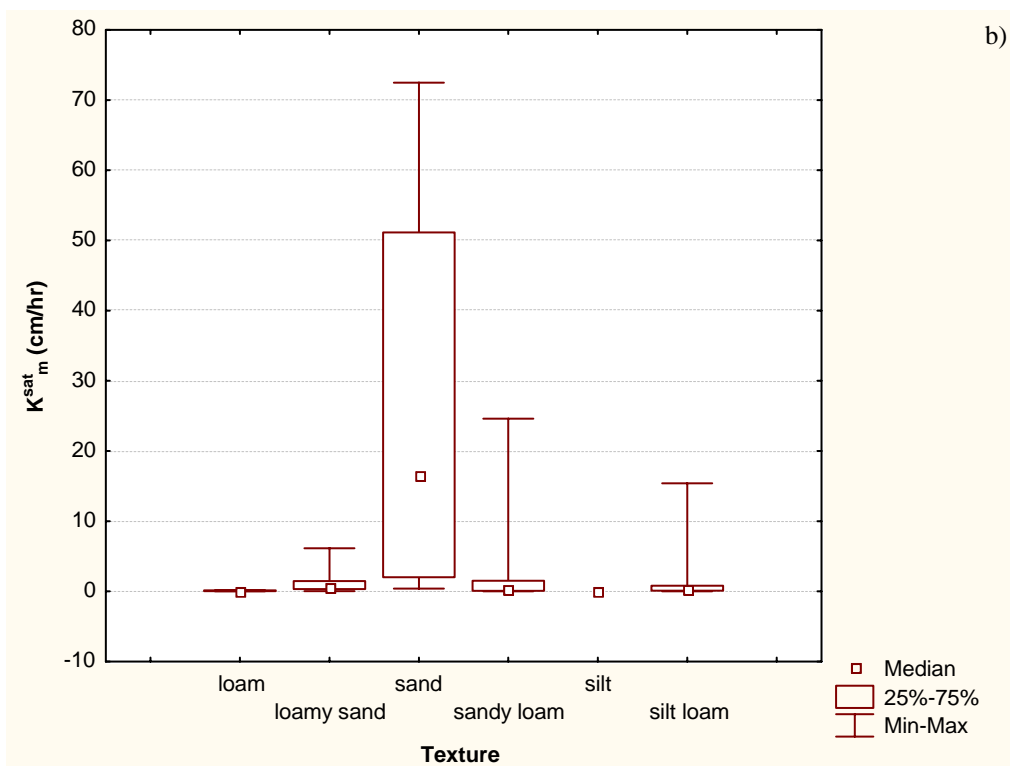
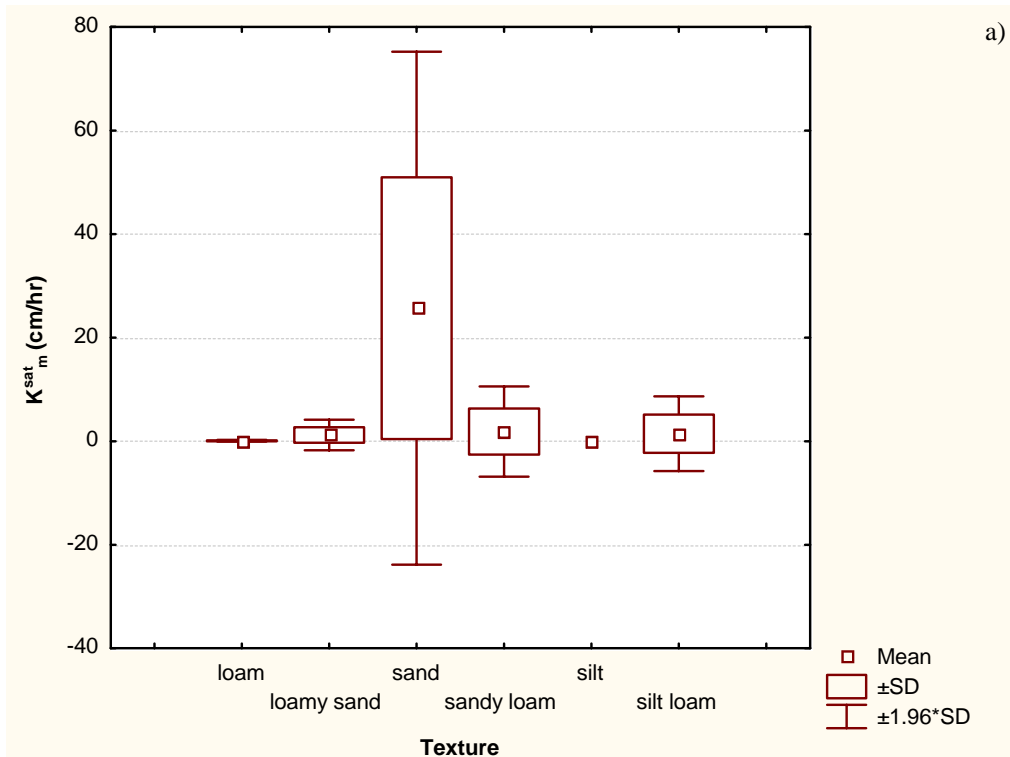


Figure 4.2.10a-b. Categorized box and whisker plots for unsaturated hydraulic conductivity.

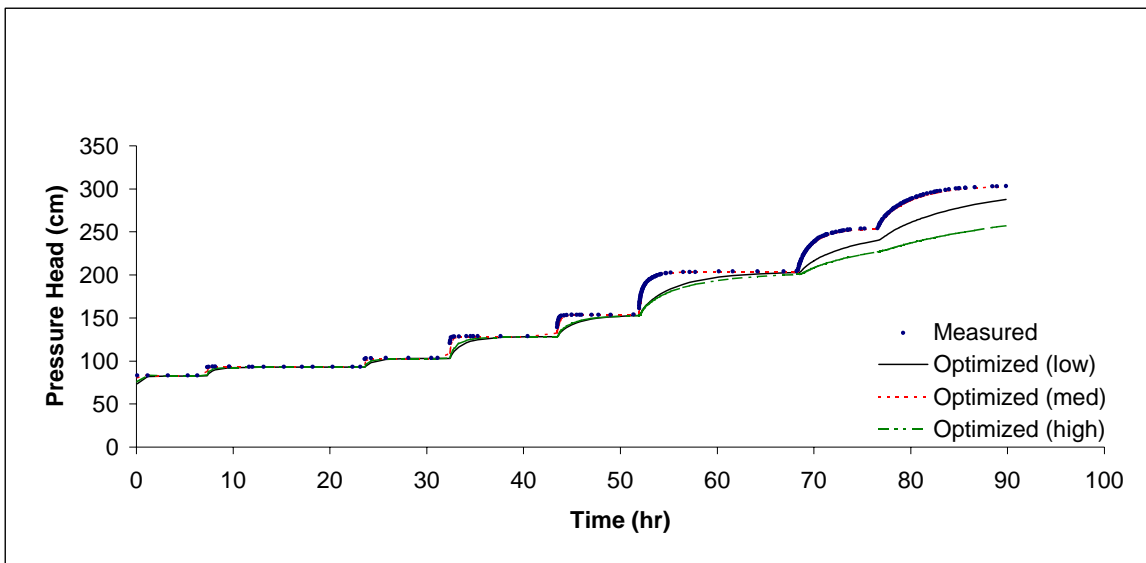
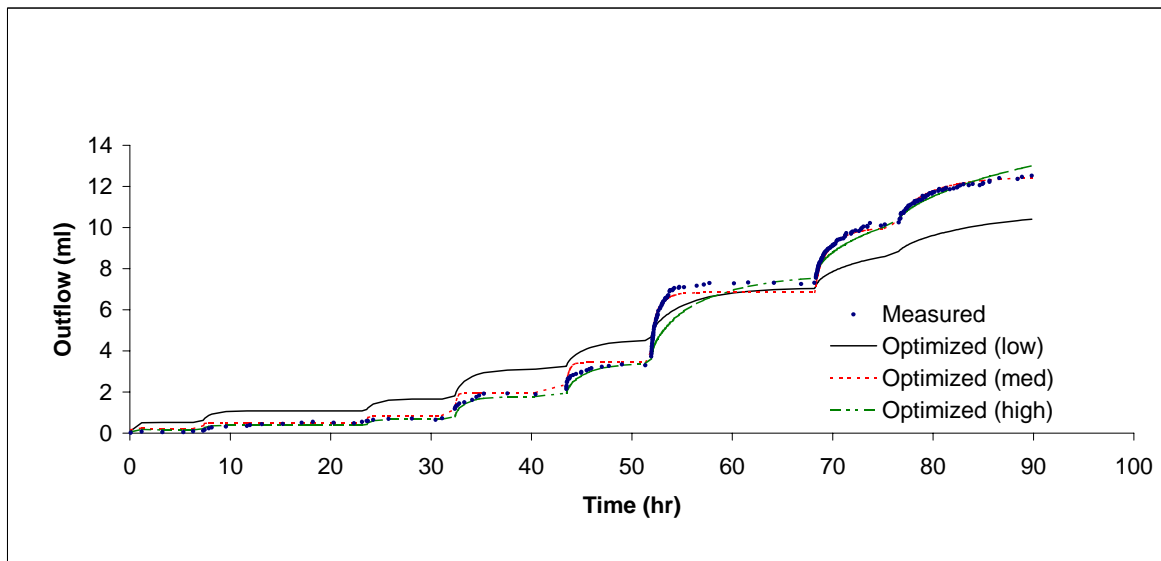


Figure 4.3.1a-b. Multi-step outflow experiment results and optimized curves for a sample with transient data.

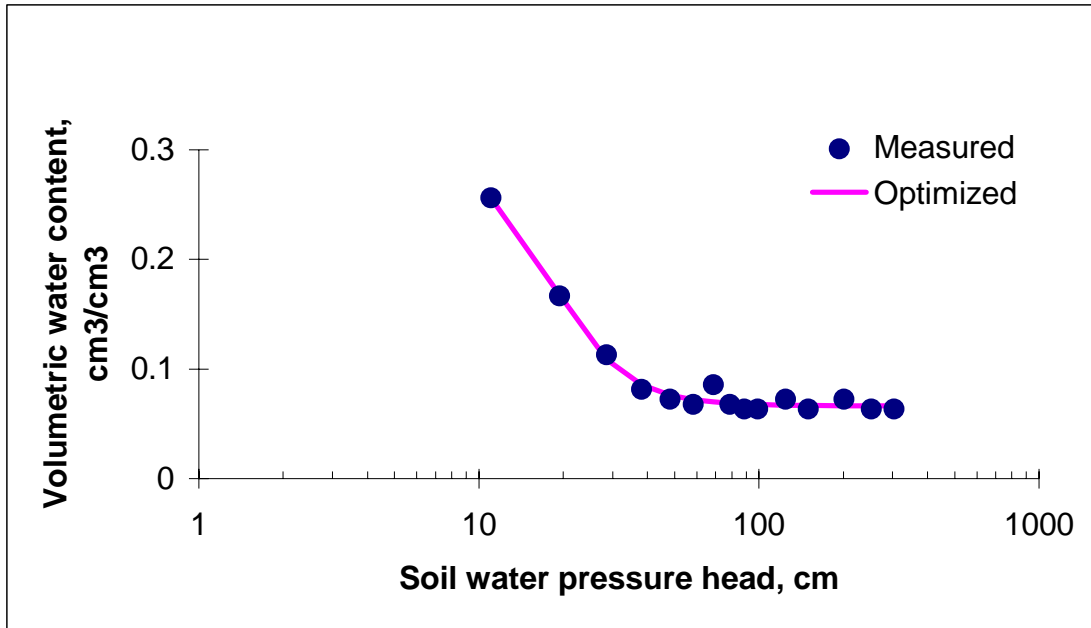
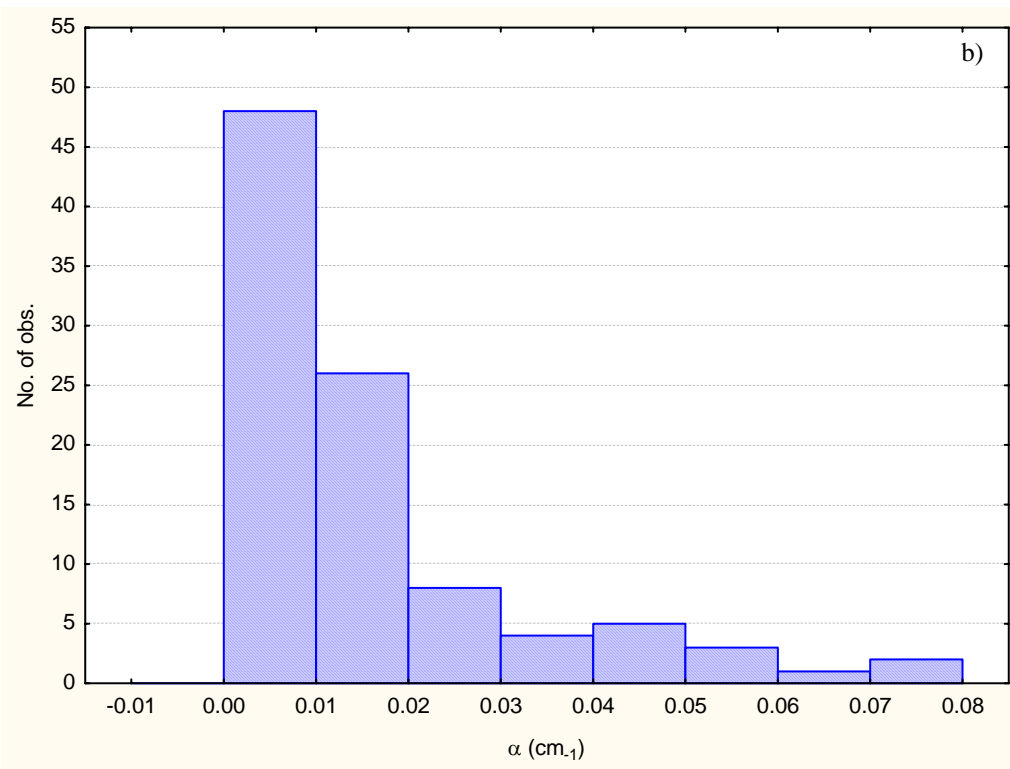
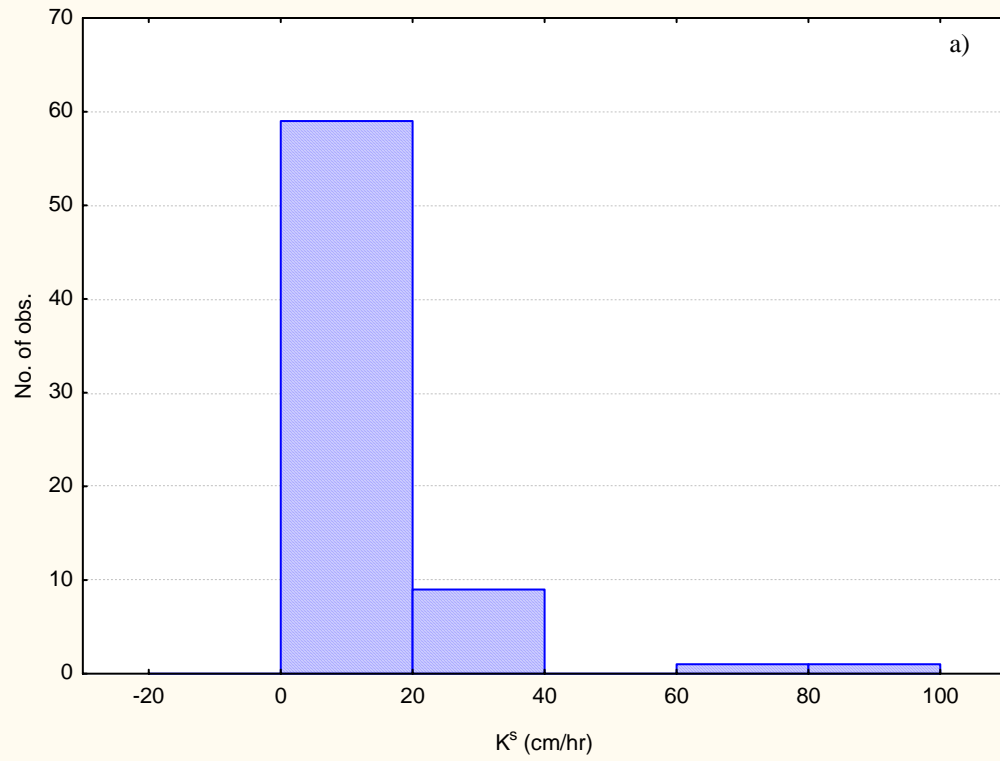


Figure 4.3.2. Multi-step outflow results and optimized curve for a sample with steady state data.



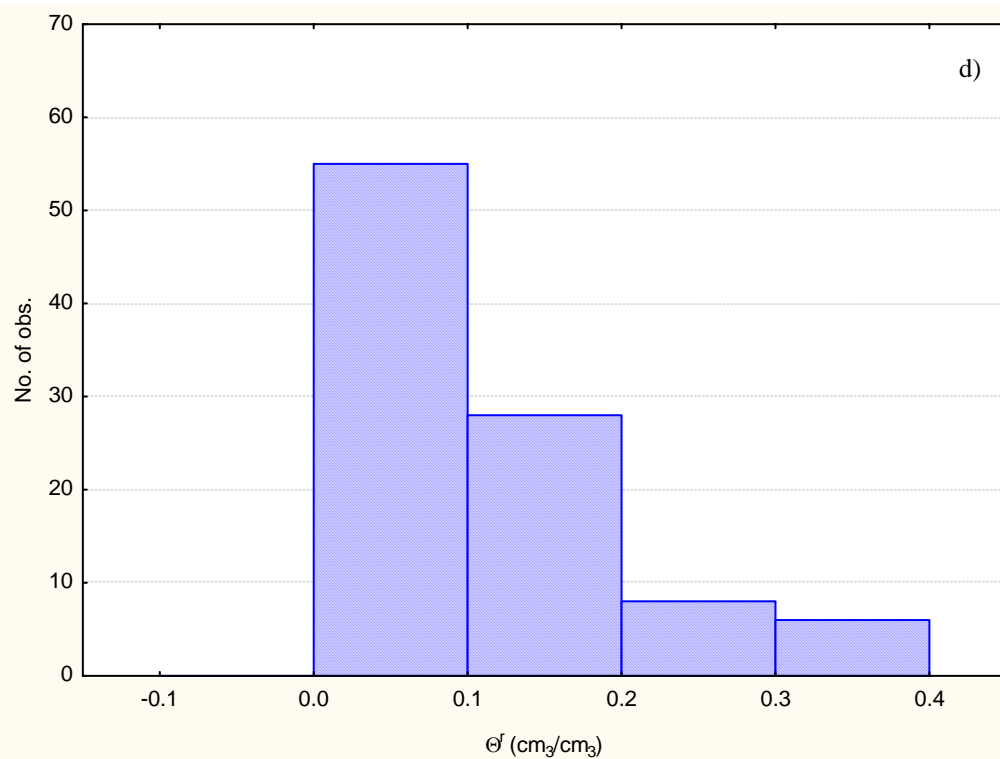
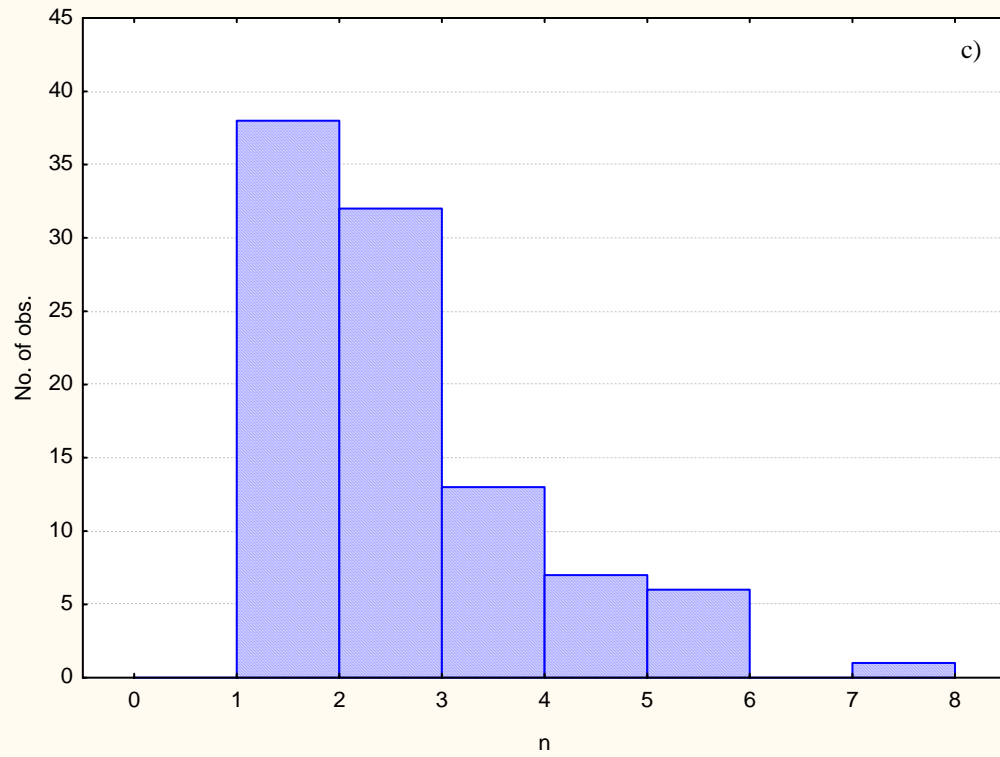
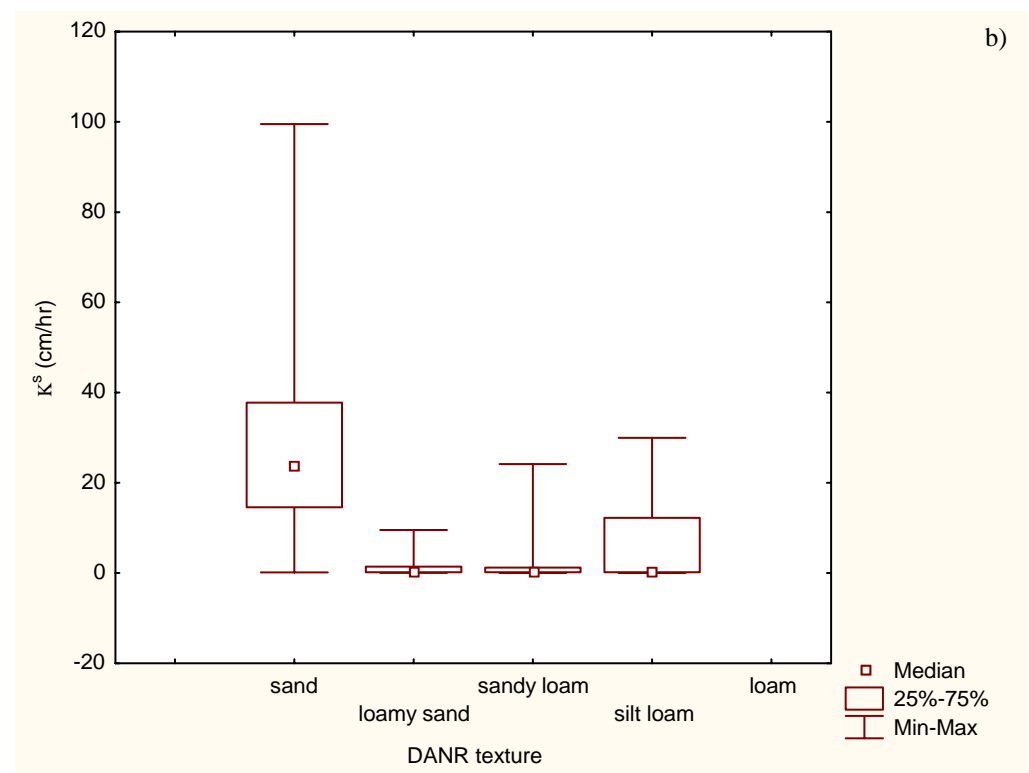
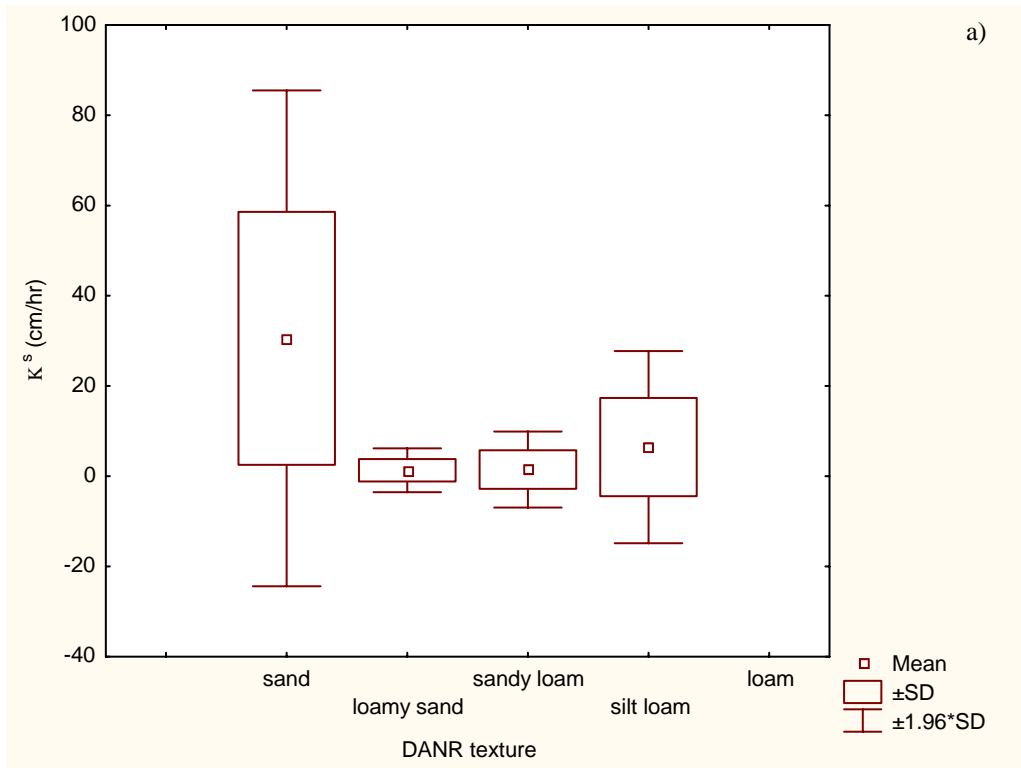
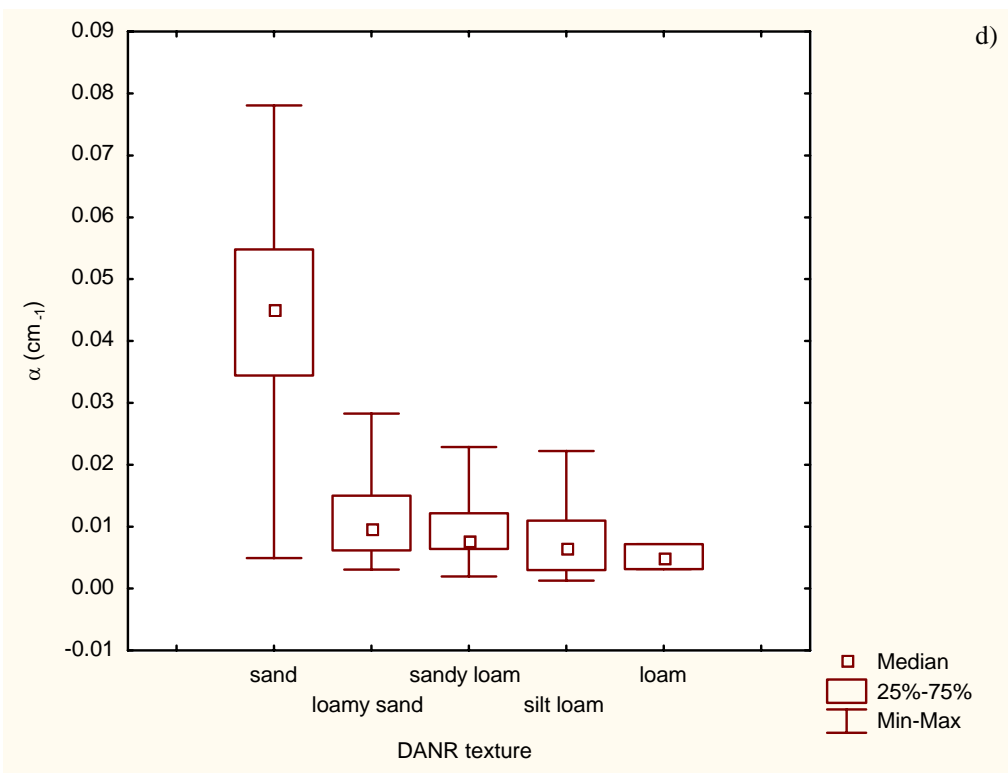
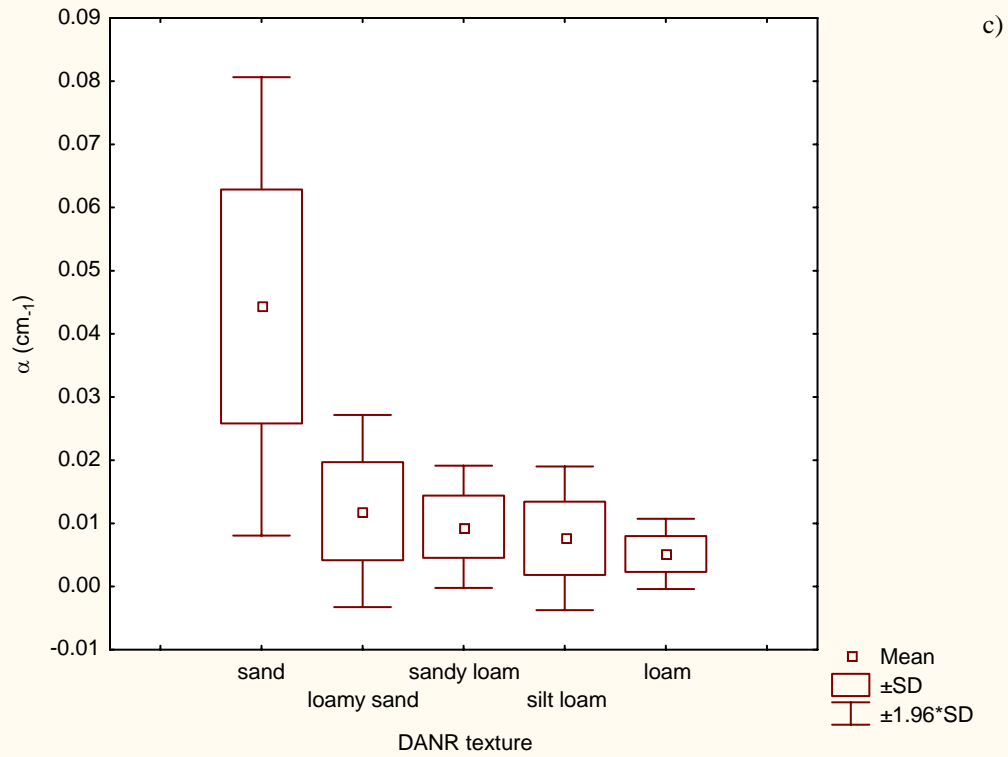
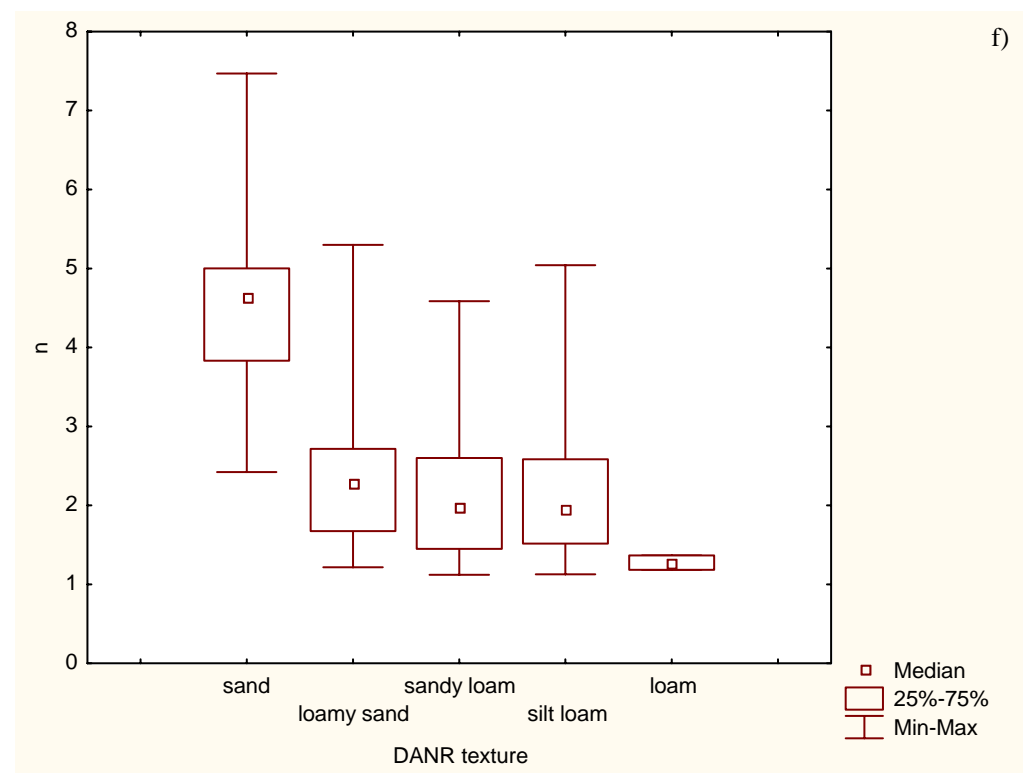
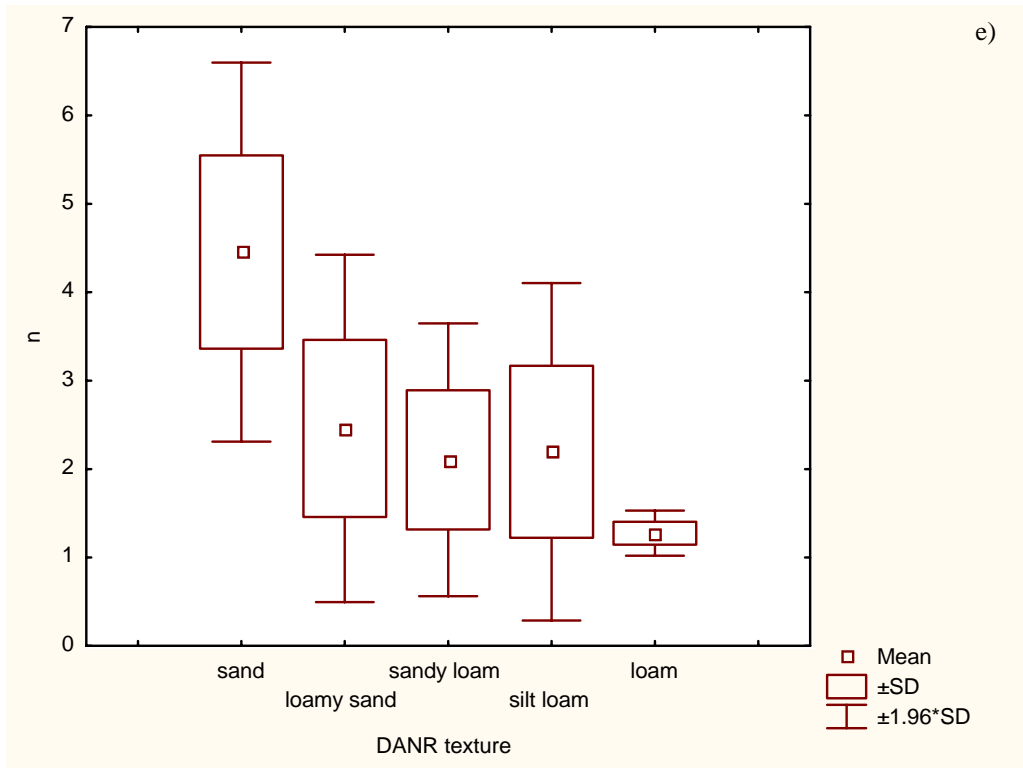


Figure 4.3.3a-d. Histograms for the van Genuchten parameters for the 97 samples.







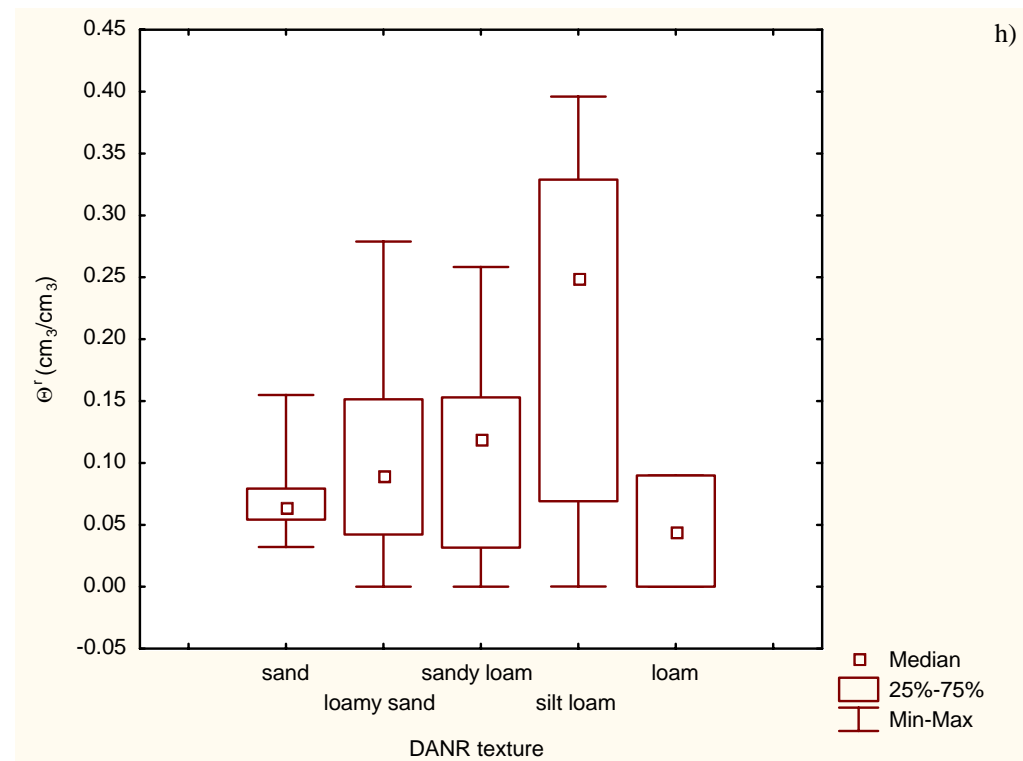
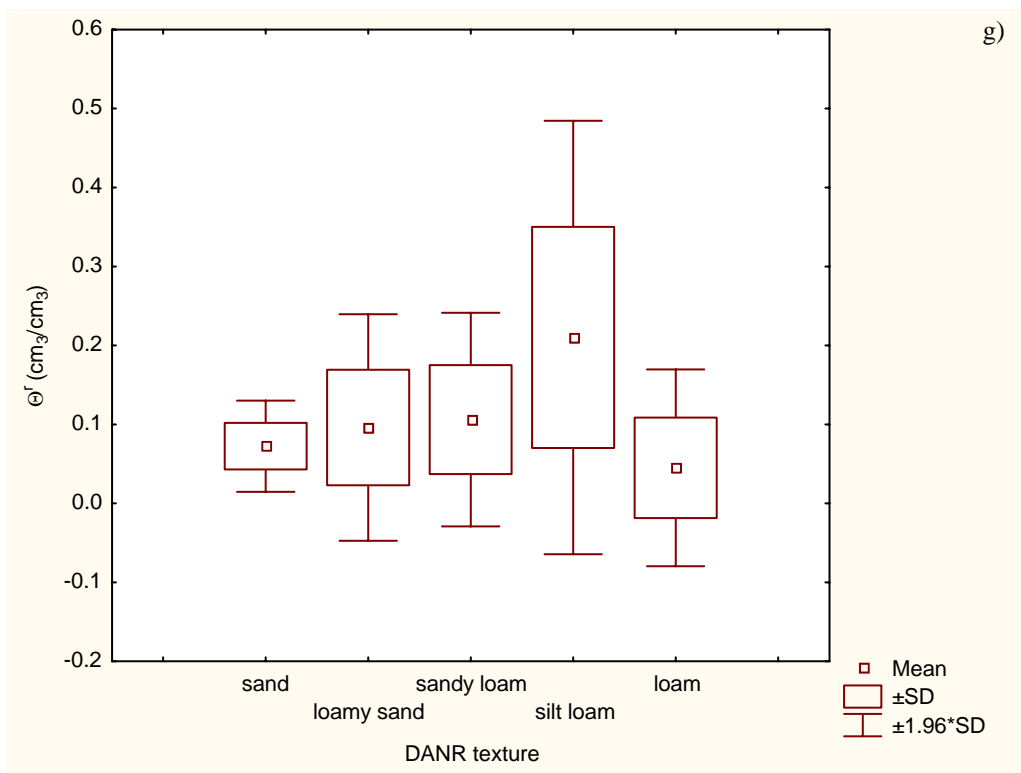
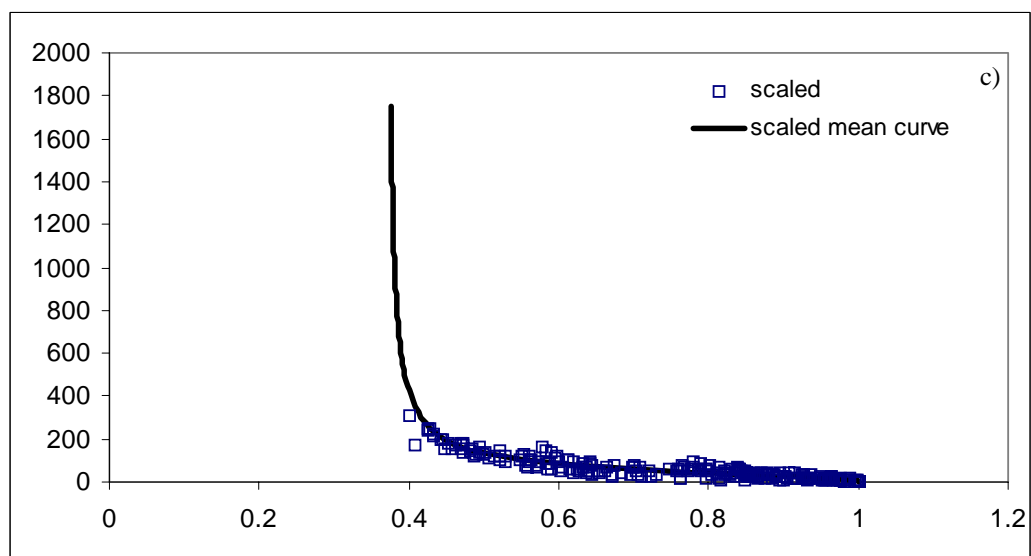
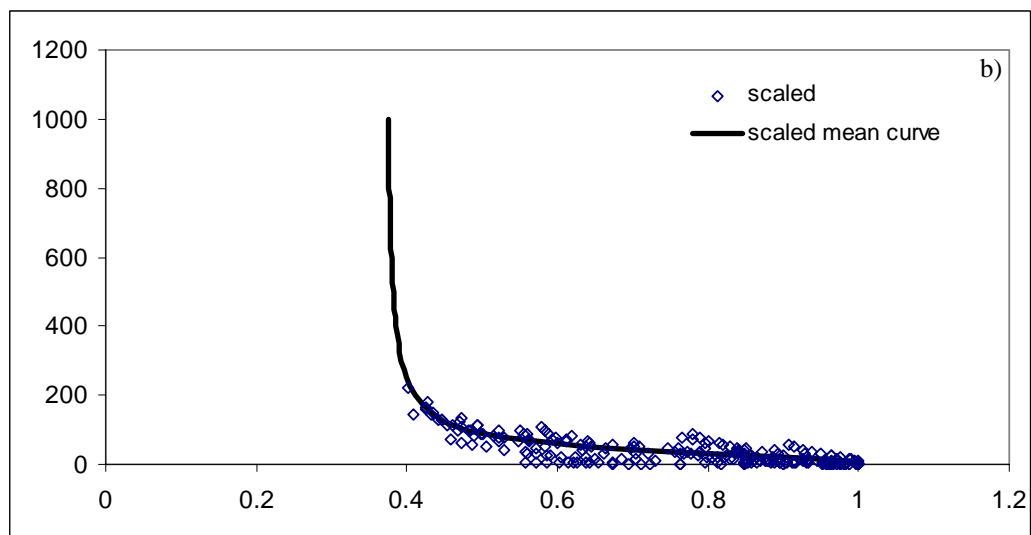
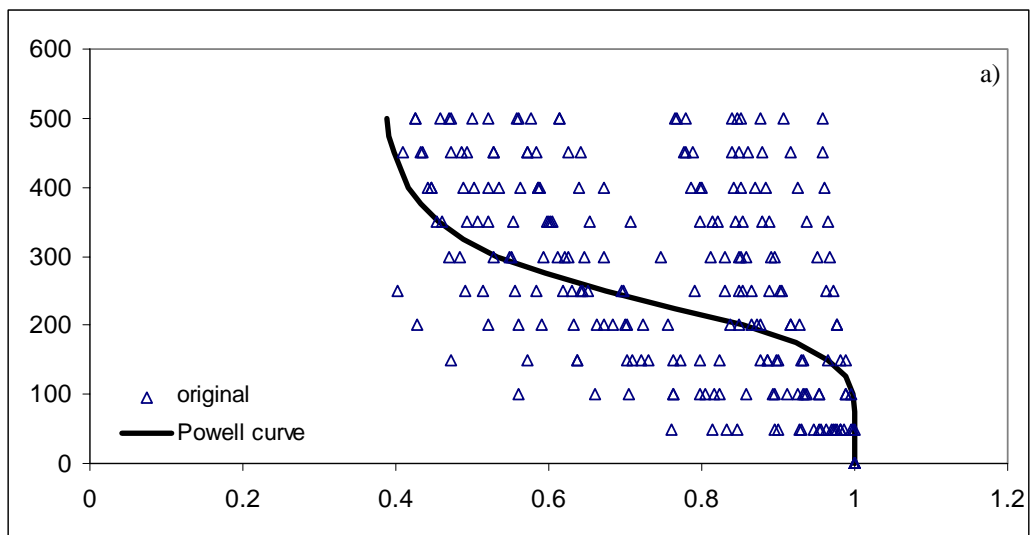


Figure 4.3.4a-h. Categorized box and whisker plot for the van Genuchten parameters.



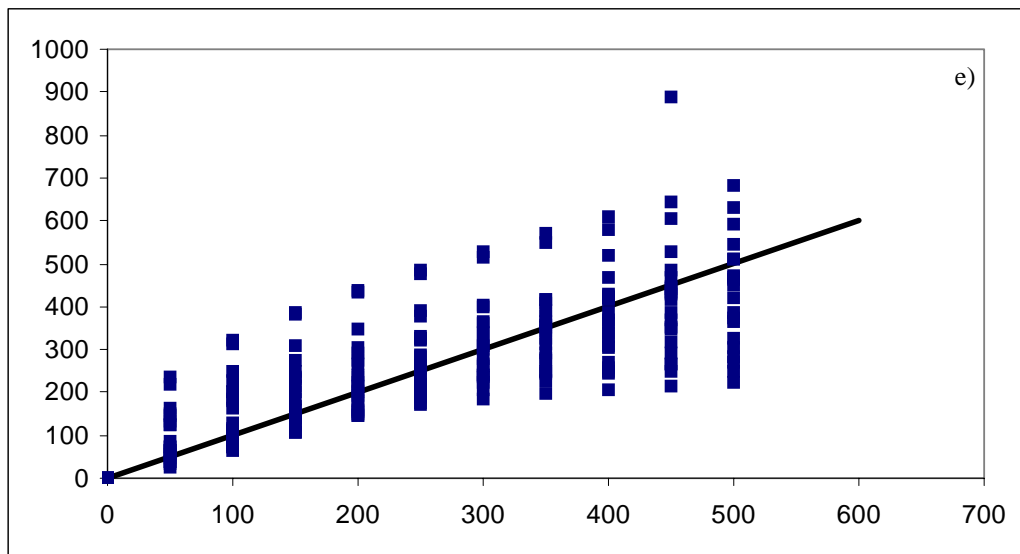
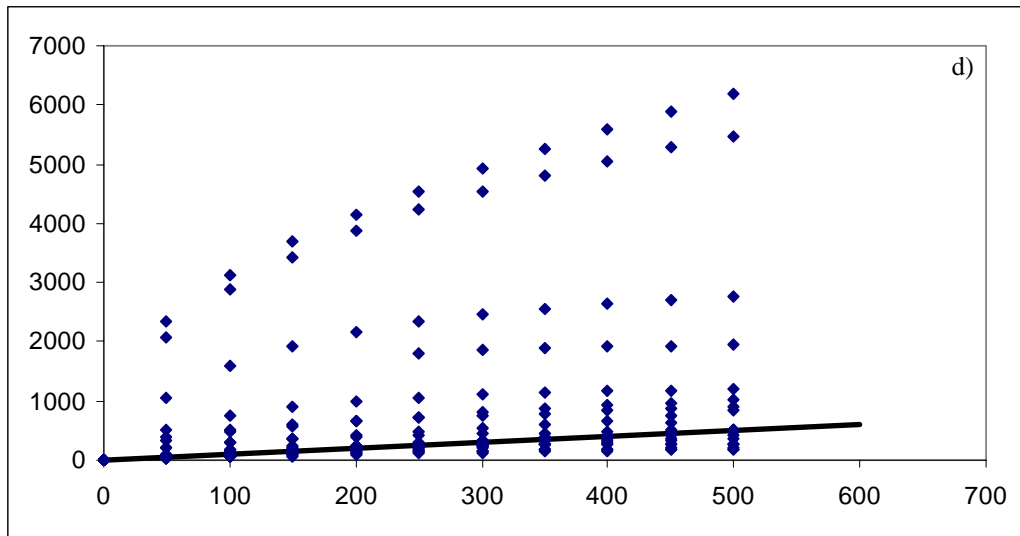
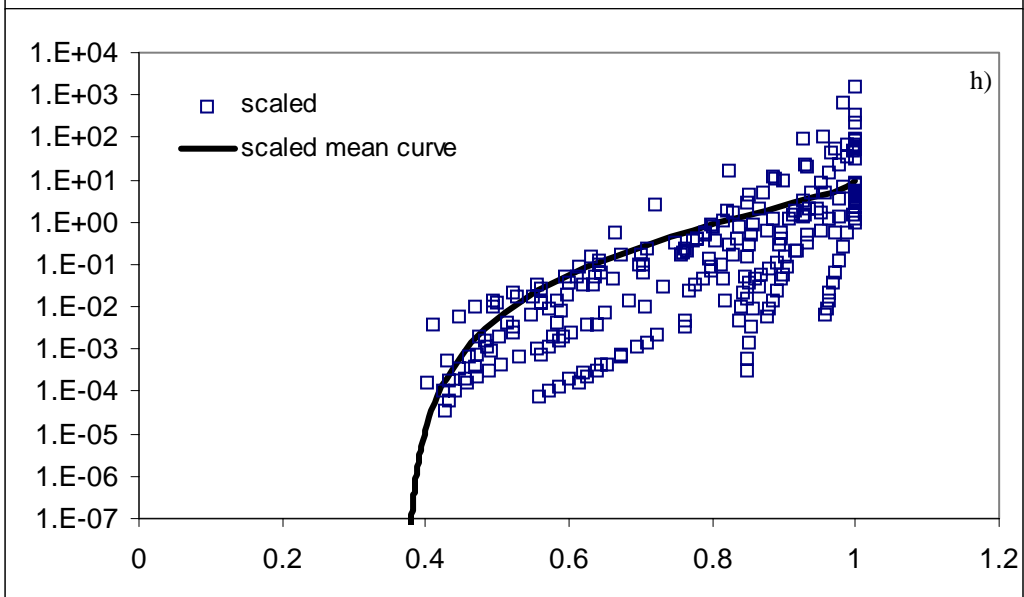
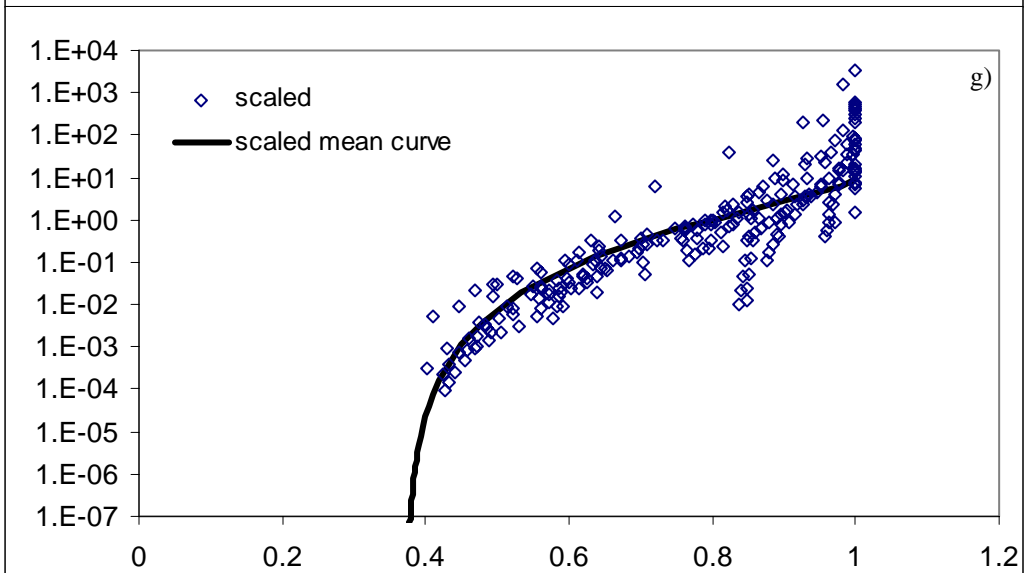
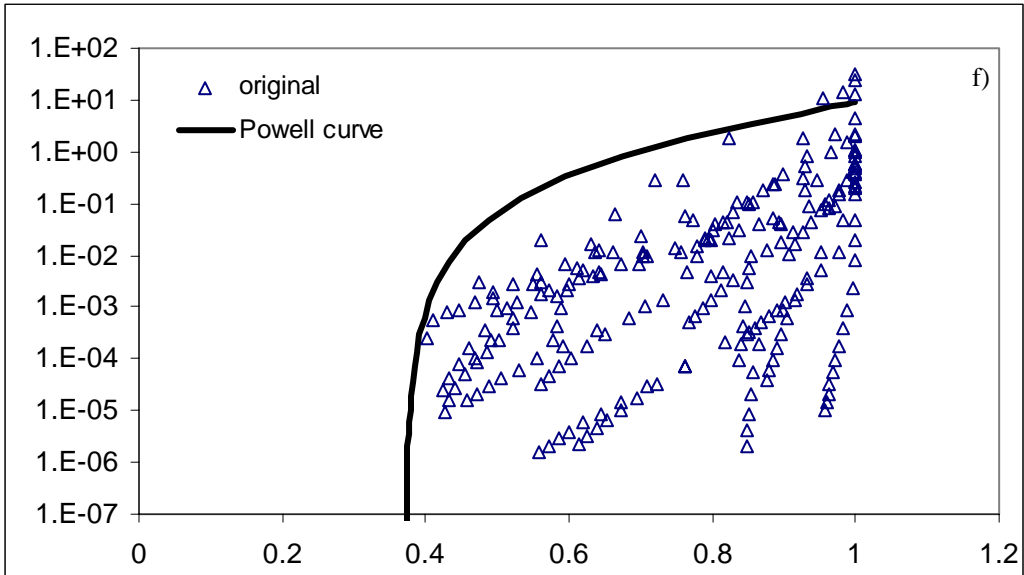


Figure 4.5.1a-e. Soil water retention (a) unscaled, (b) scaled using method 1, and (c) scaled using method 2. Original and de-scaled soil water pressure head using method 1 (d) and method 2 (e). All curves represent Group 1, Population 1.



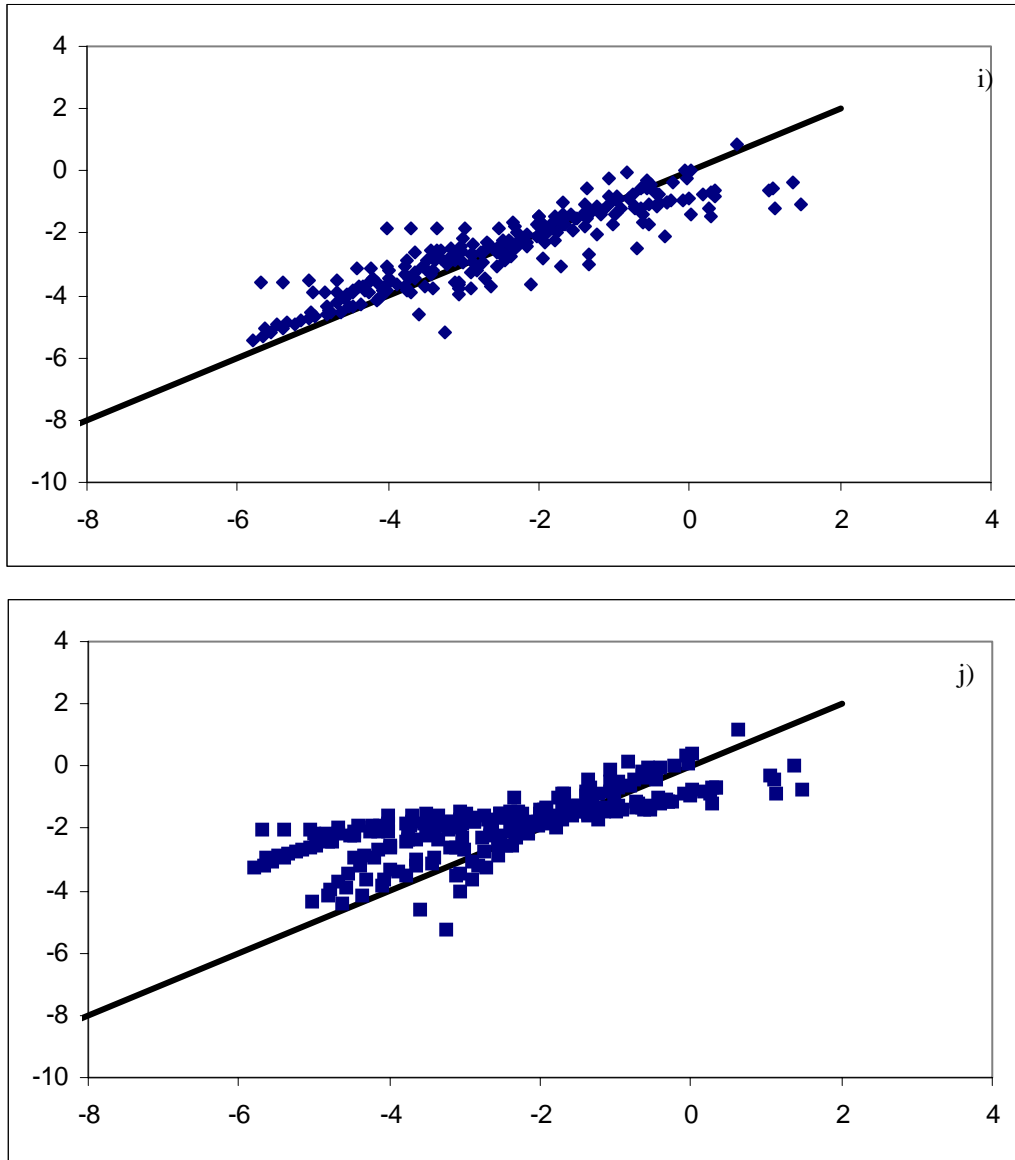
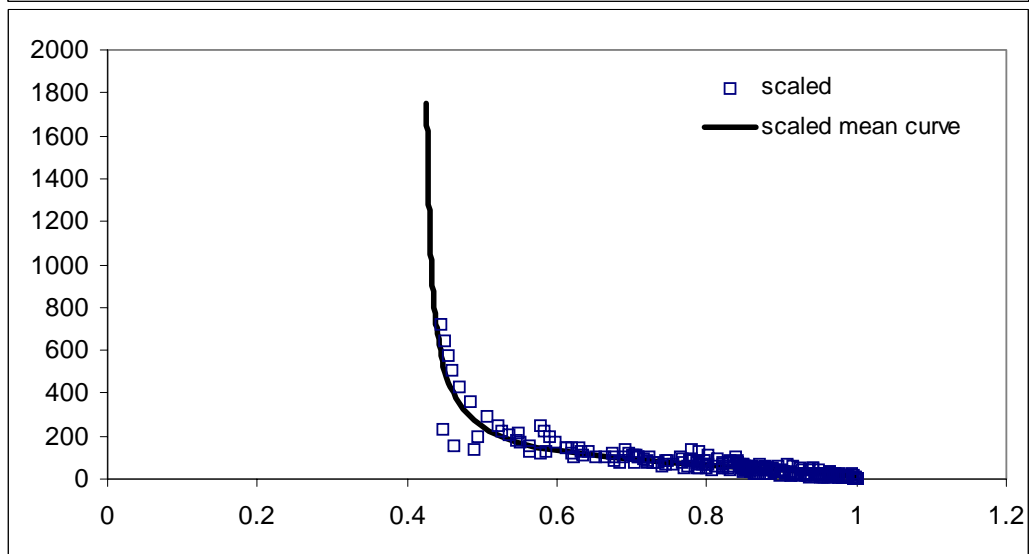
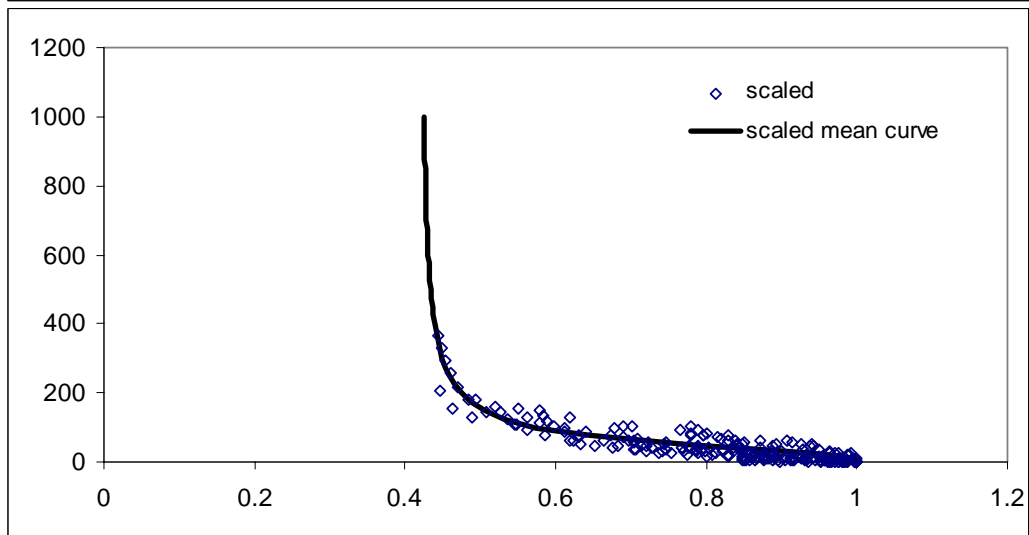
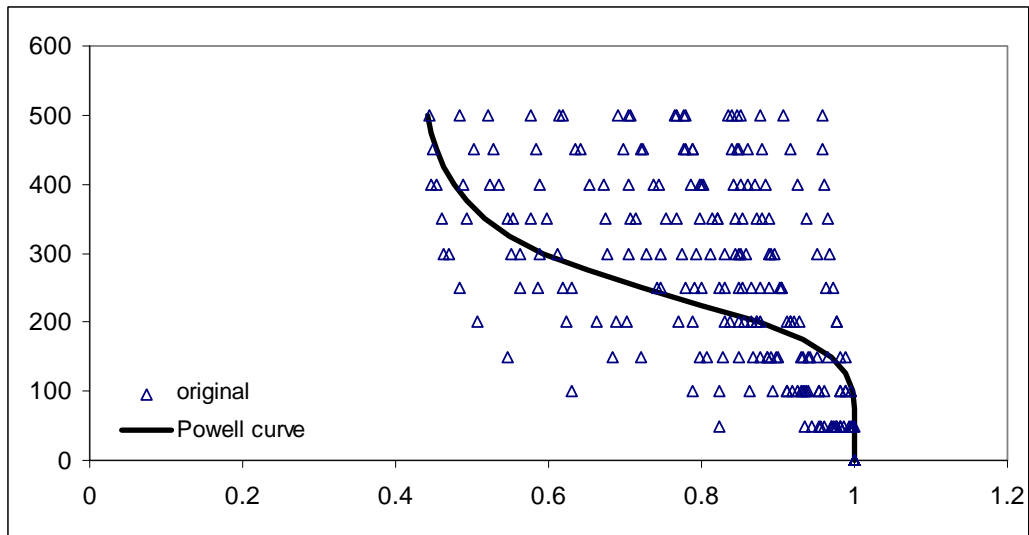


Figure 4.5.1f-j. Unsaturated hydraulic conductivity (f) unscaled, (g) scaled using method 1, and (h) scaled using method 2. Original and de-scaled unsaturated hydraulic conductivity using method 1 (i) and method 2 (j). All curves represent Group 1, Population 1.



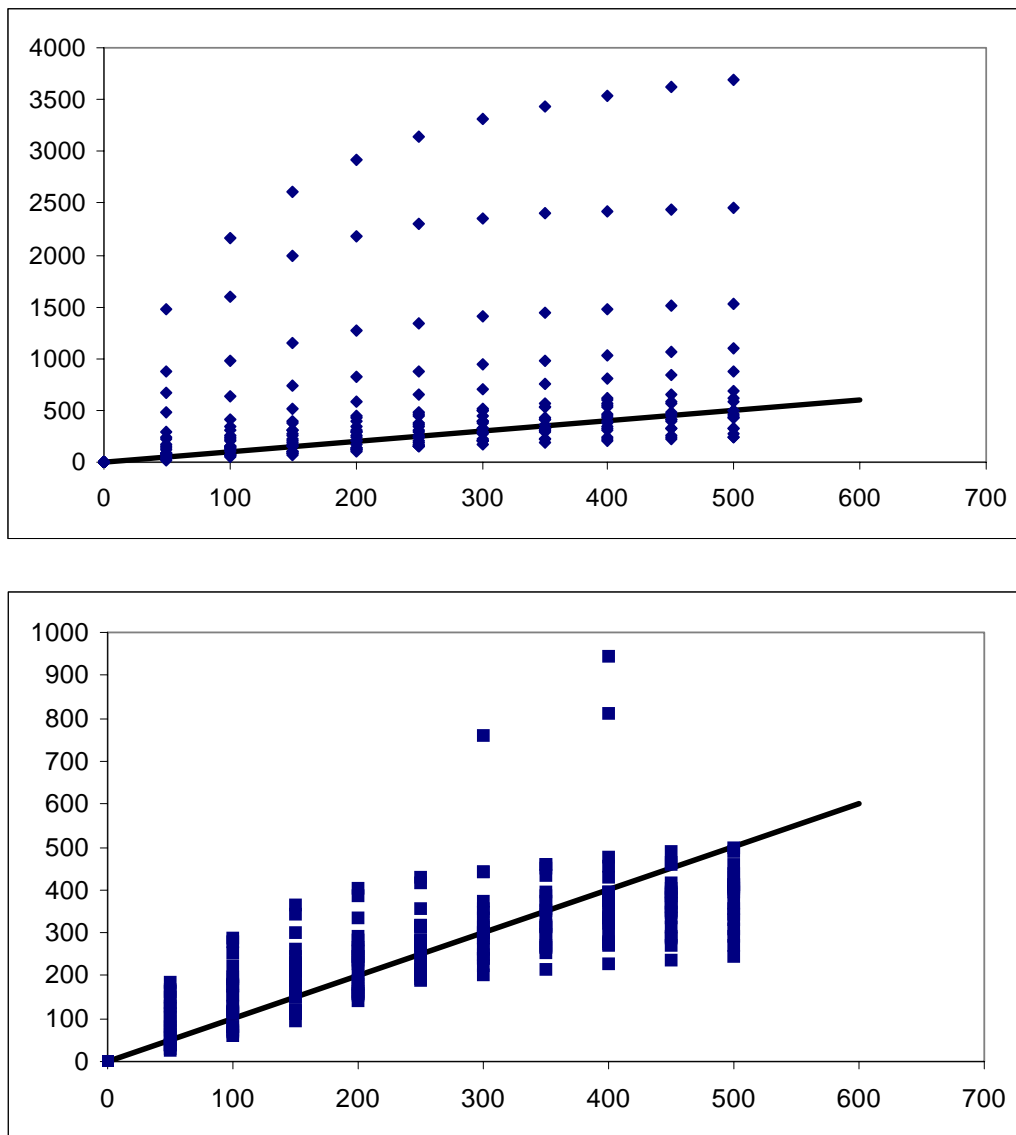
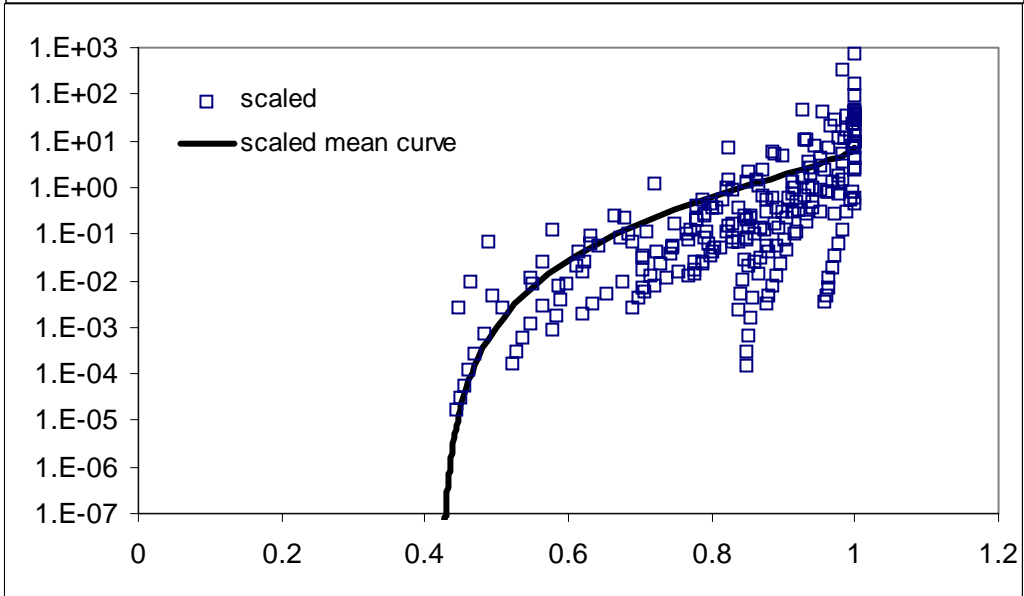
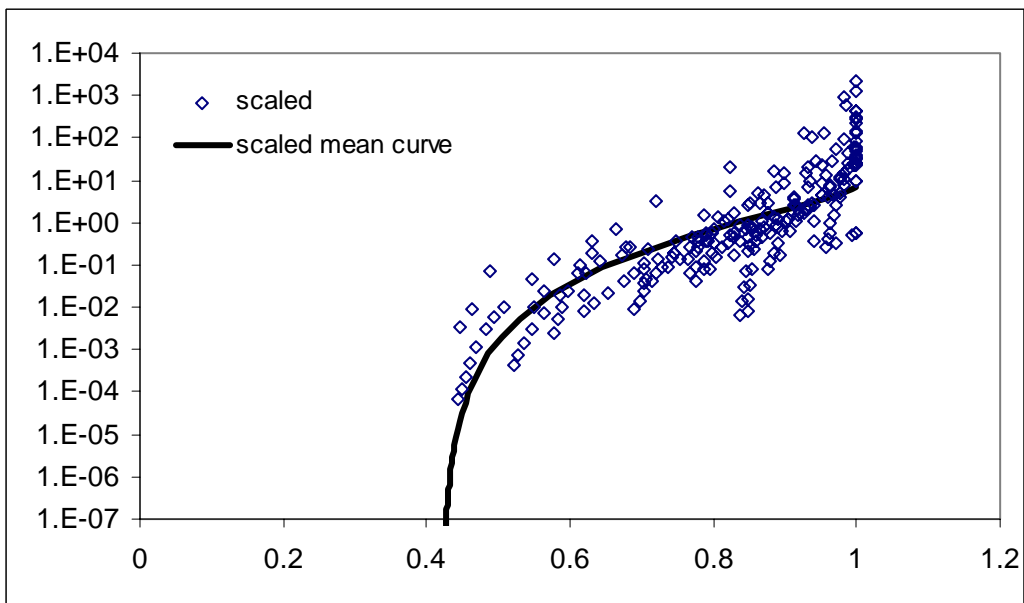
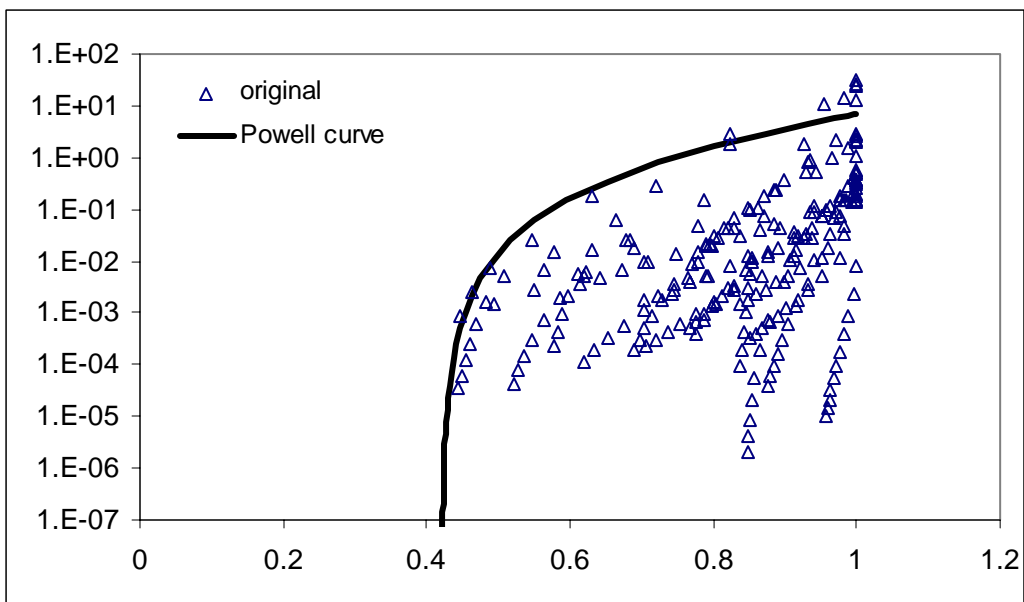


Figure 4.5.2a-e. Soil water retention (a) unscaled, (b) scaled using method 1, and (c) scaled using method 2. Original and de-scaled soil water pressure head using method 1 (d) and method 2 (e). All curves represent Group 2, Population 2.



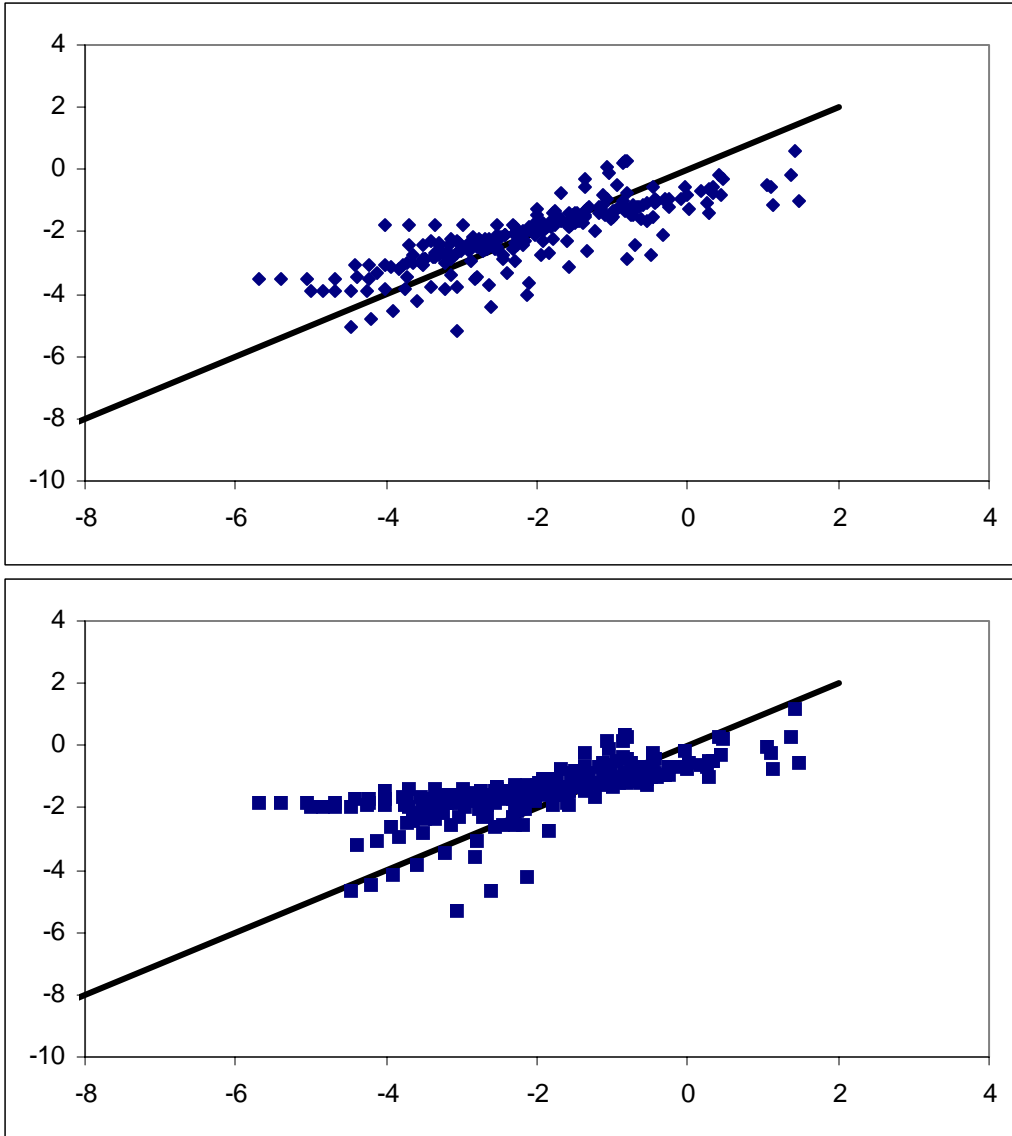
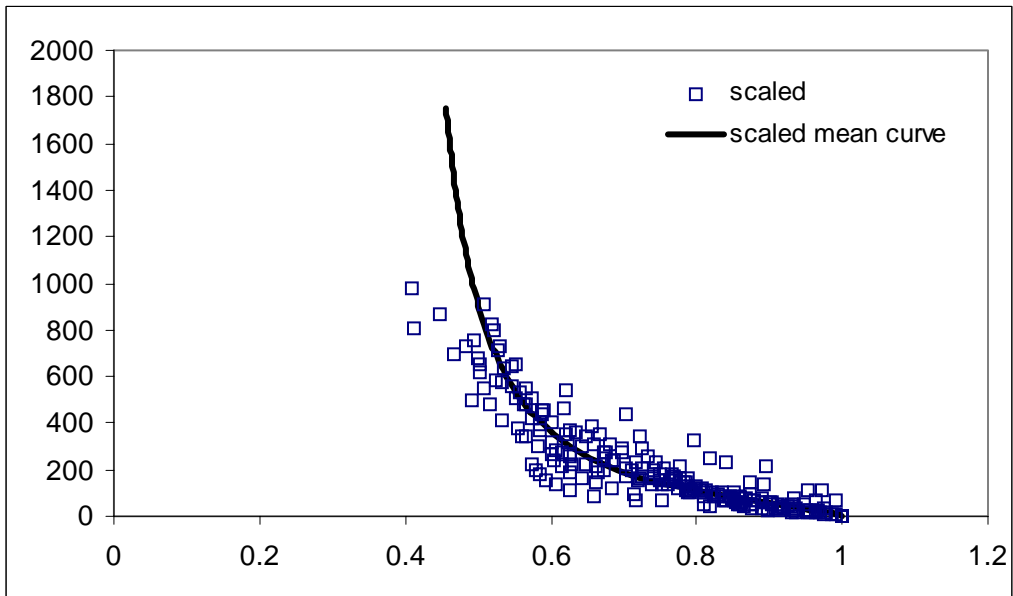
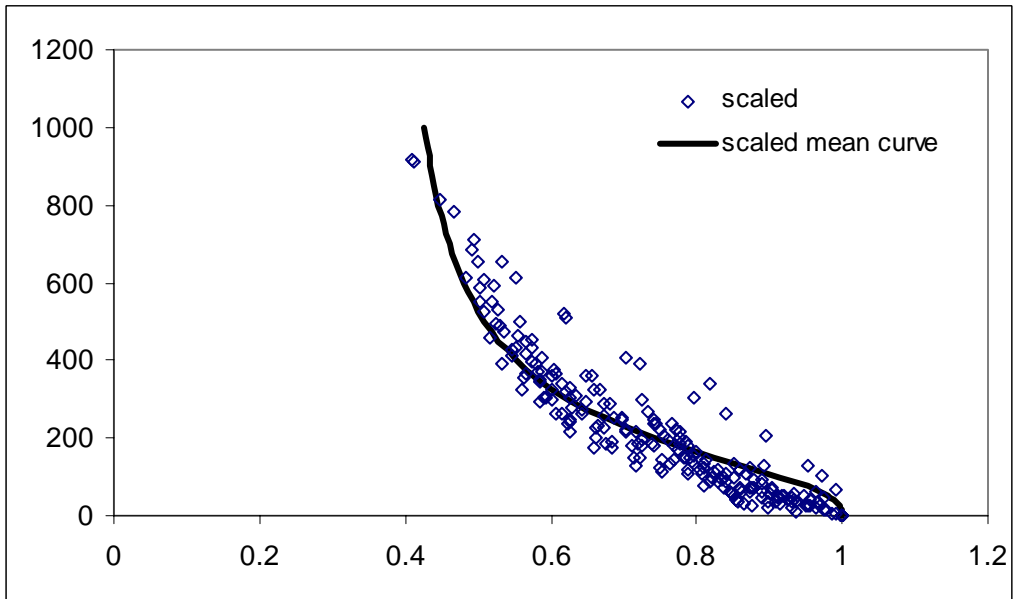
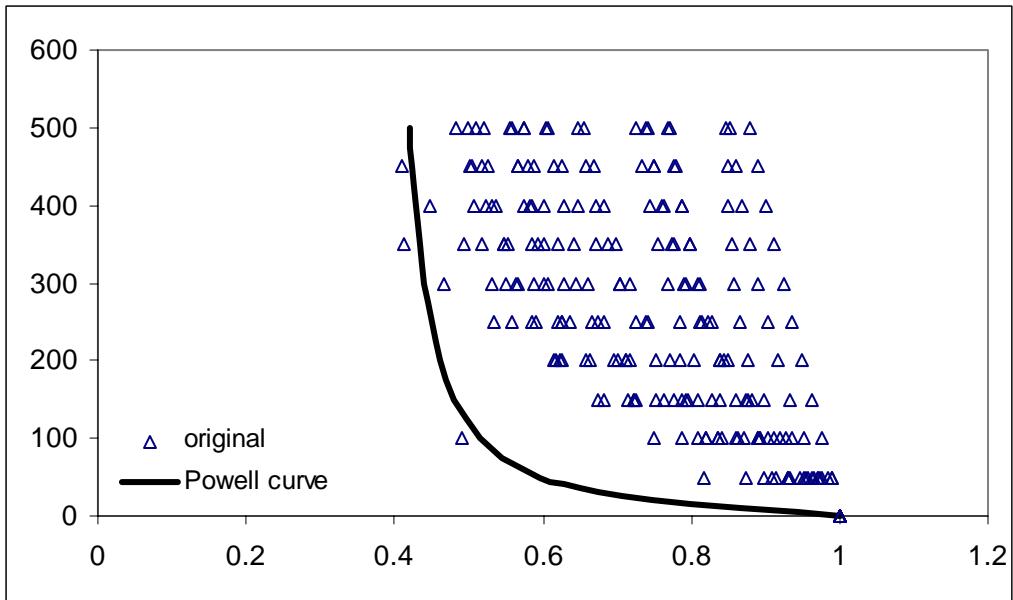


Figure 4.5.2f-j. Unsaturated hydraulic conductivity (f) unscaled, (g) scaled using method 1, and (h) scaled using method 2. Original and de-scaled unsaturated hydraulic conductivity using method 1 (i) and method 2 (j). All curves represent Group 2, Population 2.



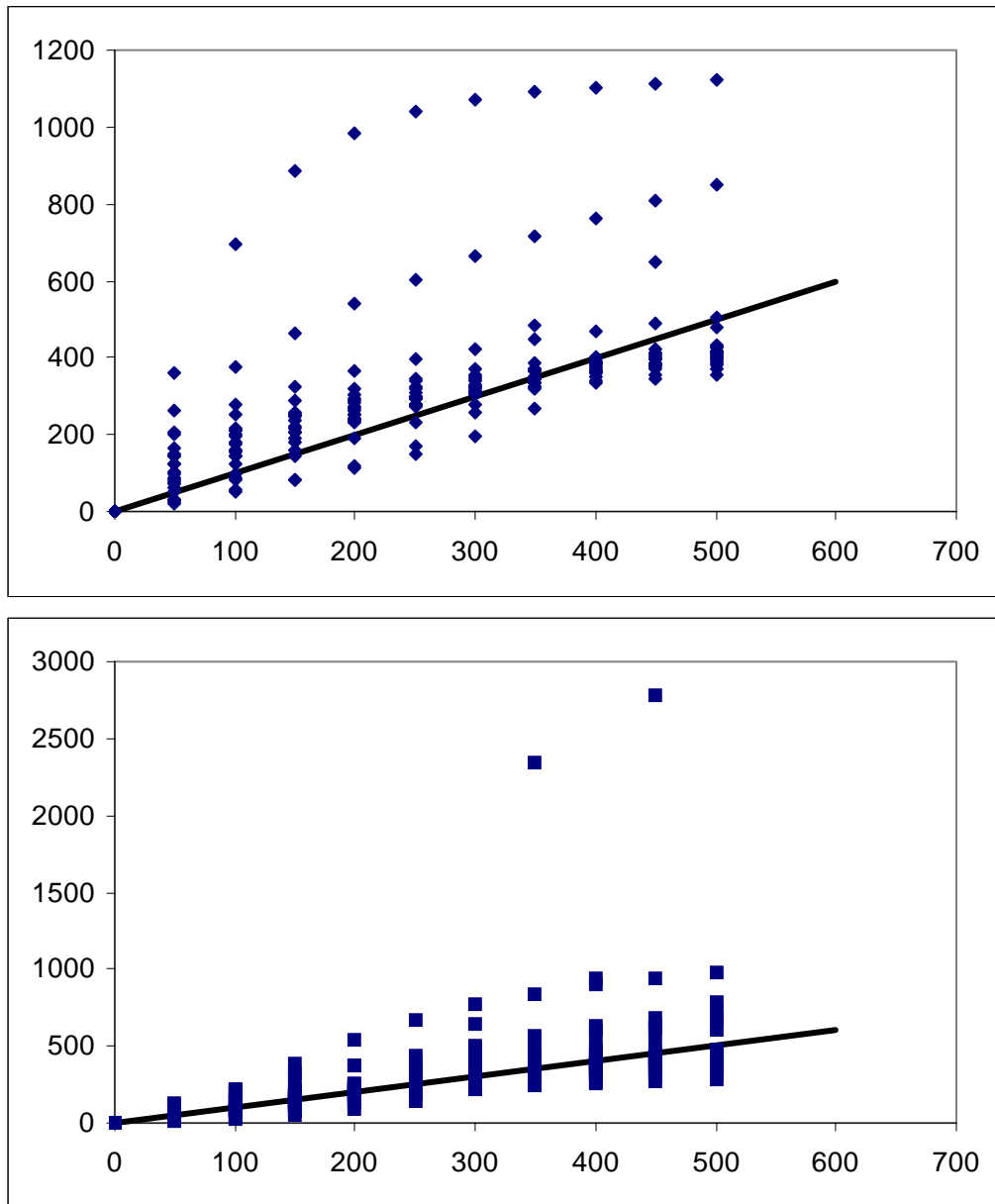
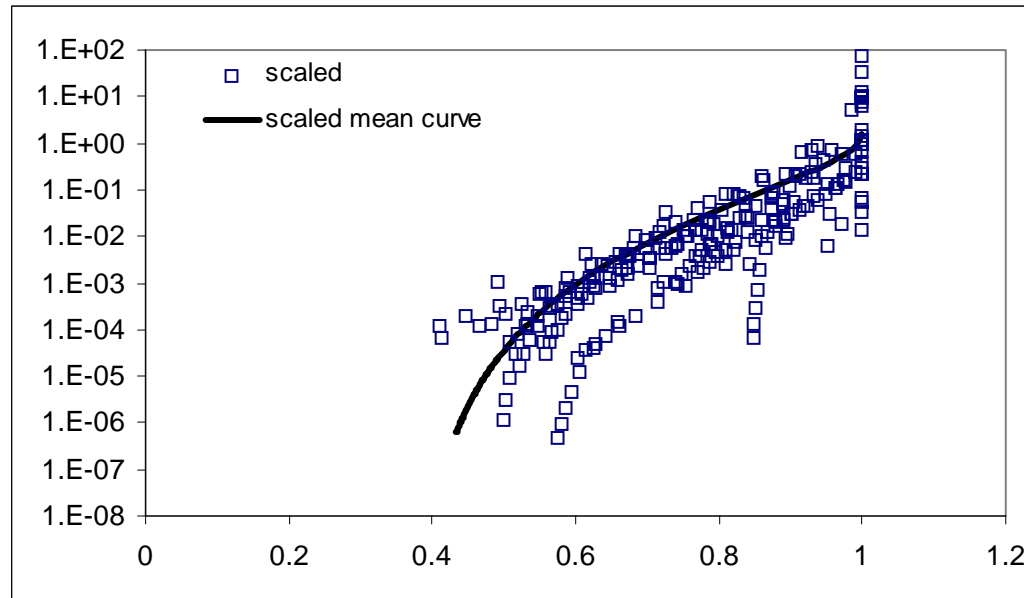
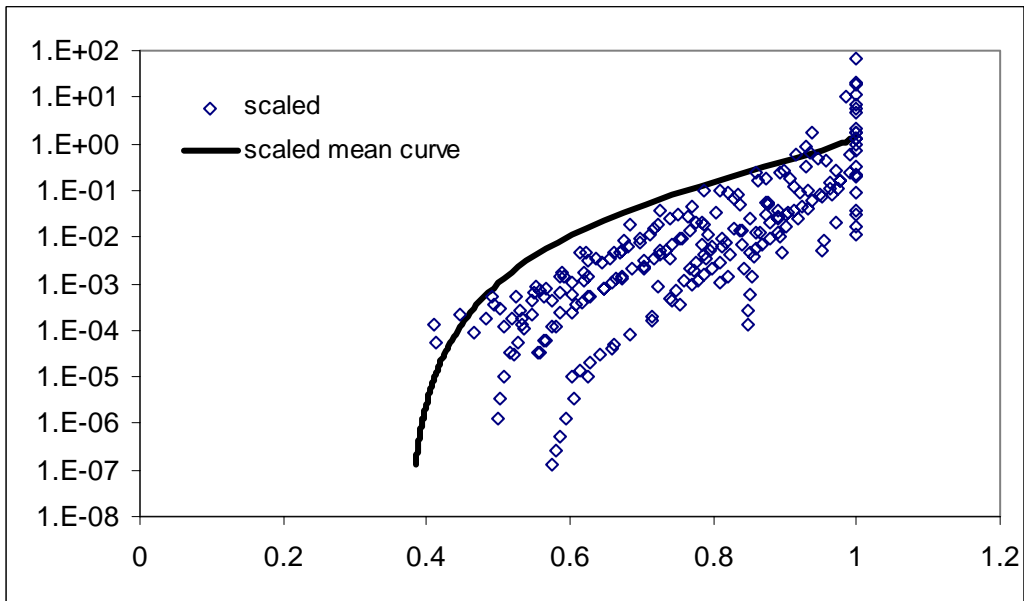
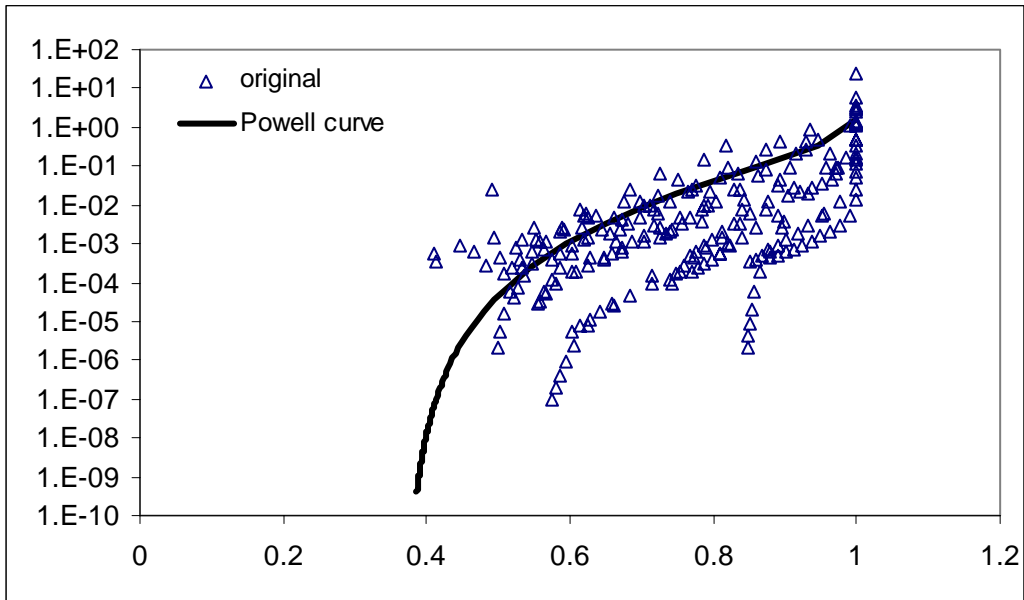


Figure 4.5.3a-e. Soil water pressure head (a)unscaled,(b) scaled using method 1, and (c) scaled using method 2. Original and descaled soil water pressure head using method 1(d) and method 2 (e). All curves represent Group 2, Population 1, subgroup sandy loam.



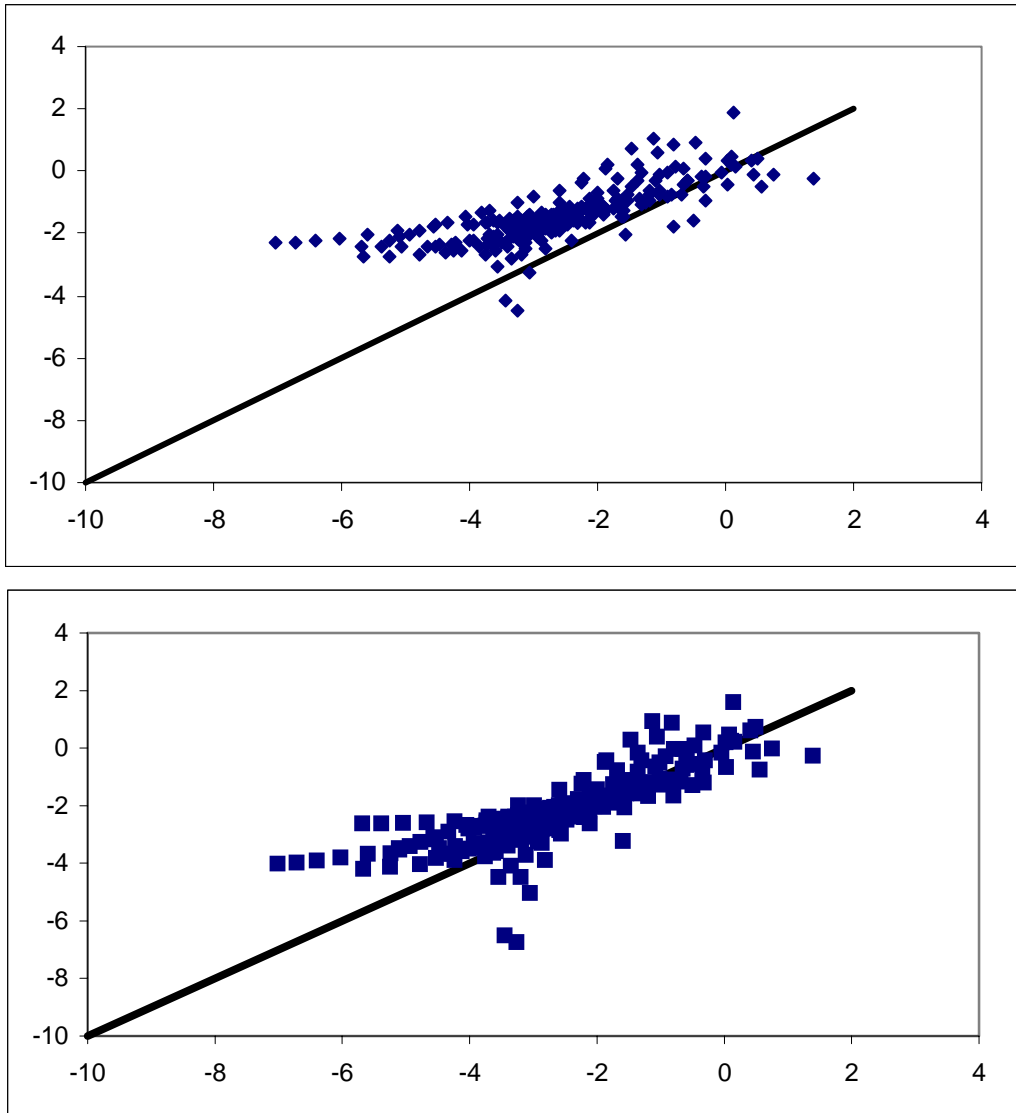
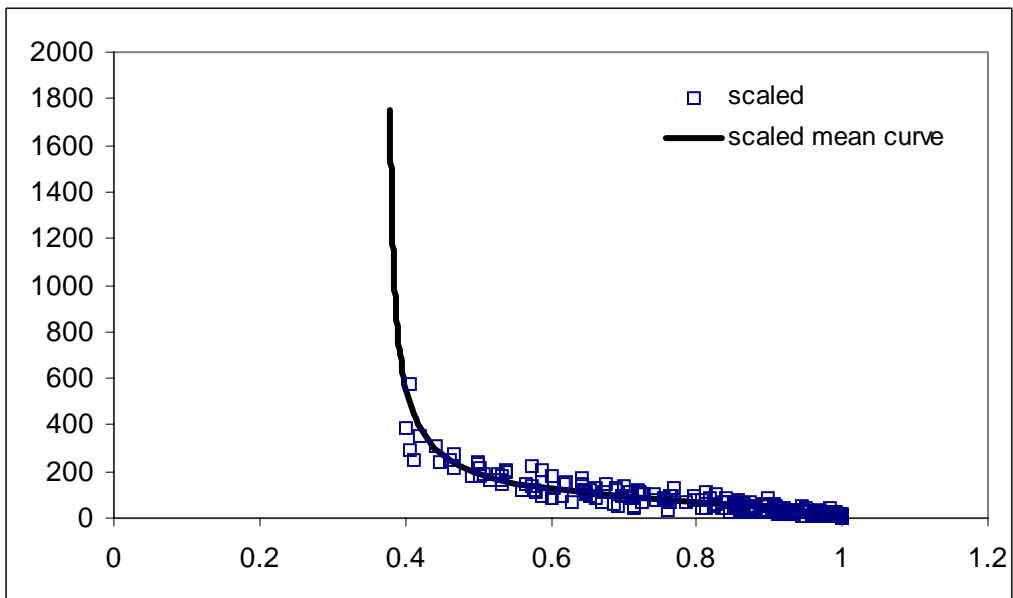
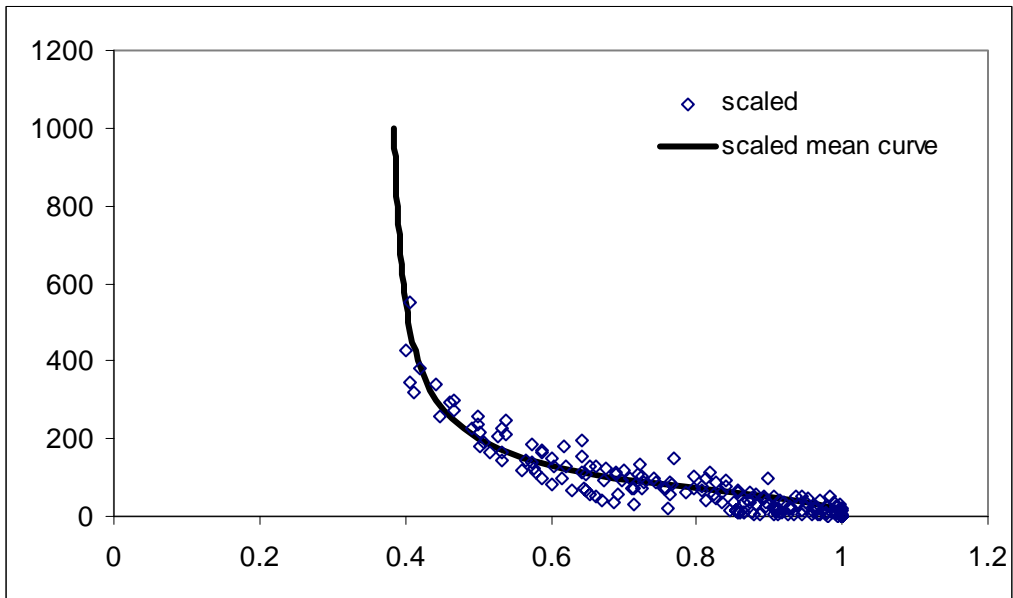
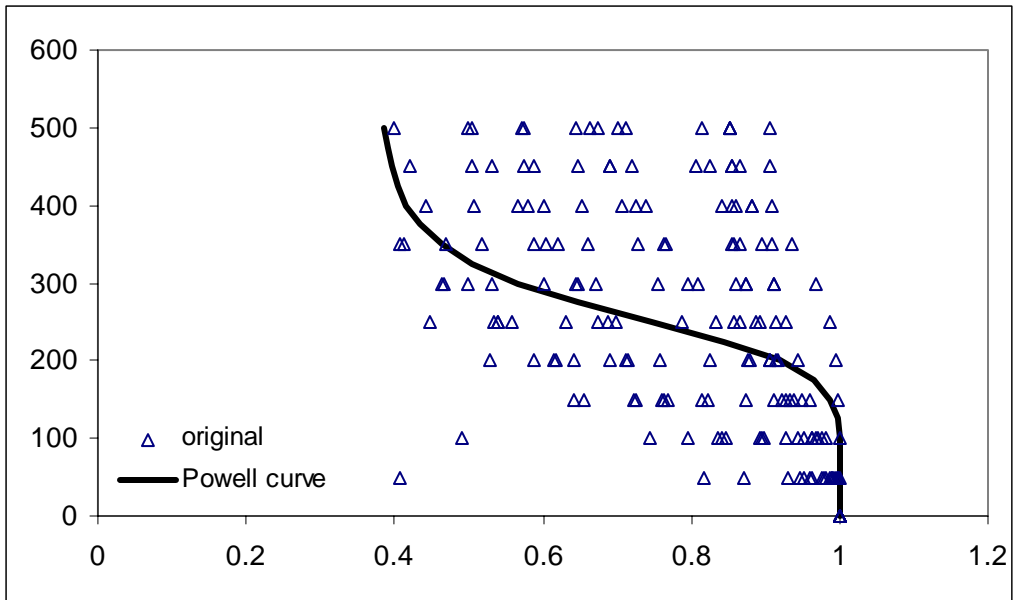


Figure 4.5.3f-j. Unsaturated hydraulic conductivity (f) unscaled, (g) scaled using method 1, and (h) scaled using method 2. Original and de-scaled unsaturated hydraulic conductivity using method 1 (i) and method 2 (j). All curves represent Group 2, Population 1, subgroup sandy loam.



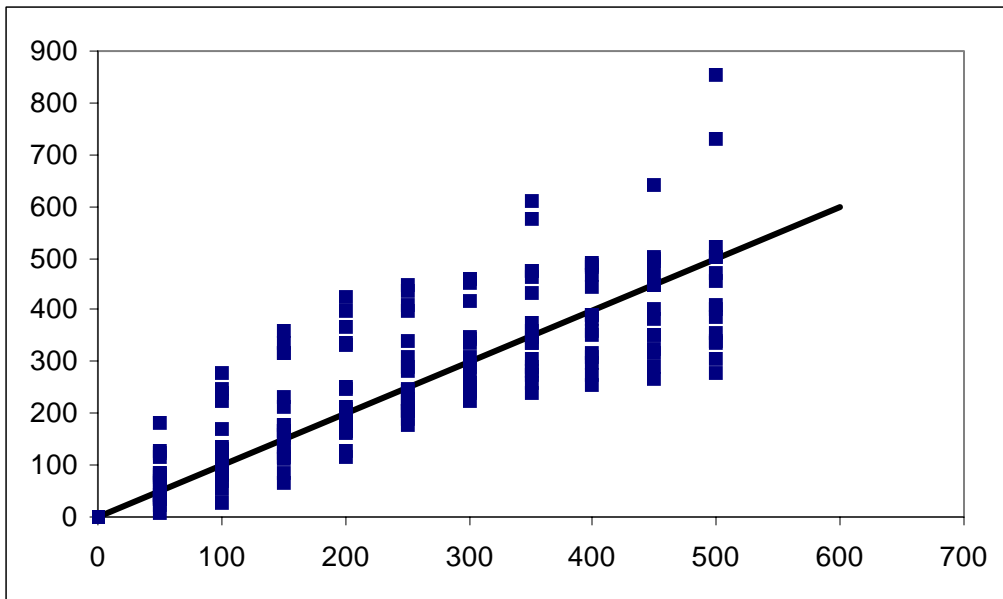
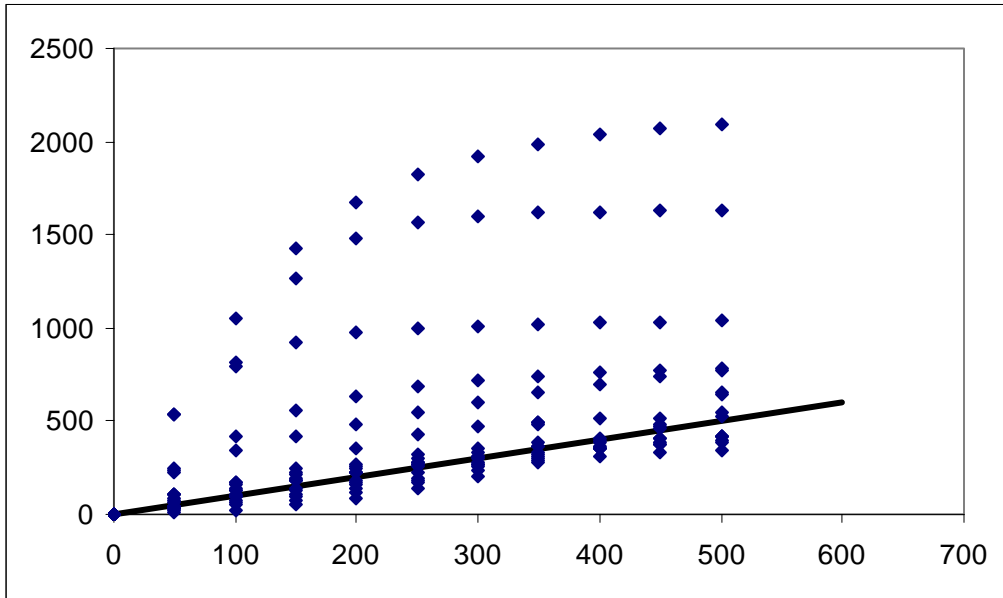
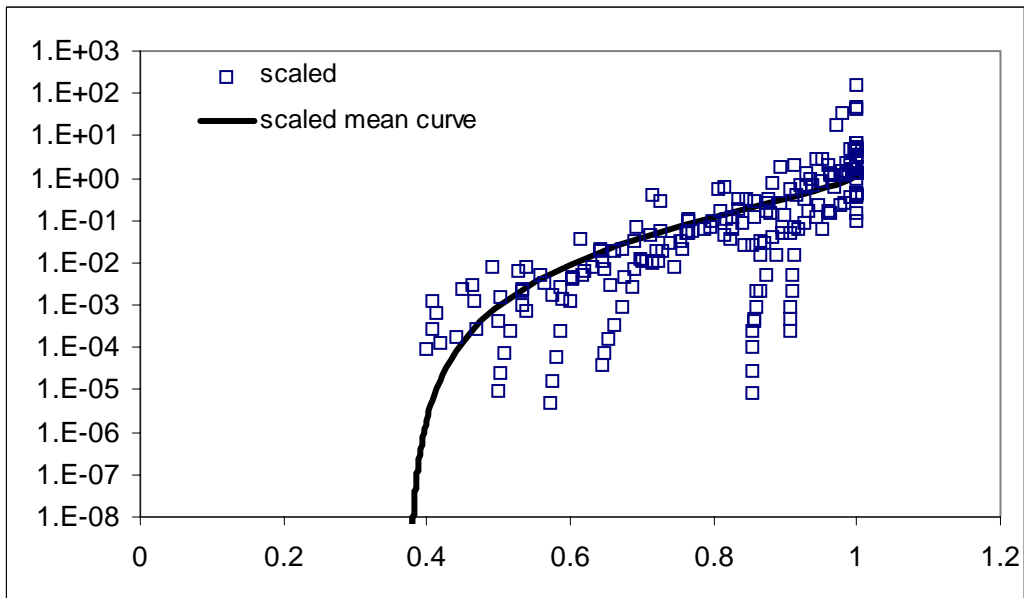
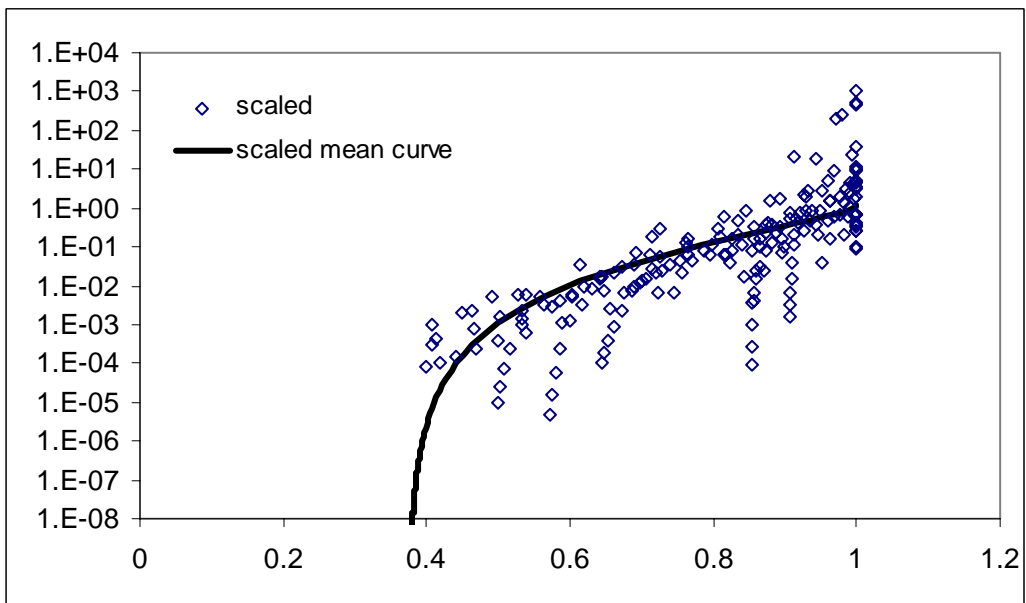
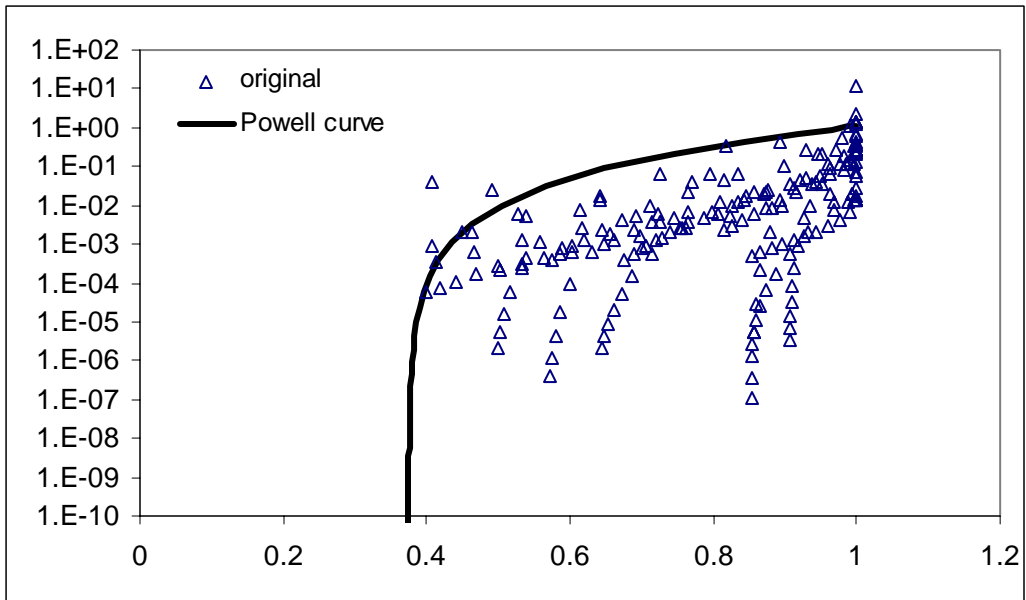


Figure 4.5.4a-e. Soil water pressure head (a) unscaled (b) scaled using method 1, and (c) scaled using method 2. Original and descaled soil water pressure head curves using method 1 (d) and method 2 (e). All curves represent Group 3, Population 1, subgroup sandy loam.



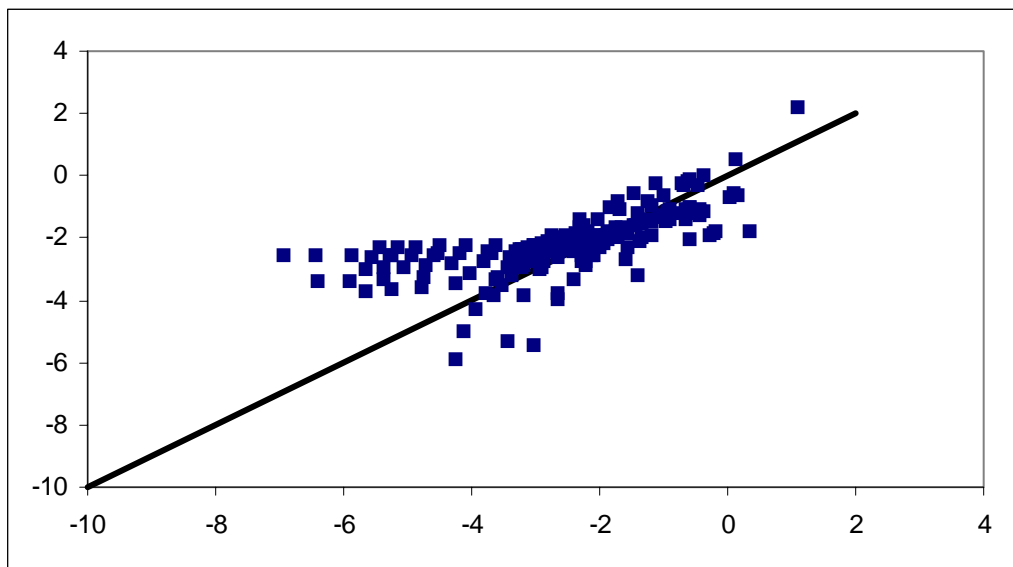
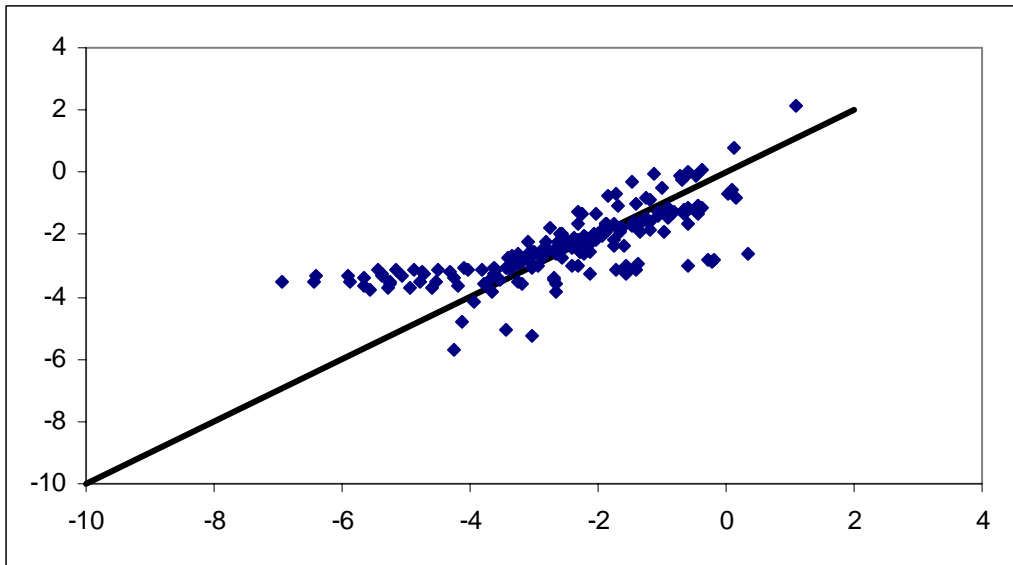
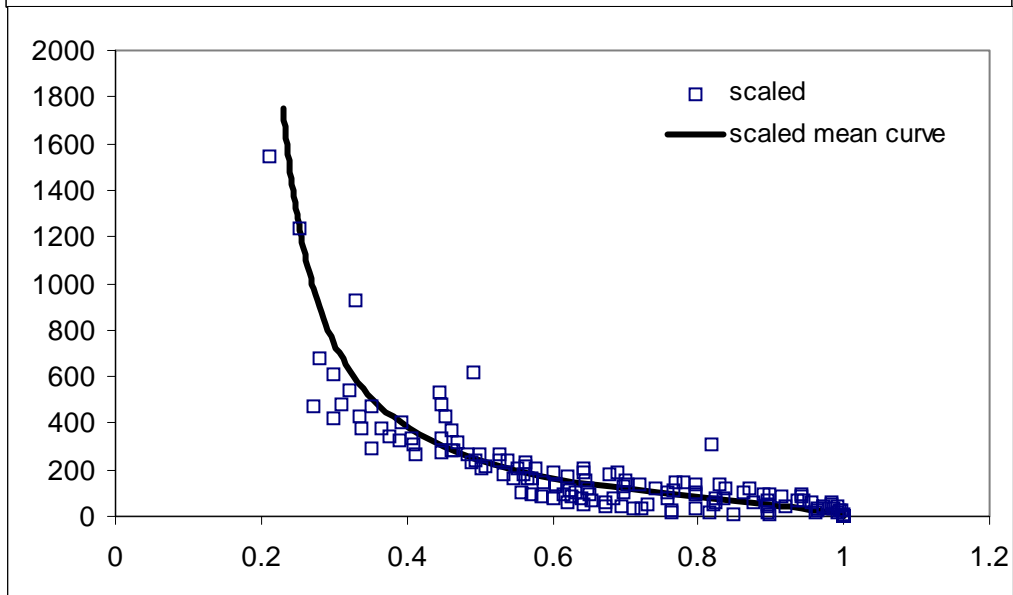
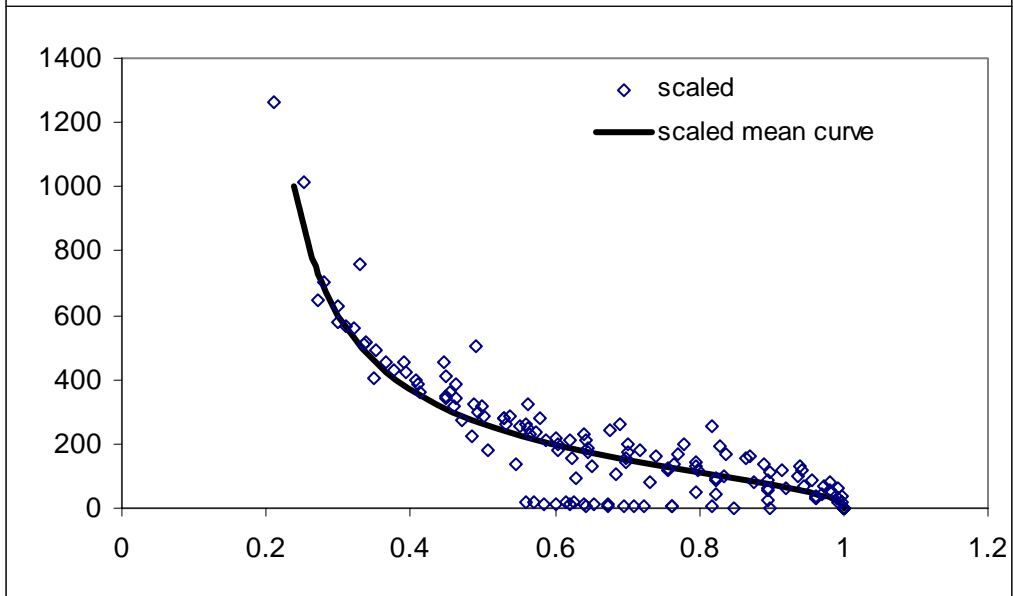
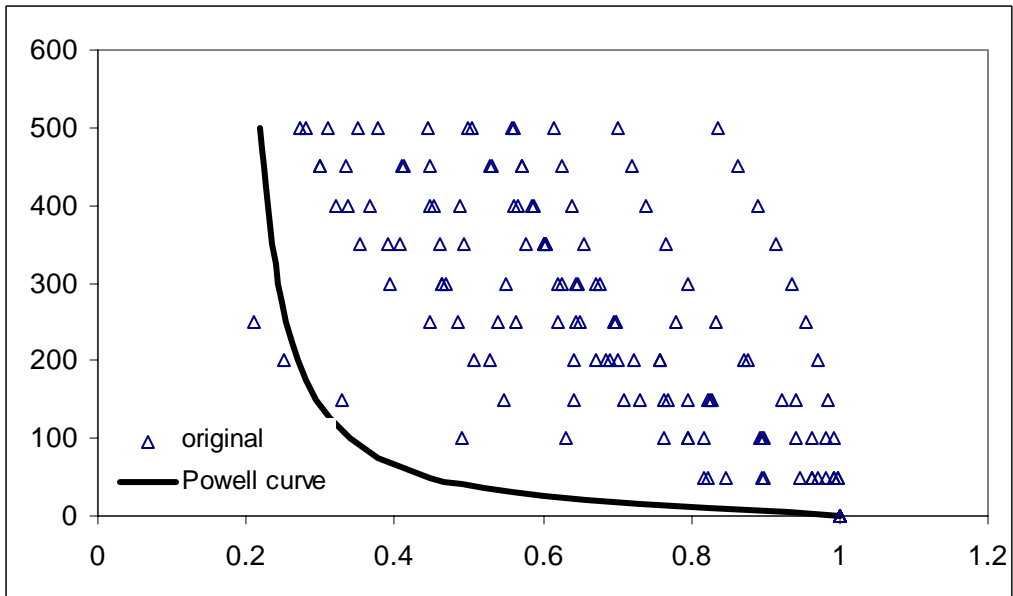


Figure 4.5.4f-j. Unsaturated hydraulic conductivity (f) unscaled, (g) scaled using method 1, and (h) scaled using method 2. Original and descaled unsaturated hydraulic conductivity using method 1 (i) and method 2 (j). All curves represent Group 3, Population 1, subgroup sandy loam.



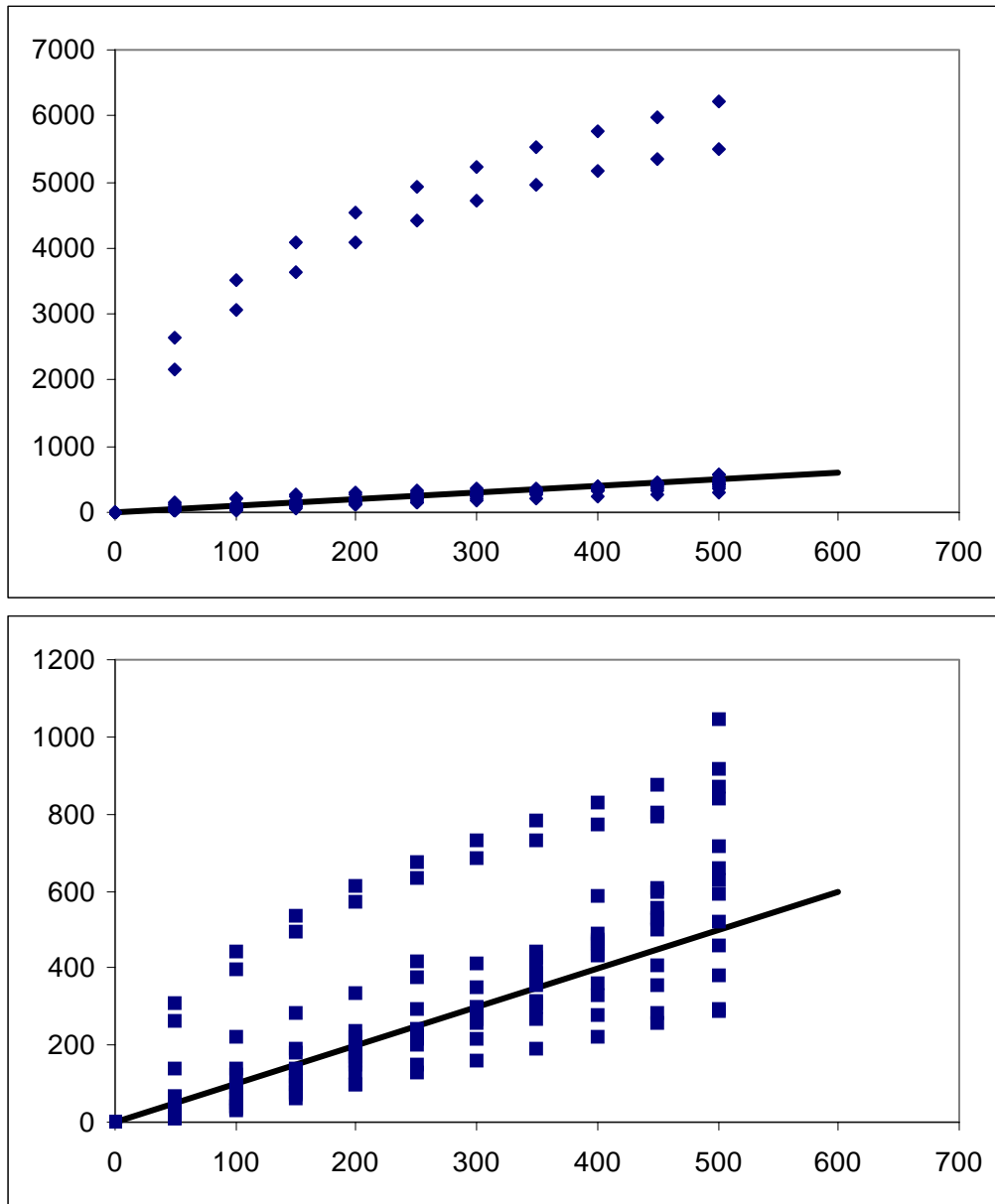
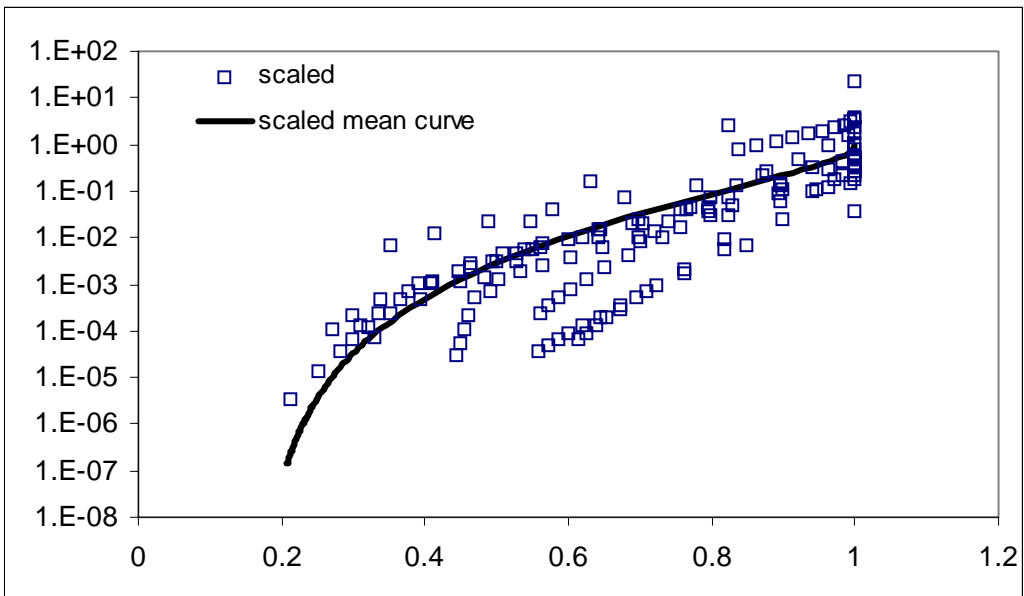
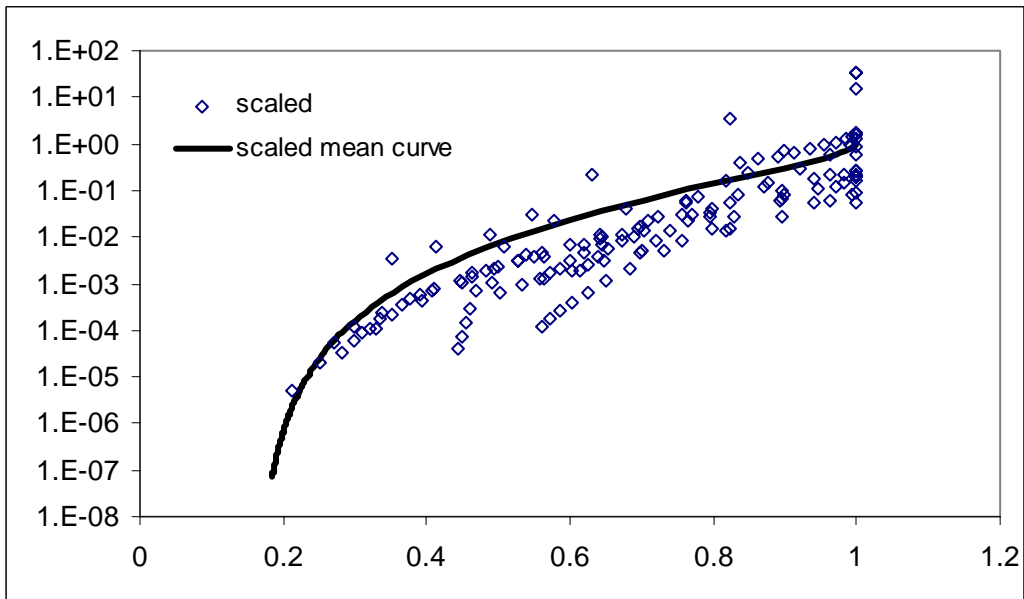
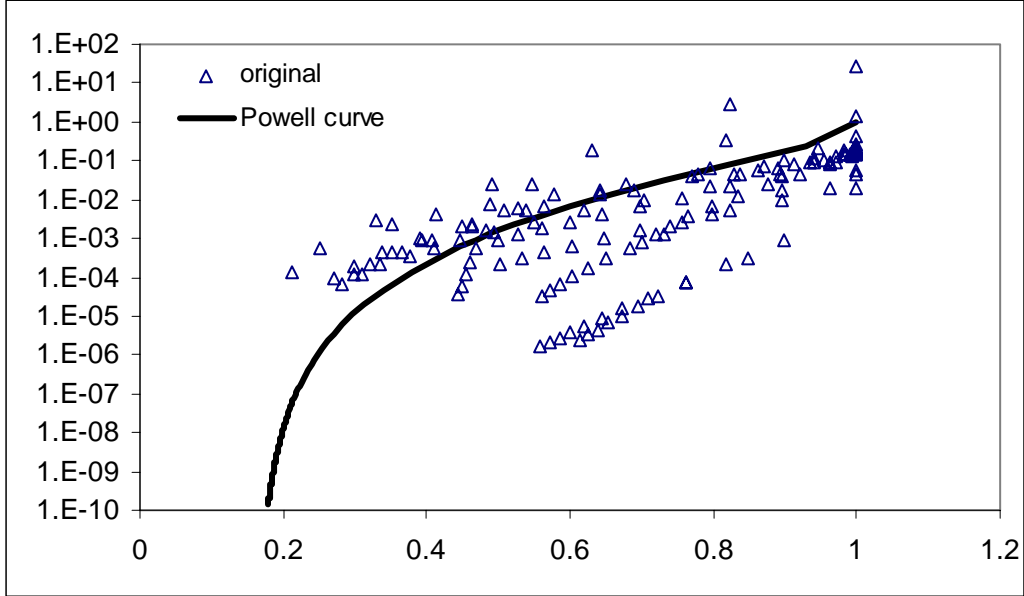


Figure 4.5.5a-e. Soil water pressure head (a) unscaled, (b) scaled using method 1, and (c) scaled using method 2. Original and descaled soil water pressure head curves using method 1 (d) and method 2 (e). All curves represent Group 4, Population 1, subgroup sandy loam.



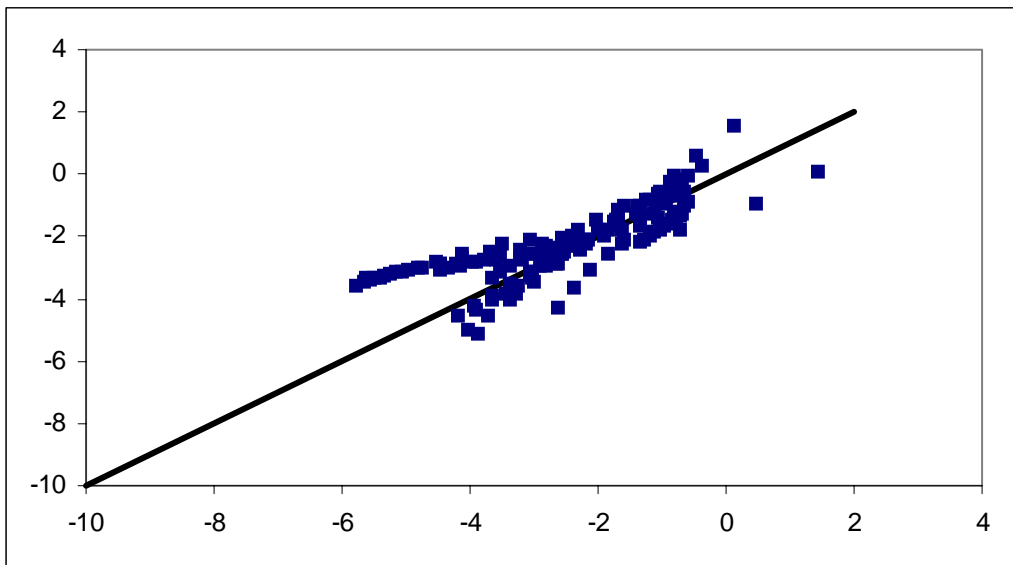
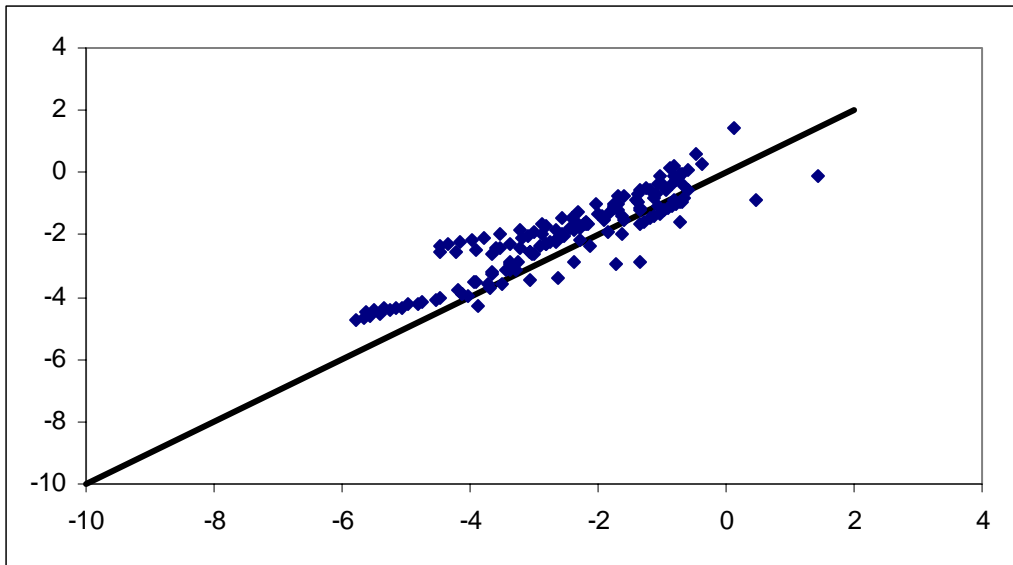


Figure 4.5.5f-j. Unsaturated hydraulic conductivity (f) unscaled, (g) scaled using method 1, and (h) scaled using method 2. Original and descaled unsaturated hydraulic conductivity (i-j) for Group 4, Population 1, subgroup sandy loam.



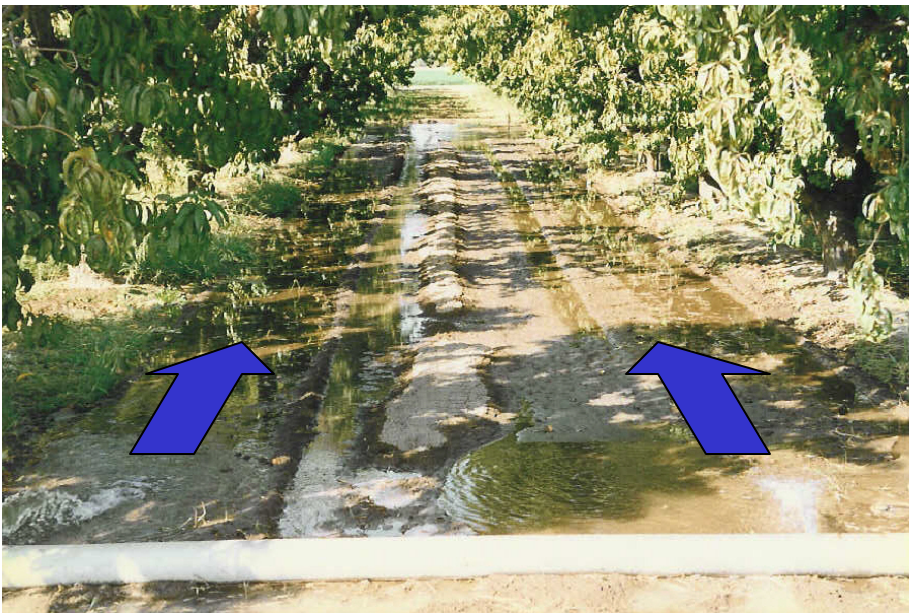
Photos 1 – 3: The irrigation begins in the afternoon. Prior to this particular irrigation, the flood basin has been mowed and rotovated to 6” depth after a application of potassium bromide (see section 2.6).



Photo 4. Another view of the irrigation pipe.



Photo 5. Overnight, the irrigation water has spread throughout the basin.



Photos 6 and 7. While water is filling the basin in the direction of the arrows, the irrigation is does not completely cover the row basin. The irrigation pipe is shown in the foreground.



Photos 8-11: Additional images of irrigation in other tree row basins (near the end of the irrigation cycle).

Appendix 1:

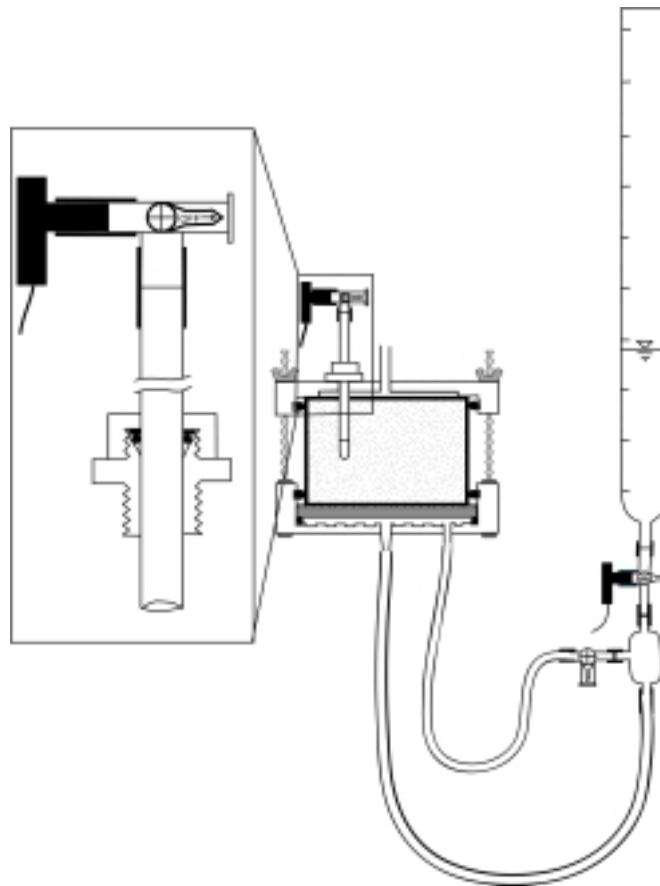
Reprint of

Tuli, A., M.A. Denton, J.W. Hopmans, T. Harter, and J.L. Mac Intyre. 2001. Multi-step outflow experiment: From soil preparation to parameter estimation . Hydrology program, Dept of Land, Air, and Water Resources, University of California, Davis, CA, Paper number 100037.

**Multi-step outflow experiment: From soil preparation to
parameter estimation**

by

Ataç Tuli, Michelle A. Denton, Jan W. Hopmans, Thomas Harter, and James L. Mac Intyre



September, 2001



Hydrology
Department of Land, Air, and Water Resources
University of California, Davis

TABLE OF CONTENTS

LIST OF FIGURES.....	iii
LIST OF TABLES	v
LIST OF PHOTOS.....	vi
1. INTRODUCTION.....	1
1.1. Synopsis	2
2. THEORY AND MODELS	4
2.1. SFOPT development and inverse parameter estimation	4
2.2. Soil water retention and hydraulic conductivity models.....	5
2.3. Objective function.....	7
3. MATERIAL AND METHODS	8
3.1. Sample preparation and bottom plate assembly.....	8
3.2. Tensiometers and transducers	11
3.3. Top and bottom plates of the Tempe cell.....	12
3.4. Adaptors for small diameter soil cores in the 2.5-inch Tempe pressure cell	13
3.5. Data collection.....	15
3.6. Keeping the experimental records.....	19
3.7. Air flushing	22
3.8. Some experimental problems and remarks	22
4. PRESSURE TRANSDUCER CALIBRATION	24
5. MULTIPLEXING	27
5.1. Multiple sensor set up	27
5.2. PC208W datalogger support software.....	29
5.3. Datalogger program for transducer multiplexing.....	36
6. DATA FILE PREPARATION PROGRAM (DATAPREP).....	38
6.1. Description and requirements of DATAPREP.....	38
6.2. Cleaning the raw experimental data	42
6.3. Making an input data file for DATAPREP program.....	43
6.3.1. Example 1.....	43

6.4. Running the data preparation program, DATAPREP	52
6.5. Corrections to DATAPREP files in the case of incomplete or erroneous transducer measurements	55
6.5.1. Example 2.....	56
6.5.2. Example 3.....	66
7. PARAMETER ESTIMATION PROGRAM (SFOPT).....	67
7.1. Description and features of the SFOPT.....	67
7.2. Troubleshooting	68
7.3. Initial estimates of parameters.....	69
7.4. Description of variables of input file.....	71
7.5. Example Problems.....	72
7.5.1. Example 1: Multi-step outflow, van Genuchten model, ceramic plate	72
7.5.2. Example 2: Multi-step outflow, lognormal model, nylon membrane	76
7.5.3. Example 3: Multi-step outflow, van Genuchten model, nylon membrane ..	79
REFERENCES.....	83
APPENDIX A. Photographs of the items used in the Multi-step outflow experiment.....	86
APPENDIX B. Source file of DATAPREP	90
APPENDIX C. Source file of SFOPT.....	96

LIST OF FIGURES

Figure 1. Flow chart of the inverse solution technique for parameter estimation of the soil hydraulic functions.....	3
Figure 2. Perforated stainless steel screen support (a), and support assembly (b).....	10
Figure 3. Modified Tempe pressure cell.	14
Figure 4. Tensiometer pressure head (solid line) and pressure head at the bottom of the porous barrier (dashed line) (a), matric pressure head (b), and cumulative outflow (c) as a function of time.	18
Figure 5. Datasheet for the saturated hydraulic conductivity experiment.....	19
Figure 6. Datasheet during the multi-step outflow experiment.....	20
Figure 7. Datasheet for the parameters obtained at the end of the experiment.....	21
Figure 8. Experimental set up for calibration (slope) of the tensiometer (a) and outflow transducers (b).	25
Figure 9. Calibration of the tensiometer (a, c) and outflow (b, d) pressure transducers at two dates.....	26
Figure 10. Schematic view of the pressure transducer multiplexing.	28
Figure 11. PC208W toolbar.	29
Figure 12. Setup connection window.....	30
Figure 13. Setup window with the connected dataloggers: (a) Hardware tab, (b) Data Collection tab, (c) Schedule tab.	31
Figure 14. Connection window: (a) before connection, (b) after connection.	32
Figure 15. Edlog program window.	33
Figure 16. Association of datalogger program: (a) Program directory, (b) after association of DLD file.	34
Figure 17. Numeric window for real-time data monitoring: (a) before adding transducers, (b) after adding transducers.....	35
Figure 18. Status window.....	35
Figure 19. Schematic diagram of data processing procedure.....	38
Figure 20. Schematic view of the experimental set up.	40

Figure 21. Outflow-transducer voltage versus time for first flushing prior to data removal.	49
Figure 22. Outflow-transducer voltage versus time for first flushing after data removal.	49
Figure 23. Final output graph of the DATAPREP program.	54
Figure 24. Graphical output window using original DATAPREP program on example2.csv.	57
Figure 25. Graphical output windows using modified DATAPREP program on example2.csv.	58

LIST OF TABLES

Table 1. Physical properties of different porous materials (l_t = thickness; $R_p = l_t / K_s$) ..	10
Table 2. Description of variables for input file 'FNAME' of the DATAPREP.....	41
Table 3. Recorded starting times for pressure applications.	43
Table 4. Recorded times for flushing events.....	44
Table 5. Data excerpt for 40 mbar pressure step.....	46
Table 6. Data excerpt for 80 mbar pressure step.....	46
Table 7. Data excerpt for 150 mbar pressure step.....	46
Table 8. Data excerpt for 300 mbar pressure step.....	47
Table 9. Data excerpt for 500 mbar pressure step.....	47
Table 10. Graphed data after removal.....	50
Table 11. Example input data file for the DATAPREP (FNAME).	51
Table 12. The lines that must be modified in the DATAPREP code.....	57
Table 13. Excerpt from SFOPT input file for Example 2 showing the times at which pressure steps begin.....	59
Table 14. "Example2.in" input data file for SFOPT with a weight of 1.0 for outflow.....	60
Table 15. "Example2a.in" input data file for SFOPT with zero weight for outflow.	61
Table 16. "Example2.in" input data file after copying and pasting.	62
Table 17. Experimental record for Example 2.	63
Table 18. Portion of "example2.in" input before and after insertion of the first handwritten value from the experimental record.	65
Table 19. Converted handwritten values from experimental record.....	66
Table 20. Initial estimates of parameters used in optimization.....	70

LIST OF PHOTOS

Photo 1. The multi-step outflow experiment set up: (A) External power supply, (B) 21X Datalogger, (C) AM416 Multiplexer, (D) Tempe cell with the ring, (E) Tensiometer and outflow pressure transducers, (F) Air trap, (G) The graduated burette.....	86
Photo 2. Porous membrane assembly for the 3.5” soil sample.	87
Photo 3. Mini-tensiometer transducer arrangement: (A) 3-way valve, (B) Pressure transducer, (C) Rubber sleeve, (D) Ferrule & O-ring, (E) Acrylic tube, (F) Copper coupler,(G) Ceramic cup	87
Photo 4. The 3.5” top cover of the Tempe cell.	87
Photo 5. The 3.5” bottom cover of the Tempe cell.	87
Photo 6. Aluminum sleeve glued with the filter paper (from the top).	88
Photo 7. Plastic liner, aluminum sleeve glued with filter paper, Plexiglas sleeve, and saturated hydraulic conductivity set up (from left to right).	88
Photo 8. The way of setting up the sample from Geoprobe Macrocore [®] for the multi-step experiment.....	88
Photo 9. Bottom cover of the 2” Tempe cell.....	89
Photo 10. Porous membrane assembly and support.....	89
Photo 11. The 2” Tempe cell set up.	89
Photo 12. Multi-step experiment set up for the ten 2” Tempe cells.....	89

1. INTRODUCTION

The success of modeling unsaturated soil water transport problems often depends on the availability of soil hydraulic functions, the water retention $\theta(h)$, and the hydraulic conductivity, (K) , as a function of soil water matric head, h , or water content, θ . Traditional techniques for determining $\theta(h)$ involve stepwise equilibrium desorption or sorption experiments. $K(\theta)$ is often determined by steady state methods. Unfortunately, it is often tedious and time consuming to determine these functions in a traditional way. Over the last several years, indirect laboratory methods have been developed that are fast, conveniently controlled, and relatively inexpensive. One such technique is the parameter estimation by the inverse modeling from transient outflow measurement.

Kool et al. (1985a) were among the first to apply the inverse technique by numerical solution of the Richards equation for a one-step outflow experiment. Subsequently, Parker et al. (1985) experimentally applied the one-step outflow method to four soils of different texture and showed that soil hydraulic functions ($\theta(h)$ and $K(\theta)$) can be optimized simultaneously by using cumulative outflow as a function of time. Although optimization of the parameters describing the soil hydraulic functions in a transient outflow experiment is a promising method to derive soil hydraulic information, estimates from one-step outflow experiments using only cumulative outflow data in the objective function are often unreliable and non-unique (van Dam et al., 1992). To overcome nonunique estimates of soil hydraulic functions, van Dam et al. (1994) introduced the multi-step outflow method, which uses a sequence of smaller pneumatic pressure increments to induce drainage of the soil core. Their laboratory experiments showed that such outflow data contain sufficient information for unique estimates of the soil hydraulic functions, using initial estimates derived from the outflow experiment itself. The experimental work by Eching and Hopmans (1993a, b) and Eching et al. (1994) showed how the multi-step method in combination with automated soil water matric head measurements during drainage of soil cores improved the estimation of parameter values of soil hydraulic functions for four different textured soils. Chen et al.

(1997) reported an updated model version (SFOPT) of the outflow experiment with data file preparation program (DATAPREP).

1.1. Synopsis

This report documents the components of the multi-step outflow method used for parameter estimation of the soil hydraulic functions by inverse modeling. In addition, it includes the documentation for the experimental data processing and the parameter estimation algorithm. The inverse modeling includes three interrelated functional parts (Figure 1): (1) a controlled transient flow experiment with prescribed initial and boundary conditions, and transient flow variables, such as cumulative outflow and matric pressure are accurately measured by pressure transducers; (2) a numerical flow model simulating the transient water flow regime of this experiment using initial estimates of the parametric soil hydraulic functions (see sections 2.1 and 2.2); and (3) a nonlinear optimization algorithm, which estimates the unknown parameters of the hydraulic functions through minimization of the difference between observed and simulated flow variables (residuals) through iterative solution of the transient flow equation (see section 2.3). The quality of the final solution of the parameter estimation problem depends on each of these three individual components as well as their integration within a computational framework. The three individual components are interfaced through input data files that include the experimental, numerical water flow model, and parameter optimization results. Parameters of the hydraulic functions are updated iteratively in the optimization routine, thereby continuously reducing the residuals until a predetermined convergence criterion has been achieved. However, achieving convergence criterion does not mean that an inverse solution is unique for a set of optimized parameters. It is generally recommended to test non-uniqueness by solving the inverse problem repeatedly using new initial parameter estimates (Figure 1).

The experimental components and procedures of the multi-step outflow method are reported in sections 3, 4, and 5. Section 3 also includes topics such as the recommended steps for soil preparation, the required measurements of the soil physical properties before starting the outflow experiment, and the way of keeping experimental records. The transducer calibration (tensiometer and outflow), a method to multiplex several

transducers to one datalogger, datalogger communication software and a sample datalogger program are described in sections 4 and 5. Moreover, the photographs of different components of the outflow experiment are shown in Appendix A. The program DATAPREP, which is used to clean collected experimental data, and to prepare input data file for the SFOPT program is introduced and explained in detail in section 6. Finally, in section 7, the description and input file structure for the SFOPT program, which includes both the numerical simulation and nonlinear optimization algorithms are presented. Initial estimates of parameters used in the hydraulic functions, the example problems, input and output files are also provided. The source codes of DATAPREP and SFOPT programs can be found in Appendixes B and C, respectively. The first 12 references on page 83 provide an excellent review of literature and procedures of this report.

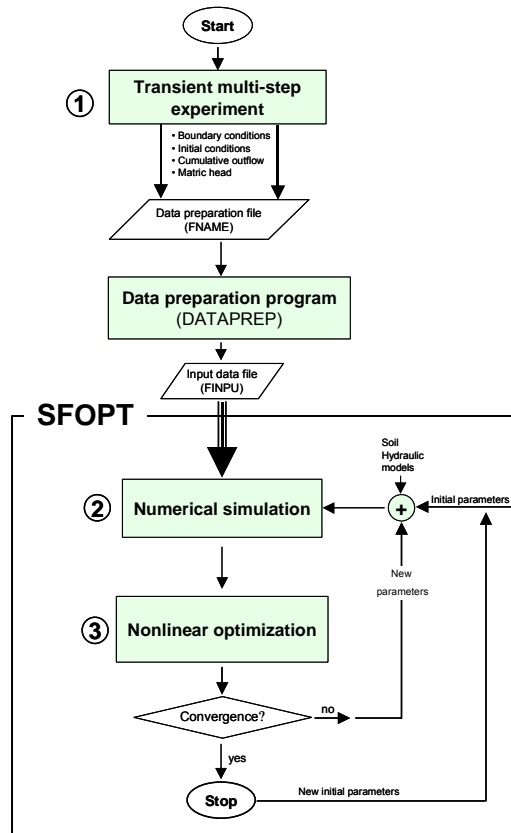


Figure 1. Flow chart of the inverse solution technique for parameter estimation of the soil hydraulic functions.

2. THEORY AND MODELS

2.1. SFOPT development and inverse parameter estimation

The nonlinear parameter optimization program SFOPT (single fluid optimization program) is originally based on the program ONESTEP, which was developed by Kool et al. (1985b) for the estimation of soil hydraulic properties from One-step outflow experiments. Van Dam et al. (1990) adapted the ONESTEP program to conduct multi-step outflow experiments (MULSTP). They made the parametric model more flexible and facilitated testing of uniqueness. Eching and Hopmans (1993a,b) modified the MULSTP code (MLSTPM) to enable the simultaneous use of cumulative outflow volume and soil water matric head data in the inversion process. Finally, Chen et al. (1997) introduced a new version of MLSTPM software (SFOPT), which includes new features and improvements in the optimization algorithm. Here, we will present the features of the SFOPT program, which are used to estimate the parameters of the constitutive functions of a soil sample from a multi-step outflow experiment, neglecting the influence of the non-wetting fluid (air) on the flow regime. Typically, the SFOPT program would be used for an air-water (nonwetting-wetting) soil system, neglecting viscosity in the air phase and its influence on water flow. Application of the inverse solution technique in a two-phase flow experiment is described in Chen et al. (1999) using an optimization code TFOPT.

Following is a general theoretical description of the inverse parameter estimation procedure for the soil hydraulic functions, specifically for the outflow method used in the SFOPT program. A detailed analysis of inverse methods on flow and optimization can be found in Hopmans et al. (2002). In the outflow method, a soil sample is saturated in a pressure cell with a porous barrier at the bottom. The porous barrier must have an air entry value larger than the maximum applied pressure, so that it remains saturated throughout the outflow experiment. The drainage induced by the soil water potential gradient is assumed to be described by the Richards equation. In its one-dimensional form with the vertical coordinate, $z(L)$, taken positive upward, it is written as

$$C(h) \frac{\partial h}{\partial t} = \frac{\partial}{\partial z} \left[K(h) \left(\frac{\partial h}{\partial z} + 1 \right) \right] \quad [1]$$

where $C = d\theta/dh$ is the water capacity (L^{-1}), h is soil matric head (L), K is unsaturated hydraulic conductivity (LT^{-1}) and t denotes time (T). The combined system of soil and porous barrier for the multi-step outflow experiment has the following initial and boundary conditions

$$\begin{aligned} h(z, t) &= h_i(z) & t &= 0 \\ q(z, t) &= 0 & t > 0, z = L \\ h &= h(0, t) - |h_a| & t > 0, z = 0 \end{aligned} \quad [2]$$

where h_i is the initial matric pressure head (L), q denotes the flux density (LT^{-1}), $z = 0$ is the bottom of the porous plate/membrane, $z = L$ is the top of the soil sample, $h(0, t)$ is the water pressure head at the bottom of the porous plate/membrane, and h_a is either the applied pneumatic gas pressure to the top of the soil core ($z = L$), or suction applied beneath the porous plate/membrane ($z = 0$). In SFOPT, a time-dependent lower boundary condition was implemented and automatically measured by the pressure transducer below the burette.

2.2. Soil water retention and hydraulic conductivity models

In order to optimize the soil hydraulic data from the inverse solution of the Richards equation (Eq. [1]), parameterization of the hydraulic functions is necessary. The soil water retention and unsaturated hydraulic conductivity functions can be defined by various expressions. In SFOPT two models are used for the description of soil hydraulic functions. The first model is the soil water retention function proposed by van Genuchten (1980)

$$S_e = \left[1 + |\alpha h|^n \right]^{-m} \quad [3]$$

with

$$S_e = \frac{\theta(h) - \theta_r}{\theta_s - \theta_r} \quad [4]$$

and $m = 1 - 1/n$, where S_e is called effective water saturation ($0 \leq S_e \leq 1$), θ_s and θ_r are the saturated and residual water content ($L^3 L^{-3}$), respectively, and $\alpha (L^{-1})$ and n are empirical parameters. Substituting Eq. [3] in the capillary model of Mualem (1976), van Genuchten (1980) derived the following unsaturated hydraulic conductivity model

$$K(h) = K_s S_e^l \left[1 - \left(1 - S_e^{1/m} \right)^m \right]^2 \quad [5]$$

where K_s and l denote saturated hydraulic conductivity (LT^{-1}) and tortuosity/connectivity parameters, respectively. S_e and m are the same parameters as used in Eq. [3]. From the analysis of a variety of soils, Mualem (1976) proposed a value for $l = 0.5$, although l can be considered as another fitting parameter as well (Hopmans et al., 1994; Hopmans et al., 2002).

The second is the lognormal model (Kosugi, 1996) that can be used in addition to the van Genuchten (1980) model. The lognormal model is physically based, and optimization results have been equally successful. The soil water retention curve and the unsaturated hydraulic conductivity functions are expressed by

$$S_e = \frac{\theta - \theta_r}{\theta_s - \theta_r} = F_n \left[\frac{\ln(h/h_m)}{\sigma} \right] \quad [6]$$

$$K = K_s S_e^l \left[F_n \left(\frac{\ln(h/h_m)}{\sigma} + \sigma \right) \right]^2 \quad [7]$$

where F_n is the complementary normal distribution function defined as

$$F_n(x) = \frac{1}{\sqrt{2\pi}} \int_x^\infty \exp\left(-\frac{x^2}{2}\right) dx \quad [8]$$

Alternative expressions for the hydraulic functions of Eqs.[6] and [7] can be written as

$$S_e(\ln h) = \frac{1}{2} \operatorname{erfc} \left(\frac{\ln h - \ln h_m}{\sigma \sqrt{2}} \right) \quad [9]$$

$$K(S_e) = K_s S_e^l \left\{ \frac{1}{2} \operatorname{erfc} \left[\operatorname{erfc}^{-1}(2S_e) + \frac{\sigma}{\sqrt{2}} \right] \right\}^2 \quad [10]$$

where erfc and erfc^{-1} denote the complementary and inverse complementary error functions, respectively. The lognormal model has six parameters h_m , σ , θ_r , θ_s , K_s , and l . The parameter h_m denotes the median matric head at which the effective saturation (S_e) is equal to 0.5 and σ is the standard deviation of the lognormal pore-size distribution. The value of h_m is usually greater than 1 and smaller than 10^6 cm. The value for σ is between 0 and 10. In SF OPT, the value of $\operatorname{LOG}_{10}(h_m)$ is used as the fitting parameter, instead of h_m to increase parameter sensitivity.

2.3. Objective function

SFOPT is a one-dimensional finite element flow model combined with a optimization algorithm using the Levenberg-Marquart (LM) maximum neighborhood method (Clausnitzer and Hopmans, 1995). The form of the objective function $O(\mathbf{b})$ to be minimized is

$$\begin{aligned} O(\mathbf{b}) = & \sum_{i=1}^N \left[W_i (Q_o(t_i) - Q_c(t_i, \mathbf{b})) \right]^2 + \sum_{j=1}^M \left[W_j V_j (h_o(t_j) - h_c(t_j, \mathbf{b})) \right]^2 \\ & + \sum_{k=1}^L \left[W_k V_k (\theta_o(h_k) - \theta_c(h_k, \mathbf{b})) \right]^2 \end{aligned} \quad [11]$$

where \mathbf{b} is a vector containing the optimized parameters (θ_s , θ_r , α , n , l , and K_s or θ_s , θ_r , $\log h_m$, σ , l and K_s). Vector \mathbf{b} contains only those parameters that need to be optimized. Values of parameters that are known such as θ_s can be fixed. Q and h denote cumulative transient outflow volume (mL) and the soil water matric head (cm), respectively. θ is soil water content, corresponding with a known soil water matric head,

h . Subscripts o and c represent observed and calculated values. N , M , and L denote the number of cumulative outflow, pressure head, and soil moisture content-matric head pairs measured during the multi-step outflow experiment, respectively.

The internal weighting (V_j in the objective function) or normalization method of Kool and Parker (1987) was adapted for weighting of input variables. The program calculates weights for the soil water matric head and soil moisture content data so that the weighting factor is inversely proportional to their mean measured values. Consequently, the measurement type with the lowest mean receives a unit weight, thus preventing one variable from dominating another because of its numerical magnitude. W is a user-supplied weight for differential weighting of each data (default = 1). For example, if a $\theta(h)$ pair is known, a weight (W) of 5 or 10 is assigned to it, thereby forcing the optimized retention curve through this point.

3. MATERIAL AND METHODS

3.1. Sample preparation and bottom plate assembly

The multi-step experiment can be conducted with either a disturbed (laboratory packed) or undisturbed soil sample. The default sample size of the standard Tempe pressure cell accommodates an 8.25-cm (3.5-inch) outside diameter and 6-cm length brass ring (component D of Photo 1 in Appendix A). Before assembling the soil sample in a Tempe pressure cell, various procedures need to be followed to saturate the soil sample. If a disturbed soil sample is used, a wet strength filter paper¹ is glued to one end of the brass ring before the ring is packed with the soil. For undisturbed soils, cheesecloth at the bottom of the soil will be sufficient to prevent soil loss. The samples (disturbed or undisturbed) are soaked in a 0.01 M CaCl_2 solution while keeping the chloride solution about 1 cm below the soil's top surface. The samples continue to be soaked until water appears on the surface. The samples are subsequently placed on a screen to measure the saturated hydraulic conductivity using a constant head method (Klute and Dirksen, 1986). After the saturated hydraulic conductivity measurement, the filter paper is removed and

¹Whatman Inc. 9 Bridewell Place, Clifton, NJ 07014. Phone: 800 631 7290. Cat No 1114125

the saturated soil sample with the ring is assembled in the Tempe pressure cell upside down. Early on, an appropriate air-entry value ceramic plate was placed in the bottom of the Tempe cell to serve as a porous barrier. However, we propose to use a nylon¹ membrane (MAGNA nylon disk filter, supported, plain type with 1.2 micron pore size and 142 mm diameter), instead of a ceramic plate (Photo 2 in Appendix A). A nylon membrane has several advantages:

- Low hydraulic resistance,
- High flow rate with high air entry value (1700 cm), although various pore sizes can be purchased,
- Pressure difference across the membrane is small,
- Do not need to specify conductivity of the membrane in flow code,
- Flow is not controlled by membrane but solely by the soil thereby improving the parameter optimization procedure,
- An estimate of $K(S_e)$, directly from outflow and tensiometer measurements can be obtained (Eching et al., 1994).

The flow properties of the nylon membrane in comparison with other porous materials are listed in Table 1. The saturated hydraulic conductivities of the nylon membrane and ceramic plate are determined from cumulative outflow volume from Tempe cells filled with water when subjected to an arbitrarily chosen pneumatic pressure of 400 mbar. To support the nylon membrane, a perforated 26-gauge stainless steel screen² (0.045" round perforations on 0.066" straight center, 225 holes per sq. in. with a 36 % open area) was cemented on a Plexiglas ring with two-ton epoxy (Figure 2a). The hydraulic resistance of the porous material, R_p , is equal to the ratio of plate thickness (l) and saturated hydraulic conductivity, K_s , of the porous material (Table 1). To prepare the support assembly, the wet strength Whatman filter paper is cut to a diameter equal to the stainless steel screen support and placed on the smooth side of the steel support (Figure 2b).

¹ Osmonics Inc. 5951 Clearwater Drive, Minnetonka, MN 55343. Phone: 800-848-1750. Catalog No: R12SP14225

² Small Parts Inc, 13980 NW South Crt, PO Box 4650, Miami Lakes, FL 33014-0650: 1-800-220-4242. Catalog No: A-PMX-045.

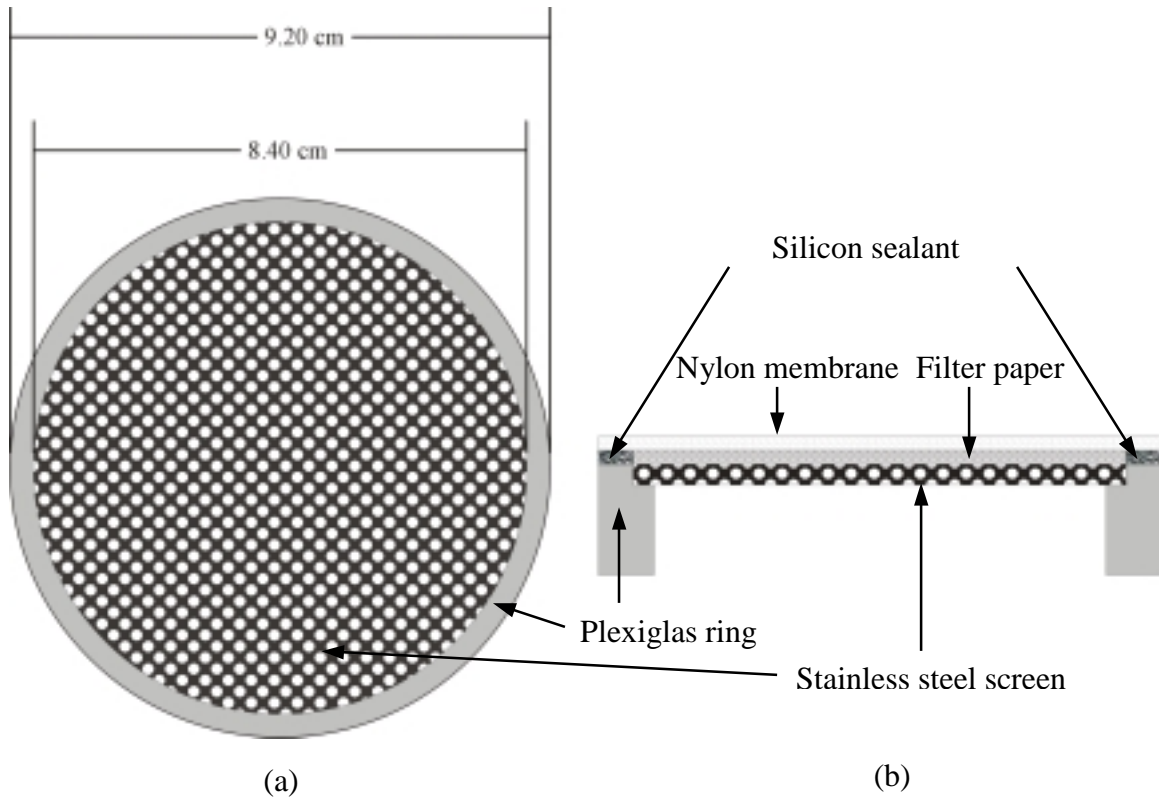


Figure 2. Perforated stainless steel screen support (a), and support assembly (b)

Table 1. Physical properties of different porous materials (l_t = thickness; $R_p = l_t / K_s$)

Porous Material	l_t (cm)	K_s (cm/h)	R_p (h)	Air-entry pressure (cm)
Ceramic	0.58	0.0071	81.48	1000
Plastic	0.05	0.017	3.01	400
Stainless Steel	0.1	0.027	3.77	250
Nylon	0.01	0.014	0.71	1700

The paper filter is used to prevent perforation of the nylon membrane. Then, waterproof silicon sealant¹ is applied to the Plexiglas ring around the filter paper and a pre-cut nylon membrane with a diameter equal to the Plexiglas ring is glued to the plate assembly. Note

¹ Bostik, RTV Silicon Sealant

that silicon sealant must be applied quite thick to give spongy effect for better airtight seal when soil sample is assembled in the Tempe cell.

3.2. Tensiometers and transducers

After laying the support assembly into the Tempe cell, the saturated soil sample is placed on the support (Figure 3). Figure 3 shows the basic arrangement of the pressure cell experiment. The soil water matric head is measured with a mini-tensiometer-transducer arrangement (Photo 3 in Appendix A). A mini-tensiometer is constructed by gluing a 1-cm long 0.635-cm O.D. ceramic cup¹ to a 12 cm long 0.63-cm O.D. acrylic tube with a copper coupler using a clear all-purpose two-ton epoxy. The acrylic tubing is connected to a three-way valve by a piece of tygon or rubber tubing. To ensure a rigid connection, the acrylic tube and three-way valve connection must be fully abutted. Flexibility of the wall of the tensiometer-transducer causes long response times of the tensiometer and fluctuation in the transducer signal. The transducer² has a working pressure range of ± 15 psi. After filling the tensiometer and three-way valve with 0.01 M CaCl_2 solution, the transducer is connected to the valve making sure that it has an open connection with the laboratory at atmospheric pressure. This ensures that the transducer membrane is not damaged during the connection of the transducer with the tensiometer as high pressures may occur. A similar procedure is used to connect the outflow transducer³ (Photo 1E and G), with an operating pressure range between ± 1 psi, to a three-way valve below the burette (Figure 3). Each transducer is checked independently for proper operation. Calibration must be done over the entire operating pressure and outflow ranges before each outflow experiment (section 4).

All transducers are connected to a 21X micrologger⁴ (Photo 1B) through an AM416 multiplexer⁴ (Photo 1C) with modular-type 4-line telephone cables. Two lines of the transducer are directly connected for excitation through an independent 10 Volts DC source⁵ (Photo 1A) while the other two lines are attached to the input (sensor) terminals

¹ Part #: 0652X03-B01M3. Soil Moisture Equipment Corp. 801 S. Kellogg Ave. Goleta 93117 CA

² 136PC15G2. Honeywell Micro switch Sensing and control. 11 West Spring Street Freeport, IL 61032.

³ 136PC01G2. Honeywell Micro switch Sensing and control. 11 West Spring Street Freeport, IL 61032.

⁴ Campbell Scientific, Inc. 815 West 1800 North. Logan, Utah 84321-1784. Phone: 435-753-2342.

⁵ Omega Engineering Inc. Stamford, CT, Power supply. Phone: 203-359-1660.

of the AM416 multiplexer. We use an external excitation source instead of the datalogger, because the AM416 does not have enough channels for both measurement and excitation of 20 transducers (see section 5).

3.3. Top and bottom plates of the Tempe cell

The cover of the Tempe pressure cell is modified to accommodate the vertical-placed tensiometer (Figure 3 and Photo 4). Airtight fitting of the tensiometer in the cover plate is ensured by a compression fitting, with a 1/4" cap and 1/8" NPT pipe thread stem. This type of compression fitting is available in most hardware stores. It needs, however, to be bored out for the tensiometer to fit. The O-ring in the assembly provides a pressure tight seal and yet allows the tensiometer to be adjusted vertically when the cap is not fully tight. Alternatively, we used a Swagelok¹ brand Stainless steel tapered thread male connector (Part#: SS-400-1-2)¹, but it also needs to be bored out for the tensiometer to fit. Instead of an O-ring, nylon front and back ferrules (Part#: NY-403-1 and NY-404-1, respectively)¹ were used to provide a pressure tight seal. The nylon ferrules do not deteriorate like the O-rings, so that they can be used for a longer time. For the top cover of the Tempe cell, a 1/4" Hose I.D. with a 1/8" NPT thread size stem male hose connector (Part#: SS-4-HC-1-2)¹ was used for the pressure inlet port. The bottom cover (Photo 5) of the cell uses a 1/4" Hose I.D. with a 1/8" NPT thread size stem male hose as a drainage port and a 3/16" Hose I.D. with a 1/8" NPT thread size stem male hose connector (Part#: SS-3-HC-1-2)¹ as the air removal port.

After attaching the top cover to the cell using threaded rods, and insertion of the tensiometer, soil samples are re-saturated and flushed by wetting through the bottom plate. Accurate outflow data requires that the tubing between the Tempe cell and burette is air free. De-aerated 0.01 M CaCl₂ solution is used to minimize dispersion of the soil. For undisturbed soil samples, a hole may need to be drilled in the soil sample to allow tensiometer insertion without too much force. However, a tensiometer can usually be easily installed in wet disturbed soils. After saturation, the 3-way valve above the air trap is turned off in the direction of air trap and water in the burette is removed to the 20 ml

¹ Swagelok, Oakland valve and Fitting, 2441 Sprig Court-Unit A, Concord, CA 94520. Phone: 925-676-4100.

level by insertion of a syringe into the burette. After connecting the air pressure hose to the top cover, an initial air pressure is applied. The magnitude depends on the soil's textural characteristics. Pressurized nitrogen gas (N₂) is used instead of air pressure to minimize dissolution of oxygen into the water phase.

3.4. Adaptors for small diameter soil cores in the 2.5-inch Tempe pressure cell

The assembling procedure described in sections 3.1 to 3.3 is exclusively for 3.5-inch O.D. soil cores, that fit the standard 3.5-inch Tempe pressure cell. However, also top and bottom plates for 2.5-inch Tempe pressure cells are available that can accommodate soil cores with outside diameters equal or smaller than 2.5" outside diameter (O.D.). Examples of the soil cores that have been adapted to fit the 2.5" pressure cell are (1) two-inch aluminum rings (0.051 wall thickness), collected with a Giddings hand sampler, (2) two-inch standard well soil cores (preferably larger than 0.064" wall thickness) as extracted by a split spoon core sampler using well drilling equipment, (3) 1.75" O.D. PVC liner of macrocore sampler from a GeoProbe[®] soil core sampler, and (4) 2" O.D. PVC liner as used in 3.25" Dual Tube (DT) sampler of GeoProbe[®]. In either case, special adaptors and procedures were developed to accommodate the various size core samples. Irrespective of size, 4" tall soil cores are needed, that will be trimmed back to a 3-inch soil core. The following procedure describes the fitting of a 1.75" PVC liner into the 2.5" Tempe pressure cell. Photographs 6 through 11 show the various components described in this procedure.

1. Trim the 4" PVC liner to a 3.5" length by cutting 0.5" off one end of the soil sample. The abrasive cutoff wheel of the Dremel tool is used to trim through the PVC;
2. Glue wet strength Whatman filter paper at one end of the 2" Aluminum sleeve (Photo 6). This sleeve contains lubricated O-rings at the bottom and top end, and ensures a watertight fit of the soil core in the sleeve. We apply high vacuum grease or white petroleum jelly, for general lubrication purposes;

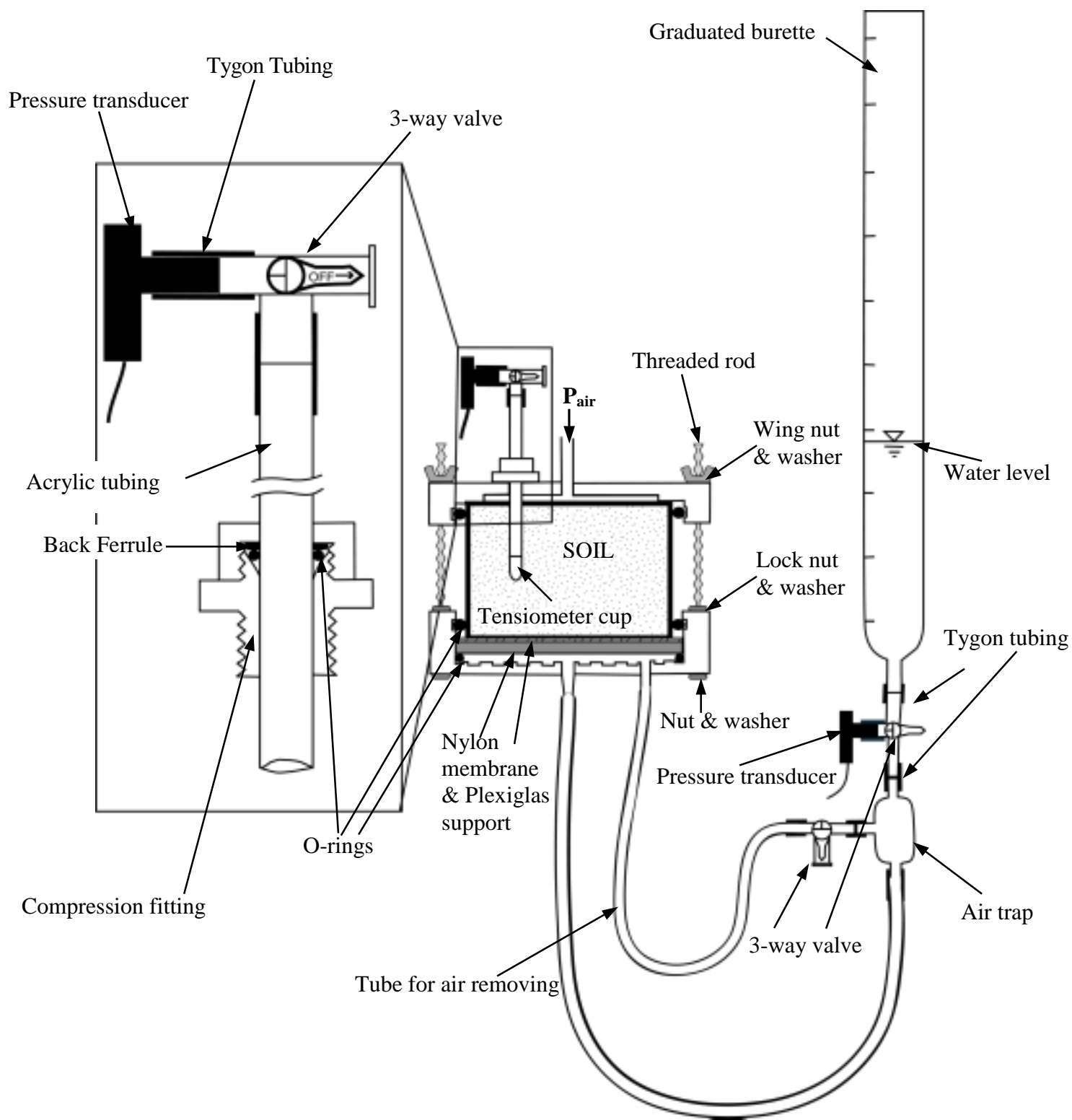


Figure 3. Modified Tempe pressure cell.

3. Push the open end of the sleeve over the trimmed end of the soil sample. To ensure hydraulic contact between the filter paper and the soil, it is recommended to wet the trimmed end of the soil sample first with a water spray. Also, to allow easy assembling, it is suggested to sand the outer edge of the PVC, thereby removing nicks and burrs that may puncture the nylon filter;
4. Turn the PVC-aluminum sleeve assembly around, and trim the other end of the soil sample;
5. Push a 2.5" O.D. Plexiglas (acrylic) (3" long) sleeve (with 2 O-rings) about one inch over the aluminum sleeve, so that the remaining 2.0" of acrylic sleeve can be used as a constant-head device (Photo 7) for the saturated hydraulic conductivity measurement (section 3.1). The soil sample is saturated first (see section 3.1) before the saturated hydraulic conductivity measurement.
6. Immediately transfer the wet soil sample (with the 2 adapters) to the 2.5" Tempe cell. Do this by placing the upright soil sample on a stand, and pushing the prepared bottom plate assembly (see Photo 8, 9, and 10) over the cleaned soil sample. The outside and bottom of the acrylic sleeve must be clean of soil particles, to prevent air leakage and puncturing the nylon membrane during pressurization. Then, turn the whole assembly back to the upright position, so that the wet strength Whatman filter paper is visible on the top of the soil sample;
7. Attach the 2.5" top plate to the pressure cell. Saturate the soil sample making sure that water is flushed out from the top. Then, install the tensiometer, while pushing it through the filter paper (Photo 11). Hereafter, the multi-step outflow procedure is similar as for the 3.5" soil samples (Photo 12).

If instead, the soil samples are 2" in diameter, they can be directly fitted into the 2.5" O.D. acrylic sleeve. For 2.5" O.D. soil cores, it is proposed to use 3.5" O.D. adapter sleeves (0.5" wall thickness) that fit the 3.5" Tempe pressure cell.

3.5. Data collection

The motivation to start the experiment at an initial soil matric potential below saturation was presented by Hopmans et al. (1992), so that the Richards' equation (Eq.

[1]) assumption of air continuity throughout the sample is valid. They suggested that better results are obtained if the sample is initially unsaturated. Therefore, an initial pneumatic pressure of a range between 20-50 mbar depending on the soil's air entry value, is applied to unsaturate the soil sample.

In this setup, either a one-step or a multi-step experiment can be conducted. Cumulative outflow volume and soil water matric head are measured as a function of time. Water pressure and outflow readings are recorded automatically at desired time intervals. A 5 minutes interval during the experiment is recommended. However, one may choose other pressure steps and time intervals by changing parameters in the datalogger program (See section 5.3).

The soil water matric head in the pressure experiments is computed as the difference between the measured tensiometer pressure and the applied pneumatic pressure (Figure 4b), because tensiometer pressure from the transducers is the sum of pneumatic and matric pressure. A typical tensiometer response during a sequence of the pneumatic pressure steps is depicted in Figure 4a. The numbers near the peaks denote drainage period for this sequence of the applied pressure steps. The water pressure head measured by pressure transducers of the tensiometer is represented by the solid line, which has a range between 0 and the pressure difference between the current and previous increment. The pressure head at the bottom of the porous barrier is plotted by the dashed line and is determined by the water level in the burette (Figure 4a). When a pressure step is applied, the tensiometer responds corresponding with an immediate peak. For the small-applied pressures, the water held in the largest pores drain quickly, which is indicated by the rapid decline of tensiometer response towards hydraulic equilibrium with the water pressure in the burette (Figure 4a). When the response curve reaches a plateau, the water pressure in the tensiometer cup must theoretically be equal to the distance between the water level in the burette and the bottom of the porous barrier. However, for the larger applied pressure increments, tensiometer response is slower and the time required for the hydraulic equilibrium increases due to the decrease in the unsaturated hydraulic conductivity with decreasing water content. Consequently, it takes more time for cumulative outflow and matric pressure curve to approach a plateau value. It is

recommended to increase the applied pressure increment if a plateau values has been attained.

In the multi-step experiment, the choice and number of pressure steps will depend on objectives. We have found for many soils, that pressure steps of 60, 80, 120, 200, 300, 400, and 550 cm are adequate. Generally, the pressure can be changed at time intervals of one day. However, in many cases we prefer to wait for near zero drainage rate before increasing the applied pressure, so that soil water retention points can be directly determined from the multi-step outflow data. Since outflow is measured continuously with the transducer of the burette (Figure 3), the cumulative outflow data can be used to determine the timing of a pressure increment (Figure 4c). The water level in the burette does not need to be adjusted to provide a constant pressure below the porous membrane. This is so because the adapted SFOPT program can handle time-dependent lower boundary conditions at the bottom of the membrane.

If the pressures are changed daily, the multi-step outflow experiment generally takes 5-6 days, however, a typical experiment lasts 10-14 days. After the experiment is completed, the soil samples are removed from the pressure cells, weighed, oven dried at 105 °C for 24 hours, and weighed again to estimate the volumetric water content at the end of the experiment. Sometimes it is preferred to include a retention point at a soil water matric potential, much lower than corresponding with the highest applied pressure. Additional retention points can be collected using the 5-bar pressure plate apparatus (Klute, 1986). The additional value combined with the cumulative outflow volume is subsequently used to calculate saturated and initial soil water content values. In the parameter optimization procedure, the cumulative outflow and corresponding water content values combined are used to compute the temporal changes in soil water content with the corresponding soil water matric head values of the draining soil core.

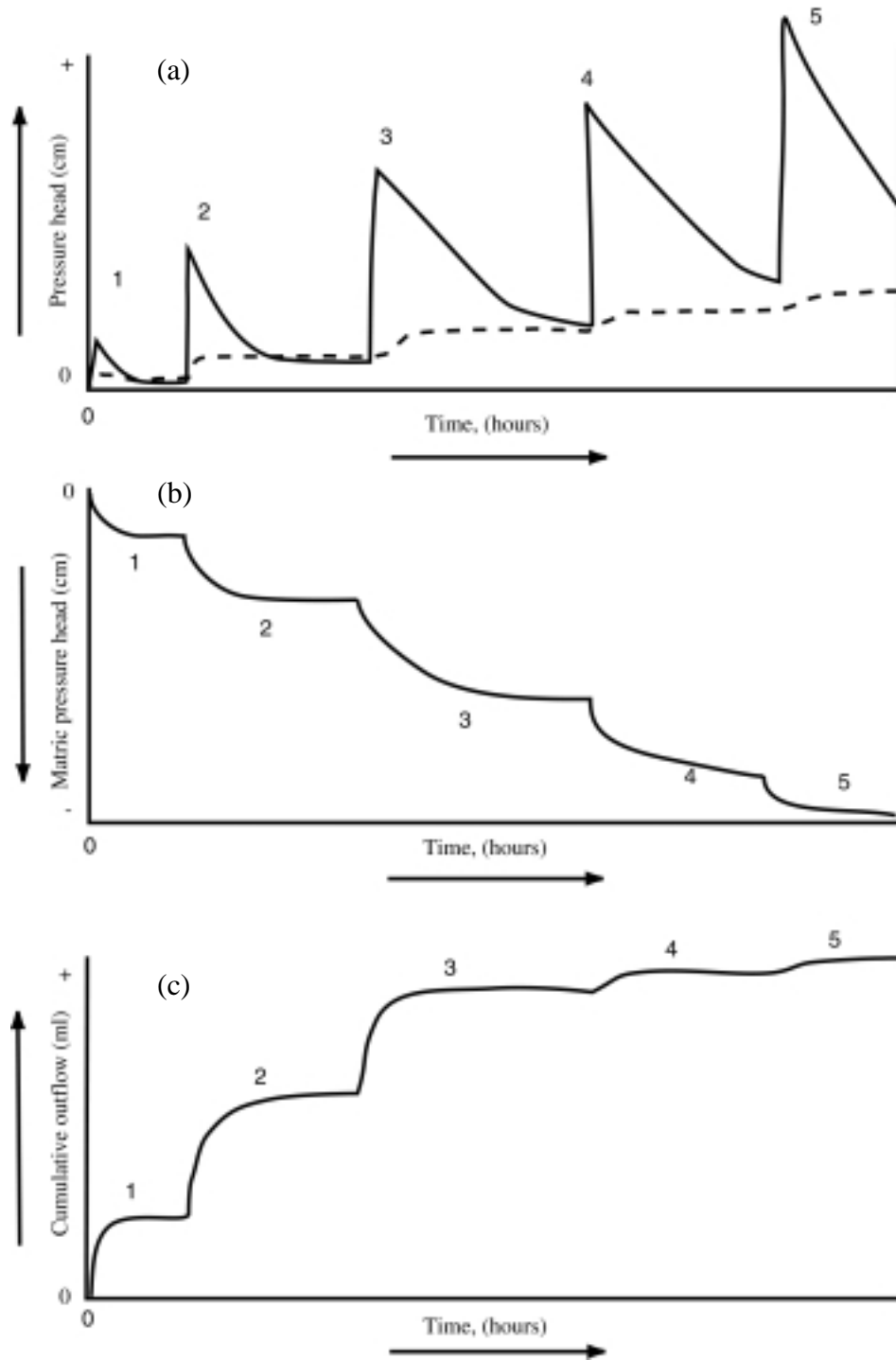


Figure 4. Tensiometer pressure head (solid line) and pressure head at the bottom of the porous barrier (dashed line) (a), matric pressure head (b), and cumulative outflow (c) as a function of time.

3.6. Keeping the experimental records

One must realize that keeping complete experimental records during the different experimental steps (before, during, and after) are vital to the experimental objectives and the later data processing. In this section, some example datasheets are presented to demonstrate the type of records that must be kept throughout the outflow experiments. For the saturated hydraulic conductivity experiment, the datasheet of Figure 5 is suggested. The numbers used in this datasheet is just for illustration purposes only.

Saturated Hydraulic Conductivity of Soils										
Plot	Depth	Sample #	Total Time	Δt	ΔH	Q	A	L	K_{sat}	K_{sat}
	cm		HH:MM	min	cm	ml	cm ²	cm	cm / min	cm / h
6-1	25	91	1:27	87.0	8.9	92.0	53.5	6	0.01334	0.800
6-2	50	92	0:55	55.0	9.1	85.5	53.5	6	0.01918	1.151
6-3	25	93	2:04	124.0	9.3	21.0	53.5	6	0.00204	0.123
6-4	50	94	2:03	123.0	9.2	65.0	53.5	6	0.00645	0.387

Figure 5. Datasheet for the saturated hydraulic conductivity experiment.

In Figure 5, ΔH is total hydraulic head difference across the soil sample, Q is amount of water collected at the corresponding time interval, Δt , A and L are the cross-sectional area and the length of the soil sample, respectively.

The most involved part of the data recording is the steps of the multi-step outflow experiment. One must record all steps and readings with the date and time during the course of the experiment. Before starting the multi-step outflow experiment, some measurements for the DATAPREP program must be taken from the experimental set up (see section 6.1 and Figure 20) and are recorded, separately. Figure 6 shows a recommended datasheet to use. The numerals with arrows of Figure 6 correspond with the following descriptions:

1. Tempe Cell number of soil sample.

2. Corresponding placed soil sample number.
3. Heading for date & time (military), current applied pressure (mbar), mV (millivolt), and ml (milliliter) readings.
4. Heading for real-time milivolt (mV) readings of tensiometer (T mV) and outflow (Q mV) from PC208W¹ program and sight-reading of outflow (Q ml) from the burette.

1	Tempe Cell #		1	2	3	4	5	6	7	8	9	10
2	Sample #		91	92	93	94						
3	Date & Time	mV & ml readings										
4	Pressure											
5	3/11/01	T mV	-0.399	-0.941	-0.381	-0.566						
6	1012 am	Q mV	1.926	1.841	1.793	1.964						
7	0 mbar	Q ml	20	20	20	20						
8												
9	1024 am	T mV	0.078	-0.422	-0.197	-0.081						
	3/11/01	T mV	-0.569	-1.06	-0.453	-0.818						
	2012 pm	Q mV	2.486	2.431	2.707	2.186						
	20 mbar	Q ml	34	34	38	30						
10	1024 am	T mV	2.380	4.580	4.539	4.290						
	3/12/01	T mV	-0.102	-0.474	-0.037	-0.187						
	0722 am	Q mV	3.154	3.304	3.854	2.822						
	100 mbar	Q ml	50	55	65.5	47						
	0745 am	T mV	2.380	4.580	4.539	4.290						
	3/13/01	T mV	1.190	-0.130	0.280	2.140						
	2144 pm	Q mV	3.610	3.860	4.460	3.410						
	200 mbar	Q ml	60.5	68.5	80	60.5						
11												
12	2215 pm	Q mV	3.216	3.562	4.320	3.210						
		Q ml	55.5	67.0	77.5	57.5						
	3/14/01	T mV	0.810	-0.280	0.260	1.910						
	0725 am	Q mV	3.510	3.850	4.370	3.360						
	200 mbar	Q ml	58.5	68.0	78.0	59.0						
13												
14	0747 am	Q mV	3.230	3.563	4.373	3.285						
		Q ml	56.0	67.0	78.0	58.5						
15												
	0820 am	T mV	8.56	13.77	14.31	14.99						

Figure 6. Datasheet during the multi-step outflow experiment.

¹ Campbell Scientific, Inc. 815 West 1800 North. Logan, Utah 84321-1784: Phone: 435.753.2342

5. Date of initial readings before the first pressure step is applied.
6. Military time of readings.
7. Current applied pressure.
8. Comment line for information on INITIAL AIR PRESSURE.
9. Time and values of the real-time tensiometer readings after pressure application.
10. Readings and sight-reading of T and Q before 100-mbar and 200-mbar NEW AIR PRESSURE applications.
11. Comment line for information on **AIR FLUSH** and what pressure is currently being applied.
12. Time of measurements of (Q mV) and (Q ml) after Air Flushing. It may not necessary to record tensiometer readings since the readings have not changed.
13. Comment line for the second **AIR FLUSH** before the 400-mbar NEW AIR PRESSURE increment is applied.
14. Time of measurements of (Q mV) and (Q ml) after the second Air Flushing and just before the 400-mbar NEW AIR PRESSURE application.
15. Comment line for the information on 400-mbar NEW AIR PRESSURE is applied.

Figure 7 shows an example datasheet that may be used for recording data to calculate the volumetric water content, dry bulk density, and porosity at the end of experiment.

Determination of water content value, dry bulk density, and porosity									
Sample #	Depth	Wet soil + Ring at the last pressure step	Oven Dry Soil + Ring	Ring weight	Ring volume	Water content @ saturation	Water content	Dry bulk density	Porosity
	cm	g	g	g	cm ³	cm ³ / cm ³	cm ³ / cm ³	g / cm ³	cm ³ / cm ³

Figure 7. Datasheet for the parameters obtained at the end of the experiment.

3.7. Air flushing

When a nylon membrane is used as porous barrier, air accumulation may occur during the high pressure steps of the experiment, due to air diffusion through the thin membrane. Two ports at the bottom of the cell and the air trap permit flushing of trapped air under the nylon membrane. For air flushing, the Luerlok type 60 cc Syringe¹ is connected to the 3-way valve closing the connection to the air trap (Component F of Photo 1). The plunger of the syringe is pulled back slowly for extracting accumulated air under the bottom of the membrane. This procedure has to be done slowly to prevent additional suction to the soil sample. By changing the valve opening direction, the extracted air is pushed back slowly into the air trap. Air escapes from the air trap through the burette, lowering the water level in the burette to the level now indicating the true drainage volume. This “Air Flushing” procedure is repeated several times during the experiment, whenever air accumulates. Air flushing times must be recorded since air accumulation gives erroneous outflow readings and must be corrected between air flushings. For that purpose, a software program DATAPREP, written in free format FORTRAN language, is used to correct the outflow data, and to transform the experimental data of tensiometer and outflow transducer readings (mV) to units of pressure (cm water). Since the number of data pairs collected by the datalogger is large, the DATAPREP program also helps to select a user-specified number (approximately between 250-500) of data pairs (tensiometer and outflow readings), and prepares the input data file for the SFOPT optimization program. Details of this program and data processing procedure are given in section 6.

3.8. Some experimental problems and remarks

Major problems that may be encountered during the outflow experiment are:

1. Poor contact between the soil sample and porous plate or nylon membrane. When the contact between the porous material and soil is poor, cumulative volume outflow can be very small. Cumulative volume outflow values for fine textured

¹ Becton Dickinson & Co. Franklin Lakes, NJ 07417-1884

soils are usually small as well. Optimized hydraulic functions are generally questionable in that case.

2. A cracked ceramic plate or perforated nylon membrane. It is possible to crack the ceramic plate if the Tempe cell pressure lid is screwed on too tight. Moreover, the edge of the brass ring touching the nylon membrane must be soil particle free, to prevent perforation of the nylon membrane. Damage of the porous membrane causes the presence of air bubbles in the burette.
3. Soil particles between the sample cylinder and the O-ring of the pressure cell will cause air leakage during the experiment. Applying soapy water on the O-ring after assembling the pressure cell provides a good leakage test. It is recommended that this is done at the beginning of each pressure increment.
4. Do not increase the pressure step immediately after air flushing. It is important to wait at least 30 minutes after air flushing, so that pressure transducers (tensiometer and outflow) can stabilize.

4. PRESSURE TRANSDUCER CALIBRATION

Pressure transducers for the multi-step outflow experiment must have a high output to input voltage ratio, low noise, and a stable calibration. There are several transducers available that fulfill these requirements, though they may not be specifically applied to soil research (Eching and Hopmans, 1993b). Here, we provide an example of how to calibrate differential pressure transducers for the tensiometer and outflow, with one side of the pressure sensitive membrane open to the atmosphere.

An experimental set up for simultaneous checking and calibrating the slope of both tensiometer and outflow transducers are shown in Figure 8a and b, respectively. Each tensiometer is filled with CaCl_2 solution, and is submerged in solution to prevent the tensiometer from draining. Initially, the 3-way valve is turned off in the direction of the tensiometer cup so that the transducer is open to the atmosphere (Figure 8a). A piece of tygon tubing connects to the open end of the valve and the pressure source (N_2 gas). The 3-way valve of the transducer below the graduated burette is closed towards the glass air trap (Figure 3 and Figure 8b), while the burette is filled with the same solution to the 100 ml level. All transducers are connected to the datalogger and the external power source¹ of 10 V. Transducers are automatically scanned at 20-seconds intervals and the one-minute average readings with the Julian date and military time is stored. A 10-minute data collection is adequate for each calibration step. Typical applied pressures are 20, 40, 80, 160, 320, and 540 mbar whereas burette levels of 100, 90, 80, 60, 40, and 20 ml provide an appropriate range of water pressures. When the new pressure is applied to the tensiometer transducers, the burette levels are lowered to the next level.

Calibration parameters are obtained using linear regression analysis to the transducer's readings (mV) and corresponding applied pressure and outflow values. Results have shown that the slope of the curves is generally stable and do not change much with the time. However the interception may change considerably between experiments (Figure 9). Therefore, only the slope is used as an input parameter for the DATAPREP program. Using this known slope value, DATAPREP finds the intercept

¹ Omega Engineering Inc. Stamford, CT, Power supply. Phone: 203-359-1660.

from subsequent experimental data measured at the beginning of the multi-step experiment, assuming that hydraulic equilibrium is attained quickly.

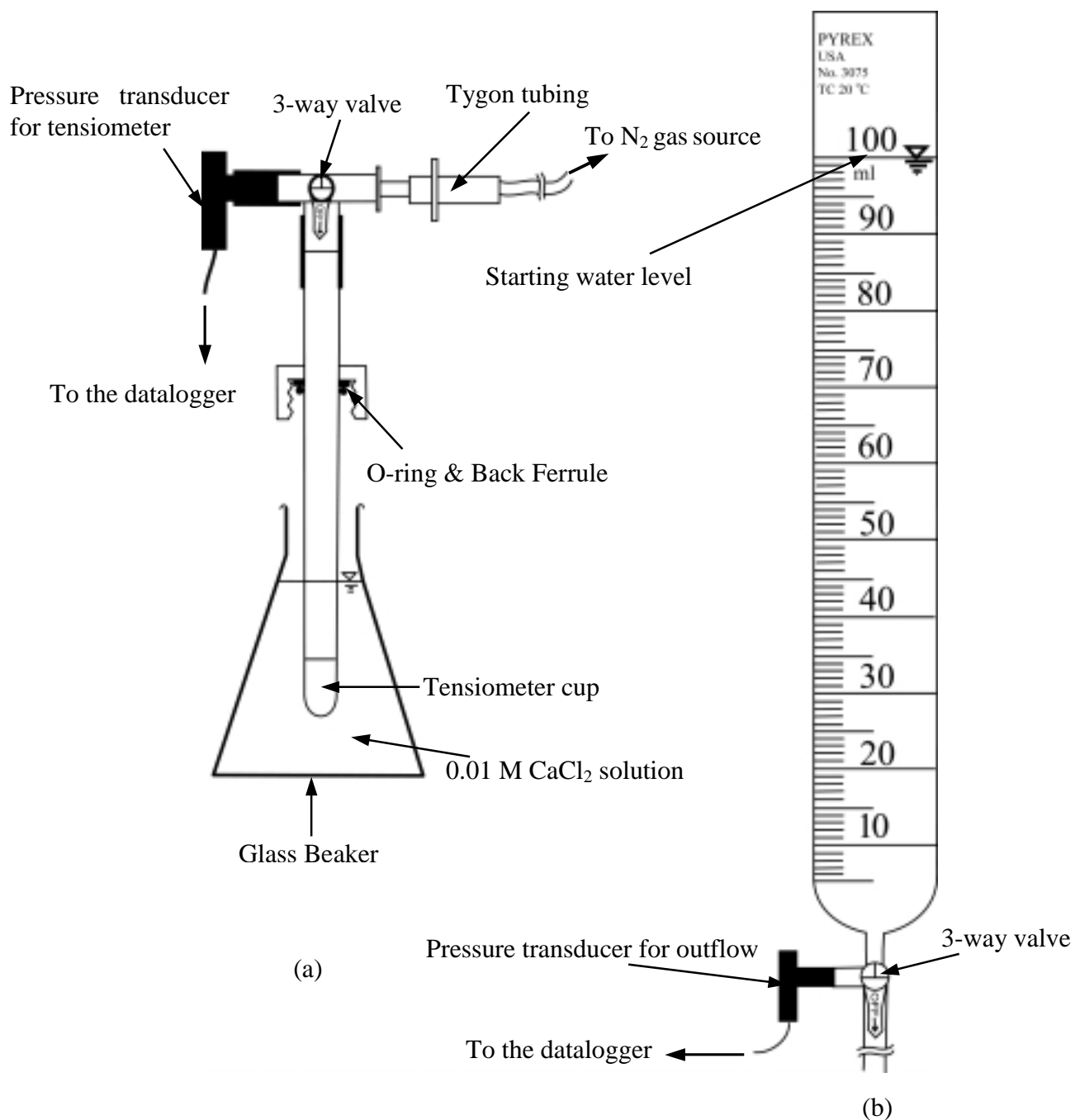


Figure 8. Experimental set up for calibration (slope) of the tensiometer (a) and outflow transducers (b).

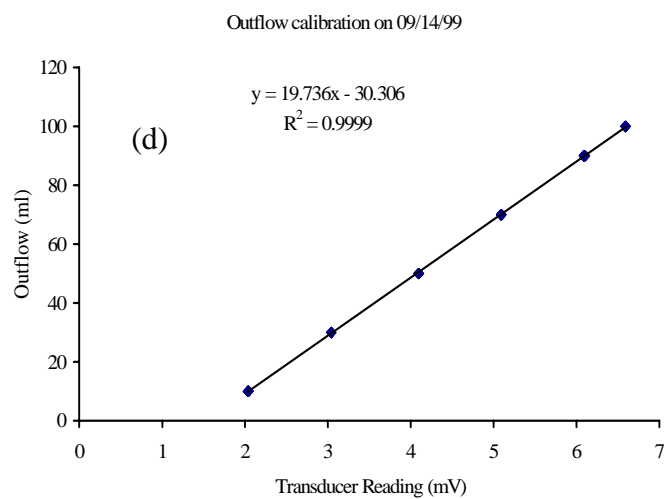
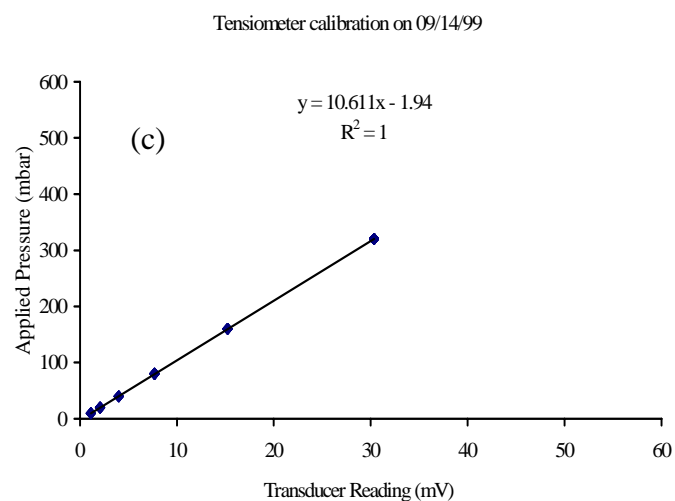
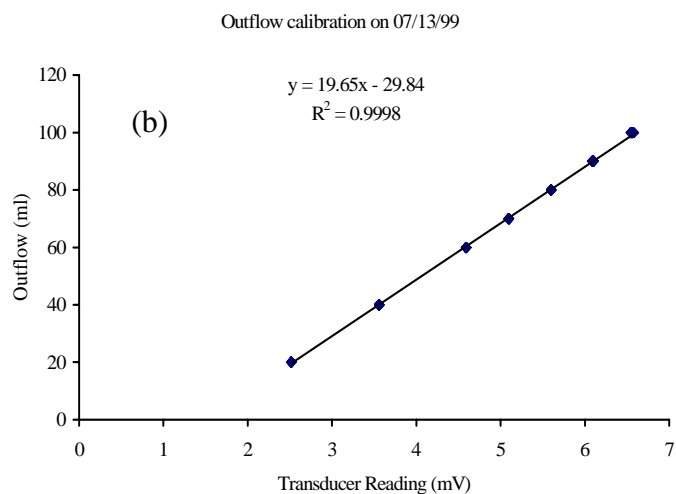
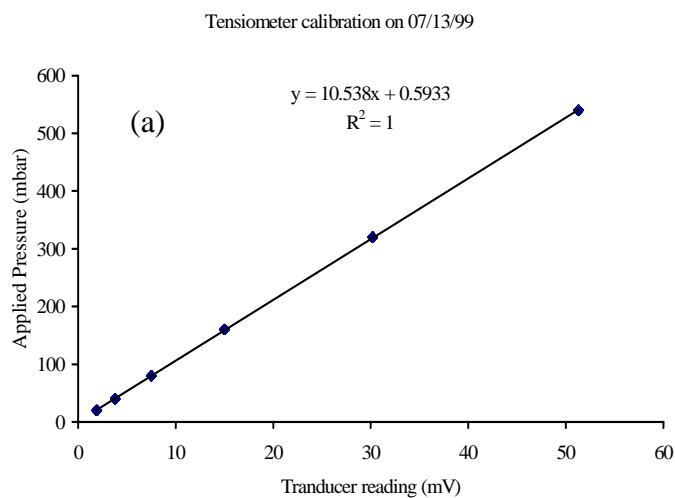


Figure 9. Calibration of the tensiometer (a, c) and outflow (b, d) pressure transducers at two dates

5. MULTIPLEXING

5.1. Multiple sensor set up

Figure 10 shows a schematic of equipment used for matrix head and outflow measurements for a set of 10 pressure cells through an AM416 multiplexer (Component C of Photo 1). The AM416 Multiplexer allows connection of a larger number of pressure transducers than there are 21X datalogger input channels. No multiplexer would be needed, if only 8 pressure transducers were used. AM416 is an acronym for **A**(nalog) **M**(ultiplexer) **4**(lines x) **16**(sets) meaning that a maximum of 16 differential full bridge transducers (consist of 4 pins) can be scanned (Campbell Scientific, 1996a). Without using an external power source, each of the common line ports (COM1 and COM2) of the AM416 can serve 8 channels. Each channel consists of 4 terminals (2 for excitation and 2 for data input). Thus, up to 16 transducers can be connected if the multiplexer is connected to and powered by the datalogger (12 VDC). For our experimental set up, however, the multiplexer and external power supply (10 VDC) are needed to connect 20 transducers (Component E of Photo 1) for monitoring 10 Tempe cells (Photo 12). A stable power (voltage) supply, such as a DC converter with voltage stabilizer is essential to reduce the transducer noise. For each pressure transducer, pin #1 and 3 (yellow and red wires) are connected to the external power supply (Component A of Photo 1) using black terminal strips in the multiplexer box (see Photo 1). The other pair (pin #2 and 4; green and black wires) are connected to the measurement (Input) terminal strips (H and L) of the channels of the multiplexer. With this configuration, in principle, up to 32 transducers can be connected and measured simultaneously with excitation voltage supplied by the external power source.

To collect data from the 20 transducers, the multiplexer must be connected to the 21X datalogger. For this purpose, two input channels 1 and 2 (with H and L terminals on the top strips) of the 21X datalogger (Component B of Photo 1) is connected to the common lines COM1 and COM2 of the AM416. Channel #1 (H and L terminals) of the datalogger is connected to the multiplexer's common line 1 (COM H1, COM L1), while channel #2 (H and L terminals) is connected to the common line 2 (COM H2, COM L2).

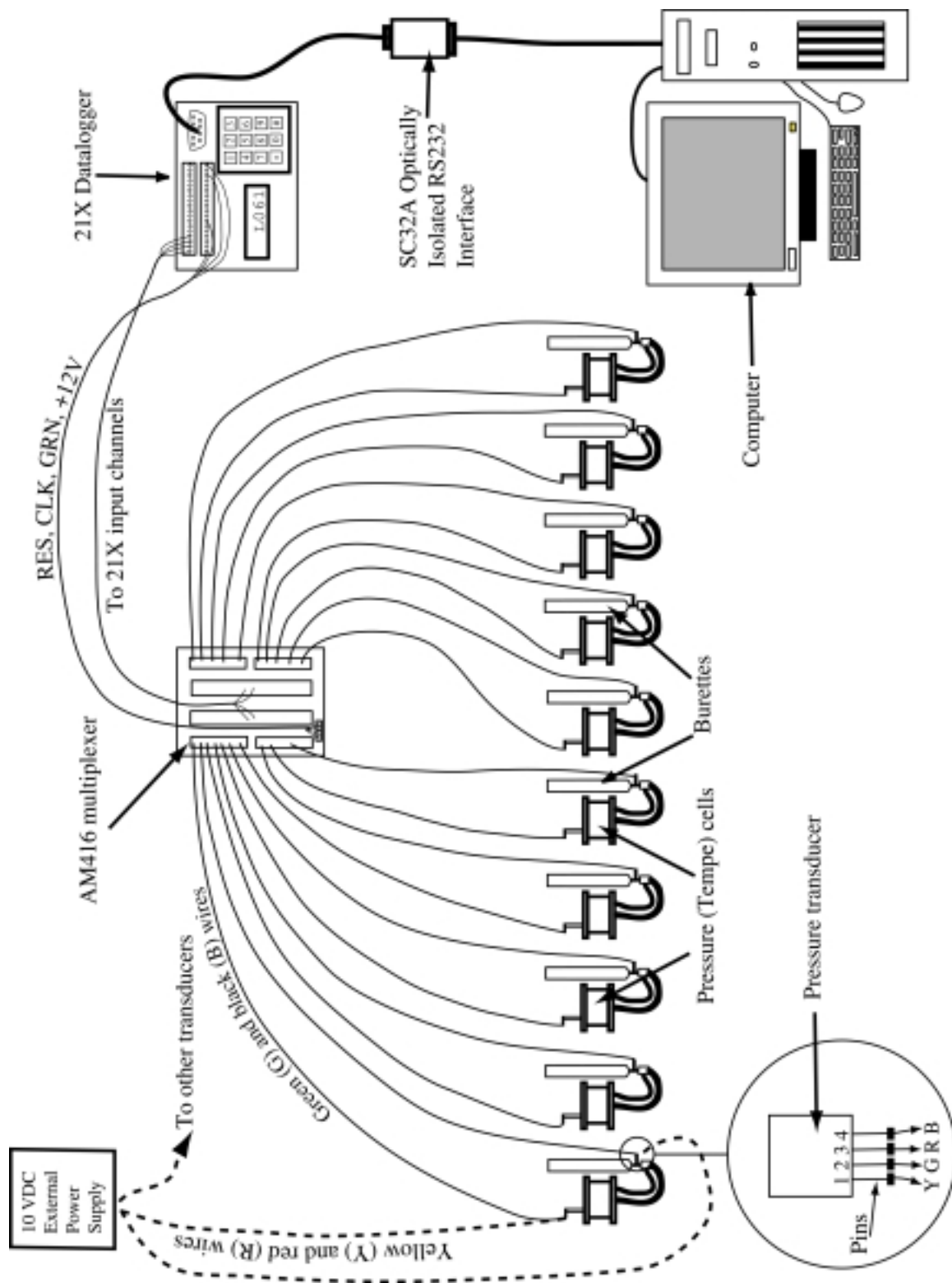


Figure 10. Schematic view of the pressure transducer multiplexing.

The AM416's RESET (RES), CLOCK (CLK), GROUND (GND) and +12V terminals are connected to the 21X's CONTROL1, EXCITATION1, GROUND, and +12V (on the bottom strip of the datalogger), respectively. These terminals are used for control and excitation of the AM416.

5.2. PC208W datalogger support software

The 21X datalogger is, in turn, connected to a computer via the SC32A¹ optically isolated RS232 interface (Figure 10). The PC208W datalogger support software is used to establish a communication link between the datalogger and computer and facilitates programming, communication, and reliable data exchange between computer and 21X¹ (Campbell Scientific, Inc. 1998). The PC208W program can handle more than one datalogger simultaneously, however the number depends on the available serial ports of the computer. The following outlines the steps for establishing communication between datalogger and PC:

1. Start PC208W program on the desktop. A toolbar with eight buttons is opened (Figure 11).

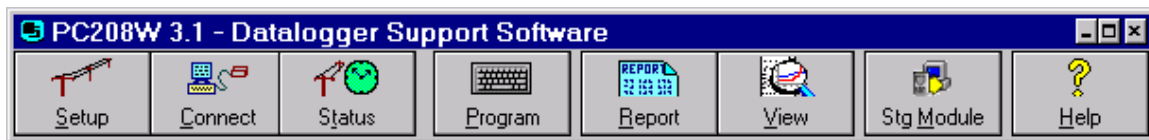


Figure 11. PC208W toolbar.

The buttons on the toolbar are:

Setup: Configure the devices for hardware, data collection, and collection schedules.

Connect: Go on-line with the datalogger to set the clock, send programs, collect data, view and graph measurements

Status: Check the communication and data collection status of all devices you work with, and trigger manual data collection.

Program: Create and edit datalogger programs with EDLOG.

¹ Campbell Scientific, Inc. 815 West 1800 North. Logan, Utah 84321-1784: Phone: 435.753.2342

Report: Process the data files and creates reports using SPLIT.

View: View any file in either ASCII or Hex (useful for checking data files).

Stg Module: Retrieve files from Storage modules.

Help: Enter the PC208W help system.

2. Click on **Setup** button. A setup connections window will be opened with default COM1 port in the **Device Map** column (Figure 12).

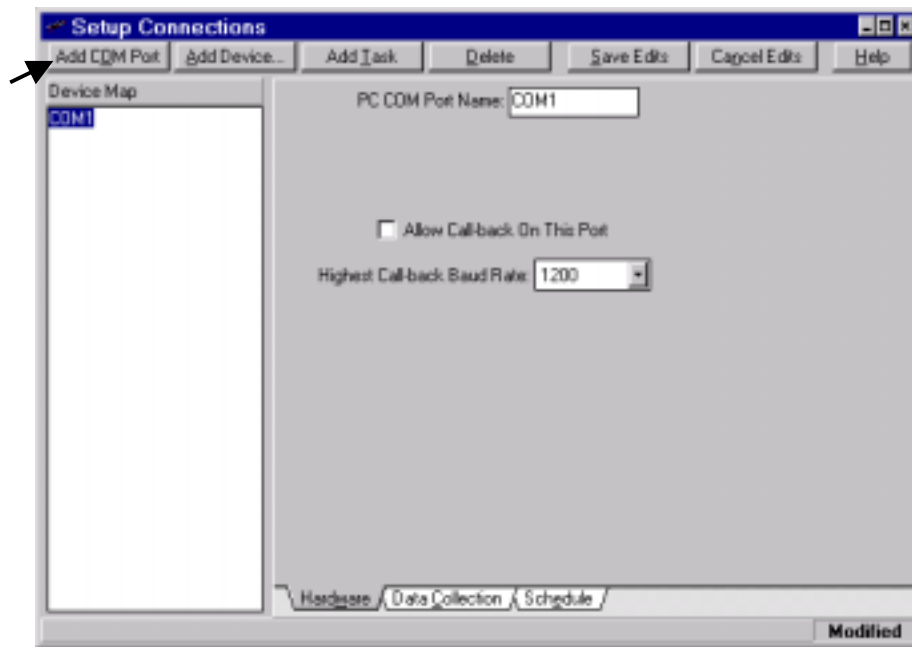
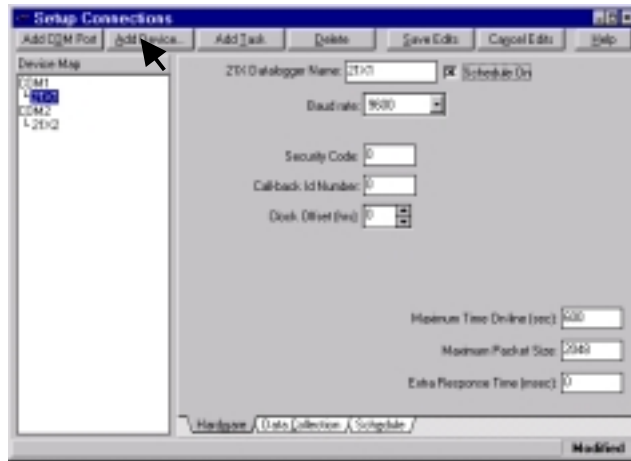


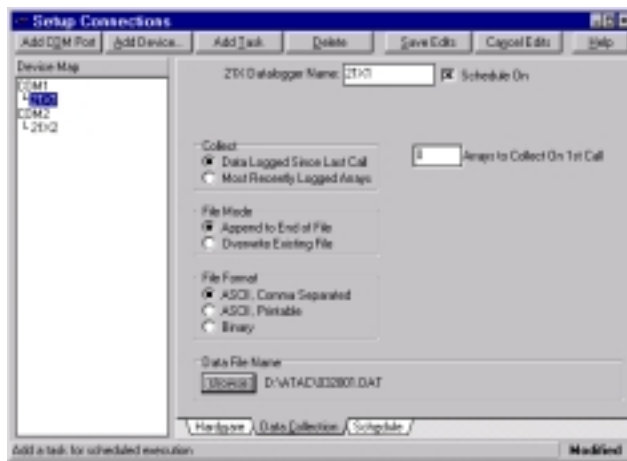
Figure 12. Setup connection window.

Since our computer has 2 serial ports, another COM port can be added by clicking **Add COM Port** button. After adding the second COM port (COM2), click **Add Device** button to connect 21X datalogger with corresponding COM ports (Figure 13a).

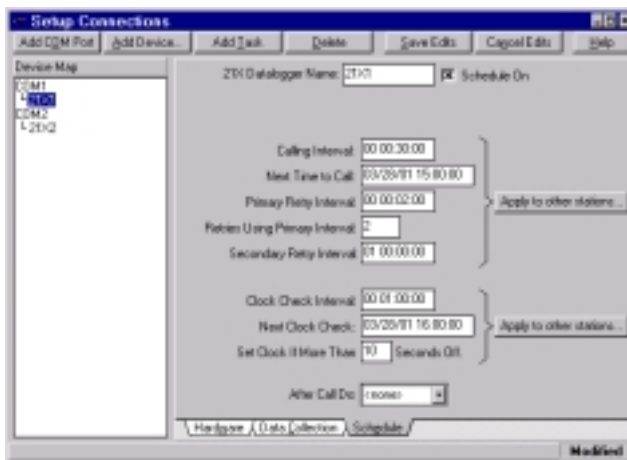
3. Highlight by clicking on device name in the **Device Map** column in Figure 13a and assign required parameters. Each device has its own **Hardware**, **Data Collection**, and **Schedule** tab. Using the **Hardware** tab, The PC208W inserts default values for most



(a)



(b)

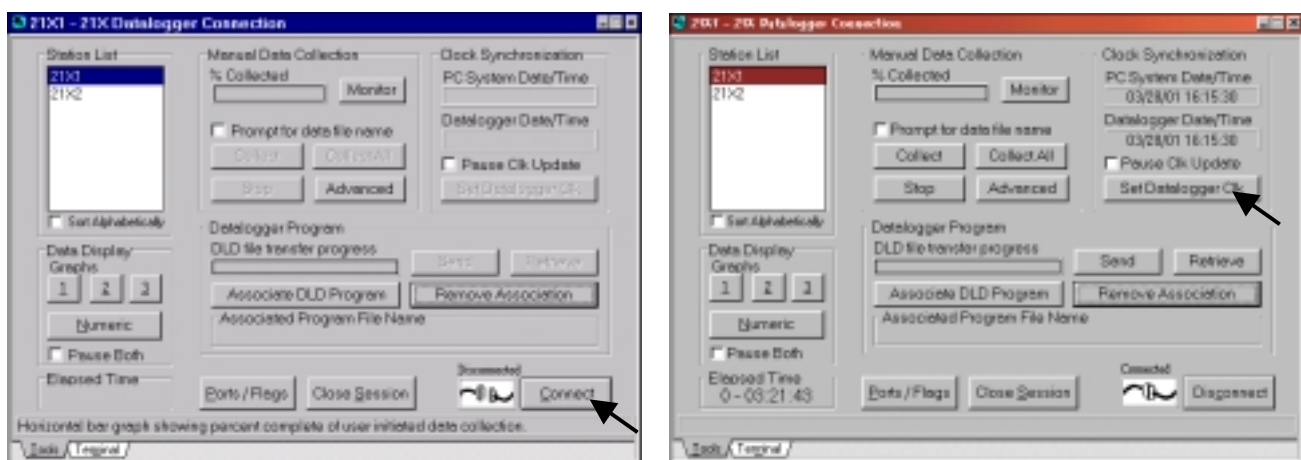


(c)

Figure 13. Setup window with the connected dataloggers: (a) **Hardware** tab, (b) **Data Collection** tab, (c) **Schedule** tab.

parameters of the 21X. Checking the “Schedule On” box enables automatic data collection from the datalogger storage to the computer’s specified directory (Figure 13a). Using the **Data Collection** tab, data manipulation is set up. While a filename for the data file is suggested, the user also can specify the data file name and its directory to collect measured data from the datalogger (Figure 13b). If one selects automatic data collection, data collection and retry information must be specified on the **Schedule** tab (Figure 13c). Moreover, the ‘Calling interval” for data collection and the datalogger clock synchronization based on PC time must be entered.

4. Click on **Save Edits** button.
5. Turn on the power of the datalogger 21X1 and wait until 11:111111 is displayed on the LCD panel of the datalogger. This indicates that the memory check was passed. When 0’s appear instead, the memory check failed and indicates bad memory.
6. Click on **Connect** button of the PC208W toolbar. **Connect** button brings up a window, which gives you real time access to any of the datalogger in your **Device Map**. Here, one can transfer programs to a datalogger, set the datalogger clock, collect data from the datalogger, and display or graph datalogger measurements. Only one datalogger is connected at any given time. If one wants to connect another datalogger in the **Station List** box, the desired datalogger must be highlighted by clicking on it.
7. Click on **Connect** button of the Connection window (Figure 14a). Wait until connection is established and then press **Set Datalogger Clk** button (Figure 14b).



(a)

(b)

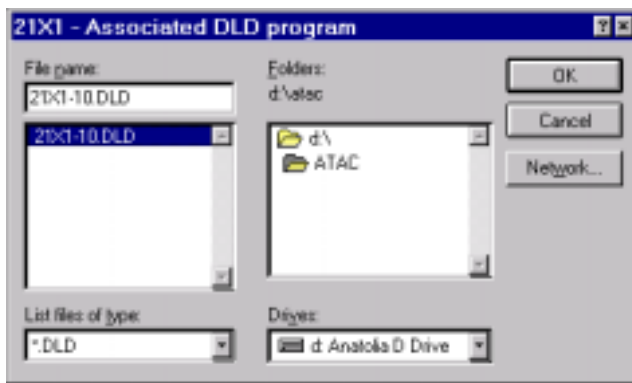
Figure 14. Connection window: (a) before connection, (b) after connection.

8. Click on the **Program** button on the toolbar (Figure 11). This invokes the program EDLOG, which is a tool for creating, editing, and documenting programs for dataloggers (section 5.3). After creating the program (Figure 15), EDLOG compiles and save the datalogger program in a specified directory. When an EDLOG program is saved, EDLOG automatically adds a .CSI extension to the program name. An existing program with .CSI extension can also be loaded for editing. Moreover, whenever an EDLOG program is compiled a file with .DLD extension is created for sending to the datalogger. Close the EDLOG program.



Figure 15. Edlog program window.

9. Go back to the Connection window (Figure 14b) and click on **Associate DLD Program** button. Open the directory, where the datalogger program was saved (Figure 16a). Find the corresponding DLD-file that you wish to send to the datalogger. Click OK, and the Associated Program File Name appears on the connection window (Figure 16b). The program is now ready to send to the datalogger.



(a)



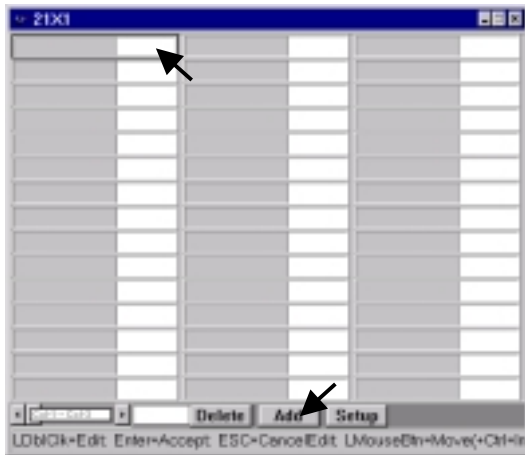
(b)

Figure 16. Association of datalogger program: (a) Program directory, (b) after association of DLD file.

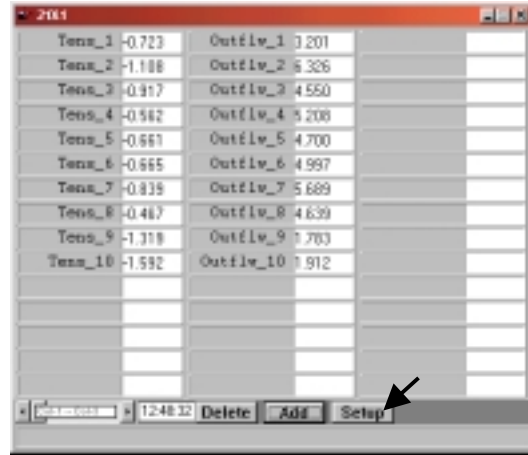
10. Click on **Send** button (Figure 16b) and wait to hear a sequence of sounds from the multiplexer. It is extremely important to remember that, when you send a DLD program to the datalogger, all existing data are deleted from the storage memory of the datalogger.
11. Click on **Numeric** button (Figure 16b) to visualize real-time transducer measurements. First select a cell (Figure 17a) and click on the **Add** button. This will open a window, which shows all transducers. Highlight the tensiometer transducers you wish to be monitored. Click on **Paste** button. Do the same thing for the outflow transducers (Figure 17b). The real-time measurements will appear and refresh when new data are collected (see **Setup** button).
12. Go back to PC208W toolbar and press **Status** button. This button displays information for all the dataloggers on the **Device Map**. One can check the status of data collection, including scheduled calls, errors, retries, and how much new data were collected (Figure 18).

In our laboratory, the outlined procedure has already been conducted. If the user wants to run a new experiment, all steps except #2 and 8 must be followed. Note that if the “Schedule on” option is selected from the Hardware tab, the computer and PC208W

program must be run continuously after the proper parameters have been entered. All other program windows can be closed.



(a)



(b)

Figure 17. Numeric window for real-time data monitoring: (a) before adding transducers, (b) after adding transducers.

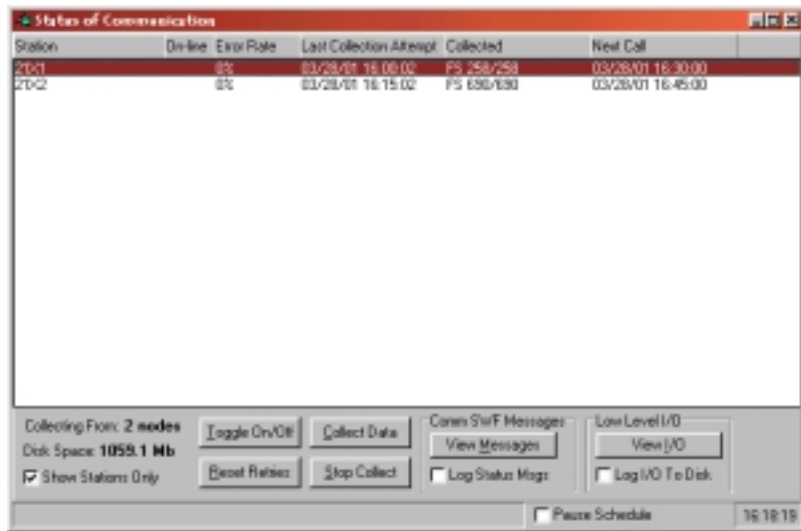


Figure 18. Status window.

5.3. Datalogger program for transducer multiplexing

The example datalogger program, which can be used with a multiplexer and 21X datalogger to measure output voltages from 20 transducers simultaneously, is provided below. Only one program line must be changed, when a different number of transducers are used. The loop count under program command P87 must be equal to half of the number of the transducers. Editing of this program allows changing the sequence and frequency of measurements. For more information, the user is referred to the program language section of the 21X datalogger and the PC208W manuals (Campbell Scientific, Inc., 1996b, 1998). The automatic collection into an indexed array (parameter 4 of the program command P2 and parameter 2 of program command P71) is discussed in the AM416 multiplexer manual (Campbell Scientific, Inc., 1996a).

;{21X}

*Table 1 Program

01: 20 Execution Interval (seconds)

1: Set Port (P20)

1: 1 Set High

2: 1 Port Number

2: Beginning of Loop (P87)

1: 0 Delay

2: 10 Loop Count

3: Step Loop Index (P90)

1: 2 Step

4: Excitation with Delay (P22)

1: 1 Ex Channel

2: 1 Delay w/Ex (units = 0.01 sec)

3: 1 Delay After Ex (units = 0.01 sec)

4: 5000 mV Excitation

5: Volt (Diff) (P2)

1: 2 Reps

2: 3 50 mV Slow Range

3: 1 DIFF Channel

4: 1 -- Loc [Tens_1]

5: 1.0 Mult

6: 0 Offset

6: End (P95)

```

7: Set Port (P20)
  1: 0    Set Low
  2: 1    Port Number

8: If Flag/Port (P91)
  1: 21    Do if Flag 1 is Low
  2: 30    Then Do

9: If time is (P92)
  1: 0    Minutes into a
  2: 5    Minute Interval
  3: 10    Set Output Flag High

10: Resolution (P78)
  1: 1    High Resolution

11: Real Time (P77)
  1: 110    Day,Hour/Minute (midnight = 0000)

12: Average (P71)
  1: 20    Reps
  2: 1    Loc [ Tens_1  ]

13: Else (P94)

14: If time is (P92)
  1: 0    Minutes into a
  2: 5    Minute Interval
  3: 10    Set Output Flag High

15: Resolution (P78)
  1: 1    High Resolution

16: Real Time (P77)
  1: 110    Day,Hour/Minute (midnight = 0000)

17: Average (P71)
  1: 20    Reps
  2: 1    -- Loc [ Tens_1  ]

18: End (P95)

*Table 2 Program
  01: 0.0000    Execution Interval (seconds)

```

*Table 3 Subroutines

End Program

6. DATA FILE PREPARATION PROGRAM (DATAPREP)

6.1. Description and requirements of DATAPREP

The program DATAPREP (Appendix B) transforms the multi-step outflow experimental data, which are collected by the datalogger, to a new file (filename is FINPU), which is used as an input file for SFOPT. To create FINPU with DATAPREP, the data preprocessing procedure of Figure 19 must be followed. One must follow the required data cleaning and preparation procedures outlined in sections 6.2 and 6.3 for creating the input data file, FNAME. Note that FNAME and FINPU are the character variables for the experimental and input file names, respectively of the DATAPREP program code (line 37 and 39 in Appendix B)

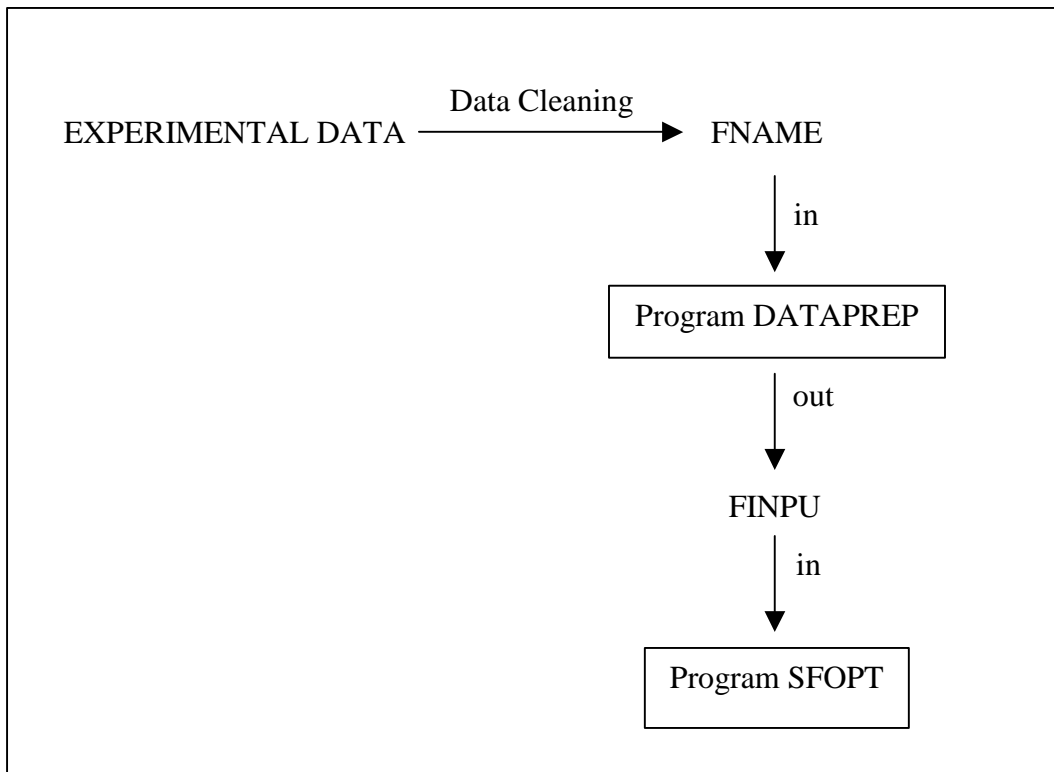


Figure 19. Schematic diagram of data processing procedure.

The program DATAPREP requires measured values for sample height (**samhe**), sample diameter (**samdi**), sample volume (**samvo**), thickness of porous membrane

(**porhe**), distance between center of the porous cup and bottom of the porous membrane (**tenhe**), burette reading at the beginning of the experiment after soil sample saturation (**watvo**), water height in burette from bottom of porous membrane at the beginning of the experiment after soil saturation (**wathe**), and change of water height in burette per ml of outflow volume (**whinc** = 0.181 cm/ml) (Figure 20). In addition, although DATAPREP does provide default values, the user must specify the total number of nodes (**nnsf**), the number of nodes in the soil sample (**lnnsf**), and the saturated conductivity of the porous membrane (**cpltsf**) used in SFOPT (see description of input file in 7.4). If the porous membrane has negligible thickness, as is the case for a porous nylon membrane, values for **nnsf** and **lnnsf** are identical and **cpltsf** can be set to a default value of 999. The variable definitions for the required input file for the DATAPREP program are presented in Table 2.

To ensure adequate number of data for the whole experiment, the maximum time interval between data pairs is set to 2 hours. After providing the DATAPREP program with the approximate number of data pairs (**ntob**) required for FINPU, the allowable change in capillary pressure and outflow volume between data pairs is computed from the difference between the maximum and minimum measured values during the outflow experiment. Unreasonable fluctuations of the measurements are removed using a computational filter, thereby providing a smooth set of data values. Outliers are treated in two ways. First, if the data value is lower than the n subsequent values for h (h denotes matric potential, $h < 0$), or higher than the n subsequent values of Q ($Q > 0$, where Q denotes cumulative drainage volume), the specific data value pair (h and Q) is removed from the data set. The current default value for n is set to 5, but this value may need to be changed depending on the number of erroneous data values. Second, if the particular data value is larger, within a specified tolerance, than the previous value for h (< 0) or smaller than the previous Q -value (> 0), this specific data pair (Q and h) is eliminated as well. Default values for these differences are 1 cm for h and 0.1 ml for Q . Also, these criteria can be changed depending on the magnitude of the measurement error. At the end of each run, DATAPREP automatically displays a graphical representation (Figure 23) on the computer screen, showing a comparison of the original and transformed cumulative

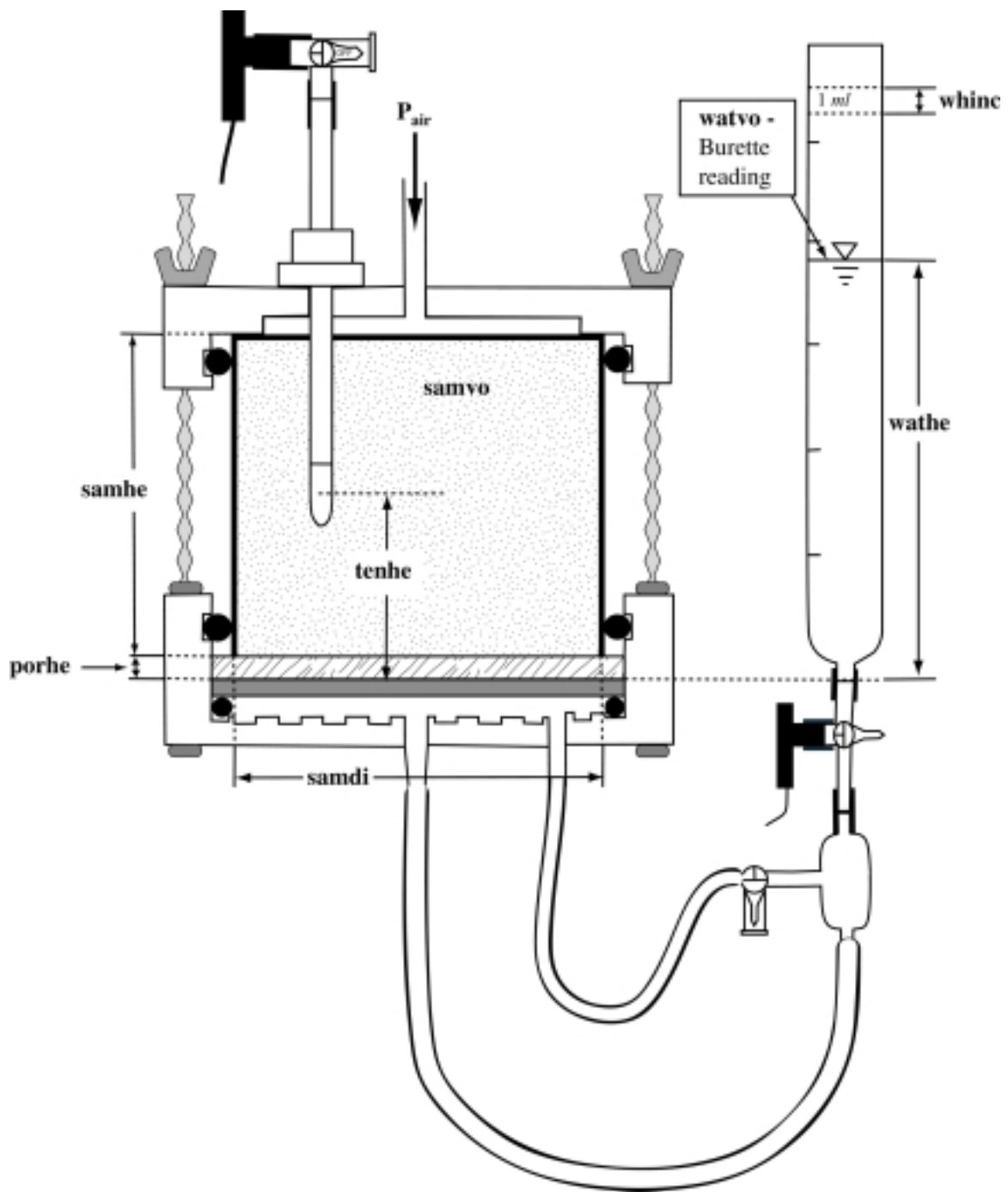


Figure 20. Schematic view of the experimental set up.

Table 2. Description of variables for input file 'FNAME' of the DATAPREP.

Line	Variable	Description
1	XSS	Saturated water content
2	APINI	Initial air pressure at hydraulic equilibrium in mbar (ZX (cm) in SFOPT)
3	QOINI	Burette reading at initial equilibrium (time = 0, ml)
4	QOEND	Burette reading at end of outflow experiment (ml)
5	A(1)	Slope of pressure transducer of tensiometer (mbar/mV)
6	A(2)	Slope of pressure transducer of burette (ml/mV)
7	NCHANGE	Number of air pressure step (AIRP in SFOPT)
8	For I=1,..., AIRP	
	CDATE(I)	Day of change of air pressure (Julian date)
	CTIME(I)	Time of change of air pressure (hhmm)
	P(I)	New air pressure (mbar)
12(if AIRP=4)	NFLUSH	Number of air flushings + 1
13-24(if NFLUSH=12)	For I=1, ...,NFLUSH	
	FDATE(I)	Day of air flushing (Julian date, I=1 corresponds with date when air accumulation started)
	FTIME(I)	Time of air flushing (hhmm, I=1 corresponds with time when air accumulation started)
25-END	DATE(I)	Day of measurement (julian date, I=1 corresponds with data at hydraulic equilibrium at t=0, and is used for calibration of pressure transducers)
	TIME(I)	time of measurement (hhmm, I=1 corresponds with data at hydraulic equilibrium at t=0, and is used for calibration of pressure transducers)
	HO(I)	pressure transducer output signal (mV) for tensiometer
	QO(I)	pressure transducer output signal (mV) for burette

outflow and soil water matric head as a function of time. The graphic also lists the difference in observed (water level in burette) and measured (pressure transducer) total outflow volume. At run time the user will be prompted to specify a file name for a file that will contain this data for graphing in a spreadsheet or other graphing program.

The user should review the description of variables in Section 7.4 to assure the correct values of input parameters for SFOPT. Additionally, it may be necessary to change assumed default values in the program DATAPREP and its input file FNAME.

6.2. Cleaning the raw experimental data

In this section the procedure for cleaning the raw experimental data collected by the data logger via the pressure transducers and for the preparation of the input data file for DATAPREP will be explained in detail. The cleanup is required because (1) the collected data is in output signal (mV) format and must be transformed to the desired units of matric head (cm water) and outflow (mL), (2) the outflow data must be corrected due to possible air accumulation, (3) there are occasional anomalous readings due to transducer malfunctions, and (4) some extra data, which do not represent the experiment, may be collected prior to and after the experiment. The DATAPREP program also selects a specified number of data pairs for use in the inverse modeling. It is necessary to reduce the data to a smaller number of pairs because the collected data may be far too exhaustive. Each of these items will be addressed in the example problem presented in Section 6.3.1. Occasionally, data can be lost or can be erroneous due to: 1) transducer malfunction (including membrane perforation), 2) tensiometer failure (including cracks and poor hydraulic contact), 3) data download failure from datalogger to computer, 4) computer hard drive failure, and/or 5) power outage lasting longer than the storage capacity of the datalogger. The procedure for dealing with these problems is presented in Section 6.5.

For any period during which air accumulates, the program assumes that air accumulation occurs uniformly. Therefore, it is necessary to define the air accumulation duration or period (step 10 in the following section) in FNAME. The term “air accumulation period” refers to the period during which air accumulates. The term “flushing event” refers to the actual act of flushing the air from the system. The first flushing day and time corresponds to the beginning of the first pressure period during

which air begins to accumulate. To identify the next flushing event time, remove noisy data that was recorded during the flushing event, and report an intermediate time value in FNAME as the endpoint of the first air accumulation period. This also acts as the beginning of the next air accumulation period. This is the basic technique that is used to identify air accumulation periods and to clean the noisy data that occurs during the flushing event. It is helpful to keep in mind that you are specifying the times at which air accumulation begins and ends. The specification of the flushing times is best illustrated in Example 1 in Section 6.3.1.

6.3. Making an input data file for DATAPREP program

The procedure for creating the preparation file is illustrated below with an example. Here we assume that the experimentalist has recorded all the information requested below during the course of the experiment, such as flushing event times and applied pressure times.

6.3.1. Example 1.

An undisturbed sandy loam soil sample was subjected to 6 pressure applications of 10, 40, 80, 150, 300, and 500 mbars. The 10-mbar pressure is applied as an air entry pressure. The recorded application times for the pressures are shown in Table 3 and the recorded times for flushing events are shown in Table 4. Remember, these times are only approximate. The volume in the outflow burette prior to any pressure application is 20 mL. The sample was completely saturated at the onset of the experiment. The sample volume is 111.64 cm³. The oven dry weight of the sample is 173.5 grams, the wet weight at the end of the experiment was 189.2 grams, and a total of 18 mL of water drained from the sample during the course of the experiment. Air accumulated and was flushed seven

Table 3. Recorded starting times for pressure applications.

Pressure, mbars	Julian date	Military time
10	77	1746
40	78	0840
80	78	1740
150	79	0830
300	80	1540
500	82	1700

Table 4. Recorded times for flushing events.

Flushing Event #	Julian Date	Military Time
1 (air starts to accumulate)	79	0831
2	79	1850
3	80	1527
4	82	1325
5	83	2148
6	84	1217
7	84	2300
8	85	0822

times. Air began to accumulate during the 150-mbar pressure. The calculations are explained below and the resulting input file (FNAME) for DATAPREP is shown in Table 11. Numerals below correspond with the line numbers of FNAME (page 51). The graphs are included to illustrate the technique used for removal of air flushing event data. This data input file was prepared with Microsoft Excel.

1. Calculate the saturated volumetric water content.

- a) Calculate the mass of water in the core as the difference between the oven dry weight and the wet weight at the conclusion of the experiment: $189.2 - 173.5\text{g} = \mathbf{15.7\text{g}}$

- b) Add to this the mass of water that has drained from the core to get the total mass of water, m_w , at saturation (recall that 1mL water weighs 1 gram):

$$m_w = 15.7\text{g} + 18\text{g} = 33.7\text{g}$$

- c) Divide by the mass of the oven dry soil to result in the saturated gravimetric water content, θ_g : $\theta_g = 33.7\text{g} / 173.5\text{g} = \mathbf{0.194}$

- d) Calculate the bulk density according to: $\rho_b = m_s / V_t$ where ρ_b is the bulk density, m_s is the oven dry soil mass, and V_t is the total volume of the soil:

$$\rho_b = 173.5\text{g} / 111.64\text{ cm}^3 = \mathbf{1.55\text{ g/cm}^3}$$

- e) Calculate the volumetric water content, θ_v , according to: $\theta_v = \theta_g \rho_b / \rho_w$ where ρ_w is the density of water: $\theta_v = 0.194 (1.55) / 1.0 = \mathbf{0.302\text{ cm}^3\text{cm}^{-3}}$

or directly from $\theta_v = m_w / \rho_w V_t$

2. Enter the initial pressure step that is applied (i.e. “air entry” pressure) (**10 mbars**).
3. Enter the burette reading at the onset of the experiment. That is, the reading prior to any application of pressure. (**20 mL**).
4. Enter the burette reading at the conclusion of the experiment. (**38 mL**).
5. Enter the slope of the calibration curve for the tensiometer-transducer. To see an example of a calibration curve, we refer to Figure 9 in Section 4. The slope for this sample was **10.638**.
6. Enter the slope of the calibration curve for the outflow-transducer. To see an example of a calibration curve, we refer to Figure 9 in Section 4. The slope for this sample was **20.647**.
7. Enter the number of pressure applications minus one. That is, the air entry pressure is excluded (**6 - 1 = 5**).
8. For each pressure increase (except for the air entry value), enter the Julian date, military time, and pressure value (in mbars) The number of lines in this step must agree with the number declared in step 7 (**5**). The times declared here may not exactly match the times declared in the experimental folder since the datalogger records several times per minute and can be programmed to average these values every minute or every five minutes. Therefore, it is necessary to look through the data to pinpoint when a pressure step began. The following outlines this procedure:

Table 5 shows an excerpt from the data file for this example problem. It can be seen that the readings for the tensiometer-transducer are fairly uniform until 08:41 at which time there is a marked change. This change can either be a drop in the value or an increase. What is important to note is that the readings are maintained at some relatively uniform level until some marked change occurs that coincides approximately with a recorded pressure application. Recall that the experimentalist recorded the pressure application time for 40 mbars to be 08:40 (Table 3) but we see in Table 5 that it is instead 08:41. Some data excerpts for the remaining pressure applications are shown in Table 6 through Table 9.

Table 5. Data excerpt for 40 mbar pressure step.

Julian Date	Military Time	Tensiometer transducer	Outflow transducer
78	835	-1.1195	2.3118
78	836	-1.1172	2.3106
78	837	-1.1172	2.3141
78	838	-1.116	2.3129
78	839	-1.1138	2.3118
78	840	-1.1172	2.3153
78	841	-0.96706	2.3448
78	842	-0.60072	2.3744
78	843	-0.64734	2.4381
78	844	-0.72014	2.4802
78	845	-0.80321	2.5099

Table 6. Data excerpt for 80 mbar pressure step.

Julian Date	Military Time	Tensiometer transducer	Outflow transducer
78	1734	-1.0408	2.5218
78	1735	-1.0351	2.5207
78	1736	-1.0363	2.5219
78	1737	-1.0386	2.5242
78	1738	-1.0203	2.6015
78	1739	-1.042	2.5741
78	1740	-0.55625	2.5527
78	1741	0.08758	2.5754
78	1742	-0.15242	2.5845
78	1743	-0.51073	2.5856
78	1744	-0.6882	2.5914

Table 7. Data excerpt for 150 mbar pressure step.

Julian Date	Military Time	Tensiometer transducer	Outflow transducer
79	825	-1.0227	2.6243
79	826	-1.0249	2.6255
79	827	-1.0238	2.6243
79	828	-1.0249	2.6230
79	829	-1.0260	2.6219
79	830	-1.0260	2.6241
79	831	1.1443	2.6366
79	832	4.4054	2.6457
79	833	3.4337	2.6582
79	834	2.8742	2.6628
79	835	2.4874	2.6696

Table 8. Data excerpt for 300 mbar pressure step.

Julian Date	Military Time	Tensiometer transducer	Outflow transducer
80	1534	-0.42545	2.8039
80	1535	-0.48571	2.8289
80	1536	-0.53693	2.8414
80	1537	-0.60516	2.8062
80	1538	-0.6518	2.8004
80	1539	-0.68705	2.8016
80	1540	8.3433	2.8073
80	1541	12.416	2.8209
80	1542	12.246	2.8198
80	1543	12.086	2.8266
80	1544	11.932	2.83

Table 9. Data excerpt for 500 mbar pressure step.

Julian Date	Military Time	Tensiometer transducer	Outflow transducer
82	1655	0.4435	3.0933
82	1656	0.44124	3.0945
82	1657	0.43213	3.0922
82	1658	0.42985	3.0945
82	1659	0.42873	3.0922
82	1700	0.42189	3.1035
82	1701	19.589	3.0966
82	1702	19.554	3.0968
82	1703	19.547	3.0945
82	1704	19.546	3.0956

9. Enter the number of air flushings plus one. Remember that this number signifies the endpoints of the air accumulation periods or intervals (**7 + 1 = 8**).
10. Enter the Julian date and military time corresponding to the beginning of each air accumulation period. For example, the first flushing day and time corresponds to the start time for the first pressure during which air accumulates (150 mbars) because what you are actually specifying is the time at which air accumulation commenced. So, the time reported for the first air accumulation period is the same as the start time for the 150 mbar pressure, or day 79, at time 08:31 (Table 4). For the remaining flushing events it is necessary to graph the outflow data in order to determine the time to report and to determine which data should be deleted from the file. The outflow-

transducer data for the second flushing event prior to any data removal is graphed in Figure 21. Notice in Figure 21 the plot is relatively flat until a peak begins at 18:46 with a second, smaller peak at 18:52. We removed data from 18:45 to 18:54 and reported an air flushing time of 18:50 (refer to line 38 in Table 10). One could have chosen any other time between 18:46 and 18:53. What is important is that some time during the flushing event is reported to delineate between two periods of air accumulation. Figure 22 shows outflow-transducer versus time for first flushing event after data removal.

11. Follow this same procedure for the remaining air accumulation periods.
12. The remainder of the file consists of the recorded data in the following order per line:
Julian date, military time, tensiometer-transducer reading, and outflow-transducer reading.
13. Remove all data after the final flushing event except for the endpoint after the last flushing event because otherwise you will incorporate data that includes uncorrected air accumulation.
14. Save the file as a comma delimited file (*.csv).

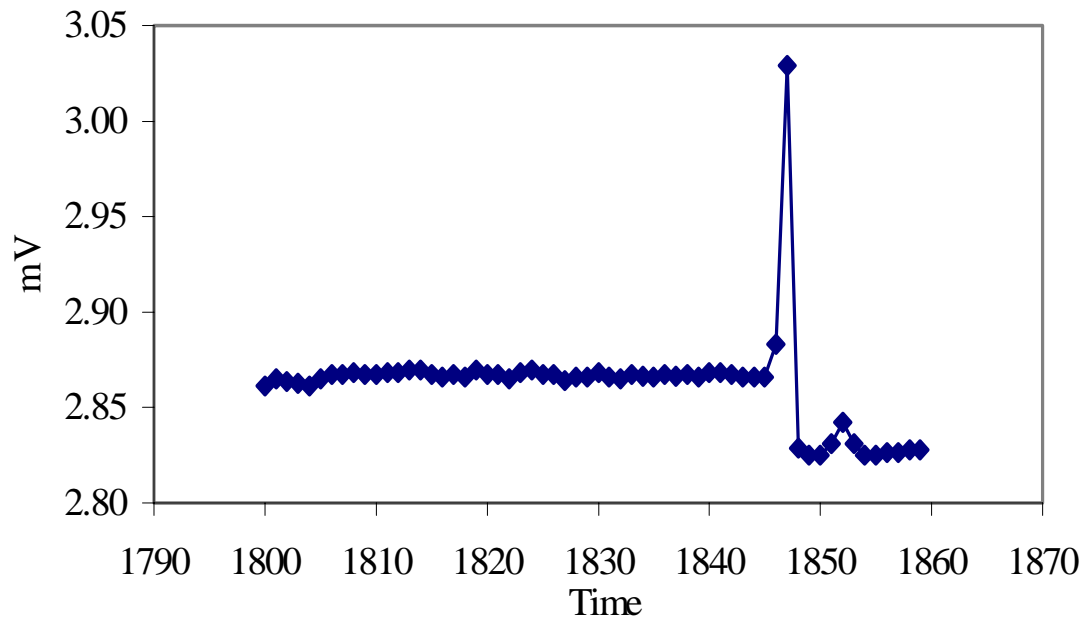


Figure 21. Outflow-transducer voltage versus time for first flushing prior to data removal.

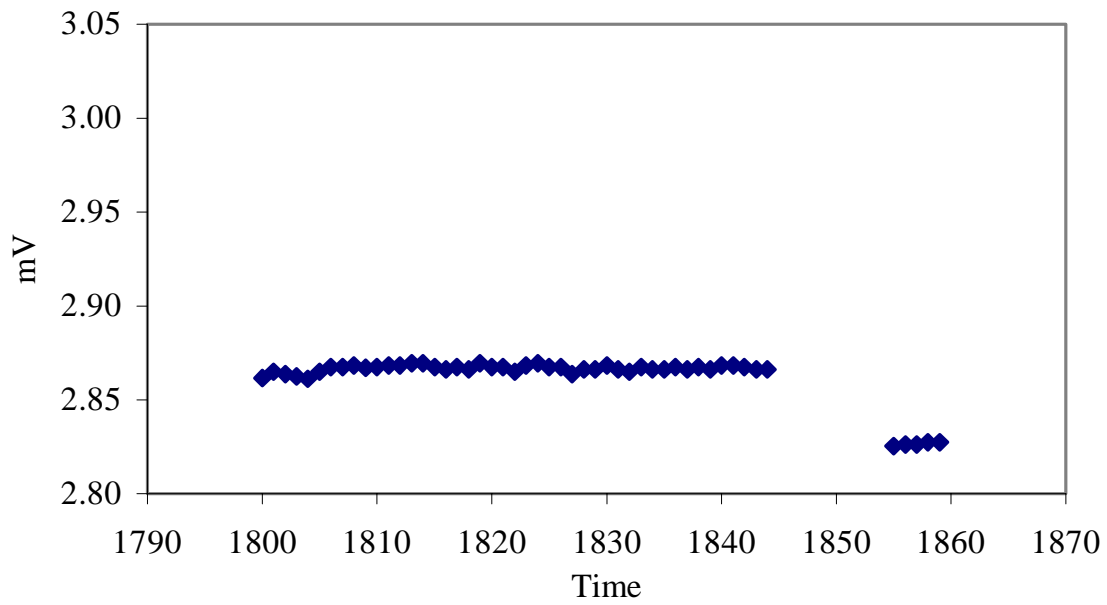


Figure 22. Outflow-transducer voltage versus time for first flushing after data removal.

Table 10. Graphed data after removal.

Line	Military Time	Outflow transducer
1	1808	2.8684
2	1809	2.8672
3	1810	2.8673
4	1811	2.8684
5	1812	2.8684
6	1813	2.8696
7	1814	2.8695
8	1815	2.8673
9	1816	2.8662
10	1817	2.8674
11	1818	2.8662
12	1819	2.8696
13	1820	2.8674
14	1821	2.8674
15	1822	2.8650
16	1823	2.8684
17	1824	2.8696
18	1825	2.8673
19	1826	2.8673
20	1827	2.8639
21	1828	2.8662
22	1829	2.8662
24	1830	2.8684
25	1831	2.8662
26	1832	2.8650
27	1833	2.8674
28	1834	2.8663
29	1835	2.8662
30	1836	2.8673
31	1837	2.8663
32	1838	2.8673
33	1839	2.8662
34	1840	2.8684
35	1841	2.8685
36	1842	2.8674
37	1843	2.8662
38	1844	2.8662
39	1855	2.8253
40	1856	2.8264
41	1857	2.8264
42	1858	2.8277
43	1859	2.8277

Table 11. Example input data file for the DATAPREP (FNAME).

1	0.302			
2	10			
3	20			
4	38			
5	10.63820763			
6	20.64745309			
7	5			
8	78	841	40	
↓	78	1740	80	
	79	831	150	
↓	80	1540	300	
	82	1701	500	
9	8			
10	79	831		
11	79	1850		
↓	80	1527		
	82	1325		
	83	2148		
	84	1217		
↓	84	2300		
	85	822		
12	78	841	-0.96706	2.3448
↓	78	842	-0.60072	2.3744
	78	843	-0.64734	2.4381
	78	844	-0.72014	2.4802
	78	845	-0.80321	2.5099

	85	814	10.885	3.4127
	85	815	10.883	3.4115
	85	816	10.88	3.4127
	85	817	10.878	3.4115
	85	818	10.876	3.4138
	85	819	10.874	3.4127
	85	824	10.936	3.2452
	85	832	10.868	3.2591
	85	833	10.866	3.2759
	85	834	10.864	3.2793
↓	85	835	10.861	3.2805
	85	836	10.861	3.2816

6.4. Running the data preparation program, DATAPREP

Due to its graphics requirement, the DATAPREP program must be run using Digital Visual Fortran 5.0 (Visual Fortran), which uses Microsoft® visual development environment. The visual development environment is also known as Microsoft Developer Studio™. DATAPREP uses run-time library modules (DFLIB) of Visual Fortran for drawing the final output graph to show the end result of the data preparation (cleaning) procedure. Module DFLIB includes run-time functions and subroutines to assist user in special tasks. Thus, DATAPREP has to be opened as a Fortran QuickWin Application project. If a different version of Visual Fortran is used, the run-time library module name (DFLIB) needs to be changed. To run the DATAPREP program, follow the given instructions below

1. From the Windows Start Menu, Select Visual Fortran.
2. Select Developer Studio.
3. To create a new project, choose the File menu and select New. A dialog box opens that has the following tabs:
 - Files
 - Projects
 - Workspaces
 - Other Documents

The Projects tab displays various project types. Specify the project name and location. Click the QuickWin Application type of Fortran project to be created.

4. Click OK to create the new project.
5. To add Dataprep.f90 file to the project, Select “Add To Project” from the Project menu.
6. Select “Files” from the submenu. The “Insert Files into Project” dialog box appears. Use this dialog box to select the Dataprep.f90 file to be added to the Project.
7. Click OK. The editor appears allowing you to type in source code. The file name appears in the FileView pane.

8. Open prepared folder, double click on Dataprep.f90 file (might have to select View workspace). For new experimental set-up, parameters at the beginning of the program must be changed. If you want to change the weighting it must be done here.
9. After changes made in source code (Dataprep.f90), the program must be re-compiled.
10. Choose the Build Menu and select “compile Dataprep.f90”.
11. Choose the Build Menu and select “Build”.
12. Choose the Build Menu and select “Execute”.
13. Type in file name including .csv extension, give input file name that is wanted for the FINPU file (same name different extension, i.e., *.in), give graph file name (i.e., *.g), give 250 points as the number of desired points. This seems to be ignored, anyway, because it seems that the number of points chosen is never the number you specify.
14. At the end of program run, another window will be opened and shows a final output graph (Figure 23). The gray plot in Figure 23 corresponds to the original outflow data, green is corrected outflow, blue is chosen outflow data points for use in SFOPT, pink is original pressure data, and red are chosen pressure points for SFOPT.
15. Look at the graph to see if there is any additional cleanup to be done. If so go back to the file with the csv extension in MS Excel spreadsheet program and clean up, then re-run DATAPREP.
16. Close workspace.

The user must note that the file with the csv extension has to be in the same project directory created above as the source code (DATAPREP). The output file of the DATAPREP Program is the input file for the SFOPT optimization program. The SFOPT program can be run by a similar procedure as outlined above with the required input file. But this is not a rule of thumb. On the contrary, SFOPT is independent of the program environment. It can be executed with different type of Fortran compilers.

```

Experimental file name : example1.csv
Input file name :      example1.in
Number of time points : 247    10.638    20.647    8.924    -28.414
Difference between final outflows by burette and transducer : -1.343 ml
Time : 0 to 167.9 hr  Press. : 0 to -383.2 cm  Outflow : 0 to 19.3 ml

```

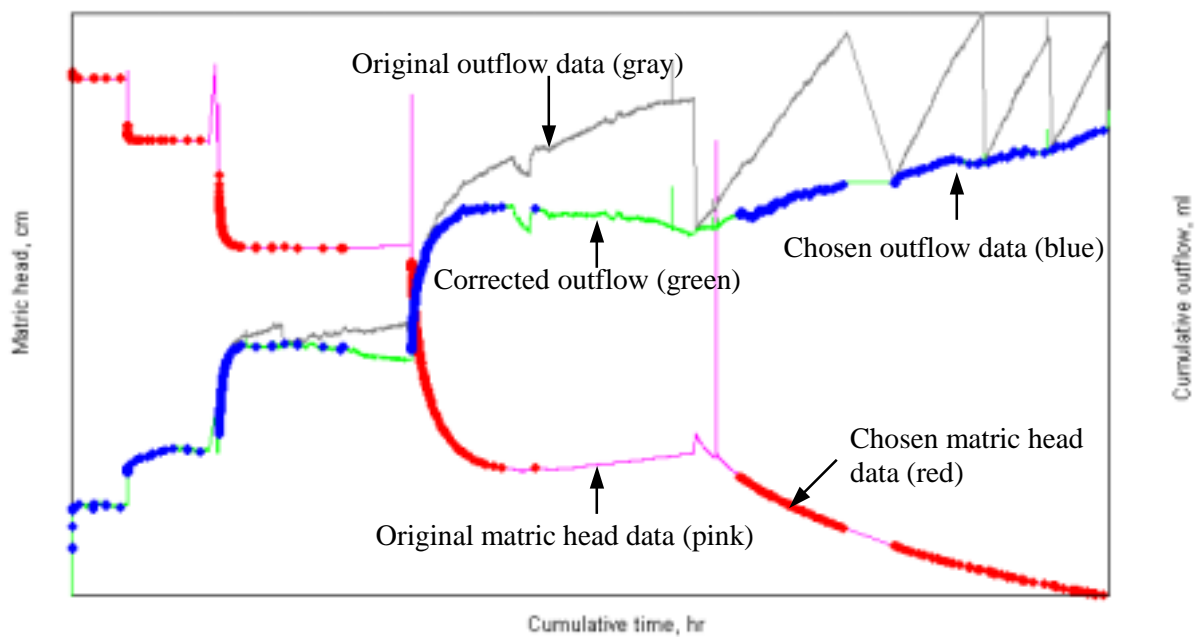


Figure 23. Final output graph of the DATAPREP program.

6.5. Corrections to DATAPREP files in the case of incomplete or erroneous transducer measurements

The DATAPREP program assumes that experimental conditions during the multi-step procedure are according to protocol. It does not account for failure of one or both pressure transducers or for data losses by the data logger. For such conditions it is often possible to adjust for experimental irregularities in the data, prior to inverse modeling. Most times, a repetition of the experiment is not possible, or is too time consuming, and hydraulic properties must be inferred from the available data. The following general types of irregularities may occur:

- Outflow data records from the pressure transducer in the burette are missing, erratic, or erroneous for part or all of the experimental duration; in this case, a shortened record combined with the manually recorded outflow data immediately prior to each pressure step increment must be considered together with a complete matric potential record;
- Matric potential data records from the pressure transducer in the core are missing, erratic, or erroneous for part or all of the experimental duration; in this case, a shortened or interpolated record combined with the manually recorded pressure steps must be considered;
- Automatic data records (from both pressure transducers) are completely lost due to computer failure; in this case only the manually recorded pressure and outflow data at the end of each step are available.

The principle approach in these cases is careful inspection of the available data, of the data selected by DATAPREP, and manipulation of the weights given to matric potential–outflow pairs. Manually recorded data that are deemed reliable are inserted into the records produced by DATAPREP prior to the inverse modeling with SFOPT. Only high-quality data are given a non-zero weight. Weights must be carefully chosen to reflect the imbalance in matric potential and outflow data. The resulting hydraulic data must be clearly identified as being obtained by non-standard procedures and should be documented separately.

In this section, we show two important non-standard procedures, one for an experiment with erratic or irregular outflow data recordings (first category above), and one for the extreme case of a complete loss of the electronic data record (last category above). We show that approximate data pairs may be substituted in the case when a handwritten data log is available. If transient data is lost, equilibrium data pairs can still provide enough information for parameter estimation of the retention curve.

6.5.1. Example 2.

In this example, 10 pressure increments were applied: 10, 60, 80, 90, 100, 125, 150, 200, 250, and 300 mbars. As can be seen in Figure 24, the outflow data are poor for the first eight pressure steps, but the data for the last two steps appear to be of good quality. Notice that the DATAPREP program has not selected any data pairs from pressure steps 2-7 although the pressure data appear to be of good quality. This is because the program selects data according to criteria, specified from lines 162 to line 215 in DATAPREP (See also section 6.1), which eliminate highly fluctuating data. If one type of data (either pressure or outflow) does not satisfy those criteria, the DATAPREP program will not select the data pair in question. However, the proposed modifications make use of the good pressure head data and include the handwritten outflow values from the experimental record. The following steps outline this procedure:

1. Modify the DATAPREP code (Appendix B) by changing the value of the weight parameter “wtq” in line 29 (in the “important parameters” section at the beginning of the code) from a value of 1.0 to a value of 0.0 and by commenting lines 193-197 and line 207. Table 12 reflects these changes (the original format is shown in Appendix B). These changes allow pressure head data to be chosen according to the specified criteria and allow the required outflow pair to be chosen without any restrictions. We do not want to impose any restrictions for choosing outflow since the outflow data are poor. We simply need to obtain the pairs required in SFOPT. Since we do not want erratic outflow data to be used in the parameter estimation, those data are given a weight of 0.0.

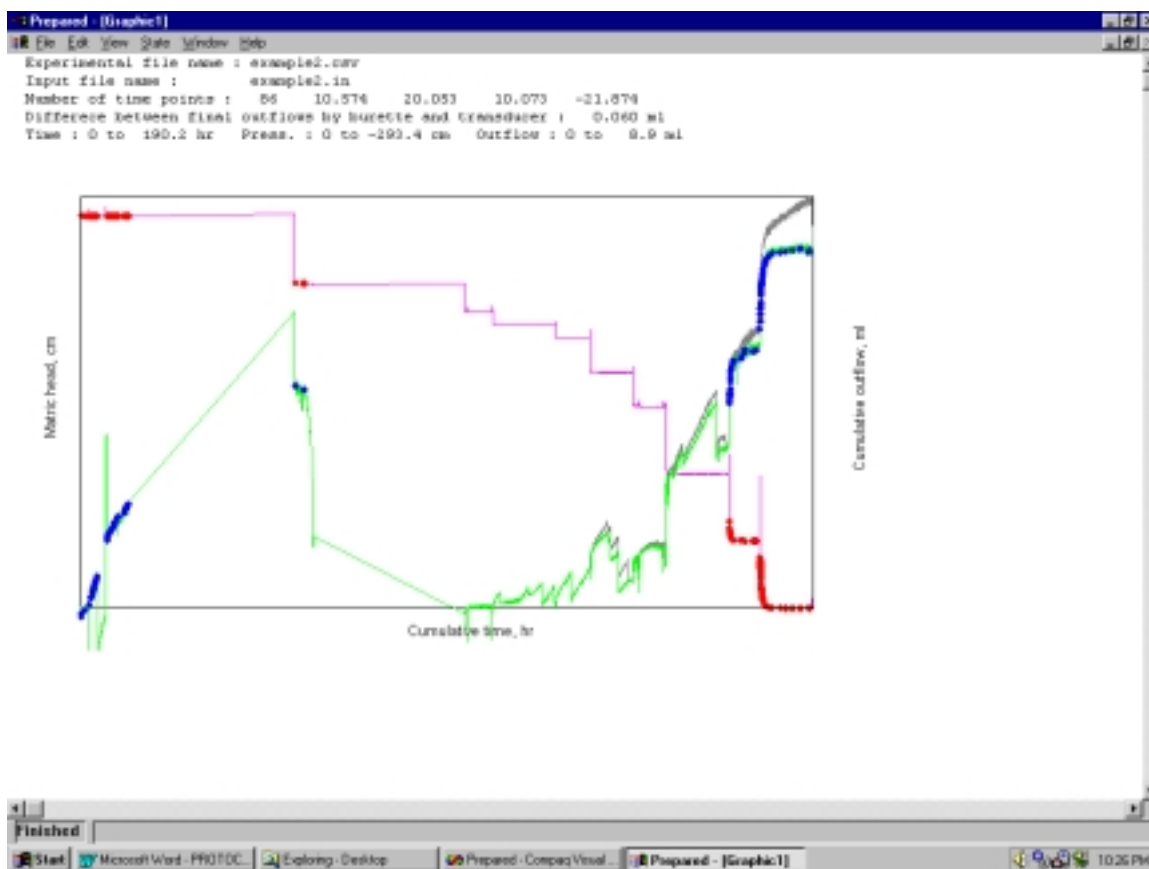


Figure 24. Graphical output window using original DATAPREP program on example2.csv.

Table 12. The lines that must be modified in the DATAPREP code.

```

      .
      .
      wtq=0.    ! Weighting factor of cumulative outflow Q-type data      (line 29)
      .
      .
! IF(Q1(N).GT.Q1(N+1)) GOTO 70                                           (line 193)
! IF(Q1(N).GT.Q1(N+2)) GOTO 70 ! If the current outflow is greater than
! IF(Q1(N).GT.Q1(N+3)) GOTO 70 ! outflows at the following five time
! IF(Q1(N).GT.Q1(N+4)) GOTO 70 ! steps, skip the current time step.
! IF(Q1(N).GT.Q1(N+5)) GOTO 70                                           (line 197)
      .
      .
! IF(Q1(N).LT.Q(M)-.25) GOTO 70                                           (line 207)

```

2. Recompile this version of the code. Be sure to close the graphical output window generated from the first model run or the compilation will result in an error message.
3. Send the data set through the DATAPREP code, but give the resulting optimization input file and graphical output file new names (i.e., “example2a.in” and “example2a.g”) since you will need both files (“example2.in” and “example2a.in”) for step 4. Figure 25 shows the new graphical output. Notice that 264 time points have been selected, whereas previously (Figure 24) only 86 time points were selected.

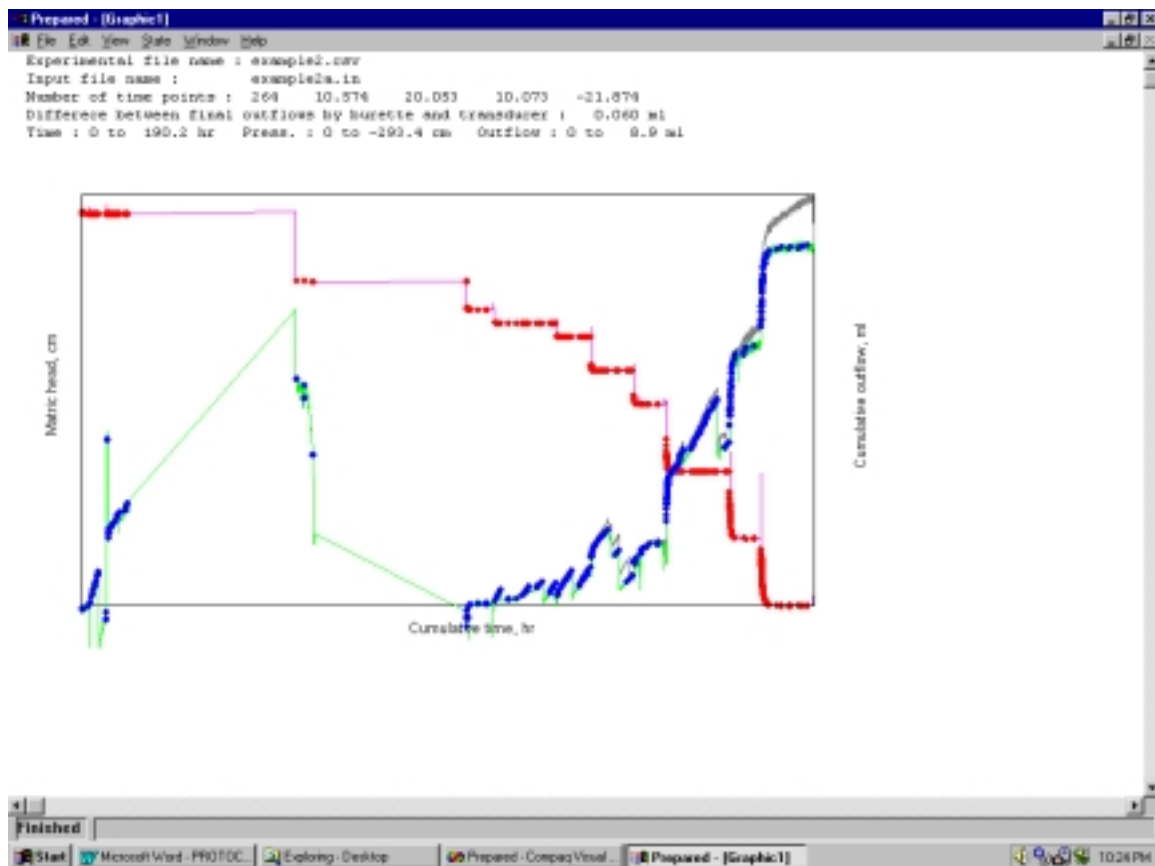


Figure 25. Graphical output windows using modified DATAPREP program on example2.csv.

4. Next, the two input files must be pieced together to provide the appropriately formatted input file for SFOPT. The time at which the two files will be assembled is just prior to the onset of the ninth pressure step of 250 mbars. The starting times for the pressure steps are declared at the end of the optimization input file (see Table 13).

Table 13. Excerpt from SF OPT input file for Example 2 showing the times at which pressure steps begin.

--- Pressure steps:	
--- Time (hr), Upper Nonwetting Pressure	
0.00	10.20
55.60	61.22
99.88	81.63
107.13	91.84
123.45	102.04
132.23	127.55
143.32	153.06
151.78	204.08
168.18	255.10
176.35	306.12

The 250 mbar (or 255.10 cm) step was applied at 168.18 hours. We want the information for the first 8 steps to come from the “example2a.in” input file, and the information from the last two steps to come from the “example2.in”. Thus,

- Delete the observation data points pertaining to the first 8 steps from the “example2.in” input file (Table 14).
- Copy the portion of the data listed in “example2a.in” (Table 15) from the beginning of the “observation data points” listing to the time just prior to 168.18 hours (i.e. 167.97).
- Paste this section into the “example2.in” file in place of the values deleted in step 4a (Table 16).

Now the file contains pairs for the first 8 pressure steps with outflow weighted at zero and the last two pressure steps with both data types weighted at 1.0.

Table 14. “Example2.in” input data file for SFOPT with a weight of 1.0 for outflow.

```

Example2.in
--- NCASES, nprint, nout, khall, nresul
    1      0      0      0      0
--- TITLE
Title
--- SAMPLE
Sample name
--- NN(total nodes), LNS(Soil nodes), DNUL, ZD(Z_obs), AIRP(Pres.step No), EPS1, EPS2
55 55 0.0010 3.7915 -10 1.0000 1.0000
--- SLL(Soil-L), PLL(Plate-L), IAM(Soil-Diam), CPLT(PlateKs)
7.583000 0.0000000E+00 4.329500 999.0000
--- NTOB(Time points),NTOA(Theta points),NTYPE,MDATA,MODE,MIT(Iter.limit)
    172      1      3      1      1      50
--- IEQ (1-van Genuchten model, 2-Lognormal model)
    1
--- Initial parameter guesses: alpha, n, thetar, thetas, Ks, l
0.0400 2.0000 0.1100 0.2370 5.0800 0.5000
--- Parameter free/fixed index (1-free, 0-fixed)
    1      1      1      0      1      0
--- Parameter limits:
--- Minimums:
0.0010 1.0100 0.0001 0.1000 0.0001 -15.0000
--- Maximums:
0.5000 10.0000 0.2070 0.9000 30.0000 15.0000
--- Ini. air pressure, Ini. outflow height:
10.20408 2.400000
--- RhoW, RhoNW (Rho:Fluid density; W:Wetting; NW:NonWetting)
1.000000 0.0000000E+00
--- Observation data points
--- Time (hr) Datatype, Obs_value, Obs_height, WT
    0.15      1      14.234      3.792      1.000
    0.15      2      -0.209      2.362      1.000
    0.20      1      14.504      3.792      1.000
    0.20      2      -0.118      2.379      1.000
      .
      .
      .
    57.97      1      65.229      3.792      1.000
    57.97      2      5.470      3.390      1.000
    168.35      1      244.001      3.792      1.000
    168.35      2      5.242      3.356      1.000
      .
      .
      .
    189.13      1      309.282      3.792      1.000
    189.13      2      8.954      4.238      1.000
    -11.60      3      0.237      10.000
--- Pressure steps:
--- Time (hr), Upper Nonwetting Pressure
    0.00      10.20
      .
      .
    176.35      306.12

```

Delete these data (step 4a) and replace with values copied in step 4b.

Table 15. “Example2a.in” input data file for SFOPT with zero weight for outflow.

```

Example2a.in
--- NCASES, nprint, nout, khall, nresul
      1      0      0      0      0
--- TITLE
Title
--- SAMPLE
Sample name
--- NN(total nodes), LNS(Soil nodes), DNUL, ZD(Z_obs), AIRP(Pres.step No), EPS1, EPS2
55 55 0.0010 3.7915 -10 1.0000 1.0000
--- SLL(Soil-L), PLL(Plate-L), IAM(Soil-Diam), CPLT(PlateKs)
7.583000 0.0000000E+00 4.329500 999.0000
--- NTOB(Time points),NTOA(Theta points),NTYPE,MDATA,MODE,MIT(Iter.limit)
      528      1      3      1      1      50
--- IEQ (1-van Genuchten model, 2-Lognormal model)
      1
--- Initial parameter guesses: alpha, n, thetar, thetas, Ks, l
0.0400 2.0000 0.1100 0.2370 5.0800 0.5000
--- Parameter free/fixed index (1-free, 0-fixed)
      1      1      1      0      1      0
--- Parameter limits:
--- Minimums:
0.0010 1.0100 0.0001 0.1000 0.0001 -15.0000
--- Maximums:
0.5000 10.0000 0.2070 0.9000 30.0000 15.0000
--- Ini. air pressure, Ini. outflow height:
10.20408 2.400000
--- RhoW, RhoNW (Rho:Fluid density; W:Wetting; NW:NonWetting)
1.000000 0.0000000E+00
--- Observation data points
--- Time (hr) Datatype, Obs_value, Obs_height, WT
0.03      1      12.957      3.792      1.000
0.03      2      -0.024      2.396      0.000
0.08      1      14.061      3.792      1.000
0.08      2      -0.090      2.384      0.000
0.22      1      14.602      3.792      1.000
0.22      2      -0.050      2.391      0.000
1.55      1      14.687      3.792      1.000
1.55      2      -0.004      2.399      0.000
.
.
167.97     1      208.392      3.792      1.000
167.97     2       4.104      3.146      0.000
168.22     1      223.976      3.792      1.000
168.22     2       4.519      3.224      0.000
.
.
188.42     1      309.368      3.792      1.000
188.42     2       9.038      4.246      0.000
-11.60     3       0.237      10.000
--- Pressure steps:
--- Time (hr), Upper Nonwetting Pressure
0.00      10.20
.
.
176.35     306.12

```

Copy these data
(step 4b) and
paste into
“example2.in”
(step 4c)

Table 16. “Example2.in” input data file after copying and pasting.

Example2.in						
--- NCASES, nprint, nout, khall, nresul						
1	0	0	0	0		
		.				
0.03	1	12.957	3.792	1.000	From "example2a.in"	
0.03	2	-0.024	2.396	0.000		
0.08	1	14.061	3.792	1.000		
0.08	2	-0.090	2.384	0.000		
0.22	1	14.602	3.792	1.000		
0.22	2	-0.050	2.391	0.000		
1.55	1	14.687	3.792	1.000		
1.55	2	-0.004	2.399	0.000		
		.				
167.97	1	208.392	3.792	1.000	From "example2a.in"	
167.97	2	4.104	3.146	0.000		
168.35	1	244.001	3.792	1.000		
168.35	2	5.242	3.356	1.000		
		.				
		.				
		.				
189.13	1	309.282	3.792	1.000	From "example2.in"	
189.13	2	8.954	4.238	1.000		
-11.60	3	0.237		10.000		
--- Pressure steps:						
--- Time (hr), Upper Nonwetting Pressure						
0.00	10.20					
		.				
		.				
176.35	306.12					

- Incorporate the hand written data of Table 17 into the “example2.in” input file by converting the known cumulative outflow and applied pressure in mbars to equivalent hydrostatic pressure and centimeters of pressure, respectively. The added data pairs correspond to the experimental times at which water flow is at hydraulic equilibrium, prior to increasing the applied air pressure.

Table 17. Experimental record for Example 2.

Tempe Cell #		1	2	3	4	5	6	7	8	9	10
Sample #		example 2									
Date & Time	mV & ml readings										
Pressure											
		Initial readings before pressure application									
2/2/99	T mV	-0.863									
0915 am	Q mV	2.075									
0 mbar	Q ml	20.0									
		INITIAL AIR PRESSURE 10 mbar on 2/2/99 0927 am									
0927 am	T mV	-1.086									
2/2/99	T mV	-1.372									
2130 pm	Q mV	2.218									
10 mbar	Q ml	22.0									
		NEW AIR PRESSURE 60 mbar on 2/4/99 1704 pm									
1710 pm	T mV	-1.323									
2/5/99	T mV	-1.426									
0806 am	Q mV	2.071									
60 mbar	Q ml	22.0									
		NEW AIR PRESSURE 80 mbar on 2/6/99 1320 pm									
1325 pm	T mV	-1.402									
2/6/99	T mV	-1.413									
2010pm	Q mV	2.092									
80 mbar	Q ml	21.0									
		NEW AIR PRESSURE 90 mbar on 2/6/99 2035 pm									
2040 pm	T mV	-1.3942									
2/7/99	T mV	-1.490									
1244 pm	Q mV	2.098									
90 mbar	Q ml	21.5									
		NEW AIR PRESSURE 100 mbar on 2/7/99 1255 pm									
0100 pm	T mV	-1.4069									
2/7/99	T mV	-1.413									
2131 pm	Q mV	2.143									
100 mbar	Q ml	21.5									
		NEW AIR PRESSURE 125 mbar on 2/7/99 2142 pm									
2148 pm	T mV	-1.3511									
2/8/99	T mV	-1.406									
0726 am	Q mV	2.146									
125 mbar	Q ml	22.0									
		AIR FLUSH 125 mbar on 2/8/99 0735 - 0743 am									
0750 am	Q mV	2.122									
	Q ml	22.0									
		NEW AIR PRESSURE 150 mbar on 2/8/99 0846 am									
0850 am	T mV	-1.0053									
2/8/99	T mV	-1.157									
1707 pm	Q mV	2.139									
150 mbar	Q ml	23.0									

- a. Convert the tensiometer transducer mV readings to pressure head in centimeters, using the slope and intercept of the tensiometer transducer. The slopes of tensiometer and outflow and the intercepts of tensiometer and outflow are listed on the third line in the graphical output window (Figure 24 and Figure 25). Multiply the mV by the slope and add the intercept to convert from mV to mbars, then subtract the applied pressure in mbars. Divide this amount by -0.98 to convert from mbars to cm. For example, the conversion for the 08:06 reading on 2/5/99 during the 60 mbar pressure is:

$$(-60\text{mbar} + 10.073 + 10.574 \cdot -1.426\text{mV}) / (-0.98) = \mathbf{66.33\text{ cm}}$$

- b. Convert the outflow to cm of hydrostatic pressure head by multiplying the number of mL's greater than the initial burette volume by 0.181, the number of centimeters per mL in the burette. For example, the 08:06 mL reading on 2/5/99 is 22.0 mL and the initial volume was 20.0 mL. Therefore, this conversion yields $(2.0)(0.181) = \mathbf{0.362\text{ cm}}$ associated with **2mL** cumulative outflow.
- c. Calculate the cumulative time at which to insert these values. Look at Table 13 and notice that the 60 mbar pressure started at 55.6 hours. In Table 17 notice that this corresponds to 17:04 on 2/4/99. Calculate the number of hours from 17:04 on 2/4/99 to 08:06 on 2/5/99 (15.03 hours) and add to the 55.6 hours to yield **70.63 hours**.
- d. Type the above values into "example2.in" and give both data types a weighting value of 1.0. The value from step 5a (**66.33 cm**) is in column 3 on the line corresponding to type 1 (pressure head) data. The values from step 5b are placed in columns 3 (**2.000**) and 4 (**0.362**) and are associated with type 2 (cumulative outflow) data. Table 18 shows the file before and after the inclusion of these values.

Don't worry that the pressure at 70.63 hours is greater than at 99.88 hours. It is normal for some noise to occur in the transducer readings. Also, don't worry that the observed value for outflow is so different from the observed values of the times before and after 70.63 hours. Remember, the reason we are going through these steps is because the outflow data recorded by the datalogger are meaningless. Hence, the outflow values before and after 70.63 hours have a weight of 0.0.

Table 18. Portion of "example2.in" input before and after insertion of the first handwritten value from the experimental record.

BEFORE				
--- Observation data points				
--- Time (hr) Datatype, Obs_value, Obs_height, WT				
		.		
		.		
59.97	1	65.439	3.792	1.000
59.97	2	3.786	3.085	0.000
99.88	1	65.253	3.792	1.000
99.88	2	-0.120	2.378	0.000
AFTER				
--- Observation data points				
--- Time (hr) Datatype, Obs_value, Obs_height, WT				
		.		
		.		
59.97	1	65.439	3.792	1.000
59.97	2	3.786	3.085	0.000
70.63	1	66.330	3.792	1.000
70.63	2	2.000	0.362	1.000
99.88	1	65.253	3.792	1.000
99.88	2	-0.120	2.378	0.000

← Insert values for
70.63 hours here

} Inserted values

The conversion for the other handwritten values from Table 17 are shown in columns 7, 8 and 9 of Table 19. Follow steps a-d to calculate these values.

- Count the number of observation data points that are now in the input file. Change the value of NTOB, on line 13 of the input file, to reflect the new number of data pairs. This number does not include the "air entry" value (NTOA), designated by type 3, that appears at the bottom of the observation data points listing.

Table 19. Converted handwritten values from experimental record.

Julian Day	Time	Applied Pressure (mbar)	Tensiometer transducer (mV)	Observed value (cm)	Outflow (mL)	Obs value (mL)	Observed height (cm)	Cumulative time (hours)
36	8:06	60	-1.426	66.332	22.0	2.0	0.362	70.63
37	20:10	80	-1.413	86.600	21.0	1.0	0.181	106.7
38	12:44	90	-1.49	97.635	21.5	1.5	0.272	123.28
38	21:31	100	-1.413	107.008	21.5	1.5	0.272	132.05
39	7:26	125	-1.406	132.443	22.0	2.0	0.362	141.96
39	17:07	150	-1.157	155.266	23.0	3.0	0.543	151.65
40	8:45	200	-1.358	208.456	25.0	5.0	0.905	167.28
40	17:40	250	-1.279	258.624	27.5	7.5	1.358	176.2
41	7:20	300	-1.252	309.353	29.0	9.0	1.629	190.05

6.5.2. Example 3.

In the occasion of a total loss of the electronic data record one must rely on the handwritten experimental record, such as that shown in Table 17. In such a case one must assume that the handwritten values are recorded at equilibrium. Since the transient data are unavailable there is not sufficient data for parameter estimation of the unsaturated hydraulic conductivity function; however, it is possible to obtain the soil water retention function parameters. If the unsaturated hydraulic conductivity prediction is desired, we suggest its estimation from either 1) substitution of retention function parameters into the Mualem (1976) model, or 2) neural networks (Schaap et al., 1998). For the estimation of the soil water retention parameters we suggest the use of the solver tool available in many spreadsheet programs (Wraith, et al., 1998).

7. PARAMETER ESTIMATION PROGRAM (SFOPT)

Several important issues that might be encountered while using SFOPT will be discussed in sections 7.1 and 7.2. Information on the initial estimates of parameters and variables are described in section 7.3. The variable descriptions of the input file will be explained in section 7.4. Following, 3 examples input and output files will be introduced for the user's convenience (section 7.5). One must note that these examples are independent of previous examples given in section 6.3.1. However, the user can refer to these examples to evaluate their own experimental data.

7.1. Description and features of the SFOPT

As mentioned in section 2.1, SFOPT (Chen et al. 1997) is a new version of MLSTPM (Eching and Hopmans, 1993b). In the presented modified version (SFOPT), the basic data and program structure were not changed from the MLSTPM code (Eching and Hopmans, 1993b). However, the described optimization model includes the following new features and modifications:

- A time dependent lower boundary condition was implemented. In MLSTPM, a constant head lower boundary condition was assumed. SFOPT allows a time-dependent head as the lower boundary condition, represented by changes in the burette reading as measured automatically by the pressure transducer.
- The optimization weighting factor calculation allows for the weighting factors to be inversely proportional to the magnitude of the data type.
- Provision of a self-explanatory input file format. The explanation lines have been added in order to increase the readability of the input file. An additional output file has been added to allow simple plotting of cumulative outflow volume and capillary pressure with time.
- Current outflow experiments make use of a thin porous nylon membrane, instead of a ceramic plate. For this new experimental procedure, the user can simply set the plate thickness (PLL) to zero. In that case, CPLT (saturated conductivity of porous membrane) is not used (section 7.4).

- We added the lognormal model to characterize retention and conductivity functions (Kosugi, 1996), in addition to the van Genuchten model as an option. The lognormal model is physically-based, and optimization results have been equally successful.

Although the DATAPREP program prepares an input file for the SFLOPT, one must make sure that the input file is correct. Input file includes the capillary pressure (positive) values instead of matric pressure head values (negative). This is just for computational conveniences in the program. Changes in the input file may be needed to obtain acceptable results. You may need to change the parameter-limits, the initial parameter estimates, or adjust the data-type weighting factors. A proper choice of the parametric model for soil water retention and conductivity function may also be needed.

The SFLOPT produces two output files. The first file includes all the optimization results and optimized parameters. The second file is for graphing purposes only, e.g. to visualize the agreement between observed and optimized cumulative outflow and matric head values. This file can be transferred to a spreadsheet program to do so. The user is free to give any name to these output files that are asked at the beginning of the SFLOPT run. One should notice that matric head values are really capillary pressure, thus they are positive per definition.

7.2. Troubleshooting

The original MLSTPM code (Eching and Hopmans, 1993b) occasionally produced erroneous simulation results with abrupt changes in computed cumulative outflow and matric head values. In most of such cases, the output file warned that "NO. OF STEPS EXCEEDS 1000 AT TIME= ??? DURING ITERATION ???". In SFLOPT, NSTEPS was set to 10000 (Line 661 in Appendix C) to fix this problem. The original NSTEPS value was 1000. However, if a similar error occurs despite this change in the code, we propose the following two ad hoc changes to the code:

- a) set EPS2 (the iteration weighing coefficient) to 0.0 (the default EPS2 value is 1.0)
- b) make line 903 in Appendix C "FC(I)=0.5*(CUMQ1+CUMQ0)" active.

Moreover, we determined that the maximum time step allowed was too large for coarse textured soils. If a large mass balance error is encountered, or large deviation between optimized and measured cumulative outflow or matric pressure occur in the output file, one may reduce the DELMAX variable (line 661 in Appendix C) from 0.5 to 0.05. In

some cases, one can also change the $DELMIN=0.005*DNUL$ to smaller values (such as $DELMIN=0.001*DNUL$), which is in DETERMINE AMOUNT OF WATER IN SAMPLE section of the subroutine FLOW (line 751 in Appendix C).

Since the DATAPREP program prepares the input file for SPOPT, the user is flexible in choosing the number of data pairs. If the number of data pairs is larger than 500, then SPOPT gives an error message and stops running, because the SPOPT processes only 500 data pairs by default. In that case one must change the parameter “NO” accordingly in the SFOPT program (Lines 19, 650, and 1134 in Appendix C). However, one should note that optimization time can become exceedingly high when a large number of data pairs are used. We recommend no more than 200-300 data pairs.

7.3. Initial estimates of parameters

The unknown parameters (elements of vector **b** in the objective function) are optimized by numerical inversion using soil water matric head and cumulative volume outflow as a function of time in the objective function. Although the hydraulic conductivity of the ceramic plate and other known parameters, such as θ_s are fixed to known values, the hydraulic conductivity of the nylon membrane is fixed to 999, indicating that the membrane hydraulic conductivity is much higher than the soil itself. To test uniqueness, each inversion problem is run on the computer three times using different initial estimates of parameters. Initial parameter values are chosen as a combination of low, medium, and high values within their range of possible values. An example of initially chosen parameter values, in our study, for each case, is given in Table 20. These initial estimates were used for both models in the examples of section 6 and 7. One should refer to Hopmans et al. (2002) for more detailed description of the recommended optimization procedures.

Table 20. Initial estimates of parameters used in optimization.

Parameters for Van Genuchten's models						
Case & Range	α	n	θ_r	θ_s	K_s	l
Low	0.004 ^v	1.01 ^v	0.055 ^v	0.414 ^f	0.07 ^v	0.5 ^f
Medium	0.02 ^v	2.0 ^v	0.11 ^v	0.414 ^f	0.07 ^v	0.5 ^f
High	0.04 ^v	4.0 ^v	0.22 ^v	0.414 ^f	0.07 ^v	0.5 ^f
Range	0.001-0.5	1.0-10	0.0-0.3	0.0-0.7	0.0001-1000	-15.0-15.0
Parameters for Lognormal models						
Case & Range	$Logh_m$	σ	θ_r	θ_s	K_s	l
Low	1.6 ^v	1.0 ^v	0.015 ^v	0.414 ^f	0.07 ^v	0.5 ^f
Medium	2.0 ^v	2.0 ^v	0.15 ^v	0.414 ^f	0.07 ^v	0.5 ^f
High	3.0 ^v	3.0 ^v	0.30 ^v	0.414 ^f	0.07 ^v	0.5 ^f
Range	0.0-10.0	0.1-10	0.0-0.44	0.1-0.9	0.0001-1000	-15.0-15.0

f: fixed; v: variable

7.4. Description of variables of input file

The variable descriptions are mostly same as listed by S.O. Eching and J.W. Hopmans (1993b). The newly introduced variables are denoted by the '*' notation.

Line	Variable	Description
1		Comment line
2	NCASES	Number of cases considered
	NPRINT	Number of times $h(z)$ and $\theta(z)$ are printed in DISTP.DAT
		Blank = do not print
	NOUT	Observations: 0 = print in output file 1 = do not print in output file
	KHALL	Option to fix the retention curve and optimize α , n , K_s , and/or I of the conductivity function 0 = simultaneous optimization of $\theta(h)$ and $K(h)$
	NRESUL	1 = Print the simulated data in OBSERV.DAT Blank = do not print
4	TITLE	Title of the problem
6	SAMPLE	Sample number or name
8	NN	Total number of nodes
	LNS	Number of nodes in soil (LNS = NN if PLL ≈ 0 , as for nylon porous membrane instead of ceramic plate)
	DNUL	Initial time step (h)
	ZD*	Distance from soil core surface to soil water pressure measurement position (cm, >0)
	AIRP	Positive: One step method \rightarrow value of pneumatic pressure used (cm of water) Negative: Multi step method \rightarrow number of pressure steps
	EPS1	Temporal weighting coefficient
	EPS2	Iteration weighting coefficient
10	SLL	Length of soil core (cm, >0)
	PLL	Thickness of porous plate (cm, >0)
	DIAM	Diameter of soil core (cm)
	CPLT	Saturated conductivity of porous plate (cm/h, not used if LNS=NN)
12	NTOB	Number of capillary pressure and/or cumulative outflow observations with time (used in line 30)
	NTOA	Number of soil water retention points in objective function
	NTYPE	Number of data types (1,2 or 3)
	MDATA	Observed data from: 1 = transient flow data only
	MODE	Mode for type of calculation: 0 = flow equation is solved for initial parameter values 1 = optimization is continued until parameter values converge or number of iteration reaches MIT; all intermediate parameter values are printed
	MIT	Maximum number of iteration in optimization routine
14	IEQ*	Index for retention and conductivity model option: 1 = van Genuchten model (VG) 2 = Lognormal model (LN)
16	B(1)	Initial value of parameter α (VG) or $^{10}\log h_m$ (LN)
	B(2)	Initial value of parameter n (VG) or σ (LN)
	B(3)	Initial value of parameter θ_r
	B(4)	Initial value of parameter θ_s
	B(5)	Initial value of parameter K_s (cm/h)
	B(6)	Initial value of parameter I
18	INDEX(I)	Index indicating a parameter is fixed or it is to be optimized: 0 = parameter B(I) is known and is kept constant 1 = parameter B(I) is unknown and will be optimized
21	BMIN(I)	Minimum parameter value for range to be optimized
23	BMAX(I)	Maximum parameter values for range to be optimized
25	ZX*	Initial applied air pressure (cm of water equivalent, >0)
	HO0*	Initial height of water in burette, relative to bottom of porous membrane (cm)
27	RhoW*	Wetting fluid density (1.0 for water)
	RhoNW*	Nonwetting fluid density (0.0 for air)
30 ..	TIME(I)	Observation time (hour)
	Datatype	1 (Capillary pressure), 2 (Cumulative outflow)
	Observation	Capillary pressure head h_c (cm), or cumulative outflow (Q , $\text{cm}^3 = \text{ml}$) at time I
	HO(I)*	ZD*(line 8) for datatype 1, or height (cm) of water in burette, relative to bottom of porous membrane at time I (datatype 2)
	WT(I)	Weight factor for observation I
..	$I = 1, 2, \dots$, (NTOB) lines	
	For each of the following NTOA lines	
	h	Soil water pressure head (<0, cm)
	Datatype	3, and
	θ	Corresponding water content of soil core (each pair corresponds with independently measured soil water retention point)
	WT	Weight factor for each independent soil water retention point
End...	TPRESS(J)	Times at which pressures are changed (h , since start of experiment)
	PRESSU(J)	Applied pneumatic pressure (cm of water)
...	$J = 1, 2, \dots$, AIRP lines	

7.5. Example Problems

In this section, we have included 3 examples. Example 1 is identical to the first example in Eching and Hopmans (1993b), which corresponds to data obtained with a ceramic plate and optimized using the van Genuchten model (Eqs [3]-[5]). However, because of changes made in the program the optimized results are slightly different. Furthermore, Examples 2 and 3 correspond to data obtained using a low impedance nylon membrane with an assumed zero thickness, using the lognormal (Eqs. [6]-[10]; example 2) and van Genuchten model (example 3), respectively.

7.5.1. Example 1: Multi-step outflow, van Genuchten model, ceramic plate

Input File

```

--- NCASES,nprint,nout,khall,nresul
    1      0      0      0      0
--- TITLE
EXAMPLE
--- SAMPLE
YOLO
--- NN(Total nodes),LNS(Soil nodes),DNUL,ZD(Z_obs),AIRP(Pres.step No.),EPS1,EPS2
    48      43      1.00E-03      3.08      -6      1      1
--- SLL(Soil-L), PLL(Plate-L), DIAM(Soil-Diam), CPLT(PlateKs)
    6      0.58      8.25      0.00722
--- NTOB(hc&Q points), NTOA(theta points), NTYPE, MDATA, MODE, MIT(Iter.limit)
    88      1      3      1      1      50
--- IEQ (1-van Genuchten model, 2-Lognormal model)
    1
--- Initial parameter guesses: alpha, n, thetar, thetas, Ks, l
    0.015      2      0.15      0.558      1.55      0.5
--- Parameter free/fixed index (1-free, 0-fixed)
    1      1      1      0      1      0
--- Parameter limits:
--- Minimums:
    0.001      1.00      0.00001      0.10      0.0001      -15.00
--- Maximums:
    0.5      10.00      0.45      0.90      100.00      15.00
--- Ini. air pressure, Ini.outflow height:
    31.0      3.58
--- RhoW, RhoNW (Rho:Fluid density; W:Wetting; NW:Nonwetting)
    1      0
--- Observation data points:
--- Time (hr), Datatype, Obs_value, Obs_height, WT
    0.183      1      35.200      3.080      1.0
    0.183      2      0.500      3.580      1.0
    0.533      1      36.500      3.080      1.0
    0.533      2      1.100      3.580      1.0
    0.933      1      37.000      3.080      1.0
    0.933      2      1.600      3.580      1.0
    1.117      1      37.200      3.080      1.0
    1.117      2      1.800      3.580      1.0
    1.450      1      43.800      3.080      1.0
    1.450      2      5.000      3.580      1.0
    1.783      1      47.000      3.080      1.0
    1.783      2      8.000      3.580      1.0

```

2.433	1	51.100	3.080	1.0
2.433	2	11.800	3.580	1.0
2.983	1	53.500	3.080	1.0
2.983	2	14.000	3.580	1.0
4.267	1	56.600	3.080	1.0
4.267	2	17.000	3.580	1.0
5.733	1	58.000	3.080	1.0
5.733	2	19.000	3.580	1.0
6.267	1	66.500	3.080	1.0
6.267	2	22.000	3.580	1.0
7.033	1	70.500	3.080	1.0
7.033	2	25.000	3.580	1.0
8.600	1	74.700	3.080	1.0
8.600	2	28.000	3.580	1.0
9.767	1	76.200	3.080	1.0
9.767	2	29.400	3.580	1.0
11.350	1	77.300	3.080	1.0
11.350	2	30.400	3.580	1.0
13.150	1	78.000	3.080	1.0
13.150	2	31.000	3.580	1.0
15.000	1	79.300	3.080	1.0
15.000	2	32.800	3.580	1.0
15.217	1	89.800	3.080	1.0
15.217	2	35.000	3.580	1.0
15.550	1	102.600	3.080	1.0
15.550	2	38.000	3.580	1.0
15.917	1	108.900	3.080	1.0
15.917	2	40.000	3.580	1.0
16.633	1	118.800	3.080	1.0
16.633	2	43.000	3.580	1.0
17.383	1	128.000	3.080	1.0
17.383	2	45.000	3.580	1.0
18.300	1	138.600	3.080	1.0
18.300	2	47.000	3.580	1.0
19.867	1	152.700	3.080	1.0
19.867	2	49.000	3.580	1.0
22.083	1	166.500	3.080	1.0
22.083	2	51.000	3.580	1.0
24.050	1	175.000	3.080	1.0
24.050	2	52.000	3.580	1.0
26.550	1	182.500	3.080	1.0
26.550	2	52.800	3.580	1.0
38.750	1	195.400	3.080	1.0
38.750	2	54.300	3.580	1.0
39.200	1	203.700	3.080	1.0
39.200	2	56.000	3.580	1.0
40.000	1	216.800	3.080	1.0
40.000	2	56.800	3.580	1.0
41.750	1	235.000	3.080	1.0
41.750	2	58.200	3.580	1.0
43.850	1	251.600	3.080	1.0
43.850	2	59.300	3.580	1.0
46.350	1	268.200	3.080	1.0
46.350	2	60.200	3.580	1.0
51.117	1	293.300	3.080	1.0
51.117	2	61.700	3.580	1.0
64.533	1	336.700	3.080	1.0
64.533	2	64.000	3.580	1.0
65.700	1	346.000	3.080	1.0
65.700	2	67.000	3.580	1.0
71.417	1	386.400	3.080	1.0
71.417	2	68.000	3.580	1.0
76.250	1	411.500	3.080	1.0
76.250	2	69.000	3.580	1.0
88.317	1	467.300	3.080	1.0

88.317	2	69.800	3.580	1.0
94.650	1	484.700	3.080	1.0
94.650	2	70.000	3.580	1.0
109.733	1	526.000	3.080	1.0
109.733	2	72.400	3.580	1.0
119.267	1	549.400	3.080	1.0
119.267	2	72.900	3.580	1.0
139.683	1	588.100	3.080	1.0
139.683	2	73.600	3.580	1.0
142.417	1	613.300	3.080	1.0
142.417	2	74.400	3.580	1.0
-31.000	3	0.458		10.0

--- Pressure steps:
--- Time(hr), Upper Nonwetting Pressure

0.000	40.00
1.150	60.00
5.767	80.00
15.133	200.00
38.833	400.00
64.583	700.00

Output file

```

1 *****
*
*EXAMPLE
*          SAMPLE  YOLO
*
*****

PROGRAM PARAMETERS
=====
NUMBER OF NODES.....(NN)..... 48
NODE AT SOIL-PLATE BOUNDARY.....(LNS)..... 43
INITIAL TIME STEP.....(DNUL)..... .10E-02
PNEUMATIC PRESSURE.....(AIRP)..... -6.000
TEMPORAL WEIGHTING COEFF.....(EPS1)..... 1.00
ITERATION WEIGHTING COEFF.....(EPS2)..... 1.00
MAX. ITERATIONS.....(MIT)..... 50
DATA MODE.....(MDATA)..... 1
NO. OF OBSERVATIONS.....(NOBB)..... 89

SOIL AND PLATE PROPERTIES
=====
SOIL COLUMN LENGTH.....(SLL)..... 6.000
COLUMN DIAMETER.....(DIAM)..... 8.250
THICKNESS OF PLATE.....(PLL)..... .580
PLATE CONDUCTIVITY.....(CONDS(2))..... .7220E-02
SATURATED MOISTURE CONTENT.....(WCS)..... .558
RESIDUAL MOISTURE CONTENT.....(WCR)..... .150
FIRST COEFFICIENT.....(ALPHA)..... .015
SECOND COEFFICIENT.....(N)..... 2.000
SATURATED CONDUCTIVITY SOIL.....(CONDS(1))..... .1550E+01
EXPONENT L MUALEM-GENUCHTEN.....(EXPL)..... .500

OBSERVED DATA
=====
OBS      HRS      Data      Data-type
1        .1830     35.2000        1
2        .1830      5.0000        2
3        .5330    36.5000        1
4        .5330     1.1000        2
5        .9330    37.0000        1
6        .9330     1.6000        2
7        1.1170    37.2000        1
8        1.1170     1.8000        2

```

9	1.4500	43.8000	1
10	1.4500	5.0000	2

79	94.6500	484.7000	1
80	94.6500	70.0000	2
81	109.7330	526.0000	1
82	109.7330	72.4000	2
83	119.2670	549.4000	1
84	119.2670	72.9000	2
85	139.6830	588.1000	1
86	139.6830	73.6000	2
87	142.4170	613.3000	1
88	142.4170	74.4000	2
89	-31.0000	.4580	3

INITIAL CAPILLARY PRESSURE HEAD AT TOP OF SAMPLE : 34.0

6 STEPS IN PNEUMATIC PRESSURE :
TIME PRESSURE

.00	40.0
1.15	60.0
5.77	80.0
15.13	200.0
38.83	400.0
64.58	700.0

ITERATION NO	SSQ	ALPHA	N	WCR	CONDS
1	.9223D+01	.0244	1.4130	.1688	1.9289
2	.5185D+01	.0398	1.5697	.1941	4.3536
3	.1231D+01	.0352	1.5864	.1597	4.8155
4	.1199D+01	.0358	1.5888	.1610	4.9946
5	.1199D+01	.0358	1.5888	.1610	4.9946

MASS BALANCE ERROR IN FE SOLUTION DURING FINAL RUN WAS 1.5359 %

RSQUARE FOR REGRESSION OF PREDICTED VS OBSERVED = .99993

CORRELATION MATRIX

=====

	1	2	3	4
1	1.0000			
2	-.4444	1.0000		
3	-.4939	.9340	1.0000	
4	.5125	.4889	.3758	1.0000

NON-LINEAR LEAST-SQUARES ANALYSIS: FINAL RESULTS

=====

VARIABLE	VALUE	S.E.COEFF.	95% CONFIDENCE LIMITS	
			LOWER	UPPER
ALPHA	.03578	.0005	.0348	.0367
N	1.58881	.0132	1.5626	1.6151
WCR	.16101	.0044	.1523	.1697
CONDS	4.99463	.2245	4.5483	5.4410

OBSERVED & FITTED			DATA		RESI-
NO	TIME (HR)	Z	OBS	FITTED	DUAL
1	.183	3.080	35.200	31.807	3.393
2	.183	3.080	.500	.927	-.427
3	.533	3.080	36.500	33.672	2.828
4	.533	3.080	1.100	2.658	-1.558
5	.933	3.080	37.000	35.027	1.973

6	.933	3.080	1.600	3.845	-2.245
7	1.117	3.080	37.200	35.553	1.647
8	1.117	3.080	1.800	4.303	-2.503
9	1.450	3.080	43.800	39.618	4.182
10	1.450	3.080	5.000	7.985	-2.985

79	94.650	3.080	484.700	488.560	-3.860
80	94.650	3.080	70.000	70.827	-.827
81	109.733	3.080	526.000	533.606	-7.606
82	109.733	3.080	72.400	71.861	.539
83	119.267	3.080	549.400	556.442	-7.042
84	119.267	3.080	72.900	72.335	.565
85	139.683	3.080	588.100	594.571	-6.471
86	139.683	3.080	73.600	73.065	.535
87	142.417	3.080	613.300	598.776	14.524
88	142.417	3.080	74.400	73.141	1.259
89	-31.000	3.080	.458	.458	.000

7.5.2. Example 2: Multi-step outflow, lognormal model, nylon membrane

Input file

```

--- NCASES,nprint,nout,khall,nresul
    1      0      0      0      0
--- TITLE
Example 2
--- SAMPLE
Sample
--- NN(Total nodes),LNS(Soil nodes),DNUL,ZD(Z_obs),AIRP(Pres.step No.),EPS1,EPS2
    55      55      0.0010      3.0000      -4      1.000      1.000
--- SLL(Soil-L), PLL(Plate-L), DIAM(Soil-Diam), CPLT(PlateKs)
    6.00      0.00      8.25      999.000
--- NTOB(hc&Q points), NTOA(theta points), NTYPE, MDATA, MODE, MIT(Iter.limit)
    254      1      3      1      1      50
--- IEQ (1-van Genuchten model, 2-Lognormal model)
    2
--- Initial parameter guesses: LOG10hm, sigma, thetar, thetas, Ks, l
    2.0      2.0      0.15      0.4411      5.0      0.50
--- Parameter free/fixed index (1-free, 0-fixed)
    1      1      1      0      1      0
--- Parameter limits:
--- Minimums:
    0.001      0.10      0.00001      0.10      0.0001      -15.00
--- Maximums:
    10.00      10.00      0.4411      0.90      100.00      15.00
--- Ini. air pressure, Ini.outflow height:
    20.408      1.40
--- RhoW, RhoNW (Rho:Fluid density; W:Wetting; NW:Nonwetting)
    1.0      0.0
--- Observation data points:
--- Time (hr) Datatype, Obs_value, Obs_height, WT
    .051      1      32.958      3.000      1.00
    .051      2      9.340      3.090      1.00
    .067      1      35.674      3.000      1.00
    .067      2      11.461      3.474      1.00
    .084      1      39.132      3.000      1.00
    .084      2      12.998      3.753      1.00
    .101      1      42.925      3.000      1.00
    .101      2      14.058      3.945      1.00

```

```

-----
-----
185.634      1      562.355      3.000      1.00
185.634      2      55.204      11.508      1.00
187.801      1      565.066      3.000      1.00
187.801      2      55.300      11.545      1.00
189.884      1      567.524      3.000      1.00
189.884      2      55.470      11.595      1.00
-22.008      3      0.441      10.00
--- Pressure steps:
--- Time(hr), Upper Nonwetting Pressure
4.557292E-04      102.040800
12.417120      204.081600
48.117120      408.163300
105.917100      714.285700

```

Output file

```

1 *****
*
*Example 2
*
*          SAMPLE  Sampl
*
*****

PROGRAM PARAMETERS
=====
NUMBER OF NODES.....(NN)..... 55
NODE AT SOIL-PLATE BOUNDARY.....(LNS)..... 55
INITIAL TIME STEP.....(DNUL)..... .10E-02
PNEUMATIC PRESSURE.....(AIRP)..... -4.000
TEMPORAL WEIGHTING COEFF.....(EPS1)..... 1.00
ITERATION WEIGHTING COEFF.....(EPS2)..... 1.00
MAX. ITERATIONS.....(MIT)..... 50
DATA MODE.....(MDATA)..... 1
NO. OF OBSERVATIONS.....(NOBB).....255

SOIL AND PLATE PROPERTIES
=====
SOIL COLUMN LENGTH.....(SLL)..... 6.000
COLUMN DIAMETER.....(DIAM)..... 8.250
THICKNESS OF PLATE.....(PLL)..... .000
PLATE CONDUCTIVITY.....(CONDS(2))..... .9990E+03
SATURATED MOISTURE CONTENT.....(WCS)..... .441
RESIDUAL MOISTURE CONTENT.....(WCR)..... .150
FIRST COEFFICIENT.....(LOG10hm)..... 2.000
SECOND COEFFICIENT.....(sigma)..... 2.000
SATURATED CONDUCTIVITY SOIL.....(CONDS(1))..... .5000E+01
EXPONENT L MUALEM-GENUCHTEN.....(EXPL)..... .500

OBSERVED DATA
=====
OBS      HRS      Data      Data-type
1      .0510      32.9580      1
2      .0510      9.3400      2
3      .0670      35.6740      1
4      .0670      11.4610      2
5      .0840      39.1320      1
6      .0840      12.9980      2
7      .1010      42.9250      1
8      .1010      14.0580      2
9      .1170      46.5850      1
10     .1170      14.9770      2

```

```

-----
-----
250 185.6340    55.2040        2
251 187.8010    565.0660       1
252 187.8010    55.3000        2
253 189.8840    567.5240       1
254 189.8840    55.4700        2
255 -22.0080      .4410         3

```

INITIAL CAPILLARY PRESSURE HEAD AT TOP OF SAMPLE : 24.2

4 STEPS IN PNEUMATIC PRESSURE :
TIME PRESSURE

```

.00    102.0
12.42   204.1
48.12   408.2
105.92  714.3

```

ITERATION NO	SSQ	LOG10hm	sigma	WCR	CONDS
1	.4303D+01	2.0230	1.8767	.1601	4.6844
2	.3899D+01	2.0180	1.7825	.1698	3.7507
3	.3528D+01	2.0121	1.6922	.1805	3.0183
4	.3167D+01	2.0071	1.6062	.1906	2.5303
5	.2833D+01	2.0038	1.5271	.1999	2.1953
6	.2544D+01	2.0026	1.4569	.2080	1.9588
7	.2311D+01	2.0036	1.3967	.2148	1.7834
8	.2137D+01	2.0062	1.3470	.2203	1.6496
9	.2014D+01	2.0102	1.3066	.2247	1.5392
10	.1952D+01	2.0429	1.1831	.2370	.9445
11	.1797D+01	2.0540	1.1528	.2389	.9696
12	.1793D+01	2.0492	1.1634	.2381	1.0216
13	.1793D+01	2.0493	1.1633	.2381	1.0219

MASS BALANCE ERROR IN FE SOLUTION DURING FINAL RUN WAS .3789 %

RSQUARE FOR REGRESSION OF PREDICTED VS OBSERVED = .99988

CORRELATION MATRIX

```

=====
          1          2          3          4
1    1.0000
2    -.5706    1.0000
3     .2502    -.8657    1.0000
4    -.9736     .5623    -.2482    1.0000

```

NON-LINEAR LEAST-SQUARES ANALYSIS: FINAL RESULTS

```

=====
VARIABLE      VALUE      S.E.COEFF.      95% CONFIDENCE LIMITS
                LOWER      UPPER
LOG10hm        2.04928        .0097      2.0302      2.0683
sigma          1.16332        .0200      1.1240      1.2027
WCR             .23814        .0019      .2343      .2419
CONDS          1.02187        .0940      .8368      1.2070

```

```

-----OBSERVED & FITTED      DATA      -----
NO  TIME (HR)      Z      OBS      FITTED      RESI-
                                DUAL
1    .051      3.000      32.958      38.512      -5.554
2    .051      3.000      9.340      8.218      1.122
3    .067      3.000      35.674      41.986      -6.312
4    .067      3.000      11.461      9.422      2.039
5    .084      3.000      39.132      45.185      -6.053

```

6	.084	3.000	12.998	10.470	2.528
7	.101	3.000	42.925	47.999	-5.074
8	.101	3.000	14.058	11.370	2.688
9	.117	3.000	46.585	50.420	-3.835
10	.117	3.000	14.977	12.132	2.845

250	185.634	3.000	55.204	54.172	1.032
251	187.801	3.000	565.066	554.332	10.734
252	187.801	3.000	55.300	54.206	1.094
253	189.884	3.000	567.524	556.639	10.885
254	189.884	3.000	55.470	54.238	1.232
255	-22.008	3.000	.441	.425	.016

7.5.3. Example 3: Multi-step outflow, van Genuchten model, nylon membrane

Input file

```

--- NCASES,nprint,nout,khall,nresul
    1      0      0      0      0
--- TITLE
Example 3
--- SAMPLE
Sample
--- NN(Total nodes),LNS(Soil nodes),DNUL,ZD(Z_obs),AIRP(Pres.step No.),EPS1,EPS2
    55      55      0.0010      3.0000      -4      1.000      1.000
--- SLL(Soil-L), PLL(Plate-L), DIAM(Soil-Diam), CPLT(PlateKs)
    6.00      0.00      8.25      999.000
--- NTOB(hc&Q points), NTOA(theta points), NTYPE, MDATA, MODE, MIT(Iter.limit)
    254      1      3      1      1      50
--- IEQ (1-van Genuchten model, 2-Lognormal model)
    1
--- Initial parameter guesses: alpha, n, thetar, thetas, Ks, l
    0.04      2.0      0.15      0.4411      5.0      0.50
--- Parameter free/fixed index (1-free, 0-fixed)
    1      1      1      0      1      0
--- Parameter limits:
--- Minimums:
    0.001      1.00      0.00001      0.10      0.0001      -15.00
--- Maximums:
    0.5      10.00      0.4411      0.90      100.00      15.00
--- Ini. air pressure, Ini.outflow height:
    20.408      1.40
--- RhoW, RhoNW (Rho:Fluid density; W:Wetting; NW:Nonwetting)
    1.0      0.0
--- Observation data points:
--- Time (hr) Datatype, Obs_value, Obs_height, WT
    .051      1      32.958      3.000      1.00
    .051      2      9.340      3.090      1.00
    .067      1      35.674      3.000      1.00
    .067      2      11.461      3.474      1.00
    .084      1      39.132      3.000      1.00
    .084      2      12.998      3.753      1.00
    .101      1      42.925      3.000      1.00
    .101      2      14.058      3.945      1.00

-----
-----

185.634      1      562.355      3.000      1.00

```

185.634	2	55.204	11.508	1.00
187.801	1	565.066	3.000	1.00
187.801	2	55.300	11.545	1.00
189.884	1	567.524	3.000	1.00
189.884	2	55.470	11.595	1.00
-22.008	3	0.441		10.00

--- Pressure steps:
--- Time(hr), Upper Nonwetting Pressure

4.557292E-04	102.040800
12.417120	204.081600
48.117120	408.163300
105.917100	714.285700

Output file

```

1 *****
*
*Example 3
*
*          SAMPLE  Sampl
*
*****

PROGRAM PARAMETERS
=====
NUMBER OF NODES.....(NN)..... 55
NODE AT SOIL-PLATE BOUNDARY.....(LNS)..... 55
INITIAL TIME STEP.....(DNUL)..... .10E-02
PNEUMATIC PRESSURE.....(AIRP)..... -4.000
TEMPORAL WEIGHTING COEFF.....(EPS1)..... 1.00
ITERATION WEIGHTING COEFF.....(EPS2)..... 1.00
MAX. ITERATIONS.....(MIT)..... 50
DATA MODE.....(MDATA)..... 1
NO. OF OBSERVATIONS.....(NOBB).....255

SOIL AND PLATE PROPERTIES
=====
SOIL COLUMN LENGTH.....(SLL)..... 6.000
COLUMN DIAMETER.....(DIAM)..... 8.250
THICKNESS OF PLATE.....(PLL)..... .000
PLATE CONDUCTIVITY.....(CONDS(2))..... .9990E+03
SATURATED MOISTURE CONTENT.....(WCS)..... .441
RESIDUAL MOISTURE CONTENT.....(WCR)..... .150
FIRST COEFFICIENT.....(ALPHA)..... .040
SECOND COEFFICIENT.....(N)..... 2.000
SATURATED CONDUCTIVITY SOIL.....(CONDS(1))..... .5000E+01
EXPONENT L MUALEM-GENUCHTEN.....(EXPL)..... .500

OBSERVED DATA
=====
OBS      HRS      Data      Data-type
1         .0510      32.9580          1
2         .0510       9.3400          2
3         .0670      35.6740          1
4         .0670      11.4610          2
5         .0840      39.1320          1
6         .0840      12.9980          2
7         .1010      42.9250          1
8         .1010      14.0580          2
9         .1170      46.5850          1
10        .1170      14.9770          2

-----
-----

247  183.4670   559.7910          1
248  183.4670    55.0950          2
249  185.6340   562.3550          1

```

250	185.6340	55.2040	2
251	187.8010	565.0660	1
252	187.8010	55.3000	2
253	189.8840	567.5240	1
254	189.8840	55.4700	2
255	-22.0080	.4410	3

INITIAL CAPILLARY PRESSURE HEAD AT TOP OF SAMPLE : 24.2

4 STEPS IN PNEUMATIC PRESSURE :
TIME PRESSURE

.00	102.0
12.42	204.1
48.12	408.2
105.92	714.3

ITERATION NO	SSQ	ALPHA	N	WCR	CONDS
1	.1125D+02	.0269	1.7137	.2402	.3955
2	.9254D+01	.0092	1.9363	.2466	.3558
3	.2455D+01	.0138	2.1243	.2588	.5637
4	.1457D+01	.0151	2.0785	.2459	.6858
5	.1454D+01	.0150	2.0942	.2463	.6892
6	.1454D+01	.0150	2.0938	.2463	.6913

MASS BALANCE ERROR IN FE SOLUTION DURING FINAL RUN WAS .5674 %

RSQUARE FOR REGRESSION OF PREDICTED VS OBSERVED = .99992

CORRELATION MATRIX

=====

	1	2	3	4
1	1.0000			
2	-.8103	1.0000		
3	-.5364	.8700	1.0000	
4	.7043	-.1886	.1029	1.0000

NON-LINEAR LEAST-SQUARES ANALYSIS: FINAL RESULTS

=====

VARIABLE	VALUE	S.E.COEFF.	95% CONFIDENCE LIMITS	
			LOWER	UPPER
ALPHA	.01498	.0004	.0142	.0157
N	2.09380	.0246	2.0454	2.1422
WCR	.24631	.0015	.2434	.2493
CONDS	.69132	.0365	.6194	.7632

-----OBSERVED & FITTED			DATA		-----
NO	TIME (HR)	Z	OBS	FITTED	RESI- DUAL
1	.051	3.000	32.958	41.678	-8.720
2	.051	3.000	9.340	8.300	1.040
3	.067	3.000	35.674	45.095	-9.421
4	.067	3.000	11.461	9.517	1.944
5	.084	3.000	39.132	48.151	-9.019
6	.084	3.000	12.998	10.573	2.425
7	.101	3.000	42.925	50.779	-7.854
8	.101	3.000	14.058	11.480	2.578
9	.117	3.000	46.585	53.012	-6.427
10	.117	3.000	14.977	12.250	2.727

243	166.884	3.000	538.087	540.150	-2.063
244	166.884	3.000	55.208	52.919	2.289

245	168.967	3.000	541.212	543.458	-2.246
246	168.967	3.000	55.183	52.956	2.227
247	183.467	3.000	559.791	564.424	-4.633
248	183.467	3.000	55.095	53.176	1.919
249	185.634	3.000	562.355	567.278	-4.923
250	185.634	3.000	55.204	53.205	1.999
251	187.801	3.000	565.066	570.065	-4.999
252	187.801	3.000	55.300	53.233	2.067
253	189.884	3.000	567.524	572.685	-5.161
254	189.884	3.000	55.470	53.259	2.211
255	-22.008	3.000	.441	.432	.009

REFERENCES

- Campbell Scientific, Inc. 1996a. AM416 relay multiplexer instruction manual. Logan, Utah.
- Campbell Scientific, Inc. 1996b. 21X(L) micrologger operator's manual. Logan, Utah.
- Campbell Scientific, Inc. 1998. PC208W datalogger support software instruction manual. Logan, Utah.
- Chen, J., K. Kosugi, and J.W. Hopmans. 1997. Parameter estimation of multi-step outflow experiments: SFOPT. Land, Air, and Water Resources Paper No. 100036, University of California, Davis, CA.
- Chen, J., J.W. Hopmans, and M.E. Grismer. 1999. Parameter estimation of two-fluid capillary pressure-saturation and permeability functions. *Advances in Water Resources*. 22(5) : 479-493.
- Clausnitzer, V. and J.W. Hopmans. 1995. Nonlinear parameter estimation: LM-OPT. General-purpose optimization code based on the Levenberg-Marquardt algorithm. Land, Air, and Water Resources Paper No. 100032, University of California, Davis.
- Eching, S.O. and J.W. Hopmans. 1993a. Optimization of hydraulic functions from transient outflow and soil water pressure data. *Soil Sci. Am. J.* 57:1167-1175.
- Eching, S.O. and J.W. Hopmans. 1993b. Inverse solution of unsaturated soil hydraulic functions from transient outflow and soil water pressure data. Land, Air, and Water Resources Paper No. 100021, University of California, Davis, CA.
- Eching, S.O., J.W. Hopmans, and O. Wendroth. 1994. Unsaturated hydraulic conductivity from transient multi-step outflow and soil water pressure data. *Soil Sci. Am. J.* 58:687-695.
- Hopmans, J.W., T. Vogel, and P.D. Koblik. 1992. X-Ray tomography of soil water distribution in one-step outflow experiments. *Soil Sci. Soc. Am. J.* 56:355-362
- Hopmans, J.W., J.C. van Dam, S.O. Eching, and J.N.M. Stricker. 1994. Parameter estimation of soil hydraulic functions using inverse modeling of transient outflow experiments. *Trends in Hydrology*, 1:217-242.
- Hopmans, J.W., J. Simunek, N. Romano and W. Durner. 2002. Simultaneous determination of water transmission and retention properties-inverse methods. In J. Dane, D.E. Elrick, D. Reynolds and B Clothier (eds). *Methods of Soil Analysis*.

Part I. Third Edition American Society of Agronomy, Monograph No. 9, Madison, WI.

- Klute A. 1986. Water retention: Laboratory methods. In A. Klute (ed). *Methods of Soil Analysis. Part I. Physical and mineralogical methods*. Second edition. American Society of Agronomy, Monograph No. 9, Madison, WI.
- Klute A. and C. Dirksen. 1986. Hydraulic conductivity and diffusivity: Laboratory methods. In A. Klute (ed). *Methods of Soil Analysis. Part I. Physical and mineralogical methods*. Second edition. American Society of Agronomy, Monograph No. 9, Madison, WI.
- Kool, J.B., J.C. Parker, and M.Th. van Genuchten. 1985a. Determining soil hydraulic properties from one-step outflow experiments by parameter estimation: Theory and numerical studies. *Soil Soc. Am. J.* 49:1348-1354.
- Kool, J.B., J.C. Parker, and M.Th. van Genuchten. 1985b. One-step: A nonlinear parameter estimation program for evaluating soil hydraulic properties from one-step outflow experiments. *Va. Agric. Exp. Stn. Bull.* 85-3.
- Kool, J.B. and J.C. Parker. 1987. Estimating soil hydraulic properties from transient flow experiment: SFIT User's Guide. VPI and SU Dept. Soils and Environmental Sciences, Blacksburg, VA 24061.
- Kosugi K. 1996. Lognormal distribution model for unsaturated soil hydraulic properties. *Water Resour. Res.* 32:2697-2703.
- Mualem, Y. 1976. A new model for predicting the hydraulic conductivity of unsaturated porous media. *Water Resour. Res.* 12:513-522.
- Parker, J.C., J.B. Kool, and M.Th. van Genuchten. 1985. Determining soil hydraulic properties from one-step outflow experiments by parameter estimation: Experimental studies. *Soil Soc. Am. J.* 49:1354-1359.
- Schaap, M.G. and F.J. Leij. 1998. Using neural networks to predict soil water retention and soil hydraulic conductivity. *Soil Till. Res.* 47: 37-42.
- van Dam, J.C., J.N.M. Stricker, and P. Droogers. 1990. From one-step to multi-step determination of soil hydraulic functions by outflow experiments. Dept. Water Resources Rep. No 7. Wageningen Agricultural Univ., Wageningen, Netherlands.

- van Dam, J.C., J.N.M. Stricker, and P. Droogers. 1992. Inverse method for determining soil hydraulic functions from one-step outflow experiments. *Soil Sci. Am. J.* 56:1042-1050.
- van Dam, J.C., J.N.M. Stricker, and P. Droogers. 1994. Inverse method to determine soil hydraulic functions from multi-step outflow experiments. *Soil Sci. Am. J.* 58:647-652.
- van Genuchten, M.Th. 1980. A closed-form equations for predicting the hydraulic conductivity of unsaturated soils. *Soil Sci. Soc. Am. J.* 44:892-898.
- Wraith, J.M. and D. Or. 1998. Nonlinear parameter estimation using spreadsheet software. *J. Nat. Resour. Life Sci. Edu.* 27: 13-19.

APPENDIX A. Photographs of the items used in the Multi-step outflow experiment

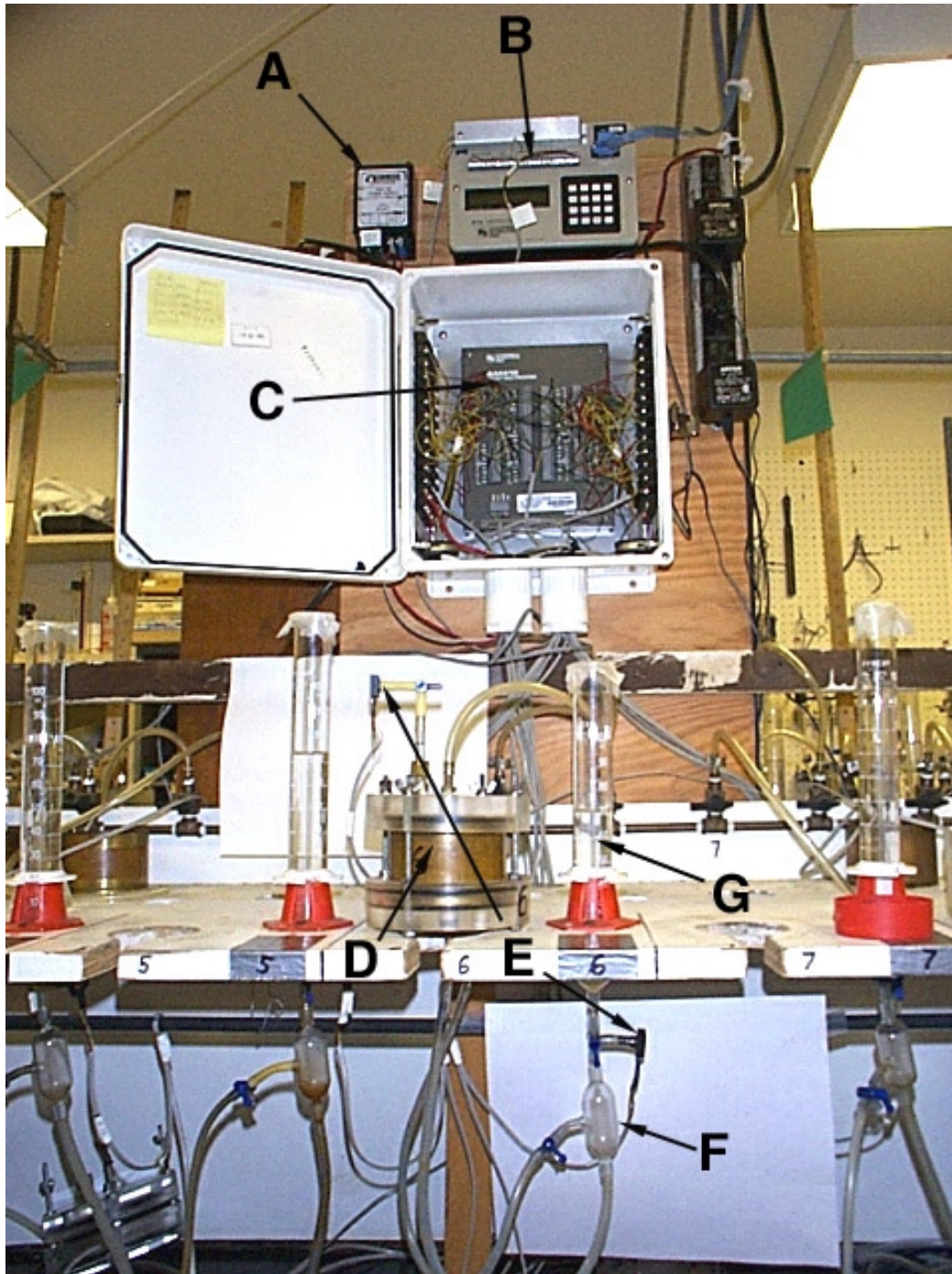


Photo 1. The multi-step outflow experiment set up: (A) External power supply, (B) 21X Datalogger, (C) AM416 Multiplexer, (D) Tempe cell with the ring, (E) Tensiometer and outflow pressure transducers, (F) Air trap, (G) The graduated burette.

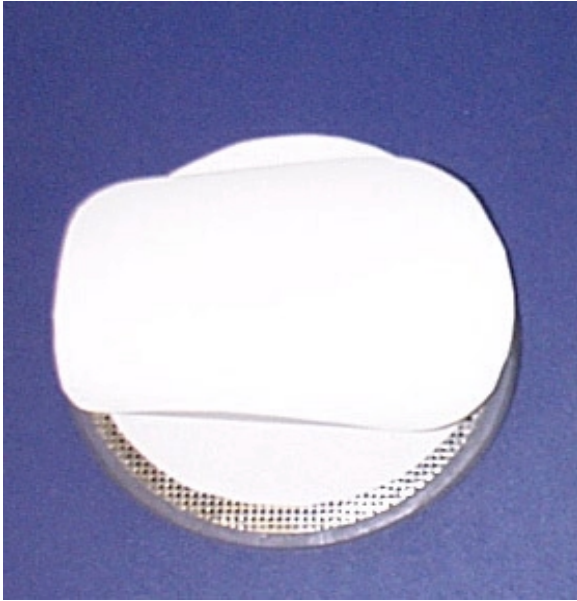


Photo 2. Porous membrane assembly for the 3.5" soil sample.

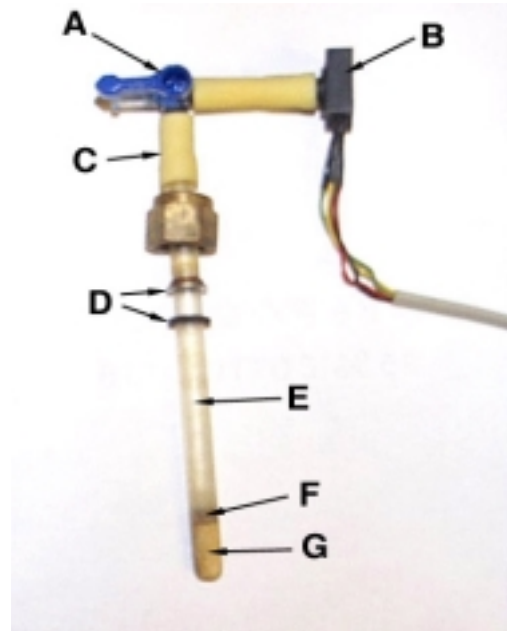


Photo 3. Mini-tensiometer transducer arrangement: (A) 3-way valve, (B) Pressure transducer, (C) Rubber sleeve, (D) Ferrule & O-ring, (E) Acrylic tube, (F) Copper coupler, (G) Ceramic cup



Photo 4. The 3.5" top cover of the Tempe cell.

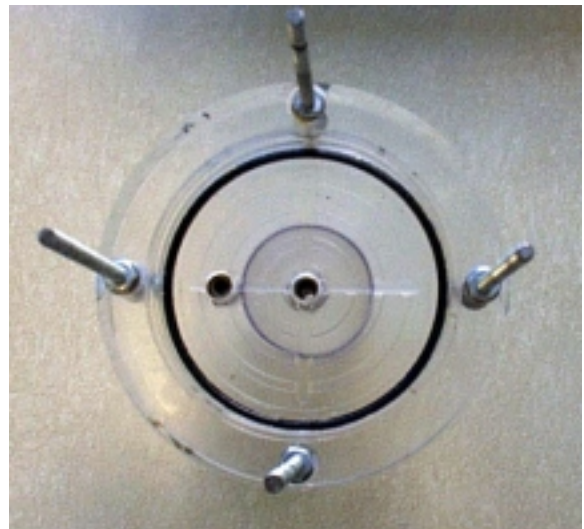


Photo 5. The 3.5" bottom cover of the Tempe cell.



Photo 6. Aluminum sleeve glued with the filter paper (from the top).

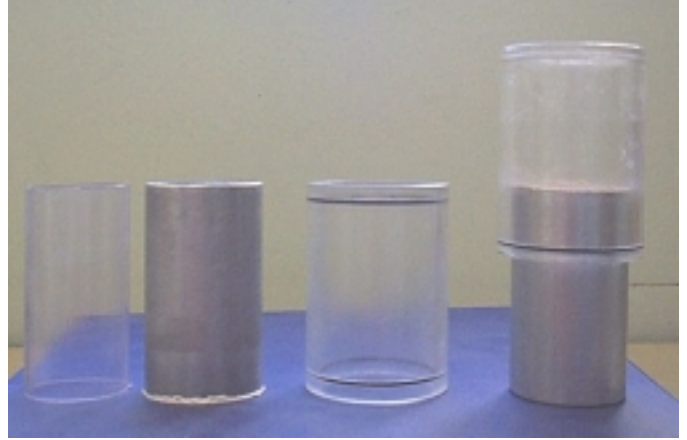


Photo 7. Plastic liner, aluminum sleeve glued with filter paper, Plexiglas sleeve, and saturated hydraulic conductivity set up (from left to right).

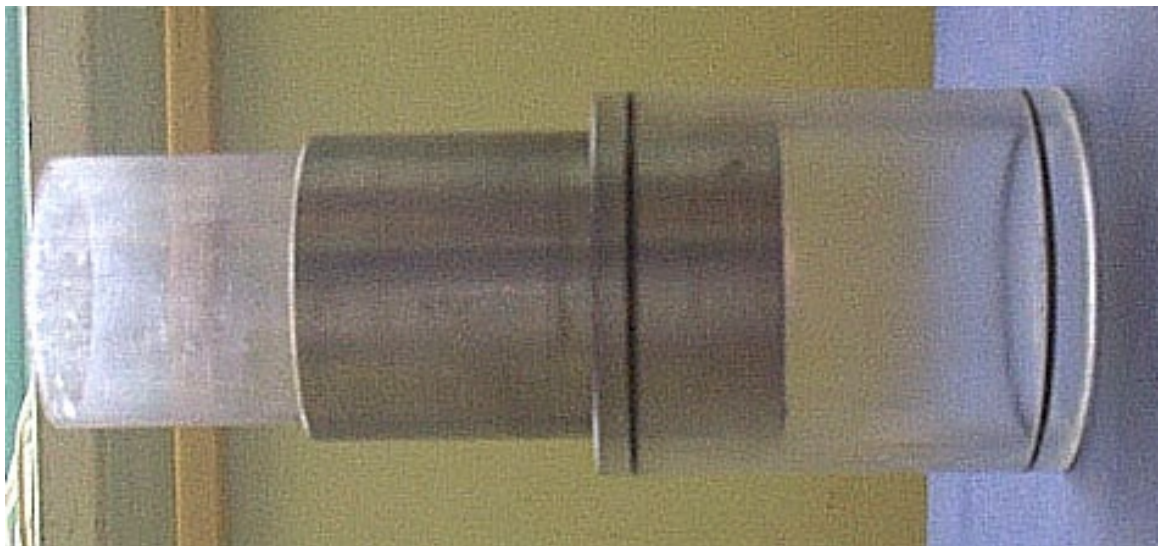


Photo 8. The way of setting up the sample from Geoprobe Macrocore[®] for the multi-step experiment.



Photo 9. Bottom cover of the 2" Tempe cell.



Photo 10. Porous membrane assembly and support.



Photo 11. The 2" Tempe cell set up.



Photo 12. Multi-step experiment set up for the ten 2" Tempe cells.

APPENDIX B. Source file of DATAPREP

```

!+++++ setting for graphics +++++
USE DFLIB
integer(2) status,index,numfonts
integer(4) deg
type (wxycoord) wxy
real(8) xmin,xmax,ymin,ymax,wxmin,wxmax,wymin,wymax,xval,yval,pymn
!+++++ setting for main program +++++
PARAMETER (ND=50000)
DIMENSION DATE(ND),TIME(ND),H0(ND),Q0(ND),A(2),B(2),B1(2),B2(2) &
& ,P(100),CDATE(100),CTIME(100),FDATE(100),FTIME(100) &
& ,Q1(ND),BC0(ND),H(0:ND),Q(0:ND),T(0:ND),BC(ND)
CHARACTER*20 FNAME,FINPU,GNAME
!+++++
!+++++ IMPORTANT PARAMETER VALUES !!! +++++
!+++++
!+++++
samhe=6. ! sample height (cm)
samdi=8.25 ! sample diameter (cm)
samvo=321. ! sample volume (cm3)
porhe=0. ! porous membrane height (cm)
tenhe=3. ! tensiometer height from bottom of porous membrane (cm)
watvo=19. ! burette reading when soil sample is saturated (ml)
wathe=1.4 ! water height from bottom of porous membrane when soil sample is
saturated (cm)
whinc=0.181 ! increment of water height in burette per 1 ml outflow (cm/ml)
nnsf=55 ! total number of nodes
lnssf=55 ! number of nodes in soil
cpltsf=999. ! saturated conductivity of porous plate (cm/h)
wthc=1. ! Weighting factor of capillary pressure hc-type data
wtq=1. ! Weighting factor of cumulative outflow Q-type data
wtheta=10. ! Weighting factor for water retention point
!+++++
!+++++
!+++++
!+++++
!+++++ file names & time points +++++
WRITE(6,*) 'ENTER EXPERIMENTAL FILE NAME'
READ(5,*) FNAME
WRITE(6,*) 'ENTER INPUT FILE NAME'
READ(5,*) FINPU
WRITE(6,*) 'ENTER GRAHING FILE NAME'
READ(5,*) GNAME

!
OPEN(20,FILE=FNAME,STATUS='UNKNOWN')
OPEN(31,FILE=FINPU,STATUS='UNKNOWN')
OPEN(41,FILE=GNAME,STATUS='UNKNOWN')

!
WRITE(6,*) 'HOW MANY TIME POINTS DO YOU NEED?'
READ(5,*) NTOB
!
!+++++ reading parameters +++++
!
READ(20,*) XSS
READ(20,*) APINI
READ(20,*) Q0INI
READ(20,*) Q0END
APINI=APINI/0.98
DO 10 I=1,2
READ(20,*) A(I)
10 CONTINUE
B2(1)=((Q0INI-watvo)*whinc+wathe-tenhe)*0.98
B2(2)=Q0INI
READ(20,*) NCHANGE
DO 15 I=1,NCHANGE
READ(20,*) CDATE(I),CTIME(I),P(I)
P(I)=P(I)/0.98
15 CONTINUE
SHOUR=REAL(INT(CTIME(1)/100.))
SMINU=CTIME(1)-SHOUR*100.

```

```

        STIME=CDATE(1)*24+SHOUR+SMINU/60.
        DO 17 I=1,NCHANGE
            HOUR=REAL(INT(CTIME(I)/100.))
            MINU=CTIME(I)-HOUR*100.
            CTIME(I)=CDATE(I)*24+HOUR+MINU/60.-STIME
17      CONTINUE
        CTIME(NCHANGE+1)=10000000.
!
        READ(20,*) NFLUSH
        IF(NFLUSH.EQ.0) THEN
            FTIME(1)=10000000.
            GOTO 22
        ENDIF
        DO 20 I=1,NFLUSH
            READ(20,*) FDATE(I),FTIME(I)
            HOUR=REAL(INT(FTIME(I)/100.))
            MINU=FTIME(I)-HOUR*100.
            FTIME(I)=FDATE(I)*24+HOUR+MINU/60.-STIME
20      CONTINUE
22      CONTINUE
!
!+++++  reading first line of data  +++++
!
        READ(20,*) DATE(1),TIME(1),H0(1),Q0(1)
            B1(1)=H0(1)
            B1(2)=Q0(1)
        DO 12 I=1,2
            B(I)=B2(I)-A(I)*B1(I)
12      CONTINUE
        B2(1)=B2(1)/0.98
!
            H0(1)=(H0(1)*A(1)+B(1))/0.98
            Q0(1)=Q0(1)*A(2)+B(2)-Q0INI
            HOUR=REAL(INT(TIME(1)/100.))
            MINU=TIME(1)-HOUR*100.
            TIME(1)=DATE(1)*24+HOUR+MINU/60.-STIME
!
!+++++  reading data  +++++
!
            NMAX=1
        DO 30 N=2,ND
            READ(20,*,END=99) DATE(N),TIME(N),H0(N),Q0(N)
            H0(N)=(H0(N)*A(1)+B(1))/0.98
            Q0(N)=Q0(N)*A(2)+B(2)-Q0INI
            HOUR=REAL(INT(TIME(N)/100.))
            MINU=TIME(N)-HOUR*100.
            TIME(N)=DATE(N)*24+HOUR+MINU/60.-STIME
            NMAX=NMAX+1
30      CONTINUE
99      CONTINUE
!+++++  calculation of lower boundary water height values  +++++
        DO 35 N=1,NMAX
            BC0(N)=(Q0(N)+Q0INI-watvo)*whinc+wathe
35      CONTINUE
!+++++  calculation of pressure head values  +++++
        ISTEP=2
        DO 40 N=2,NMAX
            IF(TIME(N).GT.CTIME(ISTEP)) THEN
                ISTEP=ISTEP+1
            ENDIF
            H0(N)=H0(N)-P(ISTEP-1)
40      CONTINUE
!+++++  correction of air flushing  +++++
        N0=NMAX+1
        DO 50 N=1,NMAX
            IF(TIME(N).GE.FTIME(1)) THEN
                N0=N
                GOTO 52
            ENDIF
            Q1(N)=Q0(N)
50      CONTINUE
52      CONTINUE
            ISTEP=2

```

```

NOX=N0
DO 55 N=N0X,NMAX
  IF (TIME(N).GT.FTIME(ISTEP)) THEN
    N1=N-1
    DQ=Q0(N1)-Q0(N)
    DT=TIME(N1)-TIME(N0)
    DO 60 NN=N0,N1
      Q1(NN)=Q0(NN)-DQ*(TIME(NN)-TIME(N0))/(TIME(N1)-TIME(N0))
60    CONTINUE
    N0=N
    ISTEP=ISTEP+1
    IF (ISTEP.GT.NFLUSH) GOTO 56
  ENDIF
55 CONTINUE
56 DO 57 N=N0,NMAX
  Q1(N)=Q0(N)
57 CONTINUE
!+++++
!+++++ data selection +++++
!+++++
!+++++
DT0=2.      !+++ maximum time interval for data selection (hr)
!+++++
!+++++
DH0=(H0(NMAX)-(B2(1)-APINI))/REAL(NTOB)
DQ0=Q1(NMAX)/REAL(NTOB)
M=0
H(0)=B2(1)-APINI
Q(0)=0.
T(0)=0.
ISTEP=1
DO 70 N=2,NMAX
  IF (TIME(N).GT.CTIME(ISTEP)) THEN
    ISTEP=ISTEP+1
    GOTO 70
  ENDIF
  HH=H0(N)-H(M)
  QQ=Q1(N)-Q(M)
  TT=TIME(N)-T(M)
  IF ((HH.LT.DH0).OR.(QQ.GT.DQ0).OR.(TT.GT.DT0)) THEN
!+++++
!+++++ CONSTRAIN 1 : constrain for data fluctuations +++++
!+++++
      IF (H0(N).LT.H0(N+1)) GOTO 70
      IF (H0(N).LT.H0(N+2)) GOTO 70 ! If the current pressure is smaller
than
      IF (H0(N).LT.H0(N+3)) GOTO 70 ! pressures at the following five time
      IF (H0(N).LT.H0(N+4)) GOTO 70 ! steps, skip the current time step.
      IF (H0(N).LT.H0(N+5)) GOTO 70
!+++++
      IF (Q1(N).GT.Q1(N+1)) GOTO 70
      IF (Q1(N).GT.Q1(N+2)) GOTO 70 ! If the current outflow is greater than
      IF (Q1(N).GT.Q1(N+3)) GOTO 70 ! outflows at the following five time
      IF (Q1(N).GT.Q1(N+4)) GOTO 70 ! steps, skip the current time step.
      IF (Q1(N).GT.Q1(N+5)) GOTO 70
!+++++
!+++++ CONSTRAIN 2 : constrain for unreasonable changes +++++
!+++++
!+++++ If the current pressure is greater than the previously chosen pressure,
!+++++ skip the current time step. (+1. is to neglect small fluctuations)
      IF (H0(N).GT.H(M)+1.) GOTO 70
!+++++
!+++++ If the current outflow is smaller than the previously chosen outflow,
!+++++ skip the current time step. (-.1 is to neglect small fluctuations)
      IF (Q1(N).LT.Q(M)-.1) GOTO 70
!+++++
      M=M+1
      H(M)=H0(N)
      Q(M)=Q1(N)
      T(M)=TIME(N)
      BC(M)=BC0(N)
    ENDIF
70 CONTINUE

```

```

!
!+++++ data output +++++
!
WRITE(31,*) '--- NCASES, nprint, nout, khall, nresul'
WRITE(31,*) 1,0,0,0,0
WRITE(31,*) '--- TITLE'
WRITE(31,*) 'Title'
WRITE(31,*) '--- SAMPLE'
WRITE(31,*) 'Sample name'
WRITE(31,*) '--- NN(total nodes), LNS(Soil nodes), DNUL, ZD(Z_obs),
AIRP(Pres.step No), EPS1, EPS2'
WRITE(31,200) nnsf,lnssf,0.001,samhe+porhe-tenhe,-1*NCHANGE,1.,1.
WRITE(31,*) '--- SLL(Soil-L), PLL(Plate-L), IAM(Soil-Diam), CPLT(PlateKs)'
WRITE(31,*) samhe,porhe,samdi,cpltsf
WRITE(31,*) '--- NTOB(Time points),NTOA(Theta
points),NTYPE,MDATA,MODE,MIT(Iter.limit)'
WRITE(31,*) M*2,1,3,1,1,50
WRITE(31,*) '--- IEQ (1-van Genuchten model, 2-Lognormal model)'
WRITE(31,*) 1 !+++ (1-van Genuchten model, 2-Lognormal model)
WRITE(31,*) '--- Initial parameter guesses: alpha, n, thetar, thetas, Ks, 1'
WRITE(31,210) 0.04,2.,0.11,XSS,5.08,0.5
WRITE(31,*) '--- Parameter free/fixed index (1-free, 0-fixed)'
WRITE(31,*) 1,1,1,0,1,0
WRITE(31,*) '--- Parameter limits:'
WRITE(31,*) '--- Minimums:'
WRITE(31,210) 0.001,1.01,0.0001,0.1,0.0001,-15.
WRITE(31,*) '--- Maximums:'
WRITE(31,210) 0.5,10.,XSS-0.03,0.9,30.,15.
WRITE(31,*) '--- Ini. air pressure, Ini. outflow height:'
WRITE(31,*) APINI,(Q0INI-watvo)*whinc+wathe
WRITE(31,*) '--- RhoW, RhoNW (Rho:Fluid density; W:Wetting; NW:NonWetting)'
WRITE(31,*) 1.,0.
WRITE(31,*) '--- Observation data points'
WRITE(31,890) '--- Time (hr),'',Datatype','',Obs_value','',Obs_height','',WT'
write(41,*) ' Input file name : ',gname
write(41,921) m
write(41,922) Q0END-(Q0INI+Q1(nmax))
write(41,923) time(nmax),h0(nmax),q0(nmax)
!
WRITE(41,*)
WRITE(41,895) '--Time (hr)--','--- H0 ---','--- Q0 ---','---Time (hr)--','--- H ---
','--- Q ---'
DO 90 N=1, NMAX
IF (N.LE.M) THEN
WRITE(41,915) TIME(N),H0(N),Q0(N),T(N),H(N),Q(N)
ELSE
WRITE(41,925) TIME(N),H0(N),Q0(N)
ENDIF
90 CONTINUE
DO 100 N=1,M
WRITE(31,910) T(N),1,-1.*H(N),samhe+porhe-tenhe,wthc
WRITE(31,910) T(N),2,Q(N),BC(N),wtq
100 CONTINUE
IF(Q0INI.LE.watvo) THEN
! WRITE(31,920) B2(1)-APINI,XSS
WRITE(31,920) B2(1)-APINI+tenhe-(samhe/2.+porhe),3,XSS,wtheta
ELSE
! WRITE(31,920) B2(1)-APINI,XSS-(Q0INI-watvo)/samvo
WRITE(31,920) B2(1)-APINI+tenhe-(samhe/2.+porhe),3,XSS-(Q0INI-
watvo)/samvo,wtheta
ENDIF
WRITE(31,*)'--- Pressure steps:'
WRITE(31,*)'--- Time (hr), Upper Nonwetting Pressure'
DO 110 I=1,NCHANGE
WRITE(31,930) CTIME(I),P(I)
110 CONTINUE
!
890 FORMAT(A13,1X,A10,1X,A11,2X,A11,3X,A3)
895 FORMAT(1(A15,1X),2(A12,1X),1(A15,1X),2(A12,1X))
900 FORMAT(5(F12.2,1X))
910 FORMAT(1(F10.2,4X),1(I4,7X),3(F10.3,1X))
915 FORMAT(6(F10.3,5X))
920 FORMAT(1(F10.2,4X),1(I4,7X),1(F10.3,1X),1(F21.3,1X))

```

```

925 FORMAT(3(F10.3,5X))
930 FORMAT(2(F10.2,7X))
200 FORMAT(2(I4,1X),2(F8.4,1X),1(I4,1X),2(F8.4,1X))
210 FORMAT(6(F8.4,1X))
!
!+++++ drawing graphics +++++
!
status = setbkcolor(15)
status = settextrcolor(int2(0))
status = setcolor(int2(0))
call clearscreen($gclearscreen)
!
write(6,*) ' Experimental file name : ',fname
write(6,*) ' Input file name : ',finpu
write(6,921) m, A(1), B(1), A(2), B(2)
write(6,922) Q0END-(Q0INI+Q1(nmax))
write(6,923) time(nmax),h0(nmax),q0(nmax)
!
921 format(' Number of time points : ',i4,2X,4(F8.3, 2X))
922 format(' Differece between final outflows by burette and transducer : ', &
& f7.3,' ml')
923 format(' Time : 0 to',f7.1,' hr Press. : 0 to',f7.1, &
& ' cm Outflow : 0 to',f6.1,' ml')
!
!++++
pixx=780.
pixy=530.-90.
call setviewport(int2(0),int2(90),int2(780),int2(530))
!
!++++ capillary pressure vs. time +++++
xmin=0.
xmax=time(nmax)
ymin=0.
ymax=h0(nmax)
DO n=2, nmax
    IF (h0(n).LE.ymax) THEN
        ymax = h0(n)
    END IF
END DO
!
wxmin=xmin-(xmax-xmin)/10.
wxmax=xmax+(xmax-xmin)/10.
wymin=ymin-(ymax-ymin)/10.
wymax=ymax+(ymax-ymin)/10.
!
status=setwindow(.true.,wxmin,wymin,wxmax,wymax)
status=rectangle_w($gborder,xmin,ymax,xmax,ymin)
!
numfonts = INITIALIZEFONTS ()
index = SETFONT('t','Arial','h16')
call moveto_w(((xmax-20)/2),(ymax-2),wxy)
call outgttext('Cumulative time, hr')
!
numfonts = INITIALIZEFONTS ()
index = SETFONT('t','Arial','h14')
call moveto_w((xmin-10),(ymax/1.7),wxy)
deg = 900
call setgttextrotation(deg)
call outgttext('Matrichead, cm')
!
status = setcolor(int2(13))
xval=time(1)
yval=h0(1)
call moveto_w(xval,yval,wxy)
do 310 n=2,nmax
    xval=time(n)
    yval=h0(n)
    status=lineto_w(xval,yval)
310 continue
!
status = setcolor(int2(12))
do 320 n=1,m

```

```

        xval=t(n)
        yval=h(n)
        eval=0.004*xmax
        evaly=eval*(ymax-ymin)/(xmax-xmin)*pixx/pixy
        status=ellipse_w($gfillinterior,xval-eval,yval+evaly,xval+eval,yval-evaly)
320 continue
!
!+++++ cumulative outflow vs. time +++++
status = setcolor(int2(0))
xmin=0.
xmax=time(nmax)
ymin=0.
ymax=q0(nmax)
DO n=2, nmax
    IF (q0(n).GE.ymax) THEN
        ymax = q0(n)
    END IF
END DO

!
wxmin=xmin-(xmax-xmin)/10.
wxmax=xmax+(xmax-xmin)/10.
wymin=ymin-(ymax-ymin)/10.
wymax=ymax+(ymax-ymin)/10.
!
status=setwindow(.true.,wxmin,wymin,wxmax,wymax)
status=rectangle_w($gborder,xmin,ymax,xmax,pymin)
numfonts = INITIALIZEFONTS ()
index = SETFONT('t' 'Arial' 'h14')
call moveto_w((xmax+10),(ymax/3),wxy)
deg = 900
call setgtextrrotation(deg)
call outgtxt('Cumulative outflow, ml')
!
status = setcolor(int2(8))
xval=time(1)
yval=q0(1)
call moveto_w(xval,yval,wxy)
do 330 n=2,nmax
    xval=time(n)
    yval=q0(n)
    status=lineto_w(xval,yval)
330 continue
!
status = setcolor(int2(10))
xval=time(1)
yval=q1(1)
call moveto_w(xval,yval,wxy)
do 340 n=2,nmax
    xval=time(n)
    yval=q1(n)
    status=lineto_w(xval,yval)
340 continue
status = setcolor(int2(9))
do 350 n=1,m
    xval=t(n)
    yval=q(n)
    eval=0.004*xmax
    evaly=eval*(ymax-ymin)/(xmax-xmin)*pixx/pixy
    status=ellipse_w($gfillinterior,xval-eval,yval+evaly,xval+eval,yval-evaly)
350 continue
call setviewport(0,0,799,610)
!+++
end

```

APPENDIX C. Source file of SFOPT

```

C *****
C *
C * EVALUATION OF SOIL HYDRAULIC PROPERTIES FROM
C * OUTFLOW DATA BY PARAMETER ESTIMATION
C *
C * version 1.2, mass-lumped FE
C *
C * J.B. Kool, 1984,1985,1986,1987
C * J.C. v Dam, 1988,1989
C * Modified by S.O Eching to include H(z,t) data, 1991
C * Modified by Jiayu Chen (1996) to include :
C * - Time dependent lower boundary condition
C * - Improved weighting factor calculation
C * - New input file format
C * - Correction of outflow calculation
C * Modified by Ken'ichirou Kosugi (1997) to include Lognormal
C * model of retention and conductivity functions.
C *****
C
PARAMETER (NO=500,NZ=100)
CHARACTER*65 TITLE
CHARACTER*20 TTYPE,FIN,FOUT1,FOUT2
CHARACTER*7 BI(12)
CHARACTER*15 SAMPLE
DOUBLE PRECISION DELZ(NO,6),FC(NO),FO(NO),R(NO),OBS_HEIGHT(NO),
+WT(NO),A(6,6),D(6,6),E(6),Q(6),C(6),CHI(6)
DOUBLE PRECISION ANGLE,ARG,GA,SCAL,SSQ,SUM,SUMB,SUM1,SUM2,SUM3,
+STEP,STOPCR,ZERO,HO(NO),HOO,HOO
DOUBLE PRECISION SUMFO(10),NOBS(10),SETWT(10),AVFO(10)
DIMENSION TB(12),AS(6,6),TH(12),BMIN(6),BMAX(6),Z1(NZ),B(6)
REAL THETA(30),KUNS(30),SSQ01,SSQ02
COMMON/AAA/delx,P(NZ),NN,AREA,LNS,PLL,SLL,PN1,TO(NO),DNUL,
*NOB,NOB2,TMINIT,EPS1,EPS2,IINDEX(6),NVAR,CPLT,ITYPE(NO),NOB1,NOBB,
*PIN(NZ),IRUN,ZD,BC_P,ZX
COMMON/HYPR/BIN(6),RHOW,RHONW,IEQ
common/theta/at,rt,wcr,wcrst,khall
common/press/airp,pressu(10),tpress(10),npress,tprint(NZ),nprint
DATA STOPCR/.01D0/,TTYPE/' DATA',QRTPI/0.78539816/
DATA BI(7)/'ALPHA ',BI(8)/'N ',BI(9)/'WCR '/
DATA BI(10)/'WCS ',BI(11)/'CONDS ',BI(12)/'EXPL '/
DATA MAXTRY/20/,ZERO/0D0/
NVAR=6
NU1=NVAR+1
NU2=2*NVAR

C
C ----- OPEN INPUT & OUTPUT FILES -----
C
C
WRITE(*,'(A)') ' ENTER INPUTFILE NAME '
READ(*,'(A)') FIN
WRITE(*,'(A)') ' ENTER OUTPUTFILE NAME1 '
READ(*,'(A)') FOUT1
WRITE(*,'(A)') ' ENTER OUTPUTFILE NAME2 '
READ(*,'(A)') FOUT2
OPEN(20,FILE=FIN,STATUS='OLD')
OPEN(21,FILE=FOUT1,STATUS='UNKNOWN')
OPEN(23,FILE=FOUT2,STATUS='UNKNOWN')
open(22,file='extract.dat',status='UNKNOWN')

C
C ----- READ & WRITE TITLE AND PARAMETERS -----
C
READ(20,*)
READ(20,*) NCASES,nprint,nout,khall,nresul
if (nresul.eq.1) open(25,file='observ.dat',status='UNKNOWN')
DO 144 ICASE=1,NCASES
WRITE(21,1002)
READ (20,*)
READ(20,'(A65)') TITLE
WRITE(21,1006) TITLE
READ(20,*)
READ(20,'(A15)') SAMPLE
WRITE(21,1007) SAMPLE
WRITE(21,1008)

```

```

      READ(20,*)
      READ(20,*) NN,LNS,DNUL,ZD,AIRP,EPS1,EPS2
      READ(20,*)
      READ(20,*) SLL,PLL,DIAM,CPLT
      READ(20,*)
      READ(20,*) NTOB,NTOA,NTYPE,MDATA,MODE,MIT
      NOBB=NTOB+NTOA
      MODEX=MODE
C      DELX1=SLL/FLOAT(LNS-1)
C      IF (NN .NE. LNS) DELX2=PLL/FLOAT(NN-LNS)
      delx=(sll+pll)/float(nn-1)
      WRITE(21,1018) NN,LNS,DNUL,AIRP,EPS1,EPS2,MIT,MDATA,NOBB
      READ(20,*)
      READ(20,*) IEQ
      if(ieq.eq.2) then
        BI(7)='LOG10hm'
        BI(8)='sigma'
      endif
C
C      ---- READ INITIAL VALUE OF COEFFICIENTS ----
      READ(20,*)
      READ(20,*) (B(I),I=1,NVAR)
      READ(20,*)
      READ(20,*) (IINDEX(I),I=1,NVAR)
      READ(20,*)
      READ(20,*)
      READ(20,*) (BMIN(I),I=1,NVAR)
      READ(20,*)
      READ(20,*) (BMAX(I),I=1,NVAR)
      if(ieq.eq.1) then
        WRITE(21,1026) SLL,DIAM,PLL,CPLT,B(4),B(3),B(1),B(2),B(5),B(6)
      endif
      if(ieq.eq.2) then
        WRITE(21,10268) SLL,DIAM,PLL,CPLT,B(4),B(3),B(1),B(2),B(5),B(6)
      endif
C
C      ----
      npress=0
      IRUN=0
      NITT=0
C
C      ----- REARRANGE PARAMETER ARRAY -----
4 NP=0
  DO 5 I=NU1,NU2
    I1=I-NVAR
    BIN(I1)=B(I1)
    TB(I)=B(I1)
    IF(IINDEX(I1).EQ.0) GO TO 5
    NP=NP+1
    BI(NP)=BI(I)
    TB(NP)=B(I1)
    TH(NP)=B(I1)
    IF(IRUN.LT.2) THEN
      BMIN(NP)=BMIN(I1)
      BMAX(NP)=BMAX(I1)
    ENDIF
5 TH(I)=B(I1)
C
C      ---- READ INITIAL CONDITONS ----
      READ(20,*)
      READ(20,*) ZX,HOO
      READ(20,*)
      READ(20,*) RHOW,RHONW
C
C      ----- READ & WRITE INPUT DATA -----
C      ITYPE = 1: HC(X,T) MEASUREMENT
C              = 2: CUMULATIVE OUTFLOW MEASUREMENT
C              = 3: THETA(h) MEASUREMENT
C      if(nout.eq.0) then
        write(21,*)
        write(21,*) '              OBSERVED   DATA'
        write(21,*) '              ====='
        WRITE(21,*) '              OBS      HRS      Data      Data-type'

```

```

endif
N1=0
NOBW=0
KK=0
READ(20,*)
READ(20,*)
DO 6 N=1,NTOB
  READ(20,*) TO(N),ITYPE(N),FO(N),OBS_HEIGHT(N),WT(N)
  IF (ITYPE(N).EQ.2) THEN
    KK=KK+1
    HO(KK)=OBS_HEIGHT(N)
  ENDIF
11  IF (NOUT.EQ.0) WRITE(21,13) N,TO(N),FO(N),ITYPE(N)
    N1=N1+1
6  CONTINUE
DO 7 II=1,NTOA
  N=NTOB+II
  READ(20,*) TO(N),ITYPE(N),FO(N),WT(N)
  TO(N)=-1.*abs(TO(N))
  NOBW=NOBW+1
  IF (NOUT .EQ. 0) WRITE(21,13) N,TO(N),FO(N),ITYPE(N)
7  CONTINUE
IF (MODE .EQ. 9) GO TO 144
NOB=N1
NOB2=NOBB-NOB
13  FORMAT(1X,I10,2(F10.4,1X),I10)
    HOO=0.5*(HOO+HO(1))
    HT_BC=-ZX+HOO-(SLL+PLL)*RHOW
    WRITE(21,1023) -1.*HT_BC
DO 10 L=1,NN
  IF (L .LE. LNS) THEN
c    X=(L-1)*DELX1
    x=(l-1)*delx
    P(L)=HT_BC+X*RHOW
    Z1(L)=SPR(1,P(L),X)
  ELSE
c    X=SLL+(L-LNS)*DELX2
    x=(l-1)*delx
    P(L)=HT_BC+X*RHOW
  ENDIF
10 CONTINUE
AREA=QRTPI*DIAM**2
C
C... wls : adjust weights according to ITYPE -----
DO 51 I = 1,NTYPE
  SUMFO(I) = 0.
  NOBS(I) = 0
51  CONTINUE
DO 61 I = 1,NOBB
  SUMFO(ITYPE(I)) = SUMFO(ITYPE(I))+FO(I)
  NOBS(ITYPE(I)) = NOBS(ITYPE(I))+1
61  CONTINUE
DO 70 I = 1,NTYPE
  IF (NOBS(I) .GT. 0) AVFO(I) = SUMFO(I)/(NOBS(I))
70  CONTINUE
DO 73 I = 1,NTYPE
  SETWT(I) = DABS( DBLE(AVFO(2) / AVFO(I)) )
73  CONTINUE
DO 81 I = 1,NOBB
  WT(I) = WT(I) * DABS(DBLE(AVFO(2) /AVFO(ITYPE(I))))
81  CONTINUE
C
c  ----- read applied pressure steps -----
if (airp .lt. 0) then
  npress=-int(airp-0.5)
  write(21,1088) npress
  read(20,*)
  read(20,*)
  do 19 i=1, npress
    read(20,*) tpress(i),pressu(i)
    write(21,1090) tpress(i),pressu(i)
19  continue
  pn1=HOO-pressu(1)

```

```

        bc_p=pressu(1)
    else
        pn1=HOO-airp
    endif
    pn10=pn1
C
C      ----- read times on which pressure distribution is printed -----
C      if (nprint.gt.0) read(20,*) (tprint(i),i=1,nprint)
C
C      ----- COMPUTE OUTFLOW FOR INITIAL PARAMETER VALUES -----
20  GA=1.0D-02
    NOCON=0
    NITT=0
    CALL FLOW(TH,FC,NITT,NOCON,MDATA,MODE,ERRMB,HO,HOO)
    IF (MODE.EQ. 9) GO TO 144
    SSQ=ZERO
    DO 32 I=1,NOBB
        R(I)=WT(I)*(FO(I)-FC(I))
32  SSQ=SSQ+R(I)*R(I)
    rmsd=sqrt(ssq/nobb)
    IF (NP.EQ.0. OR. MODE.EQ.0) THEN
        WRITE(21,1040)
        WRITE(21,1042)NITT,rmsd
        WRITE(21,1044)ERRMB
        GO TO 110
    ELSE
        WRITE(21,1040) (BI(I),I=1,NP)
    ENDIF
    if (mode.ne.0.and.icas.eq.1.and.(irun.eq.1.or.irun.eq.0))
1write(22,1047)
    do 33 i=1,np
        e(i)=zero
33  continue
C
C      ----- BEGIN OF ITERATION -----
34  NITT=NITT+1
    WRITE(6,1045) sample,irun,nitt
    NET=0
    GA=0.1D0*GA
    DO 38 J=1,NP
        TEMP=TH(J)
        TH(J)=1.01*TH(J)
        Q(J)=ZERO

        CALL FLOW(TH,DELZ(1,J),NITT,NOCON,MDATA,MODE,ERRMB,HO,HOO)
        IF (MODE.EQ. 9) GO TO 144
        DO 36 I=1,NOBB
            DELZ(I,J)=WT(I)*(DELZ(I,J)-FC(I))
36  Q(J)=Q(J)+DELZ(I,J)*R(I)
        Q(J)=100.D0*Q(J)/DBLE(TEMP)
C
C      ----- STEEPEST DESCENT -----
38  TH(J)=TEMP
    DO 44 I=1,NP
        DO 42 J=1,I
            SUM=ZERO
            DO 40 K=1,NOBB
40  SUM=SUM+DELZ(K,I)*DELZ(K,J)
            D(I,J)=1.0D04*SUM/(TH(I)*TH(J))
42  D(J,I)=D(I,J)
C
C      ----- D = MOMENT MATRIX -----
    SCAL=DSQRT(DMAX1(D(I,I),1.0D-30))
44  E(I)=DMAX1(E(I),SCAL)
50  DO 52 I=1,NP
        DO 52 J=1,NP
52  A(I,J)=D(I,J)/(E(I)*E(J))
C
C      ----- A IS THE SCALED MOMENT MATRIX -----
    DO 54 I=1,NP
        C(I)=Q(I)/E(I)
        CHI(I)=C(I)
54  A(I,I)=A(I,I)+GA

```

```

      CALL QRSOLV(A,NP,C)
C
C      ----- C/E IS THE CORRECTION VECTOR -----
      STEP=1.0D0
56 NET=NET+1
      DO 58 I=1,NP
         TB(I)=SNGL(C(I)*STEP/E(I))+TH(I)
         IF(TB(I).LT.BMIN(I)) TB(I)=BMIN(I)
         IF(TB(I).GT.BMAX(I)) TB(I)=BMAX(I)
         C(I)=DBLE(TB(I)-TH(I))*E(I)/STEP
58 CONTINUE
60 DO 62 I=1,NP
         IF(TH(I)*TB(I))66,66,62
62 CONTINUE
      SUMB=ZERO
      CALL FLOW(TB,FC,NITT,NOCON,MDATA,MODE,ERRMB,HO,HO0)
      IF (MODE .EQ. 9) GO TO 144
      DO 64 I=1,NOBB
         R(I)=WT(I)*(FO(I)-FC(I))
64 SUMB=SUMB+R(I)*R(I)
66 SUM1=ZERO
      SUM2=ZERO
      SUM3=ZERO
      DO 68 I=1,NP
         SUM1=SUM1+C(I)*CHI(I)
         SUM2=SUM2+C(I)*C(I)
68 SUM3=SUM3+CHI(I)*CHI(I)
      ARG=SUM1/DSQRT(SUM2*SUM3)
      ANGLE=57.29578*DATAN2(DSQRT(1.-ARG*ARG),ARG)
C
C      -----
      DO 72 I=1,NP
         IF(TH(I)*TB(I))74,74,72
72 CONTINUE
         IF(NET.GE.MAXTRY) GO TO 79
         IF(SUMB/SSQ-1.0D0)80,80,74
74 IF(ANGLE-30.0D0)76,76,78
76 STEP=0.5D0*STEP
      GO TO 56
78 GA=DMIN1(100.D0,10.D0*GA)
      GO TO 50
79 WRITE(21,1086)
      GO TO 96
C
C      ----- PRINT COEFFICIENTS AFTER EACH ITERATION -----
80 CONTINUE
      DO 82 I=1,NP
82 TH(I)=TB(I)
      rmsd=sqrt(sumb/nobb)
      WRITE(21,1042)NITT,rmsd,(TB(I),I=1,NP)
90 DO 92 I=1,NP
      IF(ABS(C(I)*STEP/E(I))/(1.0E-20+ABS(TH(I)))-STOPCR) 92,92,94
92 CONTINUE
      GO TO 96
94 SSQ=SUMB
      IF(NITT.LT.MIT) GO TO 34
C
C      ----- END OF ITERATION LOOP -----
96 CONTINUE
      IF(SUMB.GT.10.0D0) GO TO 143
      IF(SUMB.LT.1.0D0) IRUN=IRUN+1
      WRITE(21,1044) ERRMB
      CALL MATINV(D,NP)
C
C      ----- WRITE RSQUARE, CORRELATION MATRIX -----
      SUMS=SNGL(SUMB)
      SUMS1=0.0
      SUMS2=0.0
      DO 98 I=1,NOBB
         FOS=SNGL(FO(I))
         SUMS1=SUMS1+FOS
98 SUMS2=SUMS2+FOS*FOS
      RSQ= 1.-SUMS/(SUMS2-SUMS1*SUMS1/NOBB)

```

```

        WRITE(21,1050) RSQ
        IF (NP.EQ. 1) GO TO 106
        DO 100 I=1,NP
100  E(I)=DSQRT(DMAX1(D(I,I),1.0D-30))
        WRITE(21,1046) (I,I=1,NP)
        DO 104 I=1,NP
        DO 102 J=1,I
102  AS(J,I)=SNGL(D(J,I)/(E(I)*E(J)))
104  WRITE(21,1048) I,(AS(J,I),J=1,I)
C
C      ----- CALCULATE 95% CONFIDENCE INTERVAL -----
106  Z=1./FLOAT(NOBB-NP)
        SDEV=SQRT(Z*SUMS)
        WRITE(21,1052)
        TVAR=1.96+Z*(2.3779+Z*(2.7135+Z*(3.187936+2.466666*Z**2)))
        DO 108 I=1,NP
            SECOEF=SNGL(E(I))*SDEV
            TSEC=TVAR*SECOEF
            TMCOE=TH(I)-TSEC
            TPCOE=TH(I)+TSEC
108  WRITE(21,1058) BI(I),TH(I),SECOEF,TMCOE,TPCOE
C
C      ----- PREPARE FINAL OUTPUT -----
110  WRITE(21,1066) TTYPE
        DO 118 I=1, NOBB
            FOS=SNGL(FO(I))
            FCS=SNGL(FC(I))
            RS=FOS-FCS
            if (nresul .eq. 1) write(25,'(2f10.3)') TO(I),fcs
            IF (I.LE.NOBB-1) THEN
                WRITE(21,1068) I,TO(I),OBS_HEIGHT(I),FOS,FCS,RS
            ELSE
                WRITE(21,1068) I,TO(I),ZD,FOS,FCS,RS
            ENDIF
118  CONTINUE
        WRITE(23,119) '#','TIME(hr)','HC_OBS(cm)','HC_OPT(cm)','DFHC',
        + 'Q_OBS(ml)','Q_OPT(ml)','DFQ'
119  FORMAT(1X,A6,2X,A9,2X,A7,4X,A7,5X,A5,6X,A6,5X,A6,7X,A4)
        DO 120 I=1,NOBB,2
            DHC=ABS(FO(I)-FC(I))
            DQ=ABS(FO(I+1)-FC(I+1))
            WRITE(23,122) I,TO(I),FO(I),FC(I),DHC,FO(I+1),FC(I+1),DQ
120  CONTINUE
122  FORMAT(1X,I6,7(F10.4,1X))
C
C      ----- WRITE SOIL HYDRAULIC PROPERTIES -----
        press=-1.412532
        ssq01=0
        ssq02=0
        x=0.
        do 140 i=1,30
            press=1.412532*press
            wc=spr(1,press,x)
            akln=spr(2,press,x)
            if (irun .eq. 1) then
                theta(i)=100*wc
                kuns(i)=akln
            endif
140  continue
144  CONTINUE
C
C      ----- END OF PROBLEM -----
1002 FORMAT(1H1,10X,67(1H*),65X,1h*/11X,1H*,65X,1H*)
1006 FORMAT(11X,1H*,A65,1H*)
1007 FORMAT(11X,1H*,23X,'SAMPLE ',A15,19X,1H*)
1008 FORMAT(11X,1H*,65X,1H*/11X,67(1H*))
1014 FORMAT(/2I5,E10.1,10X,3F10.0)
1016 FORMAT(4F10.0,4I5/)
1018 FORMAT(//11X,'PROGRAM PARAMETERS'/11X,18(1H=)/11X,
        + 'NUMBER OF NODES.....(NN).....',I3/11X,
        + 'NODE AT SOIL-PLATE BOUNDARY.....(LNS).....',I3/11X,
        + 'INITIAL TIME STEP.....(DNUL).....',E9.2/11X,
        + 'PNEUMATIC PRESSURE.....(AIRP).....',F8.3/11X,

```

```

+ 'TEMPORAL WEIGHTING COEFF.....(EPS1).....',F7.2/11X,
+ 'ITERATION WEIGHTING COEFF.....(EPS2).....',F7.2/11X,
+ 'MAX. ITERATIONS.....(MIT).....',I3/11X,
+ 'DATA MODE.....(MDATA).....',I3/11X,
+ 'NO. OF OBSERVATIONS.....(NOBB).....',I3)
1020 FORMAT(6F10.0)
1021 FORMAT(3F10.0,I5,F10.0)
1022 FORMAT(6I10)
1023 FORMAT(/11X,'INITIAL CAPILLARY PRESSURE HEAD AT TOP OF SAMPLE : '
+,F8.1)
1024 FORMAT(/11X,'PARAMETERS OF THE FIXED RETENTION CURVE :'/11X,
+ 'FIRST COEFFICIENT.....(ALPHA).....',F8.3/11X,
+ 'SECOND COEFFICIENT.....(N).....',F8.3/11X,
+ 'RESIDUAL MOISTURE CONTENT.....(WCR).....',F8.3/11X,
+ 'SATURATED MOISTURE CONTENT.....(WCS).....',F8.3)
10248 FORMAT(/11X,'PARAMETERS OF THE FIXED RETENTION CURVE :'/11X,
+ 'FIRST COEFFICIENT.....(LOG10hm).....',F8.3/11X,
+ 'SECOND COEFFICIENT.....(sigma).....',F8.3/11X,
+ 'RESIDUAL MOISTURE CONTENT.....(WCR).....',F8.3/11X,
+ 'SATURATED MOISTURE CONTENT.....(WCS).....',F8.3)
1026 FORMAT(/11X,'SOIL AND PLATE PROPERTIES'/11X,25(1H=)/11X,
+ 'SOIL COLUMN LENGTH.....(SLL).....',F8.3/11X,
+ 'COLUMN DIAMETER.....(DIAM).....',F8.3/11X,
+ 'THICKNESS OF PLATE.....(PLL).....',F8.3/11X,
+ 'PLATE CONDUCTIVITY.....(CONDS(2)).....',E9.4/11X,
+ 'SATURATED MOISTURE CONTENT.....(WCS).....',F8.3/11X,
+ 'RESIDUAL MOISTURE CONTENT.....(WCR).....',F8.3/11X,
+ 'FIRST COEFFICIENT.....(ALPHA).....',F8.3/11X,
+ 'SECOND COEFFICIENT.....(N).....',F8.3/11X,
+ 'SATURATED CONDUCTIVITY SOIL.....(CONDS(1)).....',E9.4/11X,
+ 'EXPONENT L MUALEM-GENUCHTEN.....(EXPL).....',F8.3)
10268 FORMAT(/11X,'SOIL AND PLATE PROPERTIES'/11X,25(1H=)/11X,
+ 'SOIL COLUMN LENGTH.....(SLL).....',F8.3/11X,
+ 'COLUMN DIAMETER.....(DIAM).....',F8.3/11X,
+ 'THICKNESS OF PLATE.....(PLL).....',F8.3/11X,
+ 'PLATE CONDUCTIVITY.....(CONDS(2)).....',E9.4/11X,
+ 'SATURATED MOISTURE CONTENT.....(WCS).....',F8.3/11X,
+ 'RESIDUAL MOISTURE CONTENT.....(WCR).....',F8.3/11X,
+ 'FIRST COEFFICIENT.....(LOG10hm).....',F8.3/11X,
+ 'SECOND COEFFICIENT.....(sigma).....',F8.3/11X,
+ 'SATURATED CONDUCTIVITY SOIL.....(CONDS(1)).....',E9.4/11X,
+ 'EXPONENT L MUALEM-GENUCHTEN.....(EXPL).....',F8.3)
1027 FORMAT(/11X,'INITIAL CONDITIONS'/11X,18(1H=)/11X,'NODE',2X,'DEPTH
1',2X,'PRESSURE HEAD',5X,'MOISTURE CONTENT')
1028 FORMAT(2I5,2F10.0)
1030 FORMAT(/5X,8(1H*), 'ERROR ENCOUNTERED WHILE READING INITIAL CONDIT
IONS, CHECK NODE',I4,1X,'EXECUTION TERMINATED',9(1H*))
1032 FORMAT(/11X,'OBSERVED ',A/11X,16(1H=)/14X,'OBS',5X,'HRS',5X,A,4X,
1'TYPE',4X,'WEIGHT')
1038 FORMAT(42X,6(F8.4,3X))
1040 FORMAT(/2X,'ITERATION NO',6X,'SSQ',5X,6(5X,A))
1041 FORMAT(T2,A5,I3,F8.3,F8.2,F8.4,5F8.3,2F8.1)
1042 FORMAT(6X,I2,5X,D12.4,8X,6(F8.4,3X))
1044 FORMAT(/11X,'MASS BALANCE ERROR IN FE SOLUTION DURING FINAL RUN W
LAS ',F12.4,' %')
1045 FORMAT('+',T4,'SAMPLE: ',A15,' PAR. SET: ',I8,' ITERATION: ',I2)
1046 FORMAT(/11X,'CORRELATION MATRIX'/11X,18(1H=)/14X,10(4X,I2,5X))
1047 FORMAT(T2,' NR IT SSQ MBAL ALFA N ORES',
1 ' OSAT KSAT L')
1048 FORMAT(11X,I3,10(2X,F7.4,2X))
1050 FORMAT(/11X,'RSQUARE FOR REGRESSION OF PREDICTED VS OBSERVED =',
1F7.5)
1052 FORMAT(/11X,'NON-LINEAR LEAST-SQUARES ANALYSIS: FINAL RESULTS'/
11X,48(1H=)/53X,'95% CONFIDENCE LIMITS'/11X,'VARIABLE',8X,'VALUE',
27X,'S.E.COEFF.',4X,'LOWER',8X,'UPPER')
1058 FORMAT(13X,A,4X,F10.5,5X,F9.4,3X,F9.4,3X,F9.4)
1062 FORMAT(10X,I4,1X,F7.2,F11.3,8X,F9.4)
1066 FORMAT(/10X,8(1H-),'OBSERVED & FITTED ',A,8(1H-)/54X,'RESI-'/1
10X,'NO',3X,'TIME (HR)',6X,'Z',6X,'OBS',4X,'FITTED',4X,'DUAL')
1068 FORMAT(7X,I5,2F10.3,1X,3F9.3)
1069 FORMAT(1H1,10X,'PRESSURE',4X,'LOG P',6X,'WC',7X,'REL K',5X,'LOG RK
1',6X,'ABS K',4X,'LOG KA',5X,'DIFFUS',5X,'LOG D')
1070 FORMAT(10X,E10.3,F8.3,F10.4,3(E13.3,F8.3))

```



```

      B(NP)=B(NP)/A2(NP)
      DO 260 I=NR,1,-1
        SS=0.0D0
        DO 250 J=I+1,NP
          SS=SS+A(I,J)*B(J)
250      CONTINUE
          B(I)=(B(I)-SS)/A2(I)
260 CONTINUE
C
C      ----- DONE, SOLUTION IS RETURNED IN B -----
300 RETURN
      END
C
C      -----
      SUBROUTINE MATINV(A,NP)
C
C      PURPOSE : TO INVERT J'*J
C      -----
      DOUBLE PRECISION A(6,6),INDX(6,2),P,AMAX
      DO 2 J=1,6
2      INDX(J,1)=0
      I=0
4      AMAX=-1.0D0
      DO 12 J=1,NP
        IF(INDX(J,1).NE.0.0) GO TO 12
6      DO 10 K=1,NP
        IF(INDX(K,1).NE.0.0) GO TO 10
8      P=DABS(A(J,K))
        IF(P.LE.AMAX) GO TO 10
        IR=J
        IC=K
        AMAX=P
10     CONTINUE
12     CONTINUE
        IF(AMAX) 30,30,14
14     INDX(IC,1)=IR
        IF(IR.EQ.IC) GO TO 18
        DO 16 L=1,NP
          P=A(IR,L)
          A(IR,L)=A(IC,L)
16     A(IC,L)=P
          I=I+1
          INDX(I,2)=IC
18     P=1./A(IC,IC)
          A(IC,IC)=1.0D0
          DO 20 L=1,NP
20     A(IC,L)=A(IC,L)*P
          DO 24 K=1,NP
            IF(K.EQ.IC) GO TO 24
            P=A(K,IC)
            A(K,IC)=0.0
            DO 22 L=1,NP
22     A(K,L)=A(K,L)-A(IC,L)*P
24     CONTINUE
            GO TO 4
26     IC=INDX(I,2)
            IR=INDX(IC,1)
            DO 28 K=1,NP
              P=A(K,IR)
              A(K,IR)=A(K,IC)
28     A(K,IC)=P
            I=I-1
30     IF(I) 26,32,26
32     RETURN
      END
C
C
      SUBROUTINE FLOW(BN,FC,NITT,NOCON,MDATA,MODE,ERRMB,HO,HOO)
      PARAMETER (NO=500,NZ=100)
      DOUBLE PRECISION FC(NO),HO(NO),HOO,HOO
      DIMENSION T(NZ),PE(NZ),TE(NZ),BN(12),D(NZ),COND(NZ)
      DIMENSION CAP(NZ),A(NZ),F(NZ),DEPTH(NZ)
      COMMON/ST1/IOBS,SMT1,ISTP1,IFLAG,OLDT
      COMMON/HYPR/PARM(6),RHOW,RHONW,IEQ

```

```

common/theta/at,rt,wcrt,wcst,khall
common/press/airp, pressu(10),tpress(10),npress,tprint(NZ),nprint
COMMON /AAA/delx,P(NZ),NN,AREA,LNS,PLL,SLL,PN1,TO(NO),
+ DNUL, NOB,NOB2,TMINIT,EPS1,EPS2,IINDEX(6),NVAR,CPLT,ITYPE(NO),
+ NOB1,NOBB,PIN(NZ),IRUN,ZD,BC_P,ZX
DATA NITMAX/10/,TOL1/0.50/,TOL2/0.0025/,NSTEPS/10000/,DELMAX/0.05/
DATA NOMAX/45/

C
C ----- DEPTH FOR DISTRIBUTION -----
DO 3 I=1,NN
C     IF (I .LE. LNS) DEPTH(I)=(I-1)*DELX1
C     IF (I .GT. LNS) DEPTH(I)=SLL+(I-LNS)*DELX2
        depth(i)=(i-1)*delx
3  CONTINUE
TREFF=0.123

        HOO=0.5*(HOO+HO(1))
DO 35 L=1,NN
C     IF (L .LE. LNS) THEN
C         P(L)=(-ZX+HOO-(SLL+PLL)*RHOW)+(L-1)*DELX1*RHOW
C     ELSE
C         P(L)=(-ZX+HOO-(SLL+PLL)*RHOW)+(SLL+(L-LNS)*DELX2)*RHOW
C     ENDIF
        P(L)=(-ZX+HOO-(SLL+PLL)*RHOW)+(L-1)*DELX*RHOW
35  CONTINUE

        if (airp .lt. 0) then
            pn1=HOO-pressu(1)
            bc_p=pressu(1)
        else
            pn1=HOO-airp
            bc_p=airp
        endif

C ----- UPDATE PARAMETER ARRAY -----
K=0
NU1=NVAR+1
NU2=NVAR*2
DO 2 I=NU1,NU2
    IF(IINDEX(I-NVAR).EQ.0) GO TO 2
    K=K+1
    BN(I)=BN(K)
2  CONTINUE
    PARM(1)=BN(7)
    PARM(2)=BN(8)
    PARM(3)=BN(9)
    PARM(4)=BN(10)
    PARM(5)=BN(11)
    PARM(6)=BN(12)

C ----- DEFINE INITIAL CONDITIONS & CALCULATE OUTFLOW
C ----- DURING SATURATED STAGE-----
NE=NN-1
iprint=1
ipress=2
PNB=PN1
DRAIN=0.0
NMB=0
ERRMB=0.0
EPSM=1.-EPS2
ISTP1=1
IOBS=1
QOUT=0.
IFLAG=0
SMT1=0
IF((NITT.GT.0).OR.(IRUN.GT.1)) GO TO 5
DO 4 I=1,NN
    PIN(I)=P(I)
4  CONTINUE
    NOB1=NOB-1
    IF(MDATA.LE.1) NOB1=NOB
5  DO 6 I=1,NN
    P(I)=PIN(I)
6  CONTINUE

```

```

      P(NN-1)=PNB
C
C      ----- SOLVE FOR FIRST STAGE OF OUTFLOW -----
      CUMDR=QOUT
      DO 8 I=1,NN
        PE(I)=P(I)
        IF (I .LE. LNS) THEN
C          X=(I-1)*DELX1
          X=(I-1)*DELX
          IF (KHALL .EQ. 0) T(I)=SPR(1,P(I),X)
          IF (KHALL .NE. 0) T(I)=SPRT(1,P(I))
        ENDIF
      8 CONTINUE
C
C      ----- DETERMINE AMOUNT OF WATER IN SAMPLE -----
      TMIN=AREA*TOTALM(T,DELX,LNS)
      TMINIT=TMIN+QOUT
      TMW0=TMINIT
      CUMQ0=0.
      CUMQ1=0.
      CUMQ2=0.
      DELT=DNUL
      DELMIN=0.00005*DNUL
      SUMT=SMT1+DELT
      ISTEP=ISTP1
C
C      ----- DYNAMIC PART OF PROGRAM -----
      10 NIT=0
      12 NIT=NIT+1
      DO 14 I=1,NN
        T(I)=PE(I)
C      ----- NODAL CONDUCTIVITY & CAPACITY -----
        IF (I .LE. LNS) THEN
C          X=(I-1)*DELX1
          X=(I-1)*DELX
          PR=0.5*(P(I)+PE(I))
C          COND(I)=SPR(2,PR,X)/DELX1
          COND(I)=SPR(2,PR,X)/DELX
C          CAP(I)=SPR(3,PR,X)*DELX1/DELT
          CAP(I)=SPR(3,PR,X)*DELX/DELT
        ELSE
C          COND(I)=CPLT/DELX2
          COND(I)=CPLT/DELX
          CAP(I)=0.0
        ENDIF
      14 CONTINUE
C
C      ----- CONSTRUCT GENERAL MATRIX EQUATION -----
      F(1)=(2.*CAP(1)+CAP(2))/6.
      A(1)=-0.5*(COND(1)+COND(2))
      D(1)=-A(1)+F(1)
      DO 16 I=2,NE
        F(I)=(CAP(I-1)+4.*CAP(I)+CAP(I+1))/6.
        A(I)=-0.5*(COND(I)+COND(I+1))
        D(I)=0.5*(COND(I-1)+2.*COND(I)+COND(I+1))+F(I)
      16 CONTINUE
      F(NN)=(CAP(NE)+2.*CAP(NN))/6.
      D(NN)=-A(NE)+F(NN)
      FNN=F(NN)
      F(1)=F(1)*P(1)-0.5*DELX*(COND(1)+COND(2))*RHOW
      DO 18 I=2,ne
        F(I)=F(I)*P(I)+0.5*DELX*(COND(I-1)-COND(I+1))*RHOW
      18 CONTINUE
C      IF (NN .NE. LNS) THEN
C      F(LNS)=F(LNS)*P(LNS)+(DELX1*COND(LNS-1)-DELX1*COND(LNS+1))*RHOW/2.
C      DO 19 I=LNS+1,NE
C      F(I)=F(I)*P(I)+0.5*DELX1*(COND(I-1)-COND(I+1))*RHOW
C      19 CONTINUE
C      ENDIF
      F(NN)=F(NN)*P(NN)+0.5*DELX*(COND(NE)+COND(NN))*RHOW
C
C      ----- LOWER BOUNDARY CONDITION -----
      20 PE(NN)=PNB

```

```

DRAIN=F(NN)-D(NN)*PE(NN)
F(NN)=PE(NN)
D(NN)=1.
ANE=A(NE)
F(NE)=F(NE)-ANE*PE(NN)
A(NE)=0.
C
C
C ----- SOLVE FOR NEW PRESSURE HEAD VALUES -----
22 DO 24 I=2,NN
   R=A(I-1)/D(I-1)
   D(I)=D(I)-R*A(I-1)
   F(I)=F(I)-R*F(I-1)
24 CONTINUE
   PE(NN)=F(NN)/D(NN)
   DO 26 I=2,NN
     J=NN-I+1
     PE(J)=(F(J)-A(J)*PE(J+1))/D(J)
26 CONTINUE
   DRAIN=DRAIN-ANE*PE(NE)
C
C
C ----- CHECK ITERATIVE PROCESS -----
28 DO 30 I=1,NN
   TOL=TOL1+TOL2*ABS(T(I))
   IF (ABS(PE(I)-T(I)) .GT. TOL) GO TO 32
30 CONTINUE
C   WRITE(21,1002) NIT,DELT,ISTEP,SUMT,(PE(I),I=1,NN)
   IF (DELT .LT. DELMIN) GO TO 38
   GO TO 46
32 IF (NIT .GE. NITMAX) GO TO 36
   DO 34 I=1,NN
     TEMP=EPS2*PE(I)+EPSM*TE(I)
     TE(I)=PE(I)
     PE(I)=TEMP
34 CONTINUE
   GO TO 12
36 NOCON=NOCON+1
   DELT=0.5*DELT
   IF (DELT.GE.DELMIN .AND. NOCON.LE.NOMAX) GO TO 42
   IF (NOCON .GT. NOMAX) WRITE(21,1007)
38 IF (DELT .LT. DELMIN) WRITE(21,1008) DELT,DELMIN,SUMT,NITT
   WRITE(21,1009)
   DO 40 I=1,NN
     IF (I .LE. LNS) X=(I-1)*DELX1
c     IF (I .GT. LNS) X=SLL+(I-LNS)*DELX2
c       x=(i-1)*delx
   WRITE(21,1010) I,X,P(I),PE(I)
40 CONTINUE
   MODE=9
   RETURN
42 SUMT=SUMT-DELT
   DO 44 I=1,NN
44 PE(I)=0.5*(P(I)+PE(I))
   GO TO 10
C
C
C -----
46 DRINC=AREA*DELT*DRAIN
   CUMDR=CUMDR+DRINC
C
C
C ----- calculate distribution of p and theta -----
c   if ((sumt.ge.tprint(iprint)) .and. (iprint.le.nprint) .and.
c     *(nprint.gt.0)) then
       write(24,1020) tprint(iprint)
       write(24,1022)
       do 31 i=1,lms
c         x=(i-1)*delx1
c         x=(i-1)*delx
         delf=(sumt-tprint(iprint))/delt
         prt=pe(i)-delf*(pe(i)-p(i))
         theta=spr(1,prt,x)
         write(24,1021) depth(i),prt,theta
31       continue
         do 33 i=lms+1,nn

```

```

                                write(24,1021) depth(i),pe(i)
33      continue
        iprint=iprint+1
    endif
C
C      ---- CALCULATE CUM. OUTFLOW IF IFLAG=1 ----
C      IF (IFLAG .EQ. 0) GO TO 50
    DO 47 I=IOBS,NOB
        IF (TO(I). GT. TO(IOBS)) GO TO 49
C      TERM=ZD/DELX1
        TERM=ZD/DELX
        NMIN=INT(TERM)+1
        NPLUS=MIN0(NMIN+1,NN)
        XINT=NMIN-TERM
        DELF=(SUMT-TO(I))/DELT
        TDRAIN=CUMDR-DELF*DRINC
C      DO 48 J=1,LNS
        X=(J-1)*DELX1
C      X=(J-1)*DELX
        PRT=PE(J)-DELF*(PE(J)-P(J))
        T(J)=SPR(1,PRT,X)
    48  CONTINUE
        IF (ITYPE(I) .EQ. 2) THEN
C      -----CUMULATIVE DRAINAGE-----
            TMIN=AREA*TOTALM(T,DELX,LNS)
            FC(I)=DBLE(TMINIT-TMIN)
C      IF (ITYPE(I) .EQ. 2) THEN
C      -----CUMULATIVE DRAINAGE-----
C      FC(I)=0.5*(CUMQ1+CUMQ0)
            HOO=0.5*(HO(I/2-1)+HO(I/2))
            PNB=HOO-BC_P
            ELSEIF (ITYPE(I) .EQ. 1) THEN
C      -----H(X,T)-----
                TPLUS=DELF*P(NPLUS)+(1.-DELF)*PE(NPLUS)
                TMIN=DELF*P(NMIN)+(1.-DELF)*PE(NMIN)
                FC(I)=0.5*SLR*RHONW-DBLE(XINT*TMIN+(1.-XINT)*TPLUS)
            ENDIF
    47  CONTINUE
    49  ERRMB=ERRMB+100.*((DBLE(TMINIT-TMIN)-TDRAIN)/DBLE(TMINIT
        *-TMIN))
        IOBS=I
        NMB=NMB+1
        IFLAG=0
C
C      ----- PREPARE FOR NEXT TIME STEP -----
    50  IF (IOBS.GT.NOBI .OR. ISTEP.GE.NSTEPS) GO TO 54
        DELCH=1.0
        IF (NIT .LE. 2) DELCH=1.25
        IF (NIT .GE. 6) DELCH=0.80
        DELCH=AMIN1(DELCH,DELMAX/DELT)
        DELT=DELT*DELCH
        DO 52 J=1,NN
            PE1=PE(J)-P(J)
            P(J)=PE(J)
C      PE(J)=P(J)+DELCH*PE1
    52  CONTINUE
        DO 53 J=1,LNS
C      X=(J-1)*DELX1
            X=(J-1)*DELX
            PRT=PE(J)
            T(J)=SPR(1,PRT,X)
    53  CONTINUE
        TMW1=AREA*TOTALM(T,DELX,LNS)
        CUMQ2=CUMQ1+(TMW0-TMW1)
        CUMQ0=CUMQ1
        CUMQ1=CUMQ2
        TMW0=TMW1
        sumt1=sumt
        sumt=sumt+delT
        if ((sumt.ge.tpress(ipress)).and.(ipress.le.npress)) then
            if (sumt1.eq.tpress(ipress)) then

```

```

c          pnb=pnb+pressu(ipress-1)-pressu(ipress)
          if (airp .lt. 0) then
              PNB=HOO-PRESSU(IPRESS)
              bc_p=pressu(IPRESS)
          else
              PNB=HOO-airp
              bc_p=airp
          endif
          ipress=ipress+1
          delt=dnul
          sumt=sumt1+delt
      else
          delt=tpress(ipress)-sumt1
          sumt=tpress(ipress)
      endif
  endif
  IF (SUMT .GE. TO(IOBS)) IFLAG=1
  ISTEP=ISTEP+1
  GO TO 10
C
C  -----
54 IF(ISTEP.GE.NSTEPS) WRITE(21,1014)NSTEPS,SUMT,NITT
58 DO 60 I=1,NN
    P(I)=PE(I)
60 CONTINUE
C
C  ----- CALCULATE THETA(h) AND/OR K(h) IF NOB2 > 0 -----
IF(NOB2.EQ.0) GO TO 64
N1=NOB+1
N2=NOB+NOB2
X=0.5*SLL
DO 62 I=N1,N2
    IF (ITYPE(I) .EQ. 3) FC(I)=SPR(1,TO(I),X)
    IF (ITYPE(I) .EQ. 4) FC(I)=SPR(2,TO(I),X)
62 CONTINUE
64 IF (NMB .NE. 0) ERRMB=ABS(ERRMB/FLOAT(NMB))
RETURN
C
C  -----
1001 FORMAT(11X,4E10.3)
1002 FORMAT(/11X,'PE(I) DURING ITERATION (NIT=',I3,' DELT=',E10.2,' IST
1EP=',I4,' SUMT=',E10.3,')'/(10X,10F11.3))
1003 FORMAT(11X,2F10.5)
1007 FORMAT(/11X,'TROUBLE CONVERGING, START AGAIN WITH DIFFERENT INITI
1AL VALUES ')
1008 FORMAT(/11X,8(1H*),'DELT =',E11.4,', IS LESS THAN DELMIN (=',E11.
14,')', EXECUTION TERMINATED AT TIME =',E11.4,' (NIT=)',I5)
1009 FORMAT(/11X,' LAST CALCULATED VALUES'/11X,22(1H*)/11X,'NODE',5X,'D
1EPth',9X,'P(I)',9X,'PE(I)')
1010 FORMAT(11X,I4,F10.2,2(3X,F12.4))
1014 FORMAT(/11X,'NO. OF STEPS EXCEEDS',I4,' AT TIME=',F10.3,' DURING
1ITERATION',I4)
1016 FORMAT(11X,I5,F10.3,2(2X,F10.3))
1020 FORMAT(/,' DISTRIBUTION OF PRESSURE AND WATER AFTER T = ',F8.4,
1' HOUR'/)
1021 FORMAT(T2,F8.2,F8.1,F8.3)
1022 FORMAT(T2,' DEPTH          P      THETA')
END
C
C  -----
C
FUNCTION SPR(N,PR,X)
C
C  PURPOSE: TO CALCULATE THE SOIL-HYDRAULIC PROPERTIES
C
COMMON/HYPR/A,R,WCR,WCS,CONDS,EXPL,RHOW,RHONW,IEQ
DATA SS/0.0/
C..
C... VAN GENUCHTEN MODEL
      IF (IEQ .EQ. 1) THEN
          S=1.-1./R

```

```

        P=-(X*RHONW-PR)
        IF(P)1,10,10
1      P=-P
        THETA=(1.+(A*P)**R)**(-S)
        IF(N-2) 2,4,6
2      SPR=WCR+(WCS-WCR)*THETA
        RETURN
4      T=1.-THETA*(A*P)**(R-1.)
C      IF (THETA .LT. WCR) T=S*THETA**(1./S)
        cond=conds*theta**expl*t*t
        SPR=cond
C      SPR=AMAX1(COND,1.E-08)
        RETURN
6      T=1.+(A*P)**R
        WC=WCR+(WCS-WCR)*THETA
        SPR=(WC-WCR)*(R-1.)*A*(A*P)**(R-1.)/T + WC*SS/WCS
        RETURN
10     GO TO (12,14,16,18),N
12     SPR=WCS
        RETURN
14     SPR=CONDS
        RETURN
16     SPR=SS
        RETURN
18     THETA=(P-WCR)/(WCS-WCR)
        S=R/(1.-R)
        IF(THETA.GT.0.999999) GO TO 20
        SPR=-(THETA**S-1.)*(1./R)/A
        RETURN
20     SPR=0.
        RETURN
    ENDIF
C...
C... LOGNORMAL MODEL
        IF (IEQ .EQ. 2) THEN
            P=-(X*RHONW-PR)
            IF(P)188,1088,1088
188     P=-P
            psim=10.**a
            theta=qnorm((log(p/psim))/r)
            IF(N-2) 288,488,688
288     SPR=WCR+(WCS-WCR)*THETA
            RETURN
488     t=qnorm((log(p/psim))/r+r)
            cond=conds*theta**expl*t*t
            SPR=cond
c      SPR=AMAX1(COND,1.E-08)
            RETURN
688     t=exp(-1.*(log(p/psim))**2./(2.*r**2.))
            spr=(wcs-wcr)/(2.*3.141592654)**0.5/r/p*t
            RETURN
1088    GO TO (1288,1488,1688,1888),N
1288    SPR=WCS
            RETURN
1488    SPR=CONDS
            RETURN
1688    SPR=SS
            RETURN
1888    THETA=(P-WCR)/(WCS-WCR)
            S=R/(1.-R)
            IF(THETA.GT.0.999999) GO TO 2088
            SPR=-(THETA**S-1.)*(1./R)/A
            RETURN
2088    SPR=0.
            RETURN
    ENDIF
C
    END
C
C -----
C
function sprt(n,pr)
c

```

```

c
c      purpose: to calculate the fixed retention curve and the capacity
c
      common/theta/at,rt,wcrt,wcst,khall
      COMMON/HYPR/A,R,WCR,WCS,CONDS,EXPL,RHOW,RHONW,IEQ
      data ss/1.e-07/
      write(6,*) 'The lognormal model does NOT support this option !!!'
      s=1.-1./rt
      if(pr)1,10,10
1     p=abs(pr)
      theta=(1.+(at*p)**rt)**(-s)
      if(n-2) 2,2,6
2     sprt=wcrt+(wcst-wcrt)*theta
      return
6     t=1.+(at*p)**rt
      wc=wcrt+(wcst-wcrt)*theta
      sprt=(wc-wcrt)*(rt-1.)*at*(at*p)**(rt-1.)/t + wc*ss/wcst
      return
10    go to (12,14,16,18),n
12    sprt=wcst
      return
14    sprt=conds
      return
16    sprt=ss
      return
18    theta=(pr-wcrt)/(wcst-wcrt)
      s=rt/(1.-rt)
      if(theta.gt.0.999999) go to 20
      sprt=-(theta*s-1.)*(1./rt)/at
      return
20    sprt=0.
      return
      end

c
c      -----
c
      FUNCTION TOTALM(WC,DELX,LNS)
c
c      PURPOSE: TO EVALUATE TOTAL MOISTURE IN PROFILE
c      -----
      PARAMETER (NO=500,NZ=100)
      DIMENSION WC(NZ)
      TOTALM=0.0
      N=1
      NS=LNS-2
      IF(MOD(LNS,2).NE.0.0) GO TO 4
c      TOTALM=3.*DELX1*(WC(1)+3.*WC(2)+3.*WC(3)+WC(4))/8.
c      TOTALM=3.*DELX*(WC(1)+3.*WC(2)+3.*WC(3)+WC(4))/8.
      N=4
4     DO 10 I=N,NS,2
c      TOTALM=TOTALM+DELX1*(WC(I)+4*WC(I+1)+WC(I+2))/3.
c      TOTALM=TOTALM+DELX*(WC(I)+4*WC(I+1)+WC(I+2))/3.
10    CONTINUE
      RETURN
      END

c
c      function qnorm(x)
c      implicit real*8 (a-h,o-z)
      z=abs(x/2.**(.5))
      t=1./(1.+0.5*z)
      erfc=t*exp(-z*z-1.26551223+t*(1.00002368+t*(0.37409196+
*      t*(.09678418+t*(-.18628806+t*(.27886807+t*(-1.13520398+
*      t*(1.48851587+t*(-.82215223+t*.17087277)))))))
      if(x.lt.0.) erfc=2.-erfc
      qnorm=erfc/2.
      return
      end

```


Appendix 2:

Preprint of

Minasny, B., J. W. Hopmans, T. Harter, S. O. Eching, A. Tuli, and
M. A. Denton, Neural networks prediction of soil
hydraulic functions from multi-step outflow data, Soil
Sci. Soc. of America Journal, 2004 (in print)

Neural Networks Prediction of Soil Hydraulic Functions for Alluvial Soils Using Multistep Outflow Data

B. Minasny, J. W. Hopmans,* T. Harter, S. O. Eching, A. Tuli, and M. A. Denton

ABSTRACT

Indirect methods for prediction of soil hydraulic properties play an important role in understanding site-specific unsaturated water flow and transport processes, usually via numerical simulation models. Specifically, pedotransfer functions (PTFs) to predict soil-water retention have been widely developed. However, few datasets that include unsaturated hydraulic conductivity data are available for prediction purposes. Moreover, those available employ a variety of measurement techniques. We show that prediction of soil-water retention and unsaturated hydraulic conductivity curves from basic soil properties can be improved if hydraulic data are determined by a single measurement method that is consistently applied to all soil samples. Here, we present a unique dataset that consists of 310 soil-water retention and unsaturated hydraulic conductivity functions, all of which were obtained from the multistep outflow method. With this dataset, neural networks coupled with bootstrap aggregation were used to predict the soil-water retention and hydraulic conductivity characteristics from basic soil properties, that is, sand, silt, and clay content, bulk density (ρ_b), saturated water content, and saturated hydraulic conductivity. The prediction errors of water content were about 3 to 4% by volume. Unsaturated hydraulic conductivity predictions improved significantly when a so-called performance-based algorithm was utilized to minimize residuals of soil hydraulic data rather than hydraulic parameters. The root mean squared of residuals for predicted values of water content and unsaturated hydraulic conductivity were reduced by about 50% when compared with predicted hydraulic functions using a published neural networks program *Rosetta*. Results from a sensitivity analysis suggest that the hydraulic parameters are mostly sensitive to sand content and saturated water content.

THE DYNAMIC SIMULATION of soil hydrological processes is increasingly being used to predict the unsaturated soil-water regime in environmental applications and in crop yield modeling to study agronomic management practices. Models that simulate unsaturated water flow in soil have been widely developed and adopted. Essential to their application is the availability of unsaturated soil hydraulic properties, that is, the soil-water retention and unsaturated hydraulic conductivity functions.

The soil hydraulic properties are usually represented by a parametric model. Although many of these have been developed (Kosugi et al., 2002), the most com-

monly used soil-water retention model is the one introduced by van Genuchten (1980):

$$\theta(h) = \theta_r + \frac{\theta_s - \theta_r}{(1 + |\alpha h|^n)^m}, \quad [1]$$

where $\theta(h)$ denotes the volumetric water content ($L^3 L^{-3}$) at the corresponding soil-water matric head h (L), θ_r and θ_s are the residual and saturated water content, α is a scaling parameter (L^{-1}), n is a curve shape factor ($-$), and m is an empirical constant that can be related to n , or $m = 1 - 1/n$. When substituted into the unsaturated hydraulic conductivity (K) model of Mualem (1976), the unsaturated hydraulic conductivity is described by:

$$K(S_e) = K_o S_e^l [1 - (1 - S_e^{1/m})^m]^2, \quad [2]$$

where S_e denotes the normalized water content, $S_e = (\theta - \theta_r)/(\theta_s - \theta_r)$, l is a pore geometry parameter, and K_o is a matched saturated hydraulic conductivity ($L T^{-1}$), extrapolated from fitted unsaturated K values. This fitted value for K_o is usually smaller than the true saturated conductivity, K_s , since the latter is largely controlled by soil structural elements, such as cracks and macropores. Therefore, K_o is usually considered a fitting parameter (van Genuchten and Nielsen, 1985).

Soil hydraulic properties, typically measured for small core samples with a length scale of 10^{-1} m or smaller, vary greatly in space (Nielsen et al., 1973). Consequently, a large number of samples is needed to characterize fields with length scales of 10^2 m or larger. However, measurement of soil hydraulic properties is generally difficult, time consuming, and expensive, so that few complete datasets are available. Therefore, indirect methods have been pursued that predict soil hydraulic properties from more easily measured soil parameters. An excellent review of indirect methods, including the application of neural networks, is presented by Leij et al. (2002). Wösten (1990) postulated that the use of these indirect methods is acceptable as long as it includes the uncertainty of the estimations.

Specifically, the use of PTFs was introduced by Bouma (1989). These are predictive functions of certain soil properties estimated from other simpler and routinely-measured soil properties that are generally available (McBratney et al., 2002). The application of PTFs to predict soil-water retention using basic soil properties such as sand, silt, and clay content, and ρ_b is now commonly used in soil science studies because predictions of either water content at a specific soil-water matric potential or water retention parameters (Schaap et al., 1998) have been quite successful (Romano and Palla-

B. Minasny, Faculty of Agriculture, Food, and Natural Resources, McMillan Building A05, The Univ. of Sydney, NSW 2006, Australia; J.W. Hopmans, T. Harter, and M.A. Denton, Hydrology Program, Dep. of Land, Air, and Water Resources, 123 Veihmeyer Hall, Univ. of California, Davis, CA 95616; S.O. Eching, Dep. of Water Resources, Water Use Efficiency Office, 901 P Street, Third Floor, P.O. Box 942836, Sacramento, CA 94236-0001; A. Tuli, Dep. of Environmental Sci., 2217 Geology Building, Univ. of California, Riverside, CA 92521. Received 12 June 2003. *Corresponding author (jwhopmans@ucdavis.edu).

Published in Soil Sci. Soc. Am. J. 68:— (2004).

© Soil Science Society of America
677 S. Segoe Rd., Madison, WI 53711 USA

Abbreviations: ρ_b , bulk density; MR, mean residual; OM, organic matter; PTF, pedotransfer function; RMSR, root mean squares of residual.

dino, 2002). Also the saturated hydraulic conductivity can be predicted reasonably well from such basic soil properties. Models such as Mualem's Eq. [2] are subsequently used to predict the unsaturated hydraulic conductivity from water retention data. However, more accurate unsaturated conductivity functions are expected if these are predicted directly from measured K values, for example, by neural network analysis.

Only few studies show the application of PTFs to predict unsaturated hydraulic conductivity data from basic soil properties. Among those are Bloemen (1980) in the Netherlands, who correlated parameters of the Brooks-Corey function to soil texture and organic matter (OM) content. Similar techniques were applied by Gonçalves et al. (1997) in Portugal, Jaynes and Tyler (1984) for glacial till soil in U.S., and Vereecken (1995) in Belgium using alternative analytical expressions for the $K(h)$ function. Among the first to use neural networks to predict K was Tamari et al. (1996), who included horizon designation, soil textural class, OM content, ρ_b , and water content at specific soil-water matric potential values as input variables. Wösten et al. (1999) extracted data from the European soil hydraulic database to derive van Genuchten function parameters using sand, silt, and clay content, soil ρ_b , and organic carbon content. Schaap and Leij (2000) predicted parameters l and K_o from sand, silt, and clay content, and ρ_b using neural network analysis. The latter study concluded that K -predictions were improved if soil-water retention function parameters were included as input parameters. The performance of different published PTFs in predicting $K(h)$ for selected German soils was evaluated by Wagner et al. (2001).

Among the main issues that limit the accurate prediction of unsaturated hydraulic conductivity is the lack of a soil hydraulic database that includes measured unsaturated conductivity data. Public domain databases such as UNSODA (Nemes et al., 2001) do provide both hydraulic properties and basic soil physical data from different parts of the world for various soil types. However, the unsaturated hydraulic conductivity values that are included in these data sets are generally obtained by many different measurement techniques. Typically, these methods are limited by specific assumptions and apply to relatively narrow water content ranges, so that K -prediction results are expected to depend on measurement type (Mallants et al., 1997). Although the measurement type effect applies to prediction of soil-water retention data as well, its effect may not be as consequential, because the predicted θ range of the retention curve is much smaller than the predicted unsaturated K range.

Thus, when PTFs are used to predict soil hydraulic data, uniformity of measurement methods is desirable. Specifically, Schaap and Leij (1998) showed that the PTF prediction depended on the training data set, whereas the accuracy was largely controlled by data quality. It is expected that improved prediction accuracies will be obtained when a training data set is used with soil hydraulic and related physical properties that are determined from similar measurement techniques.

In this paper, we examine the simultaneous prediction of soil-water retention and unsaturated hydraulic conductivity from soil hydraulic data that were estimated with the multistep outflow method (Eching et al., 1994b), whereby the soil hydraulic parameters of Eq. [1] and [2] are estimated with an inverse modeling technique. Characteristically, this measurement technique provides estimated soil hydraulic parameters from the matching of experimental observations of transient water flow with numerical modeling results.

The presented measured data span 310 soil samples, largely from three different datasets, representing a variety of alluvial soils and soil textures across three different regions in the California San Joaquin Valley. The main objective of the presented analysis is to show that neural network prediction of both soil-water retention and unsaturated hydraulic conductivity will improve if all analyzed data are obtained by identical measurement methods.

METHODS

Multistep Outflow Method

Many laboratory and field methods exist to determine the highly nonlinear soil hydraulic functions of the vadose zone, represented by soil-water retention and unsaturated hydraulic conductivity curves. Most methods are either static (soil-water retention) or steady state (unsaturated hydraulic conductivity), and consequently, measurements are usually time-consuming and limited to the wet water content range. The multistep outflow method applies inverse modeling for indirect estimation of both water retention and hydraulic conductivity curves in a single transient drainage experiment. The multistep outflow method has become an attractive method for estimating soil hydraulic properties (Crescimanno and Iovino, 1995; Vereecken et al., 1997).

The outflow method originates from the one-step outflow experiment of Gardner (1956). Kool et al. (1985) formulated the inverse solution for the one-step pressure outflow experiment using a numerical solution of transient water flow, that is, Richards' equation, with the van Genuchten model of Eq. [1] and [2] representing the soil hydraulic properties. Starting with initial parameter estimates, a numerical model solution computes the theoretical drainage outflow rate of an initially-saturated soil sample. Parameters of the soil hydraulic functions are updated iteratively in an optimization routine, thereby continuously reducing the residuals until a predetermined convergence criterion (reduction in objective function value between two consecutive iterations) is achieved.

Kool et al. (1985) successfully applied the inverse method to estimate θ_r , α , and n from cumulative outflow measurements. Van Dam et al. (1994) proposed the multistep outflow method, by increasing the air pressure in multiple smaller steps. Their results showed that the outflow data from a multistep experiment provided sufficient information to yield a unique solution. Alternatively, Eching et al. (1994b) demonstrated that unique solutions were obtained if the multistep outflow method was combined with automated soil-water matric head measurements of the draining soil core.

A comprehensive review of inverse modeling for estimation of soil hydraulic properties, including one-step and multistep methods was presented by Hopmans et al. (2002). Although relatively complex, inverse modeling can provide quick results. As an additional advantage, inverse modeling for soil hydro-

lic characterization allows the simultaneous estimation of both the soil-water retention and unsaturated hydraulic conductivity function from a single transient experiment. The inverse method mandates combination of experimentation with numerical modeling, thus requiring both accurate experimental procedures and advanced numerical modeling and optimization algorithms. Since the optimized hydraulic functions are mostly needed as input to numerical flow and transport models for prediction purposes, it has the added advantage that the hydraulic parameters are estimated by similar numerical models. In addition, the parameter optimization procedure provides a confidence interval of the optimized parameters, although their interpretation may be misleading. Some caution must be exercised when applying the multistep outflow method. First, laboratory measurements, although accurate, provide hydraulic information for a relatively small soil core, detached from its surroundings. Moreover, as is the case for any method, the parameter estimates are only valid for the range of the experimental conditions, and care must be exercised in their extrapolation. Finally, inverse problems for parameter estimation of soil hydraulic functions can be ill posed because of experimental design, measurement, and model errors.

Training Dataset

The presented 310 soil hydraulic data were collected from three different field projects. The first dataset consists of 144 undisturbed soil samples that were collected from seventy two 64- by 64-m plots at two depths (25 and 50 cm) in a 40-ha field (Tuli et al., 2001a). This Long Term Research on Agricultural Systems (LTRAS) project was conducted at the Russell Ranch of the University of California near Davis, CA, to study the long-term effects of irrigation and nitrate application to the sustainability of California agriculture. The field includes three different soil series: the Yolo (fine-silty, mixed, superactive, nonacid, thermic Mollic Xerofluvents), the Rincon (fine smectitic, thermic Mollic Haploxeralfs), and the Brentwood (fine, smectitic, thermic Typic Haploxerepts). Within each 64- by 64-m plot, 8.25-cm i.d. and 6-cm-long soil cores were collected with a soil core sampler. The range of values of the main soil physical properties as obtained from these soil cores were: ρ_b , 1.22 to 1.66 g cm⁻³; OM, 0.43 to 1.63%; saturated hydraulic conductivity, 0.0002 to 17.7900 cm h⁻¹; saturated water content, 0.32 to 0.50 cm³ cm⁻³; sand (50–2000 μ m), 11 to 56%; silt (2–50 μ m), 34 to 80%; and clay (<2 μ m), 3 to 22%.

The second data set consists of 88 soil cores collected from a 32-ha furrow-irrigated field (Diener) on the west side of the San Joaquin Valley (Eching et al., 1994a), near Five Points, CA. The soil is of the Panoche series (fine-loamy, mixed, superactive, thermic Typic Haplocambids), having very deep and well-drained uniform profiles with a wide range of textures. Soil texture varied from a silty loam and sandy clay loam on the south east side of the field to a loamy sand and sandy loam with patches of silty clay, clay loam, and silty clay in the rest of the field. Undisturbed soil cores were taken from the 0.3- and 0.6-m soil depth at 44 locations, uniformly distributed within the irrigated field. The range of values of the main soil physical properties as obtained from these soil cores were: ρ_b , 1.26 to 1.87 g cm⁻³; OM, 0.03 to 0.18%; saturated water content, 0.32 to 0.54 cm³ cm⁻³; sand, 13 to 99%; silt, 1 to 76%; and clay, 1 to 15%. No saturated hydraulic conductivity data were available for the Diener dataset. Extracted core locations in the field were grouped into clays (6 locations), loams (12 locations), and sands (26 locations).

The third data set consists of 69 sediment cores. Of the three data sets, this is the only data set representing unsaturated sediments below the root zone. The core samples represent

unsaturated sediments in their native, anthropogenically unaltered depositional environment. Continuous cores were extracted with a Geoprobe Systems (Salina, KS) direct push drill rig. A Geoprobe Macrocore sampler (5.2-cm o.d.) containing a PVC liner (3.8-cm i.d.) was driven in 1.2-m intervals through unsaturated sediments to a depth of >15 m. Sediment cores were obtained from 18 locations spaced 3 to 12 m apart within a 1-ha orchard at the Kearney Field Station (Parlier) in the San Joaquin Valley, CA. The location overlies the near-distal part of the Kings River alluvial fan emanating from the Kings River watershed at the foot of the generally granitic Sierra Nevada mountain range. The continuous cores were cut in 10-cm long core sections that were fitted within PVC and aluminum sleeves to fit a 5.1-cm i.d. Tempe pressure cell (Tuli et al., 2001b). The range of values of the main soil physical properties as obtained from these soil cores were: ρ_b , 1.26 to 1.87 g cm⁻³; OM, 0.01 to 0.20%; saturated water content, 0.22 to 0.47 cm³ cm⁻³; saturated hydraulic conductivity, 0.002 to 30.0 cm h⁻¹; sand, 13 to 98%; silt, 1 to 76%; and clay, 1 to 17%. Five major textural units were distinguished in the cores: sand, loamy sand, sandy loam, silt/silt loam/loam/silty clay loam, clay loam/clay, and variably thick hardpan at the 3- to 5-m depth. A former alluvial channel bed of limited width and consisting of clean medium sand was encountered at the 7- to 10-m depth. Nine additional soil data were included from Eching et al. (1994b) and Corwin et al. (2003).

For each core sample, soil properties and hydraulic functions were determined with the following procedure. Upon saturation, the soil cores were placed on a screen to measure the saturated hydraulic conductivity (K_s) with the constant head method (Klute & Dirksen, 1986). After completion of the saturated hydraulic conductivity measurement, the samples were assembled in Tempe pressure cells for estimation of soil-water retention and unsaturated hydraulic conductivity function using the multistep outflow method. The samples were resaturated with the 0.01 M CaCl₂ solution by wetting through a bottom porous membrane assembly. For Datasets 1 and 2, the bottom plate consisted of a 1-bar ceramic plate. For the third dataset, the bottom assembly included a thin porous nylon membrane with low hydraulic resistance (Hopmans et al., 2002). A positive air pressure was applied to the top of the cell, while cumulative water outflow is automatically recorded from a pressure transducer that was installed in the bottom of a burette. The soil-water matric head inside the draining soil core was simultaneously measured with a miniature tensiometer connected to a pressure transducer. The multistep pressure increments were determined by soil texture, but maximum air pressures did generally not exceed 600 cm. The air pressure was increased when the cumulative outflow curve approached a plateau value, indicating near-hydraulic equilibrium. With the transient soil-water matric head and cumulative drainage data, the parameters of the soil-water retention and unsaturated hydraulic conductivity functions were estimated from the inverse solution of the Richards' equation as presented in Eching et al. (1994b) and Hopmans et al. (2002). During the optimization, θ_s was fixed to its measured value whereas the soil tortuosity-connectivity parameter, l , was assumed to be 0.5. Therefore, the optimized parameters were θ_r , α , n , and K_o . The final dataset includes weight percentages of sand, silt, and clay content, and field dry ρ_b as determined from standard methods (Klute & Dirksen, 1986), measured θ_s and K_s , and optimized van Genuchten parameters θ_r , α , n , and K_o .

The statistics of the complete dataset are given in Table 1, whereas the soil textural distribution is presented in Fig. 1. The textural range of the combined sample set is dominated by sands to silt loams. The multistep outflow method is typi-

Table 1. Statistics of the complete training dataset.†

Variables	Units	Average	SD	Min.	Max.
Sand content	% weight	46	23.6	6	100
Silt content	% weight	41	20.3	0	80
Clay content	% weight	13	7.3	0	55
Bulk Density (ρ_b)	g cm^{-3}	1.51	0.14	1.13	1.87
Residual water content (θ_r)	$\text{cm}^3 \text{cm}^{-3}$	0.17	0.11	0.00	0.42
Saturated water content (θ_s)	$\text{cm}^3 \text{cm}^{-3}$	0.39	0.06	0.22	0.55
Scalding parameter (α)	cm^{-1}	0.019	0.018	0.001	0.124
Curve shape factor (n)	—	2.048	1.063	1.057	7.641
$\log_{10}(K_s)^\ddagger$	$\log_{10} (\text{cm h}^{-1})$	-0.68	0.99	-3.40	2.00
$\log_{10}(K_s)^\S$	$\log_{10} (\text{cm h}^{-1})$	-0.21	0.87	-3.77	1.86

† Number of samples, $N_s = 310$, except for $\log(K_s)$, for which $N_s = 219$.

‡ K_s , matched saturated hydraulic conductivity.

§ K_s , saturated hydraulic conductivity.

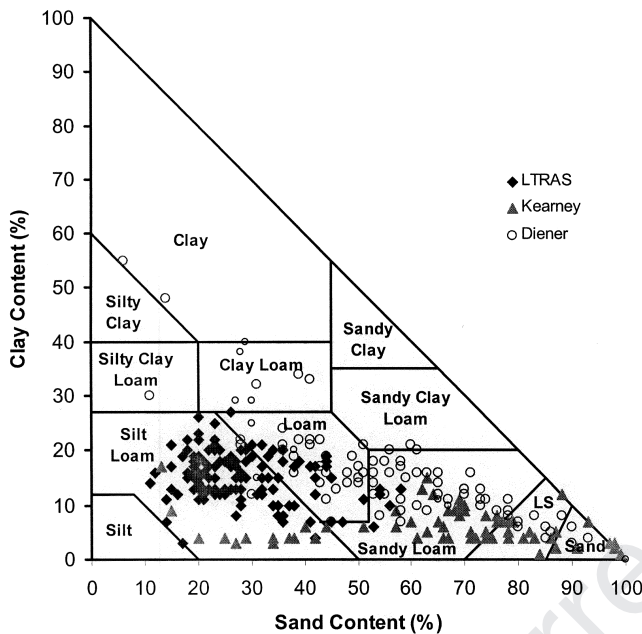


Fig. 1. Particle size distribution of the training dataset. To determine soil type, find intersection of lines, parallel to main coordinate axes.

cally not suitable for soil hydraulic property measurement of clayey soils because the maximum applied pressure step will generally not exceed 600 to 700 cm. The texture triangle shows the textural differences between the three data. The LTRAS samples are dominantly silty loam and loamy soils. The sampled Kearney soils are low in clay content, whereas the Diener samples consist mainly of loamy and sandy loam soils. For the neural network analysis, soil-water retention and unsaturated hydraulic conductivity data were extracted from the set of hydraulic functions (Fig. 2a,b) at discrete matric pressure head values: 0, 40, 60, 80, 200, 400, and 600 cm. The textural differences between the three datasets are readily apparent in Fig. 2. Specifically, the finer-textured soil materials of the LTRAS site have high soil-water retention, while the Kearney soils with their low clay content have the smallest water retention and highest hydraulic conductivity.

Neural Network Analysis

In the past decade, artificial neural networks have become an alternative method for the prediction of soil properties (Pachepsky et al., 1996; Schaap et al., 1998). A neural network is modeled after the functioning of the nervous system. Through a complex mathematical structure of interconnecting layers, knowledge is acquired through a learning process by

which interneuron connection strengths (weights) are used to store knowledge (Ripley, 1996).

The feed-forward neural networks that is applied in this study consists of a set of input units, \mathbf{x} , representing the input variables, and a set of output units, \mathbf{y} , representing the output variables, interconnected by hidden units, \mathbf{z} . Each set of the three types of units are arranged in layers. The mathematical model consists of a set of operations or network that is presented in Eq. [3]. First, an input vector \mathbf{x} is multiplied by weighting factors that are assembled in array \mathbf{W} , resulting in the hidden unit vector \mathbf{z} . In a second step, this vector \mathbf{z} is passed to a layer containing the activation or transfer function, f , which produces \mathbf{r} . Finally, in the third step, the target vector \mathbf{y} is computed from a linear combination of \mathbf{r} , with the weighting factors in array \mathbf{U} , or:

$$\begin{aligned} z_j &= \sum_{l=1}^{N_i} w_{jl} x_l + w_{j0}, \quad j = 1, \dots, N_h \\ r_j &= f(z_j), \quad j = 1, \dots, N_h \\ y_k &= \sum_{j=1}^{N_h} u_{kj} r_j + u_{k0}, \quad k = 1, \dots, N_o \end{aligned} \quad [3]$$

where N_i , N_h , and N_o denote the number of input variables, hidden units, and number of output variables, respectively. The bias values w_{j0} and u_{k0} provide for offsets for z_j and y_k , respectively. The transfer function is usually a sigmoidal function that is selected such that it accommodates the nonlinearity of the specific input–output relationship. The function that is commonly used is the hyperbolic tangent, or

$$f(z_j) = \tanh(z_j) = 1 - \frac{2}{1 + \exp(2z_j)} \quad [4]$$

The advantage of neural networks is that they can be used to predict one or more output types through a flexible network of weights, transfer functions, and input variables without a priori assuming a specific relationship between input and output and without making specific assumptions about the statistical distribution of input or output variables. Instead, the network is trained on a training dataset to find the relationship between input and output by optimizing the weighting factors in arrays \mathbf{W} and \mathbf{U} in Eq. [3] through minimization of the differences between measured and predicted output variables. Once the weights of the neural network have been determined, it can be used for prediction of output from input variables other than the training set.

Neural networks also have significant disadvantages that must be taken into consideration. First, their interpretation is often difficult and subjective, as the fitting with the transfer function is a black-box approach. Second, as is usually the case in optimization, the sets of optimized weighting factors are not necessarily mathematically unique because of the likelihood of convergence at local minima. Consequently, different initial weight values may yield different neural network results that deviate from the global minimum. To avoid non-uniqueness of the final solution, many network predictions can be obtained from multiple realizations of the input dataset by the bootstrap technique, also known as bagging (Breiman, 1996).

Neural Network Training of Soil Hydraulic Parameters

The objective of the presented study is to train the neural network so that the parameter vector $\mathbf{p} = [\theta_r, \theta_s, \alpha, n, K_0]$ can be predicted from a basic soil property vector \mathbf{x} that includes soil texture, ρ_b , saturated water content, and saturated hydraulic

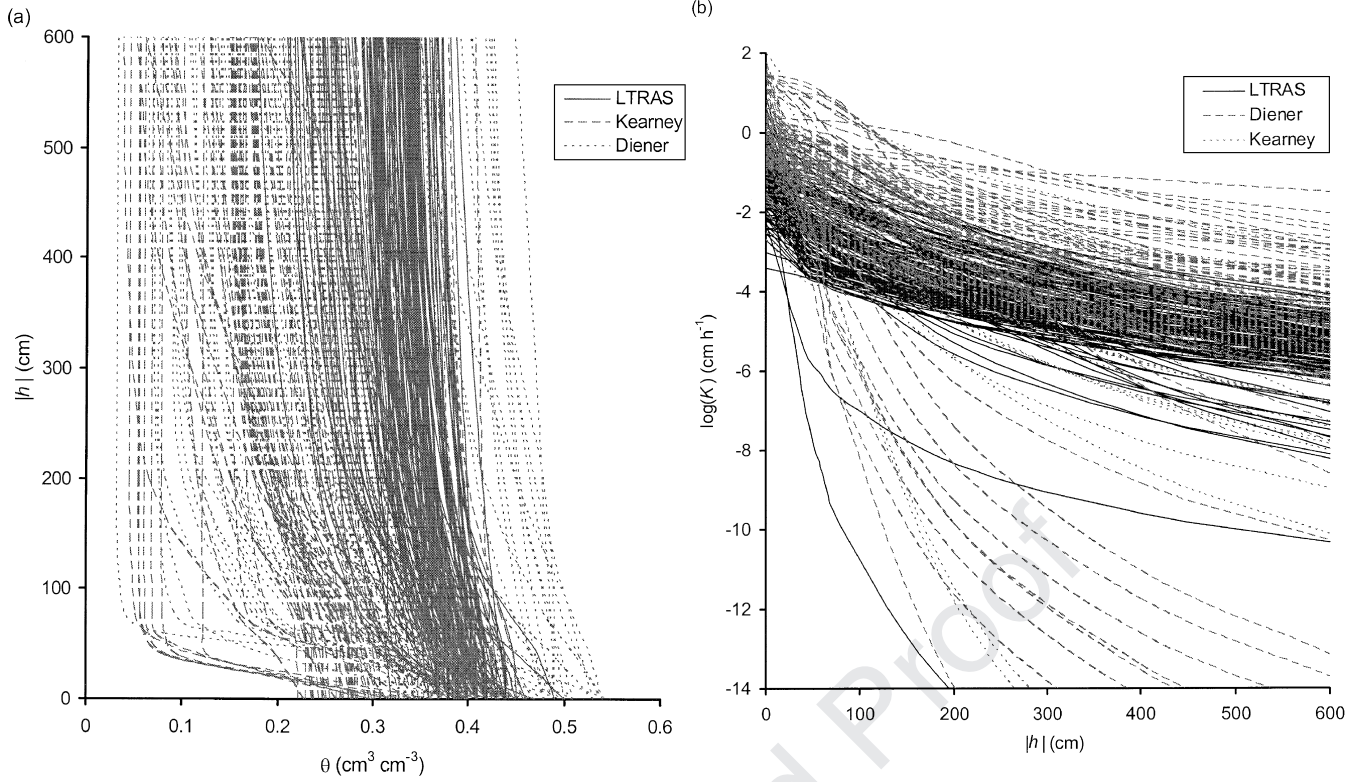


Fig. 2. (a) Soil-water retention, and (b) unsaturated hydraulic conductivity curves of the training dataset, making distinction between Long Term Research on Agricultural Systems (LTRAS), Kearney, and Diener datasets. θ , water content; h , soil-water matric head; K , hydraulic conductivity.

lic conductivity. Conventionally, this is done by optimization of the neural network weights so that the objective function that includes the sum of squares of the residuals between the measured and predicted parameters is minimized, or

$$O(\mathbf{W}, \mathbf{U}) = \sum_{i=1}^{N_s} \sum_{k=1}^{N_o} [\hat{\mathbf{p}}_{ik}(\mathbf{x}_i) - \mathbf{p}_{ik}]^2, \quad [5]$$

where N_s denotes the number of samples, N_o is the number of output parameters, and $\hat{\mathbf{p}}(\mathbf{x})$ is the output vector with the predicted parameters, as determined from the input vector \mathbf{x} .

Because the parameters in \mathbf{p} are highly nonlinear and correlated, thus possibly nonidentifiable, a fitted parameter set does not warrant an equally good prediction of soil hydraulic data. Therefore, for estimation of the soil-water retention curves, Minasny and McBratney (2002a) proposed an alternative objective function for training neural networks to predict the van Genuchten parameters from the basic input data. Instead of minimizing the hydraulic parameters, the objective function operates on the residuals of the measured and predicted soil-water retention data, that is, $\theta(h)$ data pairs. They called this the *Neuro-m* method, which was referred to by Romano and Palladino (2002) as having a performance-based objective function.

The *Neuro-m* method is extended in this study to simultaneously predict water retention and unsaturated hydraulic conductivity, with the following objective function:

$$O(\mathbf{W}, \mathbf{U}) = \sum_{i=1}^{N_i} \sum_{s=1}^{N_d(i)} \frac{[\hat{\theta}_{is}(\mathbf{x}_i, h_{is}, \mathbf{p}_i) - \theta_{is}(h_{is})]^2}{\sigma^2(\theta)} + \frac{[\log \hat{K}_{is}(\mathbf{x}_i, h_{is}, \mathbf{p}_i) - \log K_{is}(h_{is})]^2}{\sigma^2(\log K)}, \quad [6]$$

where $N_d(i)$ defines the number of water retention and conductivity data at corresponding soil-water matric head values

of soil sample i , and $\hat{\theta}(\mathbf{x}, h, \mathbf{p})$ and $\log \hat{K}(\mathbf{x}, h, \mathbf{p})$ denote the predicted water content and unsaturated hydraulic conductivity values at matric head h with the fitted parameter vector \mathbf{p} , calculated via the neural network from the input vector \mathbf{x} . Reciprocal values of the variance, σ^2 , of the respective measurements are used as weights to account for differences in magnitude between θ and $\log K$. Equation [6] was minimized with a modified version of the Levenberg-Marquardt method.

Values of K were log-transformed because K is generally found to be log-normal distributed (Schaap and Leij, 2000), so that they were computed from Eq. [2] to yield

$$\log[K(S_e)] = \log(K_0) + l \log(S_e) + 2 \log[1 - (1 - S_e^{1/m})^m] \quad [7]$$

where S_e is computed from the corresponding h value. For all unsaturated hydraulic conductivity functions, l was fixed to 0.5. Log transformations of K , α , and $n - 1$ ensured that their back-transformed values were positive and that $n > 1$.

The neural network consisted of a single hidden layer. We conducted a trial to determine the appropriate number of hidden units by training the data with a range of hidden units (Minasny and McBratney, 2002a). From this trial, we concluded that predictions did not improve significantly by use of more than six hidden units. Four different neural network models were trained to test the ability of various input parameter combinations (Table 2) to predict \mathbf{p} . These input combinations represent a hierarchical structure of data availability (Schaap et al., 1998). The least amount of input was needed for the first training set that included particle size distribution data only ($N_i = 3$). The other three training sets also included input parameters: ρ_b ($N_i = 4$), ρ_b and θ_s ($N_i = 5$), and ρ_b with θ_s and $\log K_s$ ($N_i = 6$).

The training was conducted by first minimizing the standard objective function of Eq. [5]. All the input and output values

Table 2. Hierarchical set of input variables for training neural networks.

No.	Types of input variables for vector \mathbf{x}
3	Sand, silt, and clay content
4	Sand, silt, and clay content, and bulk density (ρ_b)
5	Sand, silt, and clay content, ρ_b , and saturated water content (θ_s)
6	Sand, silt, and clay content, ρ_b , and θ_s , and $\log_{10}(K_s)^\dagger$

$^\dagger K_s$, saturated hydraulic conductivity.

were scaled to zero-mean and unit-variance so that the different magnitudes of the parameters did not affect optimization. The optimized weights after 20 iterations were used as initial estimates for the performance-based optimization, minimizing Eq. [6]. With $N_b = 6$ and $N_i = 4$, the weighting matrix \mathbf{W} consists of 6-by-5 elements, including the six bias values. If five hydraulic parameters are optimized ($N_o = 5$), the weighting matrix \mathbf{U} consists of 5-by-7 elements (including the five bias values). The neural network training algorithm was implemented in the *Neuroman* program (Minasny and McBratney, 2002b).

Bagging

Recent empirical evidence suggests that combining different neural networks can enhance the prediction accuracy (Perone and Cooper, 1993). With use of bootstrap aggregating or bagging (Breiman, 1996), one can generate many different data sets from a single original data set to fit different neural network models. These networks are then combined to form a single aggregated predictor.

The bootstrap method (Efron and Tibshirani, 1993) was developed to assess the accuracy of a prediction by generating different prediction models from different realizations of the training dataset. Dane et al. (1986) used bootstrapping to provide confidence intervals for the statistical distribution of soil ρ_b and to determine the minimum sample size needed to estimate the mean with a specified degree of precision.

Bootstrapping assumes that the training data set is a representation of the population and that multiple realizations from the population can be simulated from this single dataset. This is done by repeated sampling with replacement from the original dataset, D , of size N to obtain B bootstrap data sets, each of size N . Therefore, each bootstrap data set contains different data. Since the neural net is trained for each realization, the bagging procedure produces B neural networks. Each bootstrap dataset D^b , $b = 1, 2, \dots, B$, yields a prediction model, $\hat{\mathbf{y}}^b(\mathbf{x})$, where \mathbf{y} either represents a vector with predicted parameter (parameter-based) or θ and $\log(K)$ (performance-based) values. The bagging estimate is calculated from the mean of all B model predictions, or

$$\hat{\mathbf{y}}_{\text{bag}}(\mathbf{x}) = \frac{1}{B} \sum_{b=1}^B \hat{\mathbf{y}}^b(\mathbf{x}), \quad [8]$$

whereas the uncertainty of the model was calculated from its standard deviation. Schaap et al. (1998) applied a similar bootstrap procedure for their neural network model for predicting soil-water retention function parameters.

Bagging is especially useful when analyzing highly variable data sets. The aggregated predictor averages the prediction across all bootstrap samples, thereby reducing the prediction variance. The prediction accuracy increases if the prediction method is unstable; that is, small changes in the training data of the bootstrap can result in large changes in the resulting predictor (Breiman, 1996).

The size B of the bagged or bootstrap aggregated predictor used was 50; that is, data were resampled 50 times, thus produc-

ing 50 neural networks. For each neural net, the van Genuchten parameters were predicted, and $\theta(h)$ and $K(h)$ data pairs for each soil sample were calculated. The mean and 95% confidence interval of the predicted hydraulic parameters, water retention, and hydraulic conductivity data were computed by all B predicted data pairs, Eq. [8]. Finally, predicted soil hydraulic parameters were determined by fitting the Mualem-van Genuchten function (Eq. [1] and [2]) to the mean predicted water retention and hydraulic conductivity data. This algorithm was implemented in a program called *Neuro Multistep*, which is available upon request.

Performance Measure

The performance of the neural network was evaluated from values of the mean residual (MR) and root mean square residual. The MR is a measure of prediction bias, with negative and positive MR-values indicating underestimation and over-prediction, respectively. It is defined by

$$\text{MR} = \frac{1}{N} \sum_{i=1}^N (\hat{y}_i - y_i), \quad [9]$$

where N is equal to $N_s \times N_d$, and \hat{y} and y represent predicted and measured θ or $\log K$ values, respectively, at the seven different matric head values for each of the 310 soil samples ($N = 7 \times 310$). The root mean square of residuals (RMSRs) defines the expected magnitude of the prediction error, or

$$\text{RMSR} = \left[\frac{1}{N} \sum_{i=1}^N (\hat{y}_i - y_i)^2 \right]^{1/2}. \quad [10]$$

For soil-water content, the units of M_r and RMSR are $\text{cm}^3 \text{cm}^{-3}$, while for conductivity the units are dimensionless because the subtraction of two logarithmic K values is equal to the logarithm of their ratio.

Our prediction results were compared with those obtained by the neural network program Rosetta of Schaap et al. (2001). Briefly, Rosetta estimates soil-water retention parameters θ_s , θ_r , α , and n with a training data set of soils from the temperate and subtropical regions in Europe and the USA. Their unsaturated hydraulic conductivity parameters, K_o and l , were predicted separately by the UNSODA database.

RESULTS AND DISCUSSION

Performance of Neuro Multistep

The performance of Neuro Multistep, predicting soil hydraulic properties from the 310 sample training dataset is shown in Table 3. In addition to the performance-based optimization (Eq. [6]) proposed in this paper, we also conducted the standard parameter-based optimization (Eq. [5]) using software JMP version 5.0 (SAS Institute, 2002). Training the neural network with the performance-based objective function provided better predictive capability than with the standard parameter-based optimization. The prediction bias was also lower. Differences are most evident for the conductivity predictions. Specifically, the RMSR value of $\log(K)$ was reduced by a factor of two, and the bias was more than one order of magnitude smaller, when compared with the parameter-based optimizations. Furthermore, adding more input parameters than texture only slightly improved the prediction of conductivity with the parameter-based approach.

In part, we believe that the lesser performance of the

Table 3. Statistics of neural networks prediction of water retention and hydraulic conductivity with different combinations of input variables.[†]

Inputs	MR		RMSR	
	θ	$\log_{10}(K)$	θ	$\log_{10}(K)$
	— $\text{cm}^3 \text{cm}^{-3}$ —		— $\text{cm}^3 \text{cm}^{-3}$ —	
Parameter-based optimization				
Sand, silt, clay [‡]	−0.0142	0.2592	0.047	1.328
Sand, silt, clay, ρ_b [‡]	−0.0133	0.2311	0.043	1.356
Sand, silt, clay, ρ_b , θ_s [‡]	−0.0076	0.2377	0.039	1.383
Sand, silt, clay, ρ_b , θ_s , $\log(K_s)$ [§]	−0.0115	0.2231	0.034	1.370
Performance-based optimization				
Sand, silt, clay [‡]	0.0007	−0.013	0.042	1.065
Sand, silt, clay, ρ_b [‡]	0.0002	−0.015	0.038	0.919
Sand, silt, clay, ρ_b , θ_s [‡]	0.0001	−0.016	0.034	0.888
Sand, silt, clay, ρ_b , θ_s , $\log(K_s)$ [§]	0.0030	−0.044	0.035	0.733
Rosetta				
Sand, silt, clay, ρ_b [‡]	−0.0515	0.546	0.073	1.978
θ_s , θ , α , n [‡]	—	0.225	—	1.212

[†] α , scalding parameter; θ_s , saturated water content; ρ_b , bulk density; K_s , saturated hydraulic conductivity; MR, mean residual; N_s , number of samples; N_d , number of water retention and conductivity data; RMSR, root mean squares of residuals.

[‡] Number of data ($N_s \times N_d$) = 2170.

[§] Number of data ($N_s \times N_d$) = 1533.

Table 4. Comparison of true with predicted parameters and their respective root mean squares of residual (RMSR) values with the parameter-based (\hat{p}_{par}) and performance-based (\hat{p}_{per}) optimizations for three soils of the training data set.

Parameter [‡]	Silt loam LTRAS [†]			Sand Kearney			Loam Diener		
	p	\hat{p}_{par}	\hat{p}_{per}	p	\hat{p}_{par}	\hat{p}_{per}	p	\hat{p}_{par}	\hat{p}_{per}
θ	0.326	0.237	0.234	0.045	0.071	0.000	0.119	0.198	0.129
θ_s	0.410	0.409	0.409	0.367	0.370	0.371	0.400	0.406	0.398
α	0.015	0.011	0.011	0.036	0.037	0.032	0.013	0.017	0.013
n	1.694	1.563	1.667	4.674	3.628	4.479	1.413	1.581	1.714
$\log(K_o)$	−1.854	−1.530	−1.700	1.380	1.284	1.097	−0.928	−0.874	−1.129
RMSR θ		0.027	0.014		0.031	0.069		0.006	0.031
RMSR $\log(K)$		0.651	0.490		1.767	0.560		0.279	0.280

[†] LTRAS, long term research on agricultural systems.

[‡] α , scalding parameter; θ , volumetric water content; θ_s , residual water content; θ_s , saturated water content; K , hydraulic conductivity; K_o , matched saturated hydraulic conductivity; n , curve shape factor.

parameter-based approach is caused by the inherent assumption that hydraulic parameters are independent, whereas many studies have demonstrated that water retention and unsaturated hydraulic conductivity data are determined by the correlated set of hydraulic parameters. Therefore, an accurate prediction of one or more hydraulic parameters does not guarantee a good fit of both the water retention and hydraulic conductivity data. The performance-based optimization ensures that the predicted parameters fit both water retention and unsaturated conductivity data rather than only the hydraulic parameters. The difference in performance between the two approaches can also be attributed to the nonuniqueness or nonidentifiability of the hydraulic models. In the latter case, one may wonder whether the soil hydraulic data can be fit by more than a single parameter set. The differences between the parameter-based (\hat{p}_{par}) and performance-based optimizations (\hat{p}_{per}) for three different soil samples (silt loam from LTRAS, sand from Kearney, and sandy loam from Diener) of the training data set are highlighted in Table 4. While parameter-based optimization gives closer values of n , K_o , and similar RMSR valued for water retention, the RMSR values for $\log(K)$ are generally much higher, as expected from using Eq. [10] as the performance criterion.

Predicted soil hydraulic properties with performance-based optimization are relatively unbiased, as concluded from the near-zero value of the M_r of both θ (retention data) and $\log(K)$ (unsaturated hydraulic conductivity). The RMSR for θ is approximately 4% moisture content, whereas the RMSR for $\log(K)$ is about one order of magnitude. Increasing the number of relevant input variables to include ρ_b and θ_s improved the prediction, particularly of $\log(K)$.

The predicted soil-water content data are compared with their measured values in Fig. 3a. Whereas most θ data are concentrated near the 1:1 line across the whole water content range, some Kearney data (triangles) were underpredicted. The predicted unsaturated hydraulic conductivity values (Fig. 3b) matched their corresponding measured values except for a small number of low hydraulic conductivity values of the LTRAS samples (diamonds). As the results of Table 3 show, incorporating measured K_s values as an additional input parameter, improves the prediction of unsaturated hydraulic conductivity only slightly, while increasing the bias of

both θ and $\log(K)$. This indicates that K_s has little meaning for unsaturated K , which is better defined by K_o .

The bagging procedure yielded 50 different **W** and **U** matrices for each set of input parameters. When predicting soil hydraulic data for soils other than the training data set, these same weighting arrays are used to obtain 50 soil hydraulic functions, from which the mean and confidence limits are computed. Three examples of neural network predictions for the same soil samples as in Table 4 are presented in Fig. 4. Figure 4a presents the predicted $\theta(h)$ and $K(h)$ functions with 95% confidence intervals for a LTRAS sample with a sand and clay content of 21 and 18%, respectively, and ρ_b , θ_s , and K_s values of 1.5 g cm^{-3} , 0.41 $\text{cm}^3 \text{cm}^{-3}$, and 0.08 cm h^{-1} , respectively. For the second sample, a sand from Kearney in Fig. 4b, the sand and clay content, ρ_b , θ_s , and K_s values are 98 and 2%, 1.46 g cm^{-3} , 0.37 $\text{cm}^3 \text{cm}^{-3}$, and 60 cm h^{-1} , respectively. Finally, Fig. 4c presents the predicted curves and confidence intervals for a Diener sample with sand and clay content of 43 and 14%, and ρ_b and θ_s values of 1.53 g cm^{-3} and 0.4 $\text{cm}^3 \text{cm}^{-3}$, respectively. As expected, all predicted hydraulic data fall within the confidence bands. In this example, the prediction of the Kearney sand is quite uncertain as reflected by the high confidence interval and large RMSR values, which demonstrates the lower prediction capability for

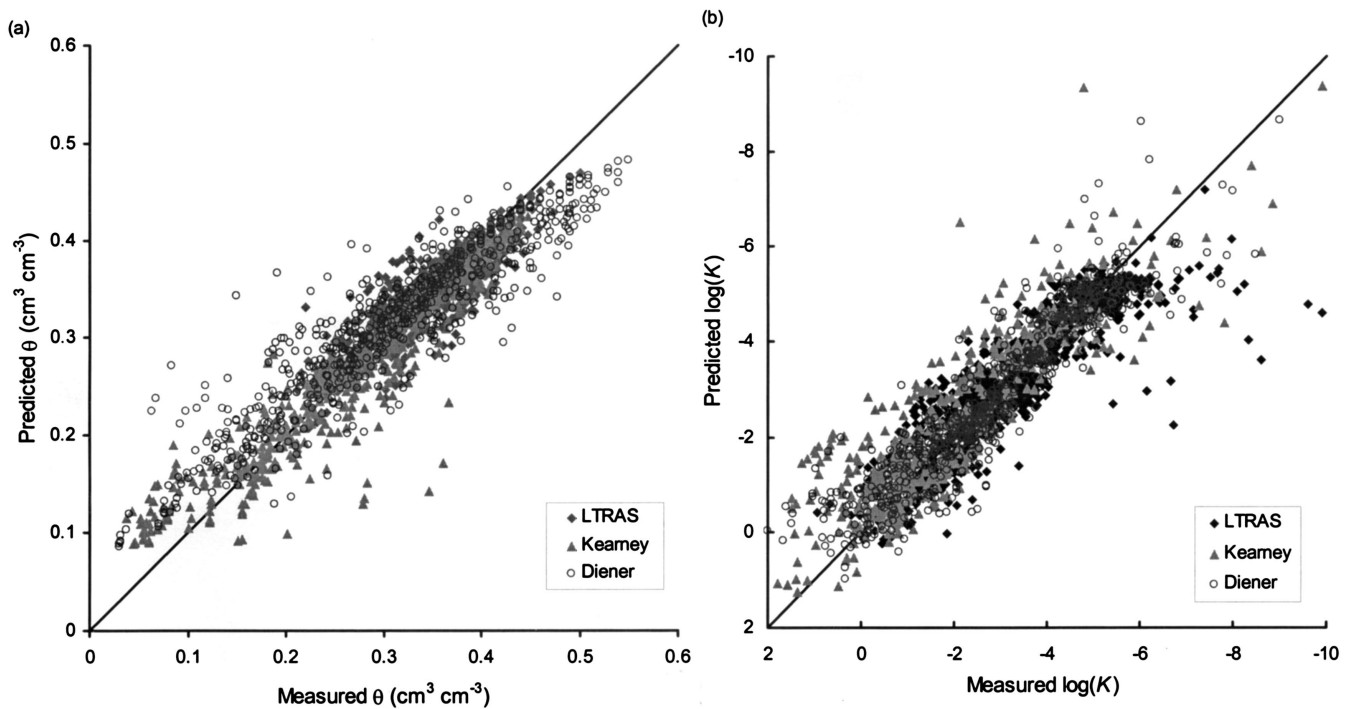


Fig. 3. Measured vs. predicted (a) water retention and (b) unsaturated hydraulic conductivity data when five input parameters are used (sand, silt, clay, bulk density, and saturated water content). θ , water content; K , hydraulic conductivity.

sand. Generally, all conductivity predictions show that the prediction uncertainty is larger as the unsaturated hydraulic conductivity decreases with decreasing matric potential values.

Comparison with Other PTFs

A key measure of the predictability performance of neural networks is the RMSR value. Literature values for RMSR of soil-water retention data range from 0.02 to 0.10 $\text{cm}^3 \text{cm}^{-3}$ (Wösten et al., 2001, Table 2). The RMSR values of Neuro Multistep with the training data of multistep outflow data are equal or better than reported elsewhere. Since studies reporting on K predictions are limited, a comparison with only few studies can be made. Specifically, Schaap and Leij (2000) reported an average RMSR value of $\log(K)$ of 1.18, using percentages of sand, silt, and clay, and ρ_b as input parameters. This value was reduced to 0.84 when K was predicted from the soil-water retention parameters θ_r , θ_s , α , and n . The average RMSR value of the study of Zhuang et al. (2001) was 1.24. The RMSR of $\log(K)$ of our training data set is of similar magnitude or lower than either reported study. In comparing the presented predictions with other studies, we must note that our study predicts the water retention and unsaturated conductivity simultaneously from the same input data, while most other training data sets apply neural networks to water retention and unsaturated hydraulic conductivity separately.

To determine the influence of the training data set on the prediction, we applied the Rosetta neural networks of Schaap et al. (2001) to our training dataset. The RMSR values with Rosetta (Table 3) were about twice as large. The larger prediction error by Rosetta

is a consequence of two factors. First, it demonstrates the value of the training data set, that is, our data set includes hydraulic data for Californian alluvial soils only, whereas the Rosetta training data set consists of a much wider range of soils across the globe. Second, we hypothesize that the higher prediction accuracy of Neuro Multistep is caused by the mere fact that all soil-water retention and unsaturated hydraulic conductivity data were determined by the multistep outflow method in the same laboratory. As also pointed out by Vereecken (2002), the evaluation of prediction methods for unsaturated hydraulic conductivity must consider the number and type of measurement methods that were used. Because of the limited number of soil types that were used in the training data set of Neuro Multistep, one must be careful in extrapolating our results to soils with larger values of clay content than included here.

To further investigate the usefulness of the prediction of neural networks to specific textural groups, we separated the training data set into two main soil textural groups: sands (sand, loamy sand, and sandy loam) and loams (loam, silt loam, sandy clay loam, clay loam, and silty clay loam), each with about an equal number of soil samples. The distribution of RMSR for both textural groups as well as for all textures combined is presented in Fig. 5a (retention) and Fig. 5b (unsaturated conductivity). This is done for Neuro Multistep with all four input data sets of Table 3, as well as for Rosetta with percentages of sand, silt, and clay, and ρ_b . Each box plot presents the median (center line) and the 25 and 75% percentiles (top and bottom) with the cross lines representing the median. Notably, the prediction error is larger for the sandy soil group than for the loamy group. We presume that the difference in prediction error is

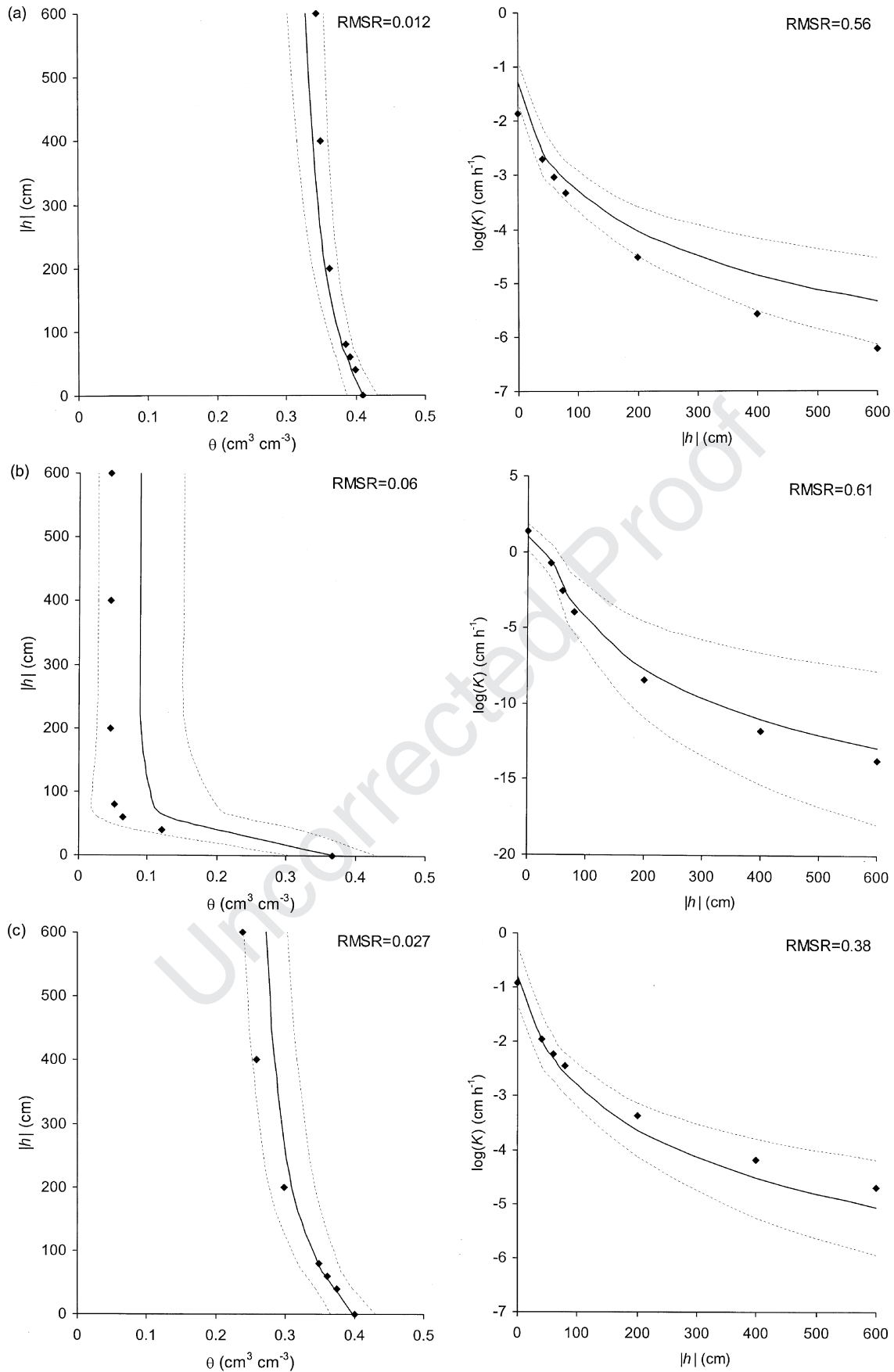


Fig. 4. Examples of measured (dots) and predicted (solid line) soil hydraulic functions with five input parameters. The dashed lines span the 95% confidence interval of the predictions. The comparison is presented for (a) Long Term Research on Agricultural Systems (LTRAS) silt loam, (b) Kearney sand, and (c) Diener loam. θ , water content; h , soil-water matric head; K , hydraulic conductivity; RMSR, root mean squares of residuals.

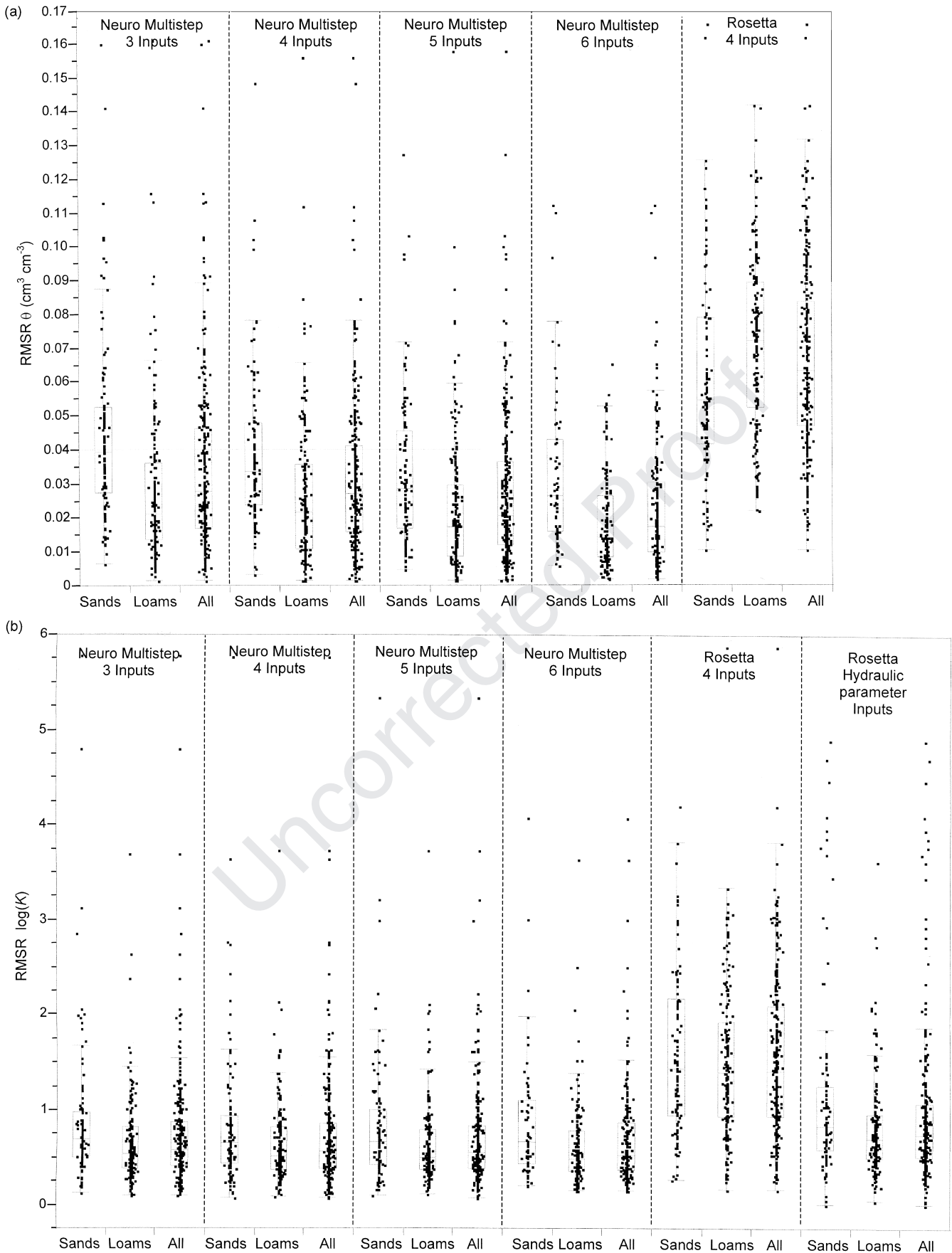


Fig. 5. Box plots of RMSR values for different neural network models predicting (a) water retention, and (b) unsaturated hydraulic conductivity. The box plots summarize the distribution of root mean squares of residuals (RMSR). The horizontal line in each box signifies the median value, whereas top and bottom of the box represent the 25th and 75th quantiles. The whiskers extend from the ends of the box to the outermost data point that falls within the distances of upper quartile + 1.5 (interquartile range), and lower quartile - 1.5 (interquartile range), respectively. θ , water content; K , hydraulic conductivity.

Table 5. Values of root mean squares of residual (RMSR) for predicted matched saturated hydraulic conductivity (K_o) with different combinations of input variables with the training data set grouped in sandy and loamy soils.

Inputs†	RMSR $\log_{10}(K_o)$		
	Sands	Loams	All
Neuro Multistep			
Sand, silt, clay‡	0.621	0.829	0.806
Sand, silt, clay, ρ_b ‡	0.579	0.813	0.788
Sand, silt, clay, ρ_b , θ_s ‡	0.594	0.800	0.777
Sand, silt, clay, ρ_b , θ_s , $\log(K_s)$ §	0.572	0.706	0.693
Rosetta			
Sand, silt, clay, ρ_b ‡	1.391	1.014	1.062
θ_r , θ_s , α , n ‡	1.011	0.966	0.968

† α , scalding parameter; θ_r , residual water content; θ_s , saturated water content; ρ_b , bulk density; K_s , saturated hydraulic conductivity.

‡ Number of samples N , for sands = 35, loams = 273, All = 310.

§ Number of samples N , for sands = 24, loams = 195, All = 219.

attributed to the high nonlinearity of the coarser soil group. However, it can be noted that opposite results were obtained with Rosetta, with lower RMSR values for sandy soils than loamy soils. This may be because of the better representation of sandy soil materials in the training dataset of Rosetta (Schaap et al., 2001).

Table 5 compares prediction results of Neuro Multistep with Rosetta for K_o only, with the same sets of input parameters as Table 3, making distinction between the sandy and loamy soil groups. In contrast to the unsaturated hydraulic data, the prediction error of K_o for sands is smaller than for the loamy soil group. It is hypothesized that the smaller prediction error is caused by the smaller measurement error of the saturated hydraulic conductivity of sandy soils. It is also noted that the K_o prediction is largely improved by including the measured saturated hydraulic conductivity, K_s , as input variable. This would suggest a two-step approach. In the first step one predicts K_o , which would be subsequently used in the second step to improve the unsaturated hydraulic conductivity predictions.

Sensitivity Analysis

Finally, it is interesting to determine the sensitivity of the various input parameters on the predicted soil hydraulic parameters. Figure 6 shows the prediction profile (SAS Institute, 2002) of five input variables on parameters: θ_r , θ_s , α , n , and $\log(K_o)$, and water retention at a matric head value of -100 cm: θ_{-100} . The input and output parameters are normalized by their respective mean (μ) and standard deviation (σ) as follows:

$$x^* = (x - \mu)/\sigma. \quad [11]$$

The sensitivity plot in Fig. 6 depicts the predicted response of the hydraulic parameters when changing each input variable across a wide range of values, as determined by its minimum and maximum value. These ranges are indicated on the x axis for each input variable. For each input variable, its value is varied while all other input variables are held constant to their respective mean values. The vertical dotted lines represent the mean values for each input parameter, whereas the horizontal dotted lines indicate the corresponding predicted values. The plot shows that the response of the outputs

is not a linear function of the input variables, particularly α and n , which is also because of log transformation in the prediction.

Sand content seems to influence most of the parameters. An increase in both sand and silt content leads to a decrease in values of θ_r , θ_s , and α , and increase in the values of n and K_o . The influence of clay content on prediction of water content at a matric head of -100 cm (θ_{-100}) appears to be relatively small compared with the other input variables, implying that the change in clay content will not affect the prediction of θ . This may be the result of the low clay content of the soil used in the training data set. The value of θ_{-100} is influenced by the combination of all input variables. Saturated water content, θ_s , appears to be another important input variable, having more influence on the parameter predictions than ρ_b . A change in θ_s value affects all parameters. It should be noted that the plot only shows the sensitivity at specific values, whereas interactions between all input variables are expected. The use of neural networks enables incorporation of the nonlinearities and interactions between the input and output variables.

CONCLUSIONS

The results confirm our initial hypothesis that the consistency of the data set plays important role in calibrating PTFs. We have compiled a unique data set of soil-water retention and unsaturated hydraulic conductivity functions that were simultaneously estimated (measured) with the multistep outflow method.

With this unique dataset, we successfully developed PTFs that simultaneously predict water retention and hydraulic conductivity by neural network analysis. We note that the predictions in this paper can only be used for the range of soil textures that were included in the training data set (sands and loams). Moreover, the predicted hydraulic properties pertain to the experimental measurement range of soil-water matric heads between 0 and -600 cm only.

The neural networks model developed in this paper has not been validated on an independent dataset. Currently, we developed the model with all available data to maximize its predictive capabilities. Additional data for other soil types and geographic regions will have to be included in the training dataset, thereby providing a more general applicable prediction. However, we doubt that a single PTF can be found that provides equal and accurate predictions for every soil and geographic region in the world as what was presented here.

The neural networks analysis in this paper is implemented in a program called Neuro Multistep. The program can be obtained by contacting either Dr. Budiman Minasny (budiman@acss.usyd.edu.au) or Dr. Jan W. Hopmans (jwhopmans@ucdavis.edu), or can be downloaded from the University of Sydney website: <http://www.usyd.edu.au/su/agric/acpa/software> (verified 19 Nov. 2003).

REFERENCES

- Bloemen, G.W. 1980. Calculation of hydraulic conductivities from texture and organic matter content. *Z. Pflanzenernaehr. Bodenk.* 143:581–605.

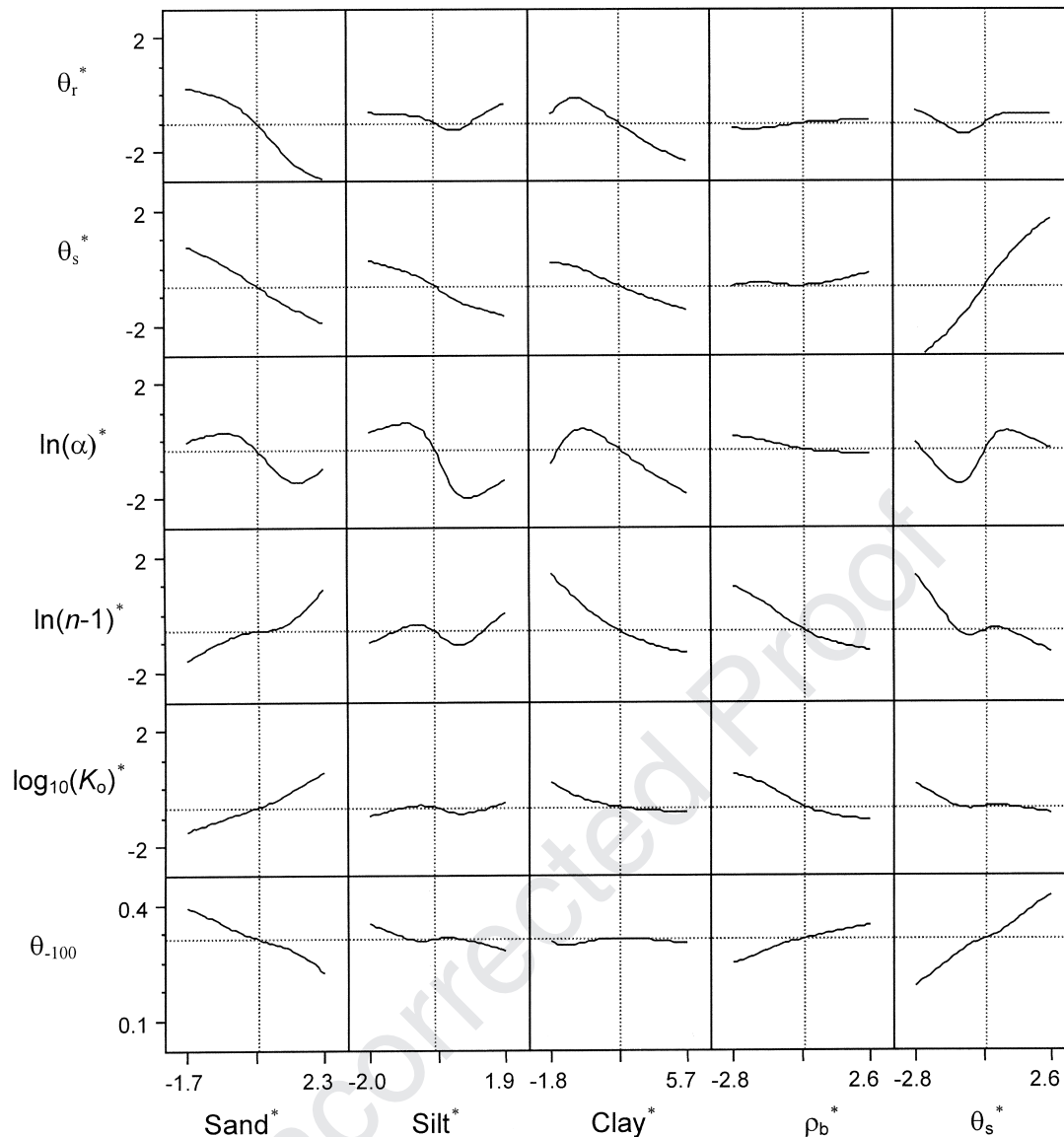


Fig. 6. Sensitivity analysis of various input data (horizontal axis) to soil hydraulic parameters (vertical axis). θ_{100} , water retention at a matric head value of -100 cm; θ_r , residual water content; θ_s , saturated water content; ρ_b , bulk density; K , hydraulic conductivity.

- Bouma, J. 1989. Using soil survey data for quantitative land evaluation. *Adv. Soil Sci.* 9:177–213.
- Breiman, L. 1996. Bagging predictors. *Mach. Learn.* 24:123–140.
- Corwin, D.L., S.R. Kaffka, J.D. Oster, J.W. Hopmans, Y. Mori, J.W. van Groenigen, C. van Kessel, and S.M. Lesch. 2003. Assessment and field-scale mapping of soil quality properties of a saline-sodic soils. *Geoderma* 114:231–259.
- Crescimanno, G., and M. Iovino. 1995. Parameter estimation by inverse method based on one-step and multi-step outflow experiments. *Geoderma* 68:257–277.
- Dane, J.W., R.B. Reed, and J.W. Hopmans. 1986. Estimating soil parameters and sample size by bootstrapping. *Soil Sci. Soc. Am. J.* 50:283–287.
- Eching, S.O., J.W. Hopmans, and W.W. Wallender. 1994a. Estimation of in situ unsaturated soil hydraulic functions from scaled cumulative drainage data. *Water Resour. Res.* 30:2387–2394.
- Eching, S.O., J.W. Hopmans, and O. Wendroth. 1994b. Unsaturated hydraulic conductivity from transient multi-step outflow and soil water pressure data. *Soil Sci. Soc. Am. J.* 58:687–695.
- Efron, B., and R.J. Tibshirani. 1993. An introduction to the bootstrap. *Monogr. 57 on Statistics and Applied Probability*. Chapman & Hall, London.
- Gardner, W.R. 1956. Calculation of capillary conductivity from pressure plate outflow data. *Soil Sci. Soc. Am. Proc.* 20:317–320.
- Gonçalves, M.C., L.S. Pereira, and F.J. Leij. 1997. Pedo-transfer functions for estimating unsaturated hydraulic properties of Portuguese soils. *Eur. J. Soil Sci.* 48:387–400.
- Hopmans, J.W., J. Simunek J., N. Romano, and W. Durner. 2002. Water retention and storage: Inverse methods. p. 963–1004. *In* J.H. Dane and G.C. Topp (ed.) *Methods of soil analysis: Part 4—Physical methods*. SSSA Book Series No. 5. SSSA, Madison, WI.
- Jaynes, D.B., and E.J. Tyler. 1984. Using soil physical properties to estimate hydraulic conductivity. *Soil Sci.* 138:298–305.
- Klute, A., and A. Dirksen. 1986. Hydraulic conductivity and diffusivity: Laboratory methods. p. 687–734. *In* A. Klute (ed.) *Methods of soil analysis. Part I. 2nd ed. Physical and mineralogical methods*. Agron. Monograph No. 9. ASA, CSSA, and SSSA, Madison, WI.
- Kool, J.B., J.C. Parker, and M.Th. van Genuchten. 1985. Determining soil hydraulic properties for one-step outflow experiments by parameter estimation. I. Theory and numerical studies. *Soil Sci. Soc. Am. J.* 49:1348–1354.
- Kosugi, K., J.W. Hopmans, and J.H. Dane. 2002. Water retention and storage: Parametric models. p. 739–757. *In* J.H. Dane and G.C.

- Topp (ed.) Methods of soil analysis: Part 4—Physical methods. SSSA Book Ser. No. 5. SSSA, Madison, WI.
- Leij, F., M.G. Schaap, and L.M. Arya. 2002. Water retention and storage: Indirect methods. p. 1009–1045. *In* J.H. Dane and G.C. Topp (ed.) Methods of soil analysis: Part 4—Physical methods. SSSA Book Ser. No. 5. SSSA, Madison, WI.
- Mallants, D., D. Jacques, P.-H. Tseng, M.Th. van Genuchten, and J. Feyen. 1997. Comparison of three hydraulic property measurement methods. *J. Hydrol. (Amsterdam)* 199:295–318.
- McBratney, A.B., B. Minasny, S.R. Cattle, and R.W. Vervoort. 2002. From pedotransfer function to soil inference system. *Geoderma* 109:41–73.
- Minasny, B., and A.B. McBratney. 2002a. The *neuro-m* method for fitting neural network parametric pedotransfer functions. *Soil Sci. Soc. Am. J.* 66:352–361.
- Minasny, B., and A.B. McBratney. 2002b. *Neuroman*: Neural networks program for generating parametric pedotransfer functions. Available at: <http://www.usyd.edu.au/su/agric/acpa/software> (verified 18 Nov. 2003). Australian Centre of Precision Agriculture, the Univ. of Sydney, NSW, Australia.
- Mualem, Y. 1976. A new model for predicting the hydraulic conductivity of unsaturated porous media. *Water Resour. Res.* 12:513–522.
- Nemes, A., M.G. Schaap, F.J. Leij, and J.H.M. Wösten. 2001. Description of the unsaturated soil hydraulic database UNSODA version 2.0. *J. Hydrol. (Amsterdam)* 251:151–162.
- Nielsen, D.R., J.W. Biggar, and K.T. Erh. 1973. Spatial variability of field measured soil water properties. *Hilgardia* 42:215–259.
- Perrone, M.P., and L.N. Cooper. 1993. When networks disagree: Ensemble methods for neural networks. p. 126–142. *In* R.J. Mammone (ed.) *Neural networks for speech and image processing*. Chapman-Hall, New York.
- Pachepsky, Y.A., D.J. Timlin, and G. Varallyay. 1996. Artificial neural networks to estimate soil water retention from easily measurable data. *Soil Sci. Soc. Am. J.* 60:727–773.
- Ripley, B.D. 1996. *Pattern recognition and neural networks*. Cambridge Univ. Press, Cambridge.
- Romano, N., and M. Palladino. 2002. Prediction of soil water retention using soil physical data and terrain attributes. *J. Hydrol. (Amsterdam)* 265:56–75.
- SAS Institute. 2002. *JMP statistics and graphics guide*. v. 5. SAS Inst., Cary, NC.
- Schaap, M.G., and F.L. Leij. 1998. Database-related accuracy and uncertainty of pedotransfer functions. *Soil Sci.* 10:765–779.
- Schaap, M.G., and F.L. Leij. 2000. Improved prediction of unsaturated hydraulic conductivity with the Mualem-van Genuchten model. *Soil Sci. Soc. Am. J.* 64:843–851.
- Schaap, M.G., F.L. Leij, and M.Th. Van Genuchten. 1998. Neural network analysis for hierarchical prediction of soil hydraulic properties. *Soil Sci. Soc. Am. J.* 62:847–855.
- Schaap, M.G., F.L. Leij, and M.Th. Van Genuchten. 2001. Rosetta: A computer program for estimating soil hydraulic parameters with hierarchical pedotransfer functions. *J. Hydrol. (Amsterdam)* 251:163–176.
- Tamari, S., J.H.M. Wösten, and J.C. Ruiz-Suárez. 1996. Testing an artificial neural network for predicting soil hydraulic conductivity. *Soil Sci. Soc. Am. J.* 60:1732–1741.
- Tuli, A., M.A. Denton, J.W. Hopmans, T. Harter, and J.L. MacIntyre. 2001b. Multi-step outflow experiment: From soil preparation to parameter estimation. Land, Air and Water Resources Rep. No. 100037. Univ. of California, Davis.
- Tuli, A., K. Kosugi, and J.W. Hopmans. 2001a. Simultaneous scaling of soil water retention and unsaturated hydraulic conductivity functions assuming lognormal pore-size distribution. *Adv. Water Resour.* 24:677–688.
- van Dam, J.C., J.N.M. Stricker, and P. Droogers. 1994. Inverse method for determining soil hydraulic functions from multi-step outflow experiments. *Soil Sci. Soc. Am. J.* 58:647–652.
- van Genuchten, M.Th. 1980. A closed-form equation for predicting the hydraulic conductivity of unsaturated soils. *Soil Sci. Soc. Am. J.* 44:892–898.
- van Genuchten, M.Th., and D.R. Nielsen. 1985. On describing and predicting the hydraulic properties of unsaturated soils. *Ann. Geophys.* 3:615–628.
- Vereecken, H. 1995. Estimating the unsaturated hydraulic conductivity from theoretical models using simple soil properties. *Geoderma* 65:81–92.
- Vereecken, H. 2002. Comment on the paper, “Evaluation of pedotransfer functions for unsaturated soil hydraulic conductivity using an independent data set.” *Geoderma* 108:145–147.
- Vereecken, H., R. Kaiser, M. Dust, and T. Pütz. 1997. Evaluation of the multistep outflow method for the determination of unsaturated hydraulic properties of soils. *Soil Sci.* 162:618–631.
- Wagner, B., V.R. Tarnawski, V. Hennings, U. Müller, G. Wessolek, and R. Plagge. 2001. Evaluation of pedo-transfer functions for unsaturated soil hydraulic conductivity using an independent data set. *Geoderma* 102:275–297.
- Wösten, J.H.M. 1990. Use of soil survey data to improve simulation of water movement in soils. Ph.D. thesis. Univ. of Wageningen, the Netherlands.
- Wösten, J.H.M., A. Lilly, A. Nemes, and C. Le Bas. 1999. Development and use of a database of hydraulic properties of European soils. *Geoderma* 90:169–185.
- Wösten, J.H.M., Y.A. Pachepsky, and W.J. Rawls. 2001. Pedotransfer functions: Bridging gap between available basic soil data and missing soil hydraulic characteristics. *J. Hydrol. (Amsterdam)* 251:123–150.
- Zhuang, J., K. Nakayama, G.R. Yu, and T. Miyazaki. 2001. Predicting unsaturated hydraulic conductivity of soil based on some basic soil properties. *Soil Till. Res.* 59:143–154.